1-1-2014

The role of osteoprotegerin and receptor activator of nuclear factor kappa-betta ligand in vascular calcification and the influence of insulin and liraglutide on this process in type 2 diabetes mellitus.

Colin Davenport
Royal College of Surgeons in Ireland

THE ROLE OF OSTEOPROTEGERIN AND RECEPTOR ACTIVATOR OF NUCLEAR FACTOR KAPPA-BETA LIGAND IN VASCULAR CALCIFICATION AND THE INFLUENCE OF INSULIN AND LIRAGLUTIDE ON THIS PROCESS IN TYPE 2 DIABETES MELLITUS

Dr Colin Davenport

MB, BCh, BAO (NUI), LRCSI, MRCPI

A thesis submitted to the Royal College of Surgeons in Ireland

for the degree of Doctor of Philosophy (PhD)

November 2014

Supervisor: Dr Diarmuid Smith

Co-Supervisor: Dr Philip M. Cummins

DECLARATION

I declare that this thesis, which I submit to RCSI for examination in consideration of the degree of Doctor of Philosophy, is my own personal effort. Where any of the content presented is the result of input or data from a related collaborative research programme this is duly acknowledged in the text such that it is possible to ascertain how much of the work is my own. I have not already obtained a degree in RCSI, or elsewhere, on the basis of this work. Furthermore, I took reasonable care to ensure that the work is original, and, to the best of my knowledge, does not breach copyright law, and has not been taken from other sources except where such work has been cited and acknowledged within the text.

Signed

Colin Davenport

Colin Davenport

RCSI Student Number

99356

Date

17/10/2014

TABLE OF CONTENTS

ACKNOWLEDGEMENTS

There are a number of groups and individuals who helped me during the three years I spent working on this thesis. First and foremost, I wish to express my sincere thanks to the patients who enrolled in Study III, without whom the clinical aspect of this research could never have taken place, and who gave freely of their time in attending for the various study visits. As a close second, I must thank the funding source for this project, the Health Research Board of Ireland, from whom I received a 3 year research training fellowship. This research grant, which was awarded after a peer-reviewed process and a competitive interview, provided my salary over the timeframe of my research, as well as providing a consumables budget and assisting my PhD registration with the Royal College of Surgeons in Ireland. I thank the interview panel for the faith they demonstrated in both the research proposal I presented and my ability to successfully complete this project.

Before my own experiments began, I was already indebted to prior members of our department's ongoing research program. Dr Eoin O'Sullivan, my immediate predecessor, established an active and exciting line of research that I was subsequently able to continue and expand upon. As I began my project, Eoin also gave me solid advice on balancing research goals with my long-term career, and continued to be available to help me long after he had re-entered the world of full-time clinical medicine. Dr David Ashley, who helped both Eoin and I as we learnt our basic laboratory skills in Dublin City University, also aided me by providing significant statistical advice during the analysis of the data generated in Study III.

Following the commencement of my research project, I required and received help from a great number of individuals. As consultants in diabetes and endocrinology in Beaumont Hospital, both Professor Christopher Thompson and Dr Amar Agha in the

endocrinology department supported my research by helping me refine my original research proposals, providing criticisms of my data, and fostering a robust academic environment that encouraged research of the highest standard. I count myself entirely fortunate to have worked in their department, and I am grateful in particular for the invaluable career advice offered by Professor Thompson over this time. My fellow research registrars within Beaumont, Dr Lucy-Ann Behan, Dr Nigel Glynn and Dr Mark Hannon, are also deserving of mention, as we all helped and supported each other on numerous occasions during the many years we spent within the department. I am also thankful to the specialist nurses and secretaries of the Diabetes Day Centre in Beaumont, who referred me numerous patients for Study III, tolerated my frequent use of their facilities and resources, and who were always a pleasure and a privilage to work with. Elsewhere within Beaumont Hospital I received support from Professor Arnold Hill, who kindly provided storage space for the significant number of samples generated by Study III, and Gillian Vale, who co-ordinated the ethics committee submissions for this hospital. Professor Gerry McElvaney supported me hugely with regards to registering my thesis with the Royal Colleage of Surgeons and by contributing significantly to the initial successful grant application. Dr Brendan McAdam provided valuable cardiology input to the the design and conduct of Study III, and Dr Frank McGrath facilitated the performance and the interpretation of the coronary artery calcification scans in the Sports Surgery Clinic in Santry. Lucy Smith, who co-ordinated the patient's attendance for said scans in the Sports Surgery Clinic, and who ensured I received the data afterwards, also deserves special mention for her efforts. Within James Connolly Hospital, my research was supported and encouraged by Professor Seamus Sreenan, Dr John McDermott, and Dr Wan Aizad Wan Mahmood. Wan, in particular, recruited 11 patients for Study III within this hospital, conducting visits at study baseline and at completion. Finally, with regards to clinical medicine, I am grateful to my colleage Dr Hannah Forde, my successor in our department's research

program, who conducted study completion visits for 22 patients in Study III, and who has already expanded upon my research with novel and exciting findings of her own.

The laboratory aspect of my research program was conducted within the environs of the Endothelium Biology Group in Dublin City University. In retrospect, I could not have asked for a more helpful and friendly group of colleageus with which to work. Dr Keith Rochfort, Dr Fiona Martin, Dr Ciaran McGinn, Dr Brian Mac Donnell, Dr Chunxu Shan and Dr Anthony Guinan, all of whom received their own doctorartes in recent years, combined to provide me with a supportive and friendly working environment, as did their various successors - Alisha McLoughlin, Laura Twomey and Robert Wallace. In addition to my research peers, Dr Ronan Murphy kindly allowed me the use of his laboratory facilities when required, and Dr Micheal Parkinson provided statistical support for the original research proposal to the Health Research Board. Dr Donal O'Gorman is also worthy of special mention, as the man who helped establish the initial diabetes and vascular research links between Beaumont Hospital and Dublin City University, who was always available for advice when I needed it, and who allowed me to use his laboratory facilities for assay performance and glucose and lactate measurement.

With regards to my supervisors, I am eternally grateful for the immense amounts of time and effort they put in over the 3 years of my research project, and in truth a significant degree of time both before and afterwards. Dr Philip Cummins, who supervised the laboratory aspect of my thesis, raised the standard of every aspect of the research program our department was pursuing, and in particular was invaluable in submitting our successful grant application and in preparing me for my thesis submission and defence. Working within his research group was an overwhelmingly positive and educational experience, and without his constant input and support the

present thesis would not exist in any form, much less a successful one. As a clinician, I consider myself entirely and especially fortunate that I was able to work for a scientist of his caliber.

With regards to Dr Diarmuid Smith, who was my clinical supervisor for my research program, I can say, simply, that I have been amazingly lucky to have Dr Smith as my mentor, colleage, and friend for nearly ten years, ever since I first worked as his intern in Beaumont Hospital. This relationship has been characterized by constant faith and support on his part for both my clinical and research careers. I cannot imagine the path my life as a doctor would have taken without his mentorship, and I continue to be inspired by his clinical and research acumen, the rapports he establishes effortlessly with both patients and colleages, his unceasingly positive attitude in the face of challenges in the Irish healthcare system, and his devotion to medicine, his family, and of course the Dublin football team.

Outside of hospitals and laboratories, I enjoyed, as I have all my life, the unceasing support of my family, who respected my reclusive researcher's lifestyle when deadlines were looming, while also being ready for me to return to the family home at short notice to seek refuge from the pressures of the world. I am immensely proud of my mother for pursuing her own academic career while simultaneously taking care of the rest of the family, myself included. With regards to my father, it can simpy be said that I will count myself well satisfied if I end up even half the man he is in the years to come. My brother, who eclipses me in possessing both science and business acumen, used his skils to help me in obtaining some of the most important consumables for my laboratory experiments. Ultimately, without the support of my family, it is doubtful that I would ever have had the drive, ambition and persistence necessary to complete this thesis.

Finally, while it may have become apparent that I have frequently been fortunate with regards to my colleages, mentors, friends and family, it is in my partner in life that I have been supremely lucky. In the first months of this research project, I travelled to Denmark to give a presentation on our initial findings to diabetes researchers from a number of different countries. That night I sat down to dinner opposite a Finnish doctor named Ksenia. Three years later, with the project complete, I asked her 'tuletko vaimokseni?'. She said yes. This thesis, as with all else that is good and positive in my life, is dedicated to her.

ABSTRACT

Background: The process of vascular calcification (VC) appears to involve certain vascular cell populations assuming an osteoblastic phenotype. Osteoprotegerin (OPG) has been proposed as an inhibitor of VC, potentially via blockade of either receptor activator of nuclear factor kappa-beta ligand (RANKL) or tumor necrosis factor-related apoptosis-inducing ligand (TRAIL). Treatments for type 2 diabetes mellitus (T2DM) such as insulin analogues and liraglutide are known to affect OPG, and may also affect VC. The aims of this thesis were to characterise the roles of OPG/RANKL/TRAIL in VC, and to measure how insulin and liraglutide affect coronary artery calcification (CAC) in T2DM. Methods: Production and secretion of OPG/RANKL/TRAIL was measured in human aortic endothelial and smooth muscle cells (HAECs & HASMCs). RANKL, TRAIL, insulin glargine and liraglutide were added to HAECs and HASMCs, and osteoblastic transformation of HASMCs was measured via alkaline phosphatase activity in the cell media and messenger ribonucleic acid (mRNA) markers of osteoblastic activity. In a clinical study, patients with T2DM who were commencing either insulin analgoues or liraglutide had CAC scans at 0 and 16 months of treatment. Results: OPG, but not TRAIL or RANKL was secreted in large amounts by HASMCs, and to a lesser extent by HAECs. The direct application of RANKL or TRAIL did not induce osteoblastic transformation of HASMCs, but application of RANKL to HAECs led to increased production of bone morphogenetic protein 2 (BMP-2), which in turn led to increased osteoblastic activity in HASMCs. Insulin glargine, but not liraglutide, decreased OPG production and increased osteoblastic activity in HASMCs *in vitro,* and insulin analogues, but not liraglutide, was associated with a trend towards accelerated CAC in the T2DM population. Conclusions: OPG inhibits osteoblastic transformation of HASMCs via prevention of RANKL-induced BMP-2 release from HAECs. Insulin analogues increase VC *in vitro* and are associated with increased CAC *in vivo* in T2DM.

LIST OF FIGURES

LIST OF TABLES

ABBREVIATIONS

ΔRN	normalized reporter signal
ΔΔCt	comparative cycle threshold method
ACEi	angiotensin converting enzyme inhibitor
Ad	adventitia
ADAM™	advanced detection and accurate measurement
AHA	America Heart Association
ALP	alkaline phosphatase
ANOVA	analysis of variance
ANCOVA	analysis of covariance
Ao	aorta
ARB	angiotensin receptor blocker
BCA	bicinchoninic acid
BMI	body mass index
BMP-2	bone morphogenetic protein 2
BMP-4	bone morphogenetic protein 4
bp	base pair
BP	blood pressure
BSA	bovine serum albumin
BSP	bone sialoprotein
Ca	calcium
CAC	coronary artery calcification
CAD	coronary artery disease
Cbfa-1	core-binding factor subunit alpha-1
cDNA	complementary DNA
CHD	coronary heart disease
CT	computed tomography
Cu^{2+}	copper ion
CV	coefficient of variation
CVC	calcifying vascular cell
CVD	cardiovascular disease
CXR	chest x-ray
DcR1	decoy receptor 1
DcR2	decoy receptor 2
DDC	Diabetes Day Centre
DMSO	dimethyl sulfoxide

DNA	deoxyribonucleic acid
dNTP	deoxynucleotide
DPP-IV	dipeptidyl-peptidase 4
DR4	death receptor 4
DR5	death receptor 5
EBCT	electron beam computed tomography
EC	endothelial cell
ECHO	echocardiography
ECS	extracapillary space
EDTA	ethylenediaminetetraacetic acid
eGFR	estimated glomerular filtration rate
ELISA	enzyme-linked immunosorbent assay
ERK	extracellular signal-regulated kinase
ESRF	end-stage renal failure
FAS	factor of apoptotic stimulus
FGF23	fibroblast growth factor 23
GIP	glucose-dependent insulinotropic peptide
GLP-1	glucagon-like peptide
H_2O	water
HAEC	human aortic endothelial cell
HASMC	human aortic smooth muscle cell
HCMB	Conditioned media from HAECs at baseline
HCMR	Conditioned media from HAECs exposed to RANKL
HCMT	Conditioned media from HAECs exposed to TRAIL
HUVEC	human umbilical vein endothelial cell
HbA1c	glycated hemoglobin A1c
HMG-CoA	3-hydroxy-3-methyl-glutaryl-CoA
hsCRP	high sensitivity C-reactive protein
IL6	interleukin 6
IHD	ischemic heart disease
kd	kilodalton
L	lumen
LAD	left anterior descending (coronary artery)
LDL	low-density lipoprotein
LM	left main (coronary artery)
MDCT	multidetector computed tomography
MDRD	modified diet in renal disease (formula)

MESA	multiethnic study of atherosclerosis
MGP	matrix gla protein
M	media
MI	myocardial infarction
mRNA	messenger ribonucleic acid
Msx2	msh homeobox 2
NFATc1	nuclear factor of activated T cells, cytoplasmic 1
NF-κB	nuclear factor kappa-beta
NNP1	ectonucleotide pyrophosphatase-phosphodiesterease 1
OCN	osteocalcin
OD	optical density
OPG	osteoprotegerin
OPN	osteopontin
Osx	osterix
p	p-value
PAD	peripheral artery disease
PBS	phosphate-buffered saline
PCR	polymerase chain reaction
Pi	phosphate
Pit1	sodium-dependent phosphate transporter
PI-3-kinase	phosphatidylinositol-3-kinase
PKA	protein kinase A
pNPP	p-nitrophenyl phosphate
PPi	inorganic pyrophosphate
PTH	parathyroid hormone
qRT-PCR	quantitative real-time polymerase chain reaction
RANK	receptor activator of nuclear factor kappa-beta
RANKL	receptor activator of nuclear factor kappa-beta ligand
RCSI	Royal College of Surgeons in Ireland
r	Pearson's product-moment coefficient
rcf	relative centrifugal force
RIPA	radioimmunoprecipitation assay
ROS	reactive oxygen species
RNA	ribonucleic acid
RQ	relative quantification
rpm	revolution per minute
RR	relative risk

RT	reverse transcriptase
Runx2	runt-related transcription factor 2
SDS	sodium dodecyl sufate
SEM	standard error of mean
shRNA	small hairpin ribonucleic acid
SMC	smooth muscle cell
sRANKL	soluble receptor activator of nuclear factor kappa-beta ligand
T1DM	type 1 diabetes mellitus
T2DM	type 2 diabetes mellitus
TAE	Tris-acetate-ethylenediaminetetraacetic acid
TNF-α	tumor necrosis factor alpha
TRAF	tumor necrosis factor receptor-associated factor
TRAIL	tumor necrosis factor-related apoptosis-inducing ligand
TR R1/R2	necrosis factor-related apoptosis-inducing ligand receptor 1/2
VC	Vascular calcification
vWF	von Willebrand factor
VSMC	vascular smooth muscle cell
Wnt	wingless-related integration site
WPB	Weibel-Palade body

LIST OF PUBLICATIONS/PRESENTATIONS

Publications:

I. **Davenport C,** Rochfort K, Martin FM, Murphy RP, Smith D, Cummins PM. The production and secretion of osteoprotegerin and its ligands by human aortic endothelial and smooth muscle cells under basal and injurious conditions. *In preparation.*

II. **Davenport C**, Rochfort K, Martin F, Forde H, Murphy RP, Smith D, Cummins PM. Receptor activator of nuclear factor kappa-beta ligand induces osteoblastic transformation of smooth muscle cells via its actions on endothelial cells; a paracrine relationship of vascular calcification. *In preparation.*

III. **Davenport C**, Mahmoud WA, Forde H, Ashley DT, Agha A, Thompson CJ, McDermott J, Sreenan S, McAdam B, Cummins PM, Smith D. The effects of exogenous insulin and liraglutide on markers of vascular calcification *in vitro* and on coronary artery calcification in patients with type 2 diabetes. *In preparation.*

Presentations:

I. **Davenport C,** Rochfort K, Martin FM, McGinn C, Murphy RP, Smith D, Cummins PM. The effects of inflammation, hyperglycemia and cyclic strain on osteoprotegerin production in human aortic smooth muscle cells.

Poster presentation, Arteriosclerosis, Thrombosis and Vascular Biology Annual General Meeting, Chicago, 2012.

II. **Davenport C,** Rochfort K, Martin FM, McGinn C, Murphy RP, Smith D, Cummins PM. The effects of inflammation, hyperglycemia and cyclic strain on osteoprotegerin production in human aortic smooth muscle cells.

Oral Presentation, Irish Endocrine Society Annual General Meeting, Malahide, 2012.
Winner: O'Donovan Medal - best oral presentation

III. **Davenport C**, Rochfort K, Martin F, MacDonnell B, Murphy RP, Smith D, Cummins PM. Endothelial cells induce osteoblastic activity in smooth muscle cells in a paracrine manner that is enhanced by receptor activator of nuclear factor kappa-beta ligand (RANKL).

Oral Presentation, Irish Endocrine Society Annual General Meeting, Kilkenny, 2013.

IV. **Davenport C**, Cummins PM, Smith D. The role of osteoprotegerin and receptor activator of nuclear factor kappa-beta ligad in vascular calcification and the influence of insulin and liraglutide on this process in type 2 diabetes mellitus.

Poster presentation, Beaumont Hospital Annual Research Day, Dublin, 2014.
Winner: First prize, PhD Poster Category

Chapter 1 - Introduction and Literature Review

1.1. Background

In the developed world, cardiovascular disease (CVD), including coronary heart disease (CHD) and stroke, remains the commonest cause of death, having accounted for 1.9 million deaths in the European Union in 2012 (and approximately 5,000 deaths in Ireland each year) [1,2]. As illustrated by the data in the European Cardiovascular Disease Statistics (2012 edition), it is clear that the twin pandemics of obesity and type 2 diabetes mellitus (T2DM) contribute significantly to these high rates of cardiovascular morbidity and mortality [1]. T2DM is worthy of particular mention in this regard, as approximately 65% of all deaths in patients with T2DM occur due to CVD [3].

Table 1.1. Risk factors for CV disease.

Modifiable risk factors	*Non-modifiable risk factors*	*Novel risk factors*
Smoking	Family history	VC
Dyslipidemia	Gender	Chronic inflammation (hsCRP, IL-6)
Hypertension	Age	Homocysteine excess [4]
Physically inactive	Ethnicity	Vitamin D deficiency [5]
Obesity		Apolipoprotein A excess [6]
Diabetes and glycemic control		
Psychological stress		
Alcohol consumption		
Renal disease		

CV, cardiovascular; IL-6, interleukin 6; hsCRP, high sensitivity C-reactive protein; VC, vascular calcification

Current efforts at reducing CVD are focused, to a large degree, on the identification and modification of traditional cardiovascular (CV) risk factors such as hypertension, dydlipidemia, cigarette smoking etc., with interventions consisting of both lifestyle changes (e.g. increased exercise, healthy diets) and the use of pharmaceutical agents (e.g. statins, anti-hypertensives) [7,8]. A number of challenges have limited the effectiveness of this approach. In clinical practice, even with the use of extensive pharmaceutical intervention optimal control of modifiable risk factors (table 1.1) can be

difficult to achieve [9]. Furthermore, even in patients who achieve their treatment goals, the risk of CVD is not entirely eliminated, as age, gender, family history and ethnicity are not modifiable. As a result of these limitations, interest has arisen in identifying novel risk factors for CV disease that target as-yet untouched aspects of the atherosclerotic process, with the goal of developing new therapeutic interventions [10]. A large number of putative risk factors are currently under investigation, and while C-reactive protein and lipoprotein-a are amongst the more notable candidates, in recent years a new process has been recognised to participate in and accelerate CVD. This process, illustrated in figure 1.1, is vascular calcification (VC) [11,12].

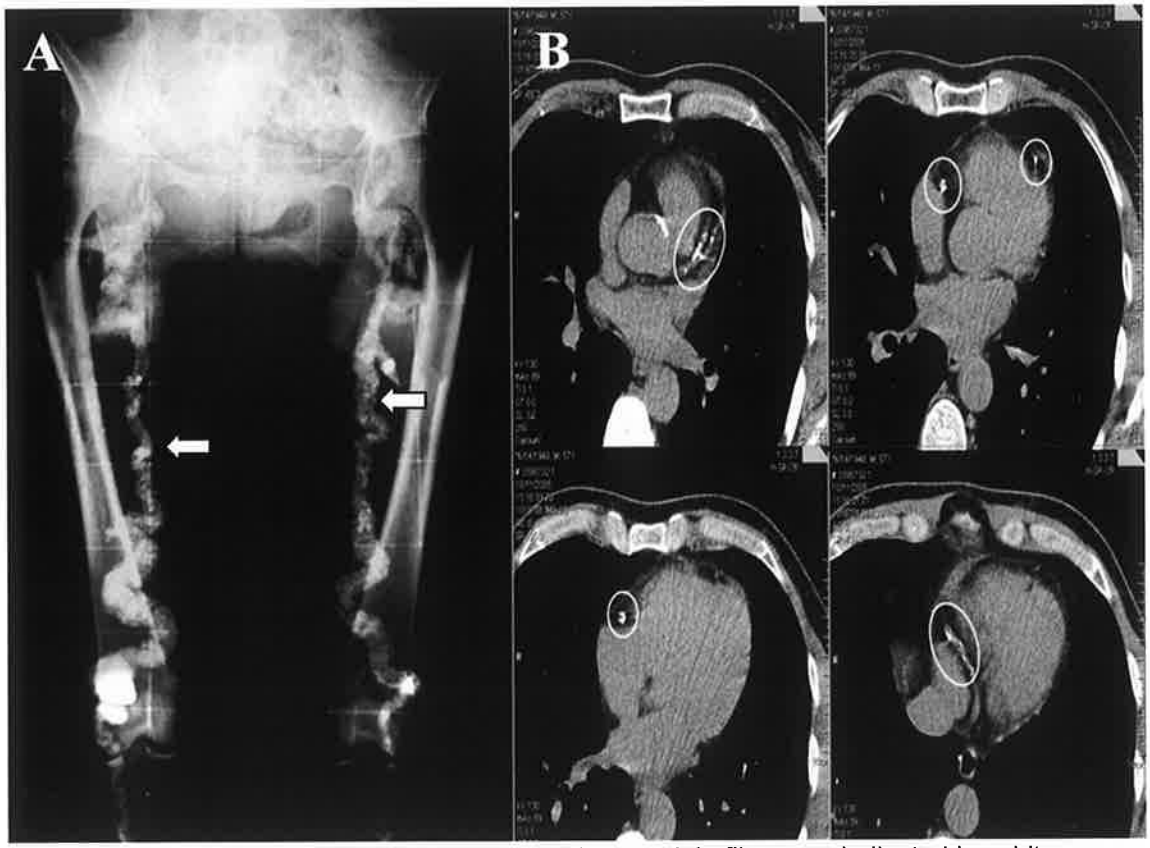

Figure 1.1. A: Extensive VC of the femoral arteries on plain film xray, indicated by white arrows. Adapted and reproduced with permission from Couri *et al* [13]. B: Computed tomogrpahy of the coronary arteries, with areas of calcification circled. Adapted and reproduced with permission from Piers *et al.* [14]. VC, vascular calcification.

As recently as 25 years ago, the widespread view of calcification within the vasculature was of a passive process of calcium deposition in the vessel walls that was essentially benign in terms of its effects on CVD [15,16]. In the intervening years that viewpoint

has shifted radically. Instead of passive deposition, it has become increasingly evident that VC is an active process involving the transformation of certain vascular cell populations into cells with osteoblastic and occasionally chondroblastic activity [17-19]. These cells secrete proteins such as collagen, which then undergo mineralization in a fashion similar to that which occurs in bone formation [20,21]. The second shift in viewpoint concerning VC is with regards to its supposedly benign nature, with mounting evidence that VC exerts a wide variety of detrimental effects on the CV system [22-28]. It is now recognized that VC is a) an active process involving cellular differentiation, and as such could potentially be inhibited or reversed, and b) a process that exerts numerous detrimental effects on CV hemodynamics and function, and as such may represent a novel CV risk factor and a target for treatment.

Osteoprotegerin (OPG) is a soluble member of the tumor necrosis receptor superfamily which exerts its biological functions by acting as a decoy receptor for either receptor activator of nuclear factor kappa-beta ligand (RANKL) or tumor necrosis factor-related apoptosis-inducing ligand (TRAIL), a relationship that is illustrated in figure 1.2 [29]. Within the skeletal system, the interaction and clinical relevance of OPG and RANKL has been well-described. In essence, OPG prevents RANKL from binding to the RANK (receptor activator of nuclear factor kappa-beta) receptor on osteoclast precursor cells, thereby preventing the maturation of osteoclasts, with the result being a net gain in bone mineral density [30].

Outside the skeletal system the clinical significance of OPG blocking RANKL and/or TRAIL signalling is not well understood. With regards to VC, an additional finding in the original OPG knockout studies, and one that did not receive a large degree of attention until recently, was that those mice who lacked OPG also developed early and severe VC [31]. At the time it was suggested that this was simply a process of calcium transfer

from bones to blood vessels, but the realization that VC involves an active osteogenic process has challenged this theory. In the interim, OPG has been identified as existing within the vasculature in significant amounts, and a study by Morony *et al.* reported that the administration of OPG to atherogenic mice led to a reduction in calcification burden [32], while in a separate study the co-administration of OPG with vitamin D prevented VC in mice [33]. *Although somewhat paradoxical, the evidence accumulating to date on OPG within the vasculature overwhelmingly indicates that while OPG encourages mineralization in the skeletal system, it exerts the opposite effect in the vasculature, acting as an important inhibitor of the calcification process [15,16,34-36].*

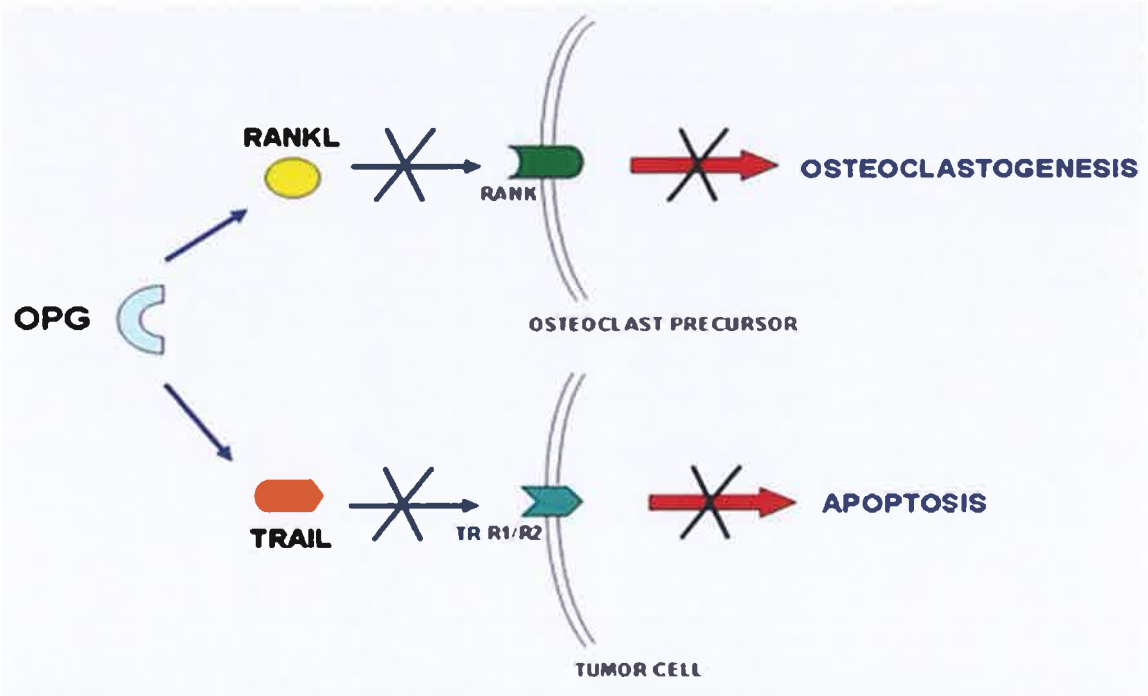

Figure 1.2. Schematic representation of the interaction between OPG molecules, RANKL molecules and TRAIL molecultes at the cell surface of osteoclasts and tumor cells. OPG molecules act as a decoy receptor for RANKL and TRAIL. When OPG molecules are present in greater amounts than RANKL or TRAIL molecules, therefore, they prevent RANKL and TRAIL from binding to and activating their cell surface receptors. Adapted and reproduced with permission from Di Lasio *et al. [37].* OPG, osteoprotegerin; RANKL, receptor activator of nuclear factor kappa-beta ligand; TRAIL, tumor necrosis factor-related apoptosis-inducing ligand, TR R1/R2, necrosis factor-related apoptosis-inducing ligand receptor 1/2.

As a potential inhibitor of VC, interest has arisen in characterizing the precise actions of OPG (and by extension its ligands RANKL and TRAIL) within the vascular wall. With this in mind, there remain at present a number of unanswered questions regarding

these proteins. With regards to the cellular context, three specific areas merit additional research at present. Firstly, the baseline production of OPG, RANKL and TRAIL from the two major vascular cell populations, endothelial cells (ECs) and vascular smooth muscle cells (VSMCs), requires qualification and quantification. Secondly, neither RANKL nor TRAIL, the two ligands whose activity OPG blocks, have been conclusively shown to induce osteoblastic activity in vascular cell populations. Thirdly, I note that there are limited data available on the effects of RANKL and/or TRAIL on co-cultures of ECs and VSMCs. This is despite the fact that ECs appear capable of producing various paracrine factors that promote osteoblastic activity in VSMCs [38]. It is these three areas of concern that form the majority of the laboratory aspect of this thesis. With regards to the clinical context, it is known that certain prescription medications in common use can alter circulating concentrations of OPG/RANKL/TRAIL, with unclear effects on VC.This area of research is of particular relevance to T2DM, which is characterisctially associated with both extensive VC and high rates of CVD. In this setting, treatment with insulin has been reported to decrease OPG production, and the hypothesis that insulin analogues (modified forms of the insulin molecule used in the treatment of T2DM) may promote VC has been expressed by a number of different groups. Conversely, newer agents for the treatment of T2DM, such as the glucagon-like peptide 1 (GLP-1) analogues, have been reported to increase OPG production and release, and may inhibit VC [39-41]. Given the high burden of VC in T2DM, the concept that these medications could promote or inhibit VC is of significant and immediate interest, and one with an extremely limited evidence base at present [42-45].

The overall goals of the present thesis are to characterise the roles of OPG, RANKL and TRAIL in the development of calcification within the vasculature, and to measure whether insulin analogues and the GLP-1 analogue liraglutide affect a) circulating concentrations of these proteins and b) coronary artery calcification (CAC) in a clinical

population with T2DM. The following sections provide an overview of the individual aims and experiments of the thesis.

1.2. Study I

An investigation of OPG, TRAIL and RANKL secretion from human aortic endothelial cells (HAECs) and human aortic smooth muscle cells (HASMCs) under basal and injurious conditions *in vitro*.

1.2.1. Aims

To qualify and quantify the release of OPG, RANKL and TRAIL under basal and injurious states from either cell population. This will provide clarity on the origins of these proteins within the vascular wall, and on the response of this system to injury.

1.2.2. Hypotheses

OPG will be secreted by HAECs and HASMCs, and this secretion will be up-regulated by injurious stimuli. RANKL and/or TRAIL will not be produced in significant quantities, indicating an alternative source for these glycoproteins in the vasculature *in vivo*.

1.3. Study II

The effects of RANKL and/or TRAIL on osteoblastic transformation of HASMCs, the paracrine influence of HAECs on osteoblastic transformation of HASMCs, and the effects of RANKL on osteoblastic activity in a perfused co-culture model incorporating both HAECs and HASMCs.

1.3.1. Aims

i) To determine whether RANKL and/or TRAIL induce osteoblastic changes in HASMCs, whether HAECs exert a paracrine influence on the osteoblastic change of HASMCs, and whether RANKL and/or TRAIL affect this relationship.

ii) To determine whether RANKL and/or TRAIL induce osteoblastic activity in HASMCs when co-cultured with HAECs in a perfused artificial capillary system.

1.3.2. Hypotheses

i) RANKL and/or TRAIL will not exert direct effects on HASMCs, but will instead act on HAECS to increase osteoblastic transformation of HASMCs via paracrine signalling.

ii) These findings will be replicated in my co-culture model, generating data with increased comparability to the arterial environment *in vivo*.

1.4. Study III

The effect of insulin analogues versus the GLP-1 analogue liraglutide on the emergence of osteoblastic activity in HASMCs and on CAC score via computed tomography (CT) in patients with T2DM.

1.4.1. Aims

i) To determine the effects of insulin glargine and liraglutide on the emergence of osteoblastic activity in HASMCs.

ii) To determine the effects of starting either insulin analogues or liraglutide on OPG, RANKL and TRAIL, and on CAC over a period of 16 months. A group of patients remaining on metformin only will constitute the control group.

1.4.2. Hypotheses

i) Insulin glargine, but not liraglutide, will be associated with increased osteoblastic activity by HASMCs *in vitro*.

ii) In the T2DM population, commencing insulin analogues will be associated with a decrease in circulating OPG concentrations, and a significant increase in CAC scores. Commencing liraglutide will not be associated with a significant increase in CAC scores.

1.5. Literature Review - Introduction

VC can be defined, at its most basic, as the precipitation of calcium crystals within the vascular wall [24]. The resultant calcium deposition may be seen on various imaging modalities and at autopsy, and is a relatively common finding within the general population [46]. Certain patient groups, such as those with T2DM, have particularly high rates of this form of calcification [47,48]. Our understanding of how and why VC occurs has undergone significant changes in recent years, as has our awareness of its role in the acceleration of CVD [16]. The first part of this literature review will focus on the history, subtypes, epidemiology and pathogenesis of VC in both the general population and those with T2DM. This will be followed by an examination of the clinical significance of VC with regards to CVD risk, and a summary of the attempts to inhibit and/or reduce VC to date. As the investigation of the roles of OPG, RANKL and TRAIL in VC is a major theme of this thesis, the available literature on these proteins, their interactions, and their putative roles in VC will be reviewed separately. Finally, the physiological actions of insulin and GLP-1, their effects on OPG, RANKL and TRAIL, and the data on how T2DM medications may affect VC will be explored.

1.6. Calcification within the Vasculature

1.6.1. History

Reports that calcification can occur within the vascular wall may be found in the literature as far back as the 1500s [16]. It was in 1906 that elements of bone marrow were first identified within a heavily calcified aortic vessel, adding significant weight to the concept of VC resembling bone formation [49]. In the 1980s, research groups reported the presence of osteopontin and bone morphogenetic proteins in calcified plaques [50], and that *in vitro* populations of vascular cells were capable of mineralization in a manner similar to osteoblasts in bone [51]. From this point onwards it has been increasingly accepted that VC involves the active deposition of osteoid and

the precipitation of calcium within the vessel wall in a manner similar to bone formation, with mounting evidence that certain vascular cell populations, including VSMCs, are capable of differentiating into an osteoblastic phenotype, with a variety of inhibitors and promoters controlling this process [24,34,52-55]. In addition to these developments, it is also in recent years that the clinical relevance of this field of research has become increasingly apparent, with a growing awareness of the detrimental effects exerted by VC on the CV system [25,34].

1.6.2. Subtypes of VC

1.6.2.1. Overview

VC is a process with a number of subtypes, differentiated by interlinked histological and anatomical criteria (table 1.2) [15,24,56]. Anatomical classification of VC, based on location within the vasculature, has perhaps the greatest representation in the medical literature, with VC typically classifed by this approach as either intimal, medial or valvular calcification [24]. It should be noted that these anatomical subtypes are not mutually exclusive. Indeed, these subtypes share many risk factors for development, have various similarities at the cellular level, and as a result often co-exist within a given individual [15,57]. A brief overview of each anatomical subtype will be explored in the following sections.

1.6.2.2. Intimal Calcification

The innermost layer of the arterial wall, the tunica intima, is composed of the endothelial cell monolayer overlying an internal elastic lamina, with connective tissue (present in significant amounts in larger arteries) and a fenestrated membrane separating it from the tunica media. Calcification of this layer (figure 1.3) is typically associated with underlying atherosclerotic disease and endothelial dysfunction, and as such is most likely to be found the coronary arteries and the aorta [24,56]. It is also

more likely to co-locate with plaque and present as patches of calcification within the vessel as opposed to diffuse or circumferential calcification [58]. This is the most common form of VC in the general population [46]. The clinical relevance of intimal calcification lies primarily in its effects on plaque stability within the coronary arteries and the aorta.

Table 1.2. Major clinical phenotypes of VC with characteristic anatomical locations and known risk factors for development.

Clinical entity	*Location within vascular wall*	*Cell population expressing osteoblastic markers*	*Location within the circulation*	*Risk factors for development*
Atherosclerotic calcification	Tunica intima	Mural pericytes ± VSMCs	Large arteries (coronary, aortic, femoral)	Atherosclerosis Dyslipidemia Hypertension ESRF T2DM Age
Medial arterial calcification	Tunica media	VSMCs	Medium sized vessels (femoral, iliac, radial)	T2DM ESRF Age
Aortic valve calcification		Myofibroblasts	Valve leaflets (facing aorta)	Dyslipidemia Bicuspid valve ESRF

ESRF, end-stage renal failure; T2DM, type 2 diabetes mellitus; VC, vascular calcification; VSMC, vascular smooth muscle cell.

1.6.2.3. Medial Calcification

Medial arterial calcification (figure 1.3) affects the tunica media of the arterial wall, which is primarily composed of smooth muscle cells and elastic tissue [59]. Medial arterial calcification is associated with increasing age, but its prevalence and severity are significantly greater in the context of conditions such as T2DM and ESRF [60-62]. While this form of calcification can affect the coronaries and the aorta, it is more frequently associated with medium-sized arteries such as the femoral, ulnar or radial vessels, and is typically diffuse, circumferential, and may extend along the entire

vascular bed. The clinical relevance of medical calcification lies primarily in its effects on cardiovascular hemodynamics [22,42,60,63].

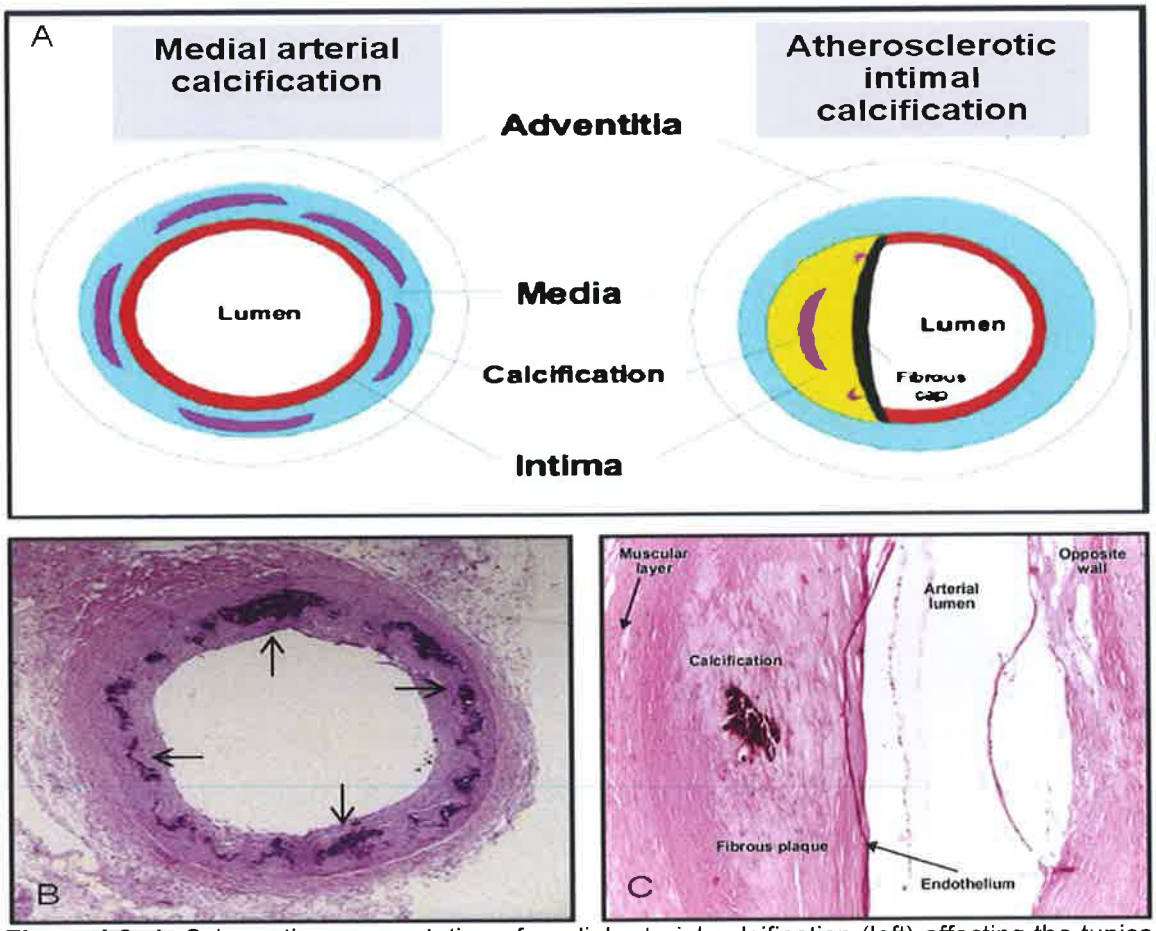

Figure 1.3. A: Schematic representation of medial arterial calcification (left) affecting the tunica media in a circumferential fashion (purple) and intimal arterial calcification (right) with an atherosclerotic plaque deforming the vessel lumen and containing a calcification deposit (purple). B: Circumferential medial calcification (arrows) within the tunica media of a peripheral artery. C: Atherosclerotic plaque arising from the intima and deforming the vessel lumen. A calcificaiton deposit (labelled) can be seen in the centre of the plaque. Adapted and reproduced with permission from Towler *et al.* [56]

1.6.2.4. Calcification of the Cardiac Valves

Calcification of the cardiac valves (figure 1.4), while occasionally considered a separate process to vessel wall calcification in the literature, is in fact quite similar at the cellular level, and has a similar negative relationship with CVD. The presence of osteogenesis in cardiac valves was most clearly demonstrated by Mohler *et al.* in 2001, when they reported mature lamellar bone tissue in over 10% of surgically excised heart valves (with more subtle markers of bone formation in the majority of the remaining valves) [64]. It was the aortic valve that was the main site of valve calcification in the vast

majority of cases [65]. Mechanical stressors, metabolic disturbances, and pro-inflammatory changes have all been implicated as inducers of aortic calcification [66].

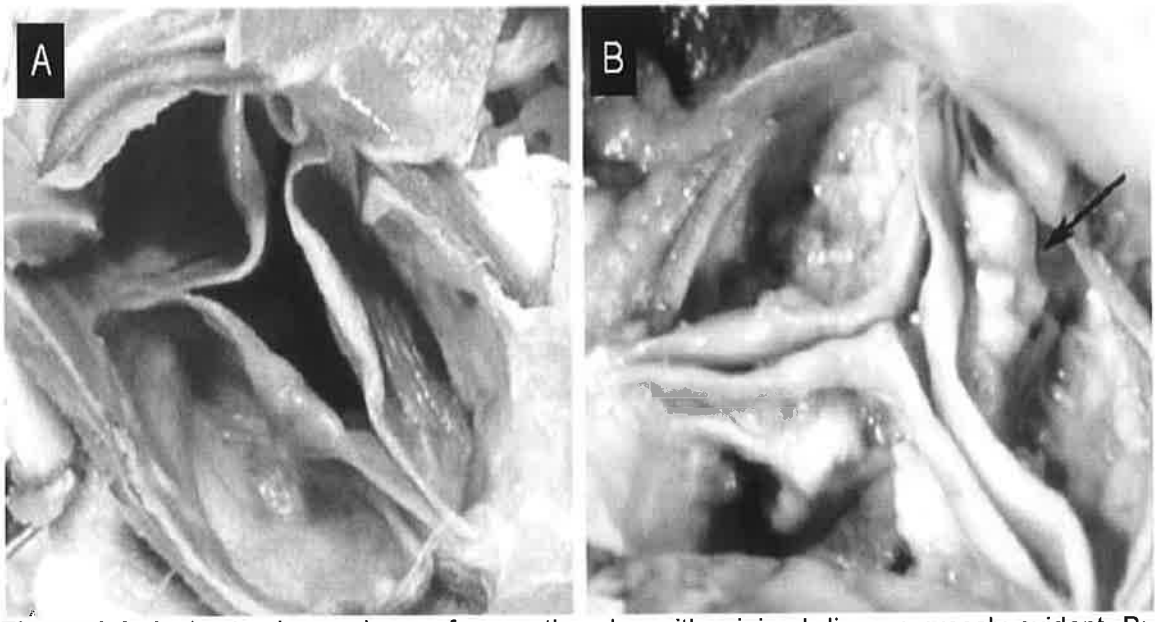

Figure 1.4. A: Anatomic specimen of an aortic valve with minimal disease grossly evident. B: Severely calcified, stenosed aortic valve with multple nodules of calcification (arrow). Adapted and reproduced with permission from Leopold *et al.* [66].

1.6.3. Epidemiology of VC on Imaging

General prevalence rates for VC are difficult to obtain. The reasons for this are that studies tend to focus on specific anatomical areas of calcification (e.g. coronary artery versus femoral calcification), prevalence rates differ depending on the imaging modality in use (e.g. CT versus x-ray), and high-risk populations such as T2DM and ESRF are often considered separately [16,46,67]. With all of the above in mind, the most recent estimates of VC from imaging studies, stratified by calcification type and/or patient population, are presented in table 1.3. Overall, these studies demonstrate that calcification is frequently present from at least the 4th and 5th decades of life in the general population, has a higher prevalence at earlier ages in T2DM and ESRF, and that with increasing age up to 100% of the population is affected.

Table 1.3. Prevalence rates for VC on imaging stratified into population studied and subtype of calcification.

Population	*Imaging modality*	*Subtype of VC*	*Results*	*References*
Asymptomatic consecutive subjects presenting for preventative medicine workup. Mean age 57.6 years, n=650.	Whole body EBCT (caudal to symphysis pubis). Prospective study.	Atherosclerotic calcification. (Specifically, coronary, aortic, iliac, carotid and femoral beds)	Exponential increase with age. Prevalence >80% in men >70 years, and 70% in women >70 years. 53% of women <50 years had no calcification, compared to 30% of men <50 years. All patients >80 years had some degree of calcification.	[46]
General population. Mean age 42 years, n=1000 patients.	EBCT. Prospective study.	Coronary arteries	Overall prevalence 17.3%, with 19.2% in white and 10.3% in black subjects.	[67]
General population. Mean age 47 years, n=116309.	CXR. Retrospective study.	Aortic arch calcification.	Prevalence 1.9% in males and 2.6% in females.	[68]
General population. Age range 55-86 years, n=552.	ECHO. Prospective study.	Aortic valve calcification.	Overall prevalence 53%.	[69]
Patients with T2DM. Age range 56-61 years, n=1059.	Plain film x-ray of femoral arteries. Prospective study.	Medial and intimal arterial calcification of the femorals.	Prevalence of medial arterial calcification 41.5%. Prevalence of intimal calcification 29.3%.	[42]
Hemodialysis patients. Age range 19 to 39 years, n=39.	MDCT. Prospective study.	Coronary arteries and cardiac valves.	Overall prevalence 92%.	[48]
Hemodialysis patients. Age range 28-74 years, n=49.	EBCT. Prospective study.	Coronary arteries and cardiac valves.	Overall prevalence 100%.	[47]

CAC, coronary artery calcification; CXR, chest x-ray; EBCT, electron beam computed tomography; ECHO, echocardiography; MDCT, multi-detector computed tomography; T2DM, type 2 diabetes mellitus; VC, vascular calcification.

1.6.4. Clinical Relevance of VC

1.6.4.1. VC in the Coronary Arteries - Predicting CV Risk

As reported by a relatively recent meta-analysis of 30 articles incorporating 218,000 subjects, the presence of VC in any arterial wall (including the cardiac valves) is associated with a 3-4 fold higher risk of CV events and all-cause mortality [70]. When patients with ESRF are considered separately, this risk is even higher, with a 6 fold increase in the incidence of CVD. With an association this strong, demonstrated across multiple patient groups, it is unsurprising that various attempts have been made to utilize VC as a risk prediction tool. In this context, quantification of the extent of calcification within the coronary arteries by CT scanning (figure 1.5) has offered the highest rates of both sensitivity and specificity for long-term CV risk prediction [71]. The two commonest techniques for measuring CAC are electron beam computed tomography (EBCT) and multidetector computed tomography (MDCT). EBCT remains, at present, the gold standard for the assessment of CAC, and the majority of the data linking CAC with CVD risk has been generated with this imaging modality [28,72]. ECBT is limited, however, in that the scanners are more expensive and bulkier when compared to traditional CT. With regards to MDCT, these scanners are cheaper, less bulky, and can be used for a variety of other scans. As a result, the measurement of CAC is increasingly being performed via MDCT. Reasonable levels of agreement have been reported between these two imaging modalities, and both were recognized as acceptable for the quantification of CAC in a recent American Heart Association (AHA) position statement [72]. With regards to the quantification process itself, most papers featuring EBCT or MDCT use the Agatson scoring system to describe CAC burden. This is the product of the area of the calcium deposits along with Hounsfield unit attenuation score [73]. CAC can also be assessed by volumetric and mass scoring systems, but the evidence underlying these approaches is limited at present.

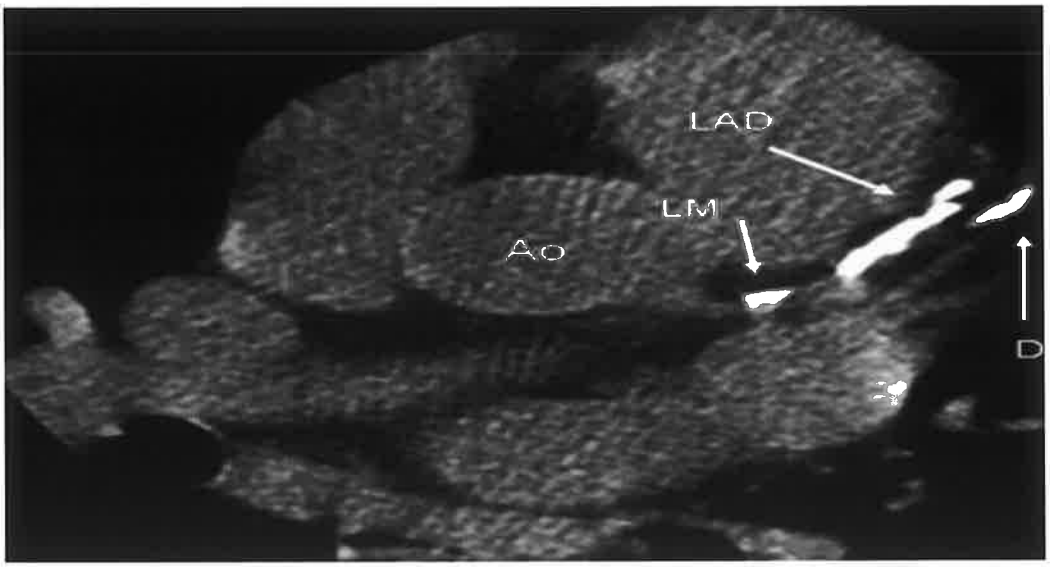

Figure 1.5. Cardiac structures on MDCT in a patient with a high CAC. Calcification is evident as a bright white colour change in the LAD and LM arteries. Adapted and reproduced with permission from Henneman et al. [74]. Ao, Aorta; CAC, coronary artery calcification; D, diagonal branch of the left anterior descending coronary artery; MDCT, multidetector computed tomography; LAD, left anterior descending coronary artery; LM, left main coronary artery.

With regards to the correlation between CAC and CVD risk on CT, an overview by the AHA can be seen in table 1.4. In a meta-analysis of nearly 28,000 patients, the presence of any CAC on CT was associated with a 4-fold increase in the risk of CHD events over the subsequent 5 years, whereas the absence of any CAC was associated with a very low risk (0.4%) of CHD [75]. Furthermore, an incremental relationship was noted, with an increased risk of CHD as the Agatson score increased. Finally, and perhaps most significantly with regards to CAC as a screening tool for high-risk patients, it has been reported by a number of different groups that CAC scores independently predict CHD risk above and beyond calculations based on traditional risk factors, including, in one study, high-sensitivity C-reactive protein (hsCRP) [76].

With regards to the usefulness of CAC scores in patients with T2DM, the evidence is somewhat limited to date. Patients with T2DM have higher CAC scores than those without, and although it has been hypothesized that this simply reflects the higher rates of atherosclerosis in T2DM, the relationship of CAC and CVD has yet to be

demonstrated convincingly in long-term outcome studies of CAC and CVD outcomes. Preliminary reports in this area have suggested that T2DM patients with low CAC scores have similar survival rates to patients without diabetes, suggesting, at least, a use for CAC scores in identifying low-risk individuals in this population [77].

Table 1.4. Association between CV disease risk and CAC score.

Category	*CAC score*	*RR (95% CI)*	*p-value*
Average risk	1-112	1.9 (1.3-2.8)	0.001
Moderate risk	100-400	4.3 (3.1-6.1)	<0.0001
High risk	400-999	7.2 (5.2-9.9)	<0.0001
Very high risk	>1000	10.8 (4.2-27.7)	<0.0001

CAC, coronary artery calcification; CI, confidence interval; RR, relative risk. Adapted with permission from the 2007 American College of Cardiology Foundation/ American Heart Association Expert Consensus Document [75].

In summary, while any form of VC appears to signify increased CV risk, this relationship has been studied to the greatest degree in the coronary arteries. Scoring CAC by CT allows for the prediction of CV events with a reasonable degree of sensitivity and specificity across multiple patient populations, adds to traditional risk prediction models, and has recently been endorsed by the AHA for the screening of asymptomatic patients with intermediate and low risk of CHD.

1.6.4.2. Detrimental Effects Caused by VC - Intimal Calcification

The relationship between intimal calcification and CVD has been studied extensively, and for longer than the other subtypes of VC, but debate continues over the relevance of this form of calcification to atherosclerotic plaque development and rupture. In general, the presence of multiple, small, discrete nodules of calcification within the atherosclerotic plaque are associated with an increased risk of plaque rupture, whereas plaques with larger, fewer foci of calcification may be at decreased risk. One hypothesis that may explain these observations is that plaques tend to rupture at

interfaces between high and low density tissue, and the increased number of interfaces that occur with multiple small foci of calcification may contribute to the higher risk of rupture with this pattern of calcium deposition. Thus, the relationship between intimal calcification and plaque stability may change over time, becoming more stable as the calcification deposits coalesce [22,25,27]. Further research will be necessary to clarify this specific relationship further, with a particular focus on the location and size of the calcification deposits within plaque.

Apart from the complex relationship described above, intimal calcification is also associated with an increased risk of coronary artery dissection following balloon angioplasty, a potentially devastating complication of angiography [28]. With regards to its effects on hemodynamic parameters, advanced intimal calcification can become confluent along a vascular tree, in a similar manner to medial calcification, and exert similar detrimental effects on vascular distensibility. With this in mind it is noteworthy that a recent analysis of the multiethnic study of atherosclerosis (MESA) cohort reported an association between intimal calcification, impaired coronary vasomotor responses and decreased myocardial perfusion [78].

1.6.4.3. Detrimental Effects Caused by VC - Medial Calcification

Once widely felt to be a benign process, medial arterial calcification is now recognized as a process that decreases arterial distensibility [22,79]. Decreased distensibility leads to loss of the Windkessel effect from large arteries, a phenomenon whereby distension of the large arteries allows 'storage' of energy and blood during systole (sometimes likened to the function of a capacitor), with relaxation of these arteries helping to overcome peripheral resistance and maintain adequate perfusion during diastole [80]. The loss of this effect may explain why medial arterial calcification is associated with a 3-fold increase in the risk of lower-extremity amputation [42]. Another consequence of the decrease in arterial distensibility with medial arterial calcification is raised pulse

wave velocity and increased pulse pressure [81]. These effects contribute in turn to left ventricular hypertrophy and decreased coronary artery filling during diastole.

1.6.4.4. Detrimental Effects Caused by VC - Valvular Calcification

The pathological nature of VC is perhaps most clearly demonstrated by calcification of the aortic valve. In recent decades, calcification of this valve has overtaken rheumatic heart disease as the commonest cause for clinically significant aortic valve disease requiring valve replacement [82]. Efficient valve function requires flexibility, which is significantly reduced by calcification. Initially this leads to stenosis of the valve and reduced cardiac output, and over time a degree of valve regurgitation will also develop. As a result, patients develop impaired peripheral circulation along with ventricular hypertrophy and an increased susceptibility to CHD [83].

1.6.4.5. Summary of Detrimental Effects Caused by VC

On reviewing the evidence base that has arisen in recent yeras, it is increasingly evident that VC exerts a variety of detrimental effects on CV hemodynamics and cardiac valve function, may increase the risk of plaque rupture, and does increase the risk of coronary artery dissection following angiography.

1.6.5. Mechanisms of VC

Over the last 25 years, it has become apparent that VC is an actively regulated process of biomineralization, very similar to processes seen in skeletal biology [16]. In recognition of the similarities between skeletal and VC, this section will begin with a brief review of the basic physiology of bone formation. This will be followed by a review of the risk factors and pathology of each major subtype (intimal, medial, valvular) of VC. VC in T2DM will be discussed as part of the section on medial arterial calcification, and the unique pathogenesis of VC in ESRF will also be reviewed.

1.6.5.1. Ossification - the Formation of Bone

Ossification, also known as osteogenesis, is, at its most basic, the deposition and organisation of bone material, both inorganic (e.g. calcium crystals) and organic (e.g. collagen), by osteoblasts. In addition to synthesising the components of bone, successful ossification also requires osteoblasts to overcome various inhibitory systems (e.g. inorganic pyrophosphate or PPi) [84,85]. Ossification is initiated, organized and completed by osteoblasts, a mononuclear cell population that arise from mesenchymal stem cells in the bone marrow and periosteum [85]. With regards to the induction of osteoblast differentiation and activity, a number of transcription factors have been identified whose upregulation appears critical to stimulating osteoblast differentiation/activation and resultant ossification. The most notable of these are runt-related transcription factor 2 (Runx2, also known as core-binding factor subunit alpha-1), its downstream mediator osterix, and msh homeobox 2 (Msx2) [22,86]. Upregulation of these transcriptional factors is associated with increased production of pro-osteogenic proteins, including alkaline phosphatase (ALP), bone sialoprotein (BSP) and the formation of matrix vesicles, while simultaneously decreasing the production of inhibitors of crystal nucleation and propagation such as osteopontin (OPN) and matrix gla protein (MGP) [19,87,88]. Signals which have been shown to upregulate Runx2 and Msx2 include the bone morphogenetic proteins 2 and 4 (BMP-2 and BMP-4), activation of the wingless-related integration site (Wnt) signalling pathway, and, with particular relevance to VC - oxidised lipids, inflammatory cytokines, and reactive oxygen species (ROS) [22].

In the initial steps of bone formation mature osteoblasts begin by depositing inorganic osteoid. This is a non-mineralized material composed primarily of type 1 collagen along with a small quantity of chondroitin sulphate. Soon after this step, osteoblasts begin to form hydroxyapatite ($Ca_{10}(PO_4)_6(OH)_2$) crystals within matrix vesicles on their cell

surfaces that are subsequently released from the cell, rupture, and form a nucleus for crystallisation within the extracellular space (figure 1.6) [87]. Further propagation of the crystals from these nuclei is facillitated by the presence of ALP, which removes the inhibitory effects of PPi. This step is a critical one in the ossification process, and as such ALP activity is viewed as a strong marker of osteoblastic activity and calcification [24,89]. The hardened composite of crystals and collagen that is the outcome of this process is termed bone matrix. Within this bone matrix, other cell types, including osteoclasts (which break down and resorb bone) accumulate and contribute to the final state of mature bone, which is a balance of ongoing resorption and synthesis [90].

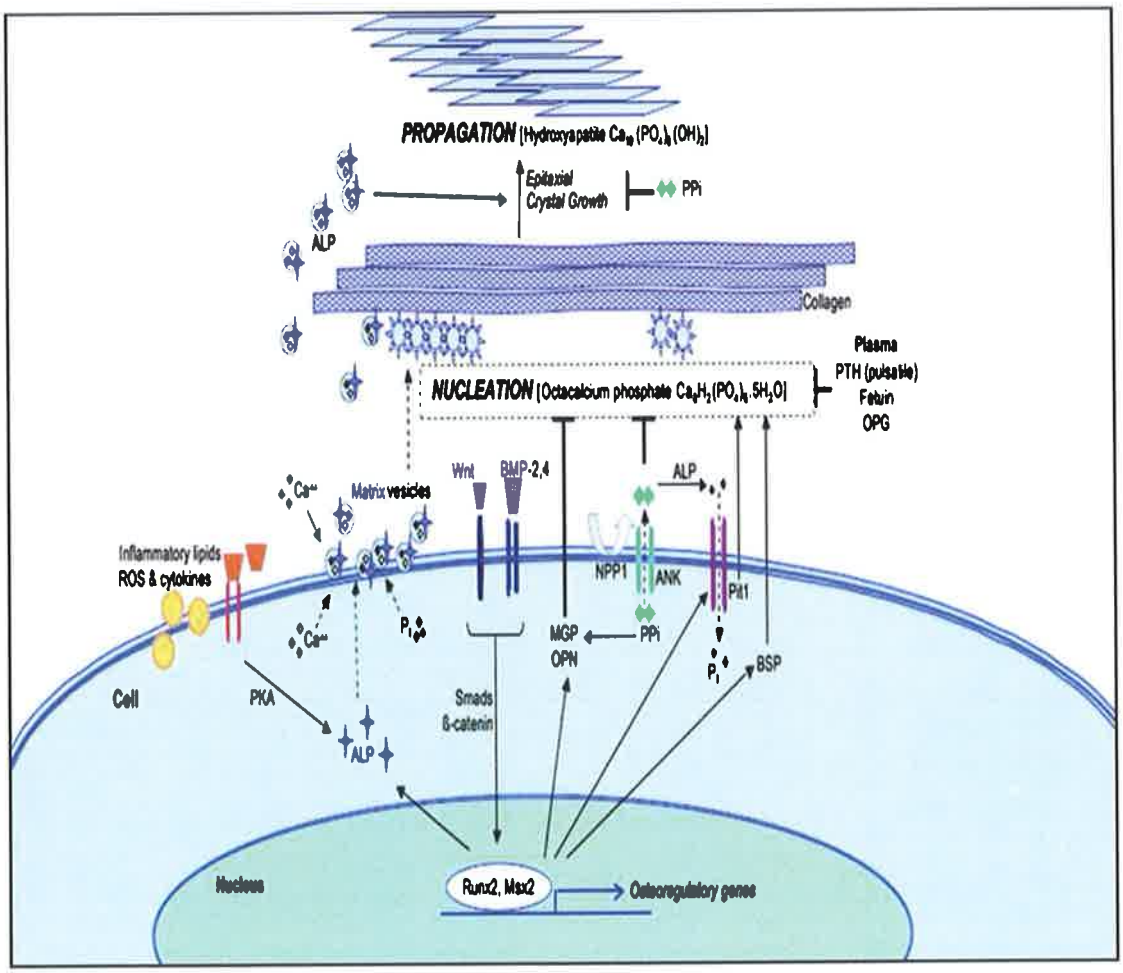

Figure 1.6. Schematic representation of the regulatory systems involved in the control of hydroxyapitite nucleation and propagation. ALP, alkaline phosphatase; BMP, bone morphogenetic protein; BSP, bone sialoprotein; Ca, calcium; MGP, matrix gla protein; NPP1, ectonucleotide pyrophosphatase-phosphodiesterease 1; OCN, osteocalcin; OPN, osteopontin; Pi, phosphate; Pit1, sodium-dependent phosphate transporter; PKA, protein kinase a; PPi, inorganic pyroposphate; PTH, parathyroid hormone; ROS, reactive oxygen species; Wnt, wingless-related integration site. Adapted and reproduced with permission from Demer et al. [24]

At the macroscopic levels, there are two pathways by which osteoblasts can organise to lay down bone. These are known as membranous and enchondral ossification, and both have been described in VC.

1.6.5.1.1. Membranous Ossification

This form of ossification is utilized in the formation of flat bones such as those found in the skull, the clavicle, and the mandible. Mesenchymal cells begin the process by laying down a sheet of dense fibrous tissue. Osteoprogenitor cells differentiate into osteoblasts throughout this tissue, and these cells begin to produce bone matrix. Activation of this form of ossification characteristically involves upregulation of the Msx2 transcription factor [91,92].

1.6.5.1.2. Enchondral Ossification

This form of ossification is utilized in the formation of the majority of bones in the human body. In this process, a dense mass of fibrous connective tissue forms the template for the final bone. Instead of immediate mineralization by osteoblasts, this process instead involves the replacement of the fibrous tissue by hyaline cartilage, secreted by chondroblasts. This hyaline cartilage is then penetrated by blood vessels, osteoclasts, and osteoprogenitor cells which differentiate into osteoblasts. The transcription factor characteristically associated with this form of ossification is Runx2 [93].

1.6.5.2. Osteogenic Cells Within the Vasculature

The process of ossification, as described above, is clearly dependent on the activation and function of the osteoblast. Indeed, at least in part, the decreasing number and reduced function of osteoblasts with advancing age that underlies the increasing incidence of osteoporosis in the elderly [94]. The critical importance of the osteoblast to skeletal ossification underscores the importance of the observation that most forms of

VC appear to involve a vascular cell lineage undergoing differentiation into a cell with an osteoblastic phenotype, and while a number of groups have demonstrated osteoblastic activity arising from harvested vascular tissue, the cell populations responsible for this activity remain an area of contention within this field of research [24]. Cell lineages which have been implicated as potential sources of osteoblastic activity include mature VSMCs from the medial layer, mural pericytes, myofibroblasts, and pericyte-like calcifying vascular cells (CVCs). Each of these cell populations have been isolated from vascular tissue and have individually demonstrated osteoblastic activity in culture. The last three lineages are somewhat pluripotential in that they can also differentiate down chondrogenic, leiomyogenic and stromogenic lines if stimulated appropriately (figure 1.7) [24,50,53,95-97]. Ultimately, osteoblastic cells within the vasculature may arise from VSMCs transdifferenting directly into an osteogenic phenotype, or dedifferentiating towards a pluripotential cell lineage, or they may arise from pericyte and myofibroblast cell populations, in turn arising from the osteochondrogenic differentiation of mesenchymal stem cells or from marrow cells migrating into the vasculature. These possiblities are not mutually exclusive, and the concept that more than one cell lineage may promtoe osteoblastic activity within the vascualture has previously been hypothesized by Towler *et al.* Additional research will be necessary to fully characterize the relationships between each of these cell lineages, and their respective relevance to the development of VC. It is noteworthy, however, that of the cell lineages mentinoed, VSMCs, as an extremely populous cell type within the vasculature, are well-positioned to contribute to the extensive, systemic VC that affects the medial layer of the vasculature. Furthermore, this cell type has a particularly strong evidence base regarding osteoblastic transformative potential (as demonstrated elegantly by Speer *et al.*, figure 1.8). As such, this cell population are of particular interest to VC in T2DM, and is the lineage of interest in the present thesis. Finally, it should also be noted that in addition to osteoblast-like cells, cells that display

markers of osteoclastic function have also been identified within advanced atherosclerotic plaques [98]. Characterization of this cell population has been limited to date, however, and their relevance to VC remains unclear.

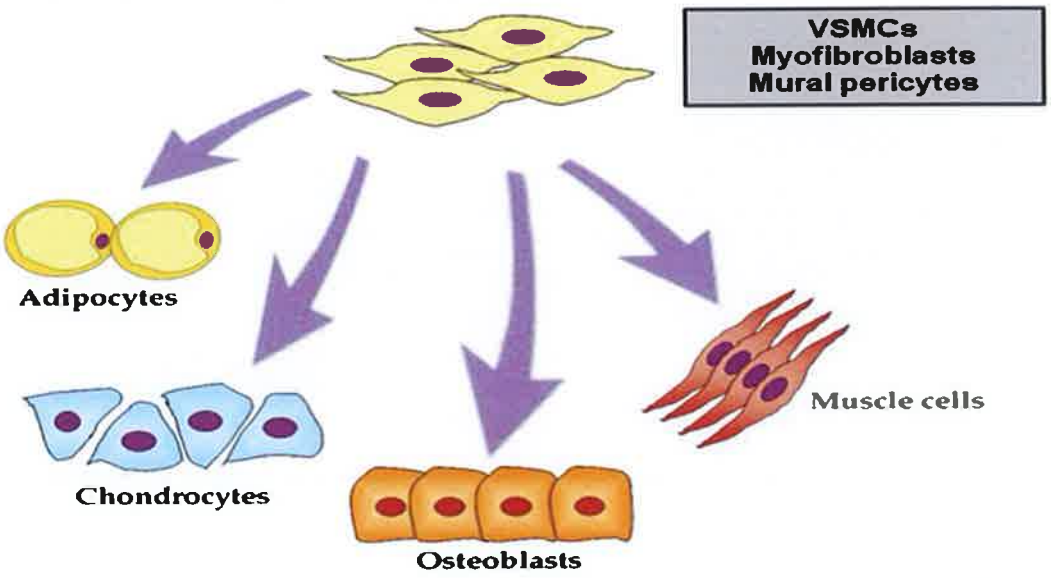

Figure 1.7. Pathways of differentiation demonstrated by the CVC sub-population of VSMCs, myofibroblasts, and mural pericytes. Adapted and reproduced with permission from Meregalli *et al.* [99].

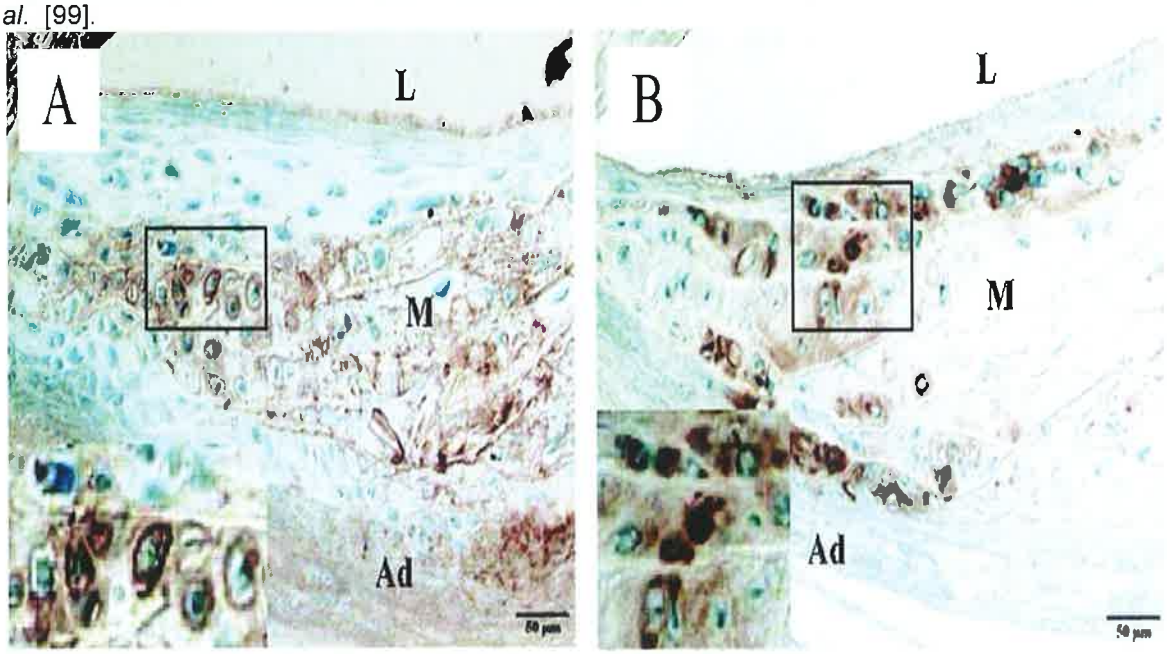

Figure 1.8. Sections of aorta from MGP knockout mice (develop severe VC at an early age) who were marked with transgenes to induce β-galactosidase expression in VSMCs. A: section was statined for β-galactosidase (blue) and osteopontin (brown), a marker of osteoblastic activity. B: section was stained for β-galactosidase (blue) and type 2 collage (brown), a marker of chondroblastic activity. Insets display higher-power magnification of the boxed areas to illustrate co-localization of SMC and osteo/chondroblastic markers. Ad, adventitia; L, lumen; M, media; MGP, matric gla protein; SMC, smooth muscle cell, VSMC, vascular smooth muscle cell. Adapted and reproduced with permission from Speer *et al.* [100].

1.6.5.3. Pathogenesis of Intimal Calcification

Intimal calcification, as noted previously, is predominantly found in association with atherosclerotic disease, and as such is the dominant form of VC in the coronary arteries, the aorta and the carotlds. The commonest vascular bed to be affected is the aorta [46,101]. The zones of calcification that characterize this subtype are typically patchy in nature, co-localizing with areas of plaque within the intima of the vessel wall, but may become confluent if particularly severe or chronic [58,102,103].

Within zones of intimal calcification, three specific forms of calcium deposition have been described. The first two are somewhat similar, involving amorphous calcium deposition within the lipid core of the plaque and amorphous deposition within the fibrous areas of the plaque. Typically, these forms do not progress to organized bone formation, instead forming amorphic granules or plates of calcium crystals. The third form involves complete enchondral ossification, including a chondrogenic stage during which cartilage is formed within the vascular wall, followed by ossification of this cartilaginous template [24,101]. It has been hypothesized that the first two forms of intimal calcification arise from apoptotic VSMCs undergoing partial transformation into osteoblast-like cells, supporting initial calcium nucleation and propagation. With regards to enchondral ossification within the intima, however, it is mural pericytes that have been implicated as the main cell population to undergo osteoblastic transformation (although VSMCs may be involved to a lesser degree, given the relative proximity of the tunica media) [52,92].

As an enchondral ossification process, intimal calcification is primarily a Runx2-driven process induced by BMP signaling, although upregulation of Msx2 signaling has also been reported [92]. A number of different processes are thought to induce osteoblastic transformation of pericytes (and/or VSMCs) and subsequent intimal calcification [24,25,28,92]. Atherosclerotic plaques, in particular, typically contain high

concentrations of inflammatory mediators such as tumor necrosis factor alpha (TNF-α), and ROS. TNF-α has been shown to increase BMP-2 production by VSMCs in culture, along with up-regulating BMP-2, Wnt and Msx2 activity in murine studies of aortic calcification [97,104]. ROS are known to act directly on VSMCs, increasing both ALP activity and decreasing levels of PPI, while also promoting calcification indirectly by inducing BMP-2 and BMP-4 production by ECs and macrophages (figure 1.9) [25,105]. Finally, the local hemodynamic effects of the atherosclerotic plaque may also be relevant to the development of intimal calcification, as hypoxia and turbulent blood flow have both been reported to increase BMP-2 production by the EC monolayer [106]. With the above in mind, therefore, it is unsurprising that intimal calcificaiton demonstrates strong epidemiological associations with dyslipidemia and hypertension [25,107-109].

1.6.5.4. Pathogenesis of Medial Calcification and the role of T2DM

1.6.5.4.1. Overview

The characteristic picture of medial arterial calcification is that of extensive calcification of medium sized arteries, affecting the entire circumference of vessels and extending in a confluent manner along these vascular beds. Severe medial arterial calcification, on plain film radiography, appears as two long, straight lines of calcification, occasionally termed 'railroad tracks' [92].

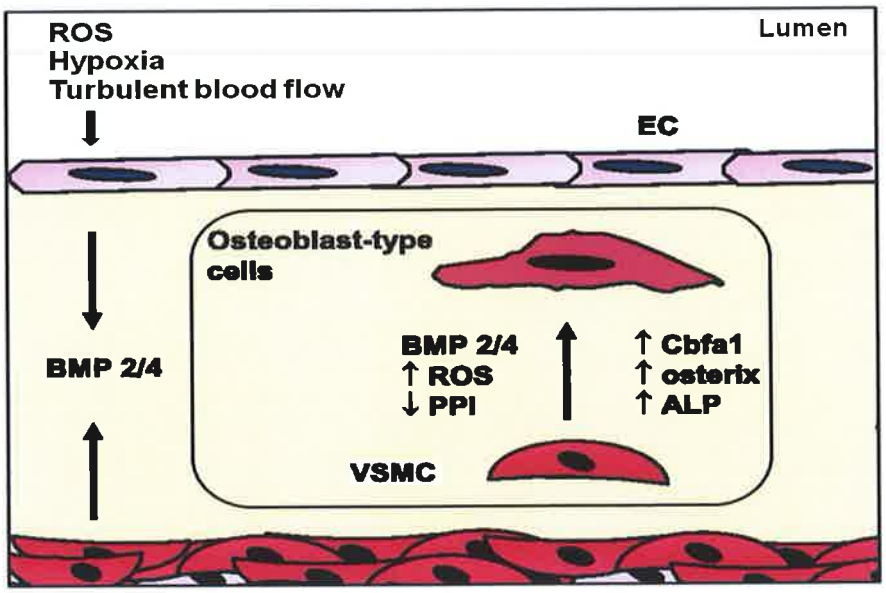

Figure 1.9. Schematic representation of local factors involved in intimal calcification. ROS, hypoxia and turbulent blood flow act on the endothelial monolayer to increase production of BMP proteins, which may also be produced by VSMCs when exposed to mediators such as TNF-α. Insert illustrates ROS and BMP proteins acting on a VSMC to induce differentiation into an osteoblast-like cell, with increased expression of osteoblastic markers. ALP; alkaline phosphatase, BMP-2/4; bone morphogenetic protein 2/4, Cbfa1; core-binding factor subunit alpha-1, EC; endothelial cell, PPi, inorganic pyrophoshate; ROS; reactive oxygen species, VSMC; vascular smooth muscle cell. Adapted and reproduced with permission from Johnson *et al.* [25].

In many ways, medial arterial calcification can best be considered by contrasting it's typical features against those of intimal calcification. Both subtypes share many of the same risk factors, involve a process of regulated ossification, and can co-exist in the same vascular bed. Nonetheless, significant differences exist between the two pathologies. Intimal calcification, as previously discussed, is a focal process, primarily promoted by the local effects of atherosclerotic plaques. Medial calcification is far more diffuse, with systemic processes (dyslipidemia, inflammation, hyperphosphatemia etc) acting directly on the adventitial and medial layers of multiple vascular beds [92]. Accordingly, medial arterial calcification characteristically occurs in the presence of conditions such as T2DM and ESRF; systemic conditions with increased circulating concentrations of various promoters of calcification that act on entire vascular beds at the same time. Indeed, while intimal arterial calcification increases with age due to increased atherosclerotic plaque, increased medial calcification in the elderly is thought

to be due, at least in part, to the general impairments in metabolism and renal function that accompany aging [36].

1.6.5.4.2. Cellular Features and Promoters

Whereas intimal calcification is characteristically associated, by nature of its location and underlying pathophysiology, with dysfunction of the endothelial layer and expansion of the intima, medial arterial calcification is instead associated with dysfunction originating within the tunica adventitia. As discussed by Towler *et al.* in their seminal review of medial calcification (figure 1.10), this external layer of the arterial wall, with its own circulatory system (the vasa vasorum), contains myofibroblast cells that are capable of orchestrating an osteogenic process within the tunica media. These myofibroblasts can be seen to express Msx2 in response to various pro-calcifying stimuli. This in turn leads to activation of the Wnt signaling pathway in VSMCs within the tunica media via paracrine signaling through the vasa vasorum [15,92]. As would be expected from an Msx2-driven process, the ossification seen in medial calcification is membranous in nature.

In terms of promoters of medial arterial calcification, inflammatory mediators appear to be an important final common pathway for a number of conditions that have been associated with this calcification subtype. T2DM, obesity and dyslipidemia, all high-risk states for calcification, are similar in that they typically generate a pro-inflammatory state, which has been shown to extend to inflammation within the adentitial layer [110,111]. Furthermore, TNF-α, the archetypal pro-inflammatory cytokine, has been shown to activate Msx2-Wnt pathways in murine models, as well as inducing osteogenic responses in VSMC populations [112,113]. The precise signaling pathways between TNF-α and increased expression of Msx2 within the tunica adventitia, however, have yet to be fully characterized. In addition to inflammation, there are a

number of other systemic inducers of medial calcification. These include vitamin D intoxication, warfarin therapy, the various components of ESRF, and T2DM [25,60].

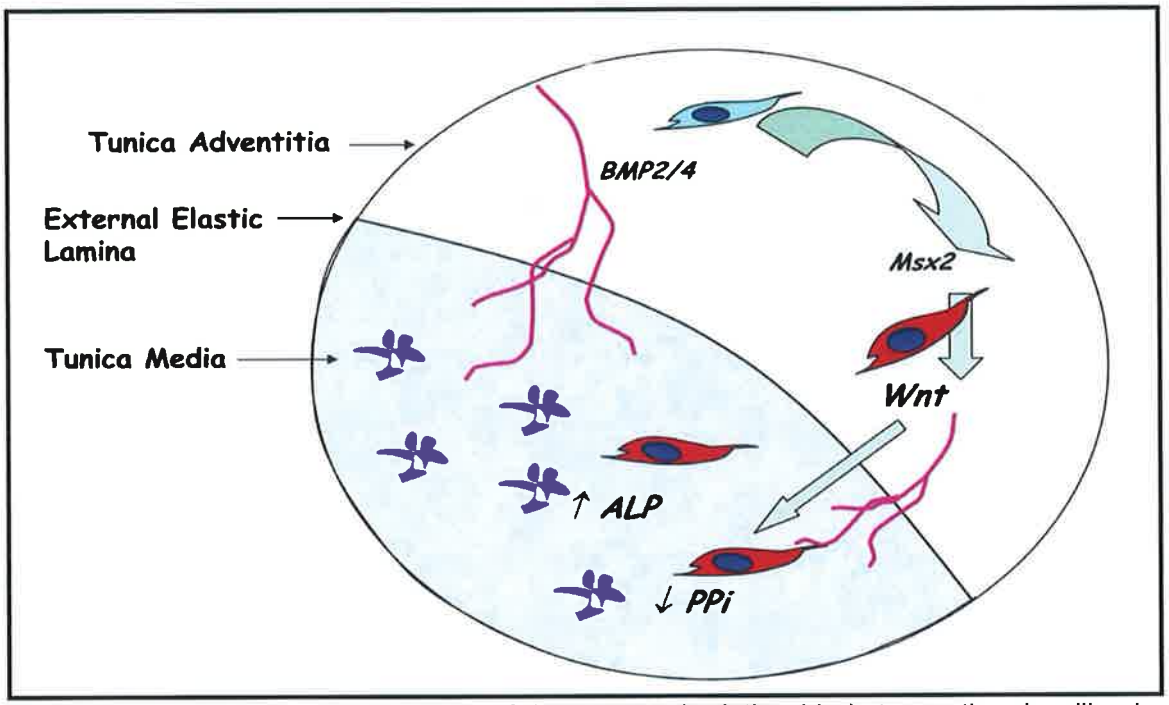

Figure 1.10. Schematic representation of the proposed relationship between the signalling in the adventitial layer and medial arterial calcification. Myofibroblasts (blue cells) in the adventitia express Msx2 in response to stimulation by BMP2/4 through the vasa vasorum (pink vessels), and activate the Wnt signalling pathway in smooth muscle cells (red cells), resulting in increased ALP, decreased PPi, and increased deposition of calcium crystals (purple). ALP, alkaline phosphatase; BMP-2/4, bone morphogenetic protein 2/4; Msx2, msh homeobox 2; PPi, inorganic pyrophosphate; Wnt, wingless-related integration site. Adapted and reproduced with permission from Towler *et al.* [92]

As noted previously, T2DM is a significant risk factor for the development of VC, predominantly medial, but the condition also increases the risk of intimal and valvular [43,62,92]. At least part of this relationship is likely due to the pro-inflammatory state that is characteristic of T2DM from an early stage. In addition to inflammation, however, both hyperglycemia and hyperinsulinemia have also been implicated as promoters of VC. With regards to hyperglycemia, a complex association between raised glucose levels, OPN expression, and calcification is currently under investigation by a number of groups [92]. As noted previously, intact OPN functions as an inhibitor of calcification. Once cleaved, however this protein appears to exert diametrically opposite effects, and has been demonstrated to induce differentiation down osteogenic pathways, along with increasing inflammation [114]. It has been suggested that as hyperglycemia increases

the production of pro-calcifying, cleaved OPN, it simultaneously diminishes the inhibitory actions of whole OPN [92]. Finally, while T2DM can be described as a state of relative deficiency in the actions of insulin, the actual circulating concentrations of insulin are frequently high, at least early in the disease process, in an effort to overcome peripheral insulin resistance [115]. Furthermore, as T2DM progresses over time, insulin analogue therapy may be initiated, which in turn may produce circulating levels in excess of the physiological range. These observations are of relevance to VC as insulin, when administered to VSMCs, has been reported to induce osteoblastic transformation and osteogenic activity [39,41]. Insulin is also known to decrease the production of OPG by vascular cell populations, and to reduce circulating OPG concentrations in patients with type 1 diabetes mellitus (T1DM) and T2DM [21,116,117]. It has been hypothesized, therefore, that insulin excess may contribute to the high prevalence of calcification in T2DM. This theory is discussed in greater detail in section 1.8.2, and is tested in the present thesis.

1.6.5.5. Pathogenesis of Valvular Calcification

Calcification of the aortic valve is by far the commonest form of valvular calcification [118]. The pathways driving aortic valve calcification share similarities with both the intimal and medial VC. BMP expression has been noted within calcified valve leaflets, along with upregulation of both Runx2 and Msx2, with activation of the Wnt signaling cascade appearing to be of particular importance in this form of VC [119] [120]. With regards to osteoblast activity, Mohler *et al.* have previously isolated a population of myofibroblasts from calcified aortic valves that undergo osteoblastic transformation, expressing the osteogenic signals noted above, producing ALP, and promoting ossification in culture [64].

In terms of promoters of valvular calcification, the MESA study has reported that T2DM, abdominal obesity, hypertension and dyslipidemia are major risk factors [62]. There

are, however, two specific promoters of aortic valve calcification worthy of note. The first is the excessive levels of mechanical stress that bicuspid valves are subjected to, which may induce endothelial dysfunction, BMP expression, and the aforementioned elastin degradation [121]. The second appears to be the presence of the bicuspid valve. As well as giving rise to pathological levels of mechanical stress, it appears that the major mutation underlying this congenital abnormality, NOTCH1, is also associated with inadequate suppression of Runx2. It is unsurprising, therefore, that patients with bicuspid aortic valves almost uniformly develop significant valvular calcification by the age of 30 [122].

1.6.5.6. Pathogenesis of VC in ESRF

VC in ESRF is often considered separately to other forms of VC due to its severity and the unique hormonal imbalances that drive calcification in this condition. It is perhaps best viewed as the addition of dysregulated hormonal/calcium/phosphate metabolism to pre-existing intimal, medial, and valvular calcification warfarin [47,48,123-125]. In essence, because many of the risk factors for renal disease are the same as those for the various subtypes of VC, the majority of patients who develop renal failure are likely to have pre-existing calcifying processes. With worsening renal failure comes a state of severe phosphate, calcium, vitamin D and parathyroid hormone (PTH) dysregulation, accelerating these pre-existing calcification processes [126].The relevance of OPG, RANKL and TRAIL to this environment is at present, unclear [124,127].

1.6.6. Inhibiting VC

Over the past 10-20 years, multiple groups have adopted a variety of different approaches in an attempt to reduce calcification burden in various patient populations. These approaches are summarized in table 1.5, and have, in the majority of cases, been disappointing in terms of producing any clear, significant reduction in VC. As a general summary, many of the large trials that aimed to inhibit VC in humans have

taken place in the ESRF population, somewhat unsurprising given the severe nature of calcification in these patients. Even in this population, however, the evidence is limited, and no coherent strategy for reducing calcification burden has been developed to date. In the general population, statins and bisphosphonates have received the greatest interest, but have failed to produce significant reductions in the progression of calcification despite the use of high doses, high risk populations, and long follow-up periods. With relevance to the present thesis, a recent review of this topic concluded that greater understanding of the regulatory mechanisms for VC is needed for successful calcification inhibitors to be designed [128].

1.6.7. Summary

It is evident, on reviewing the various clinical and pathological features of VC, that this is a heterogeneous process, driven and controlled by a wide variety of interlinked promoters and inhibitors at the systemic and cellular level, and that the clinical relevance of VC varies depending on extent and location. What is clear, however, is that VC is not a benign process, and it remains noteworthy that any degree of calcification, on any imaging modality, is associated with an increased risk of CVD. While the pathophysiology of VC is complex, the transformation of vascular cell populations into osteoblast-like cells has been a recurring theme in the studies performed on the major subtypes of this process. Numerous interventions designed to inhibit the progression of calcification have been studied, but none have demonstrated consistently beneficial results. It is in this setting that research has focused, in recent years, on characterizing the regulatory mechanisms controlling osteoblastic transformation in the hope of arresting this process, and it is in this setting that a growing interest has arisen in the activities of OPG, RANKL and TRAIL within the vascular wall.

Table 1.5. Therapies under investigation for the inhibition/reversal of VC.

Therapy	*Mode of action*	*Results*	*References*
Osteoporosis therapies			
Bisphosphonates	Prevents calcium and phosphate release from bone, inhibits crystal nucleation and propagation.	Conflicting data in human studies.	[129]
Osteoprotegerin	Unclear, potentially prevents transformation of SMCs into osteoblast-like cells via blockade of RANKL and TRAIL	Decreased aortic calcification with denosumab (monoclonal antibody that mimics OPG) in murine studies. No prospective, randomized human studies to date.	[130]
Teriparatide	Upregulates circulating concentrations of OPN, a calcification inhibitor.	Decreased valve calcification in murine studies.	[131]
ESRF therapies			
Phosphate binders	Decreases circulating concentrations of phosphate.	Conflicting data, but favoring reduced progression of calcification with non-calcium based phosphate binders.	[132]
Calcimimetics	Lower circulating calcium levels.	Reduced progression of calcification in one randomized trial in ESRF, reduced mortality in murine models.	[133]
Vitamin K	Upregulates production of MGP.	Non-significant decrease in CAC in 1 interventional study to date.	[134]

CAC, coronary artery calcification; ESRF, end-stage renal failure; HMG-CoA, 3-hydroxy-3-methyl-glutaryl-CoA; MGP, matrix gla-protein; OPN, osteopontin; OPG, osteoprotegerin; RANKL, receptor activator of nuclear factor kappa-beta ligand; SMC, smooth muscle cell; TRAIL, tumor necrosis factor-related apoptosis-inducing ligand; VC, vascular calcification.

Table 1.5 Therapies under investigation for the inhibition/reversal of VC.

Therapy	*Mode of action*	*Results*	*References*
ESRF therapies (continued)			
Sodium thiosulphate	Chelates calcium, reduces inflammation.	Recognized treatment for calciphylaxis in humans. Uncertain if benefit for other forms of calcification.	[135]
CV disease therapies			
Endothelin receptor antagonists	Hypertension is a risk factor for VC.	Significant reduction in VC in murine studies.	[136]
Statins	Dyslipidemia and inflammation are both risk factors for VC.	Inconsistent results in human trials to date	[137]

CAC, coronary artery calcification; ESRF, end-stage renal failure; HMG-CoA, 3-hydroxy-3-methyl-glutaryl-CoA; MGP, matrix gla-protein; OPN, osteopontin; OPG, osteoprotegerin; RANKL, receptor activator of nuclear factor kappa-beta ligand; SMC, smooth muscle cell; TRAIL, tumor necrosis factor-related apoptosis-inducing ligand; VC, vascular calcification.

1.7. OPG, RANKL and TRAIL

1.7.1. Introduction

OPG, RANKL and TRAIL have been identified in multiple tissue types throughout the body, and OPG's ability to block RANKL and/or TRAIL signaling has been implicated in processes as varied as tumor growth, bone turnover, immune system regulation, rheumatoid arthritis and, of course, VC. The following sections will review the interactions of all three of these proteins, and the evidence base behind a role for this system in VC, and will conclude with an iteration of the main areas of uncertainty regarding OPG/RANKL/TRAIL and VC addressed by the present thesis.

1.7.2. OPG - Overview

OPG, a molecule first discovered in 1997 simultaneously by two separate groups, is a soluble receptor that is secreted by numerous cell types into various microenvironments (e.g. bone) as well as into the circulation [30,116,138-141]. OPG is a glycoprotein, a member of the TNF receptor superfamily, coded for on chromosome 8q, and is initially formed as a 401 amino acid molecule prior to the cleaving off of 21 amino acids, producing the active 380 amino acid form (figure 1.11). Dimerization, when it occurs, does so at the heparin-binding site [139,142].

In its final, soluble form, OPG may bind to, and form stable complexes with, either RANKL or TRAIL [29,141,142]. More recently, it has emerged that OPG is also capable of binding to von Willebrand factor (vWF) [143,144].Cell lineages that produce and secrete OPG include osteoblasts, B lymphocytes, ECs and SMCs, the placenta, the lungs, the thymus gland and the kidneys [145].

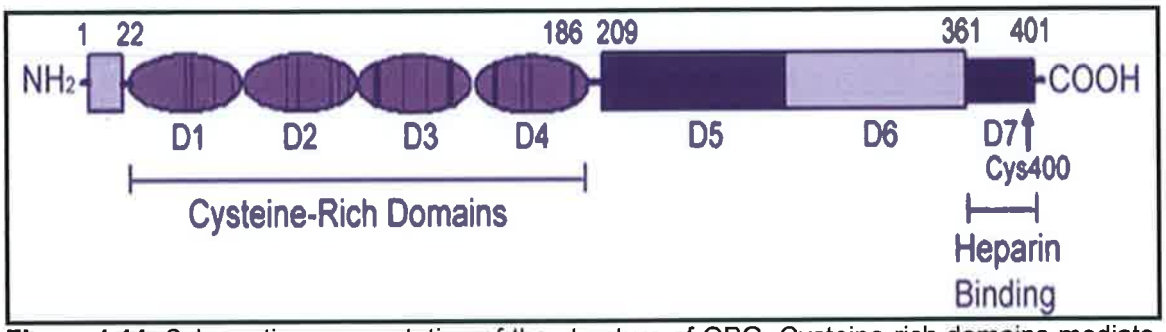

Figure 1.11. Schematic representation of the structure of OPG. Cysteine-rich domains mediate binding to RANKL. D5 and D6 are death domain homologous regions. NH_2 indicates amino-terminus. COOH indicates carboxy-terminus. Adapted and reproduced with permission from Corallini *et al.* [146].

1.7.3. RANKL and RANK - Overview

The identification of RANK on the surface of dendritic cells led to the isolation of its active ligand RANKL via direct expression screening [147-150]. RANK is a member of the TNF-receptor superfamily that exists on cell surfaces as a 616 amino acid homotrimeric transmembrane protein. It is coded for on chromosome 18q [147]. RANK is classically expressed on the surface of cells derived from a monocyte or macrophage lineage, (e.g. osteoclasts), but in addition to bone, it has also been identified within the immune system (thymus) the liver, colon, skeletal muscle, various endocrine organs and, once again, the vasculature (ECs and SMCs). RANKL is a 316 amino acid homotrimeric protein (figure 1.12) that may exist as a transmembrane protein or in a soluble form (sRANKL) if actively secreted (e.g. by T-cells) or cleaved from the cell surface by certain matrix metallopeptidases [151,152]. It has previously been shown that there are three isoforms of this protein. RANKL1 is the classic transmembrane form of the protein. RANKL3 is the soluble form of the protein. RANKL2 is also a transmembrane protein, but is much shorter than RANKL1 and appears to function differently to the other two isoforms. Whereas RANKL1 and RANKL3 have both been shown to induce osteoclastogenesis and osteoclast activation, RANKL2 may have an reduced or even opposite effect. RANKL is coded for on chromosome 13q [153]. RANKL has been identified in bone, lymphoid tissues, the

lungs, and the vasculature [145]. The precise origin of RANKL in the vasculature is an area of some debate.

With regards to RANKL binding to OPG, there is a strong affinity (23 nM at physiological temperatures) for homodimers of OPG to form stable complexes with homotrimers of RANKL. With regards to RANKL binding to RANK, the affinity is of a similar order of magnitude [29].

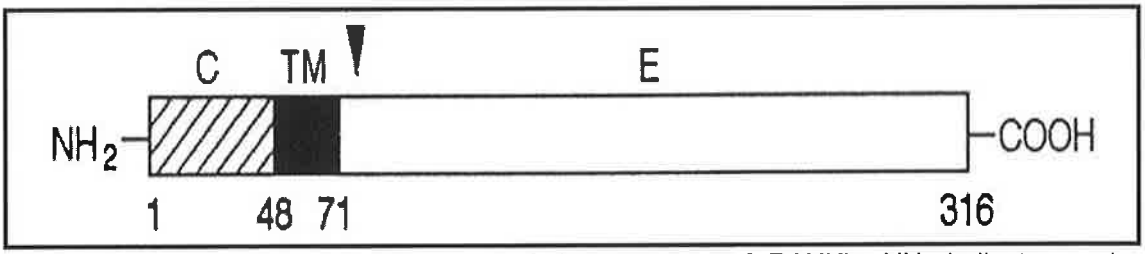

Figure 1.12. Schematic representation of the structure of RANKL. NH_2 indicates amino-terminus. COOH indicates carboxy-terminus. C, cytoplasmic; E, extracellular; TM, trans-membrane. Adapted and reproduced with permission from Yasuda *et al* [148]

1.7.4. TRAIL - Overview

TRAIL was discovered in 1995 [154], and is a 281 amino acid protein that may exist as a transmembrane protein or in soluble, circulating form, and is also a member of the TNF family (figure 1.13). TRAIL is secreted by multiple tissue types, including the immune system, the lungs, the prostate, the spleen, and the vasculature. As with RANKL, the precise origin of TRAIL within the vascular wall has not been fully defined. TRAIL is coded for on chromosome 3q.

TRAIL can bind to any 1 of 4 cell surface receptors or OPG itself. The cell surface receptors may be found on multiple cell lineages throughout the body. Two of these receptors are death domains 4 and 5 (DR4 and DR5), and the binding of TRAIL to these receptors upregulates apoptotic signaling pathways [155]. The third and fourth receptors are termed decoy receptors 1 and 2 (DcR1 and DcR2), however, and appear to oppose the apoptosis-inducing actions of TRAIL. Not only do these receptors act as alternative binding sites for TRAIL molecules, they also lead to activation of the NF-κB

pathway, which acts to inhibit apoptosis signaling from DR4 and DR5 binding [156-158]. It has been hypothesized that differential expression of these receptors may account for the varying effects of TRAIL reported in the medical literature to date [159]. Depending on the tissue types under examination, and whether the cells were under basal or injurious conditions, both pro- and anti-apoptotic effects have been demonstrated [160,161].

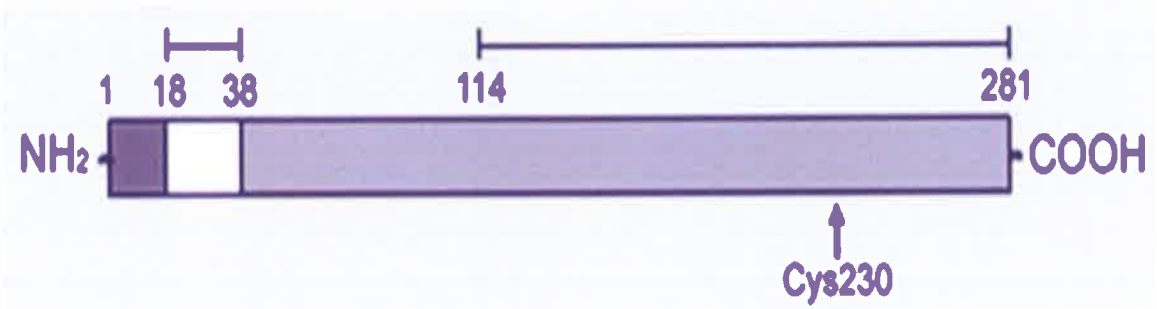

Figure 1.13. Schematic representation of the structure of TRAIL. Regions 1-18 correspond to the cytoplasmic region, resions 18-38 correspond to the trans-membrane region, and regions 114-281 correspond to the receptor binding region. NH_2 indicates amino-terminus. COOH indicates carboxy-terminus. Adapted and reproduced with permission from Di Lasio *et al.* [162]

OPG, at concentrations of 25 ng/ml or higher, has been shown to block TRAIL binding to DR4. With regards to OPG binding to TRAIL, a relatively strong affinity of 45 nM has been reported between these molecules. Finally, it should be noted that if OPG, TRAIL and RANKL are present in the same environment, OPG has roughly similar affinities for either TRAIL or RANKL and may therefore bind either one, with a preference for whichever molecule is present in greater concentration (figure 1.14) [29]. Thus, the interlinked nature of OPG, RANKL and TRAIL cannot be over-emphasized, and the failure to take these interactions into account may explain some of the discrepancies seen in the literature on OPG and its ligands to date.

1.7.5. vWF and OPG

In recent years, it has been reported that OPG and vWF co-locate in compartments within Weibel-Palade bodies (WPB) in ECs [144]. VWF is involved in clotting function and, in particular, platelet adhesion, and is released as part of the acute response to

inflammatory and thrombogenic insults [163]. OPG also appears to be released as part of this response, and in 2005, Zannettino *et al.* reported that OPG and vWF formed complexes within the WPBs, and that these complexes could also be identified in the circulation [144]. A separate group have since reported that vWF can bind to OPG, RANKL and TRAIL [143]. Interestingly, the authors of this study reported that once OPG had bound to vWF (in a complex with clotting factor VII), the ability of the resultant complex to inhibit RANKL binding to RANK was greater than that of OPG alone. On the other hand, binding of the vWF-clotting factor VII complex to OPG reduced the ability of OPG to bind to TRAIL. Thus, vWF may represent an additional modulator of interactions between OPG/RANKL/TRAIL.

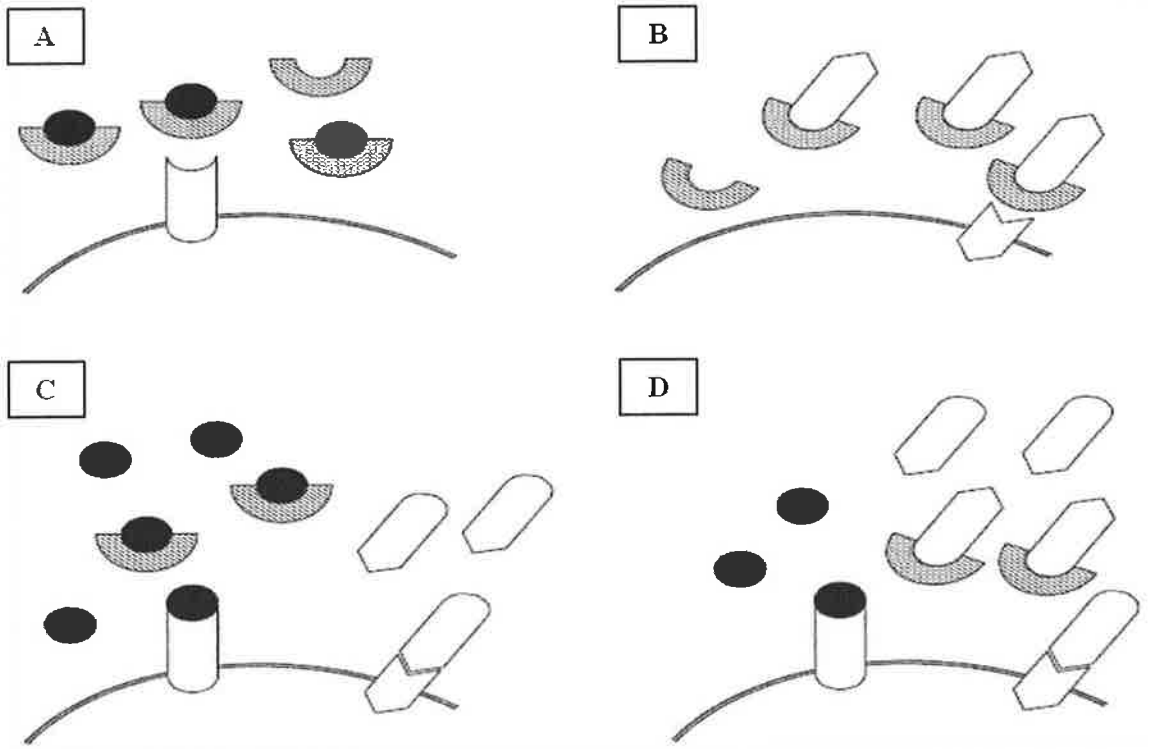

Figure 1.14. The interlinked nature of OPG, RANKL and TRAIL. A: OPG molecules (grey semicircles) are present in greater amounts than RANKL molecules (black circles), and have bound all available RANKL. B: OPG molecules are present in greater amounts than TRAIL molecules (clear elongated boxes with triangulated and convex ends), and have bound all available TRAIL. C: RANKL molecules are present in greater amounts than OPG molecules. Excess RANKL molecules are able to bind to their receptor, and there are no OPG molecules available to prevent TRAIL molecules binding to their receptor. D: TRAIL molecules are present in greater amounts than OPG molecules. Excess TRAIL molecules are able to bind to their receptors, and there are no OPG molecules available to prevent RANKL molecules binding to their receptors. OPG, osteoprotegerin; RANKL, receptor activator of nuclear factor kappa-beta ligand; TRAIL, tumor necrosis factor-related apoptosis-inducing ligand.

1.7.6. OPG - a Promoter of Bone Formation and Calcification in the Skeleton

It is in the skeleton that the interaction between OPG and RANKL has been characterized in greatest detail, and has progressed all the way from *in vitro* work to the emergence of a licensed treatment for osteoporosis in humans [164]. Indeed, the importance of OPG and RANKL to bone turnover was evident in the earliest murine models, where over-expression of OPG led to the development of osteopetrosis, whereas knockout models developed early and severe osteoporosis [31]. In keeping with these findings, the loss of RANKL led to osteopetrosis, whereas the administration of RANKL caused osteoporosis [165,166].

At the cellular level, both OPG and RANKL are produced by osteoblasts within the skeleton. OPG is produced and secreted in soluble form, whereas RANKL is produced as a transmembrane protein and in soluble form. The differential production of OPG or RANKL has been hypothesized to be an important pathway by which osteoblasts control bone turnover [152,166]. With regards to osteoclast maturation and activation, the signaling pathways activated by RANKL binding to RANK on osteoclasts are detailed in figure 1.15. In essence, binding of RANKL to RANK leads to tumor necrosis factor receptor associated factors (TRAFs) translocating within the cell and becoming associated with the RANK receptor [167]. Of the TRAF proteins which translocate, it is TRAF6 that appears most relevant to osteoclastogeneis, and has been shown to activate NF-KB, leading to its translocation to the nucleus. This increases the expression of c-Fos, which in turn upregulates the expression of NFATc1 (nuclear factor of activated T-cells, cytoplasmic 1), the master gene responsible for osteoclast maturation and activation [168,169].

In addition to illuminating various critical aspects of bone physiology, characterization of the OPG/RANKL system in bone in this fashion has also led to the emergence of a

new treatment for osteoporosis. Denosumab is a monoclonal antibody that binds to and inactivates RANKL in a manner similar to that of OPG, but does not bind TRAIL [170]. Delivered in injectable form, this novel medication favors bone formation, and has improved bone mineral density in populations such as post-menopausal women and men receiving hormone ablation therapy for prostate cancer [164].

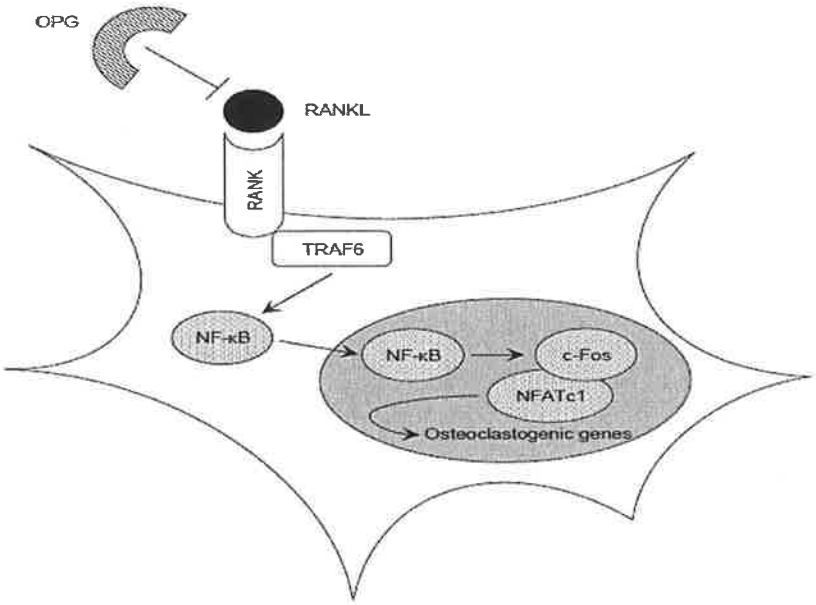

Figure 1.15. The essential signaling pathway for normal osteoclastogenesis. RANKL binds to RANK on the surface of the osteoclast precursor cell and recruits the adaptor protein TRAF6, leading to NF-κβ activation and translocation to the nucleus. NF-κβ increases c-Fos expression and c-Fos interacts with NFATc1 to trigger the transcription of osteoclastogenic genes. OPG, if present, blocks the binding of RANKL to RANK and prevents this process. NFATc1, nuclear factor of activated T cells, cytoplasmic 1; NF-κβ, nuclear factor kappa beta; OPG, osteoprotegerin; RANKL, receptor activator of nuclear factor kappa beta-ligand; TRAF, tumor necrosis factor receptor associated factor.

1.7.7. OPG - an Inhibitor of Bone Formation and Calcification in the Vasculature

1.7.7.1. Overview

In contrast to its actions in bone, the role of OPG (and by extension RANKL and TRAIL) within the vasculature remains, in many ways, unclear. As previously noted, OPG is a promoter of bone formation and calcification within the skeleton. With regards to VC, it has been demonstrated that OPG is produced and secreted in large quantities (similar concentrations to those found in bone) by SMCs, and a number of groups have

reported increased secretion of OPG by these cells when exposed to promoters of calcification such as inflammation. Furthermore, on histological examination of arterial specimens OPG has been shown to associate with areas of calcification [171]. Finally, a wealth of epidemiological data has demonstrated a clear positive correlation between circulating concentrations of OPG and the presence and extent of both VC and CVD risk [172,173]. With all of these observations in mind, it is unsurprising that early suppositions regarding OPG were that it promoted VC in a manner similar to its activities in bone. *A significant body of evidence, however, contradicts this hypothesis, and instead of promoting VC, it is now proposed by most groups within the field that OPG acts as an inhibitor of ossification and calcification within the vascular wall, and that increased OPG production within the setting of calcification represents an attempt to inhibit this process, not promote it* [15,16,34-36]. The following sections will review the evidence behind this hypothesis, as well as the potential mechanisms by which OPG could inhibit calcification within the vascular microenvironment.

1.7.7.2. OPG as an Inhibitor of VC - Animal Models

Evidence that the actions of OPG were discrepant between the bone and the vasculature was present in the earliest studies on OPG knockout mice. As previously noted, these mice developed early and severe osteoporosis, but they were also noted to develop extensive and early medial arterial calcification [31]. At the time, it was felt that this phenomenon represented a passive process of calcium and phosphate transfer from the bones to the vasculature. Since these experiments, however, the concept of VC as an active process of ossification that overcomes endogenous inhibitors of calcification (as opposed to a passive process of calcium deposition) has gained widespread acceptance [34,92]. Furthermore, OPG was identified within the vasculature of healthy mice in quantities similar to those found in bone [174]. Taken together, these observations suggested a more complex explanation for the initial findings than was originally thought. As a result, a number of experiments were

performed in which the effects of OPG on VC were studied in greater detail. To begin with, Price *et al.* administered pro-calcifying agents such as warfarin and vitamin D to rats, with or without the co-administration of OPG. They reported that rats that received OPG demonstrated significantly less VC than those that did not (figure 1.16) [33]. In keeping with these findings, Orita *et al.* administered phosphate and vitamin D to OPG knockouts and to wild type mice [175]. The knockout model, but not the wild type, developed severe medial calcification of the aorta. Furthermore, these knockouts demonstrated high levels of ALP activity in the aorta, indicating that active bone formation, as opposed to passive calcium deposition, was taking place. In terms of intimal calcification, Morony *et al.* administered recombinant OPG to atherogenic mice, and reported a decrease in the size of the calcification deposits around the atherosclerotic plaque, along with a decrease in circulating concentrations of the calcification marker osteocalcin (OCN) [32]. Bennet *et al.* adopted a different approach and generated mice that were both atherogenic and lacking in OPG, and compared them to mice that were atherogenic alone [176]. In this model, the OPG knockouts demonstrated increased calcification burden at 60 weeks. Finally, and with an additional degree of clinical relevance, some early experiments with denosumab and murine models of calcification have begun to emerge. In a 4 week experiment in which denosumab or placebo was administered to mice, Helas *et al.* reported a 50% decrease in aortic calcium deposition (measured via chemical analysis of aortic tissue) in the treatment group [130]. At present, there is only one study of denosumab on VC in humans in the literature. In this study, the authors examined the effects of denosumab on aortic calcification and reported no difference in calcification progression between placebo and the denosumab treated group. It should be noted, however, that this study was an opportunistic sub-analysis of a larger trial. Furthermore, aortic calcification was measured in a semi-quantitative manner using lateral spine x-rays, a suboptimal assessment of calcification burden [177].

Figure 1.16. Effect of osteoprotegerin on arterial calcification induced by vitamin D treatment. Calcium was stained with alizarin red. Uppermost artery: typical artery from an animal treated with vitamin D alone (carotid arteries on left). Middle artery: typical artery from an animal treated with vitamin D plus osteoprotegerin. Bottom artery: artery from an age-matched control rat. (Adapted and reproduced with permission from Price *et al.* [33]).

With the majority of the observations above supporting the hypothesis that OPG inhibits calcification in the vasculature, research has increasingly focused on elucidating the mechanisms by which OPG may accomplish this effect. As RANKL and TRAIL are the main signals blocked by OPG, studies in this area have assessed both of these proteins to determine if they have any pro-calcifying effects on vascular cells.

1.7.7.3. OPG as an Inhibitor of VC - the Actions of RANKL

While OPG has been clearly demonstrated within the vascular wall in abundant amounts, under basal and pathological conditions [34], the status of RANKL is less well defined. In general, healthy human and murine arteries express only low, or even undetectable levels of RANKL [174,178]. In atherosclerotic and calcified lesions, however, RANKL has been detected in larger quantities, typically co-localizing with inflammation, lipid deposition and, of course, areas of calcification [171,179]. The origin of RANKL in this setting is unclear, with some authors reporting that VSMCs may produce RANKL, and others suggesting that infiltrating cells of the immune system may be the source [180,181]. Of particular relevance are reports that VSMCs, a cell population capable of differentiating into osteoblast-like cells, express RANK receptors [182,183]. The presence of both OPG and RANKL within the vascular wall, along with

the expression of RANK on a cell population known to induce calcification, has led to the hypothesis that OPG inhibits VC by preventing RANKL from binding to RANK. With this in mind, a number of investigations have been conducted to test whether RANKL can induce osteoblastic and calcifying activity in VSMCs, and, if such a response occurs, does OPG prevent it. The results of these studies have been somewhat inconsistent.

Some of the earliest research on RANKL and VC was performed by Kaden *et al.* in their analysis of aortic valve calcification [184]. This group reported that administration of RANKL to a myofibroblast cell population led to increased ALP activity and expression of Runx2. More recently, Panizo *et al.* incubated VSMCs with RANKL and reported a dose-dependent increase in calcification (measured by calcium uptake and ALP activity). Co-incubation with OPG abolished this increase, as did short hairpin ribonucleic acid (shRNA) knockdown of RANK and of NF-KB pathway components [183]. With regards to *in vivo* data, Xie *et al.* studied the effects of over-expressing omentin-1 (a recently discovered cytokine that promotes OPG and inhibits RANKL production) in mice, and reported a significant decrease in VC [185]. In contrast to these findings, however, are the studies conducted by Lars Rasmussen's group. Adopting a particularly robust methodological approach, this group reported that RANKL administration had no effect on calcifying activities of VSMCs [186]. Their results were supported by the findings of Byon *et al.* in atherogenic mice, who suggested instead that RANKL may play a role in the emergence of osteoclast-like cells that may be seen in advanced VC [187]. The reasons for the discrepant findings between these studies remain unclear, although it should be noted that Rasmussen's group also reported significant limitations in the use of calcium uptake by VSMCs as a marker of calcifying activity, which may have confounded previous research in this area. Finally, it should be noted that an alternative hypothesis on how RANKL may

promote VSMC-induced calcification was recently put forward by Osako *et al.*, who reported that the administration of RANKL to ECs (which also express RANK) appeared to encourage osteogenic activity in VSMCs [38,188].

In summary, there remains a degree of controversy regarding the ability of RANKL to induce calcifying activities in vascular cell populations such as VSMCs. There also exists the possibility that the effects of RANKL may be mediated indirectly via the EC population. Accordingly, studies I and II of the present thesis include an assessment of the actions of RANKL on calcifying activity in ECs and VSMCs.

1.7.7.4. OPG as an Inhibitor of VC - the Actions of TRAIL

In comparison to RANKL, the potential actions of TRAIL in the development of VC have not received the same degree of interest until relatively recently. As with RANKL, various groups have reported a number of potential sources for TRAIL within the vascular wall, including VSMCs and infiltrating T-lymphocytes [34,160]. One of the prevailing theories with regards to TRAIL as a potential promoter of VC is that TRAIL may induce apoptosis of VSMCs, which in turn produce apoptotic bodies that act as nucleation sites for passive calcium crystal deposition and propagation [34]. While this hypothesis does not take into account the inhibitory systems, such as PPi, that resist such passive deposition, it should also be noted that apoptotic areas in the vicinity of ongoing calcification have been shown to co-locate high concentrations of OPG and TRAIL, and the possibility of this protein promoting VC cannot be dismissed [160,171]. Ultimately, by binding to and subsequently blocking the actions of TRAIL, it has been suggested that OPG may act as a survival factor for VSMCs, and may therefore reduce the number of apoptotic bodies available to act as crystal nucleation sites. Furthermore, and as previously noted, OPG may bind to either TRAIL or RANKL with similar affinity, and increased concentrations of TRAIL may reduce OPG-RANKL binding, allowing increased binding of RANKL to RANK.

At present, there are a limited number of studies testing the hypothesis that TRAIL may induce VC. While one group to date has reported a promotion of VC when human VSMCs were exposed to TRAIL, they did not elaborate upon the mechanism behind this response, and these results have not been reproduced [186,189,190]. As with RANKL, the origins and actions of TRAIL are assessed in studies I and II of the present thesis.

1.7.8. Aspects of the OPG/RANKL/TRAIL System and VC Addressed in This Thesis

On reviewing the complexities of OPG, RANKL, and TRAIL, and the conflicting evidence linking these interlinked signals to VC, it is apparent that a number of aspects of this putative regulatory system for VC require additional clarification.

With regards to basic data on the presence and concentrations of OPG, RANKL and TRAIL within the vasculature, and their relationship to calcification, it is notable that the various *in vitro* studies to date have often generated conflicting data, and are difficult to amalgamate into one coherent body of evidence. Accordingly, a comprehensive assessment of the production and secretion of OPG, RANKL and TRAIL, from primary-derived *in vitro* human cell populations (HAECs and HASMCs), under basal and pro-calcifying conditions, forms the basis of Study I of the present thesis.

In addition to the need for baseline data on OPG, RANKL and TRAIL production and secretion in the vascular microenvironment, the effects of this system on the emergence of osteoblastic activity in VSMCs also merit further assessment. Accordingly, Study II of the present thesis includes an assessment of the effects of RANKL and TRAIL on pro-calcifying activities in HAEC and HASMCs. This assessment is first performed in single cell populations, then as part of conditioned media experiments (to assess the production of paracrine signals by HAECs that induce

calcification activity in HASMCs). Finally, in order to maximize the clinical applicability of this data by simulating *in vivo* arterial hemodynamics and three-dimensional structures, Study II also includes an assessment of OPG and its ligands in a media-perfused, artificial capillary co-culture model incorporating both HAECs and HASMCs (CELLMAX® Duo).

1.8. Insulin, Liraglutide and VC

1.8.1. Introduction

As previously noted, T2DM is associated with a high prevalence of VC and CVD [3,42,43]. T2DM is recognised to be a pro-inflammatory, dyslipidemic, hypertensive state, all conditions that promote VC [191]. The extent, severity, and characteristic medial pattern of calcification in T2DM, however, suggests that other pathophysiological mechanisms, unique to T2DM, may also be contributing towards this high calcification burden. Mechanisms that have been queried include the effects of hyperglycemia on OPN and process of diabetic neuropathy [92,192]. More recently, the hormone insulin (whether endogenous or administered exogenously as an insulin analogue) has also been suggested to promote of VC by affecting the activities of OPG and RANKL within the vasculature. While hyperinsulinemia is a characteristic feature of T2DM [193], and insulin therapy has been administered to patients with T2DM for the better part of a century, there is a marked lack of evidence regarding the effects of insulin on VC, especially with regards to the insulin analogues. It should also be noted that a number of new therapies for T2DM have been developed that now offer an alternative to the early use of insulin in many patients with diabetes [44]. One new medication class in particular (the GLP-1 analogues) have, in addition to improving glycemic control, also been shown to reduce blood pressure (BP) and weight, improve lipid profiles, and improve EC dysfunction within the vasculature [45,194]. Thus, while insulin is under investigation for the promotion of calcification, newer agents for the

treatment of T2DM may have neutral or even beneficial effects on this process. Interestingly, despite the high burden of calcification and CVD in T2DM, these issues have not been tested to any significant degree to date [195].

1.8.2. Insulin

1.8.2.1. Insulin and T2DM

Endogenous insulin is a 51 amino acid peptide that is formed within the beta cells of the endocrine pancreas and is the primary hormone for the regulation of glucose within the body. There are a number of stimuli for the production and secretion of insulin, but the most important is carbohydrate ingestion with a subsequent rise in the circulating concentrations of glucose [196]. Patients with T2DM are typically resistant to the actions of insulin, and as a compensatory reaction produce increased amounts of endogenous insulin early in the course of their condition. As their disease progresses, however, endogenous production often declines, and they often require treatment with exogenously administered insulin analogues to control their hyperglycemia.

1.8.2.2. Insulin and VC

In terms of epidemiological data, while insulin resistance and hyperinsulinemia have been associated with high prevalence rates of VC in various patient populations and animal models, it has proven exceedingly difficult to differentiate the effects of insulin analogue treatment from the effects of T2DM-related co-morbidities on this process [197-199]. The majority of evidence in this area, therefore, has emerged from *in vitro* studies. One of the earliest of these studies was performed by Oleson *et al.* in 2007. In their research, the authors examined the effects of human insulin on the production of ALP, BSP, and OPG by HASMCs, along with the uptake of calcium from the media by the cells while under the influence of β-glycerophosphate (a recognised inducer of calcification). They reported that insulin at high concentrations (1000 μU/ml) increased

calcium uptake along with ALP and BSP production, indicating osteoblast-like activity, while simultaneously decreasing concentrations of OPG [39]. Insulin at lower concentrations (200 μU/ml) showed a trend towards increased calcification that did not achieve significance. Interestingly, this group also reported a wide variation in calcification activity between SMC populations from different donors which impacted upon the consistency of their data. This effect was noted once more in a follow-up study by the same group, in which certain donor SMC populations calcified significantly in the presence of human insulin and RANKL, whereas others showed no response [186]. In this follow-up study, and with this variability in mind, the authors did not demonstrate a significant effect on calcification with insulin. More recently, Yuan *et al.* revisited and explored this pathway in greater detail [41]. This group examined the effects of human insulin (10 nM concentration) on ALP expression, RANKL secretion, and the formation of calcified nodules in SMCs, and noted a significant increase in all markers of calcification following exposure to insulin. Blocking either RANKL, or the ERK 1/2 (extracellular signal-regulated kinases) pathway of insulin signalling, but not the PI3K (phosphoinositide 3-kinase) pathway, abrogated the increase in calcifying activity. This is of particular interest to patients with T2DM, as insulin resistance has been reported by some authors to involve a selective downregulation of the PI3K pathway, while the ERK 1/2 pathway may be upregulated [200,201]. When Wang *et al.* examined the effects of insulin on VSMCs, they added to the complexity of this data by reporting that insulin, when administered in isolation, was associated with decreased calcifying activity, but when the PI3K pathway was selectively blocked before the addition of insulin, a significant increase in calcification ensued [40]. Finally, in addition to these findings, insulin (primarily human insulin) has been reported to reduce the production and secretion of OPG in multiple *in vitro* and *in vivo* experiments (including the administration of insulin to a T1DM population) [21,116,117]. In summary, therefore, while the data are by no means conclusive, 3 separate groups to date have

reported insulin as a promoter of various markers of osteoblastic activity in SMCs, potentially due to alterations in OPG/RANKL. Furthermore, it is noteworthy that the *in vitro* experimental models to date have almost uniformly employed human insulin, and to the best of my knowledge there are no data available on insulin analogues and VC, despite the worldwide use of these medications in the treatment of T2DM.

1.8.3. GLP-1 analogues

1.8.3.1. GLP-1 synthesis, Signaling, Actions and Analogues

GLP-1 is a hormone produced by L cells in the small bowel in response to the ingestion of nutrients such as carbohydrates, proteins and lipids. The GLP-1 receptor is a G-protein coupled receptor that has been identified within numerous tissue types, most notably pancreatic beta cells but also both ECs and SMCs [194,202,203]. One of the main actions of GLP-1 is to temporarily increase insulin release from the pancreas following ingestion of food. In recent years, GLP-1 analogues (modified versions of the GLP-1 molecule) such as liraglutide have been approved for the treatment of T2DM. In addition to affecting insulin release these agents have also been reported to reduce weight and produce mild improvements in BP and lipid profiles, albeit with an associated increase in heart rate [204].

1.8.3.2. GLP-1 and VC

In comparison to insulin, there has been much less research performed regarding the effects of GLP-1 or its analogues on VC. In terms of indirect effects, it is reasonable to hypothesize that reductions in BP, weight and dyslipidemia might have a beneficial effect on VC. This hypothesis, however, has not been tested *in vivo* to date. In terms of direct effects, and as noted previously, GLP-1 is also capable of binding to receptors on ECs and SMCs, but the effects of this binding have not been fully characterised *in vitro* or *in vivo*. With regards to the OPG/RANKL system, there are limited data

suggesting that increasing GLP-1 activity may increase OPG production and secretion in murine models, potentially inhibiting VC [92,205-207].

1.8.4. Aspects of Insulin, GLP-1 and VC Addressed in This Thesis

In the context of the conflicting data regarding the effects of insulin on calcifying activity in vascular cells, and the lack of data regarding the effects of insulin analogues and GLP-1 analogues at both the *in vitro* and *in vivo* level, it is apparent that the effects of these medications on VC requires additional investigation. Accordingly, both insulin analogues and liraglutide are compared in terms of their ability to affect a) calcifying activity in HAECs and HASMCs, and b) CAC in a patient population with T2DM.

1.9. Concluding Remarks

By blocking the actions of RANKL and TRAIL, OPG regulates two systems whose biological relevance are still being described, especially within the vascular wall microenvironment. What is clear, however, is that the absence of OPG is associated with increased VC, and that the actions of OPG and its ligands (RANKL and TRAIL) on VSMCs, a cell population capable of acquiring an osteoblastic phenotype, merit further assessment. T2DM patients typically have high circulating concentrations of insulin, and are known to suffer from high rates of VC. To the best of my knowledge, and despite evidence that both insulin and GLP-1 effect various aspects of VC *in vitro*, no clinical study has examined the effects of either insulin analogues or the GLP-1 analogues on VC in T2DM to date. Accordingly, in the present thesis, the role of OPG, RANKL and TRAIL in VC at the cellular level, along with the systemic actions of insulin glargine and liraglutide on these proteins, and on calcification of the coronary arteries in T2DM, will be tested.

Chapter 2 - Materials and Methods

2.1. *In Vitro* Experiments

2.1.1. General Growth and Maintenance of Cells

HAECs and HASMCs were obtained from Promocell Gmbh (Heidelberg, Germany), as were the culture media for both cell populations. The HAECs (positive for vWF and CD31) were donated by a 28 year old Caucasian male, while the HASMCs (positive for α-actin) were donated by a 23 year old Caucasian male. HAECs were cultured in endothelial cell growth medium MV (catalogue number c-22120). This growth medium included the following supplements; fetal calf serum (0.05%), endothelial cell growth supplement (0.004 ml/ml), epidermal growth factor (10 ng/ml), heparin (90 µg/ml) and hydrocortisone (1 µg/ml). This media was also supplemented with penicillin (100 IU/ml) and streptomycin (100 µg/ml). HASMCs were cultured in smooth muscle cell growth medium 2 (catalogue number c-22162), which was supplemented with antibiotics in the same manner as the HAEC media, along with fetal calf serum (0.05%). epidermal growth factor (0.5 ng/ml), basic fibroblast growth factor (2 ng/ml) and insulin at 5 µg/ml (added to encourage early SMC growth during passages 2-3, then omitted for a minimum of 2 passages prior to commencement of experiments). Both HAEC and HASMC media had a basal glucose concentration of 5 mmol/l. These growth media were also used for all *in vitro* experiments.

While growing, both cell populations were maintained in a humidified incubator at 37°C and 5% CO_2, and their growth rate and morphological features were assessed on a daily basis via direct microscopy (Nikon eclipse TS100, Nikon, New York, USA). Cells were grown in P100 culture dishes (Aktiengeselischaft and Company, Numbrecht, Germany). Fresh media was added every 2-3 days, depending on the growth rate of the cell culture. Any manipulation of the cell populations took place within a sterile laminar flow cabinet (Holten Lamin-Air, Thermo Fischer Scientific, Massachusetts, USA). Passages 5-9 were utilized for experimental purposes.

2.1.2. Trypsinization of Cells

Trypsinization was required for both cell populations in order for them to be seeded to new plates, to undergo counting, and to allow them to undergo cryopreservation. Cell cultures requiring trypsinization were placed in the laminar flow cabinet, growth medium was aspirated off, and the cell culture was washed three times with 1x sterile phosphate buffered saline (PBS, Sigma-Aldrich, Dorset, United Kingdom). Pre-warmed trypsin-EDTA (Sigma-Aldrich, Dorset, United Kingdom) was then added to the cell culture. For HAECs, a 1x concentration of trypsin (10% v/v in PBS) was utilized, whereas for HASMCs a 0.25x trypsin concentration was utilized. Cells were monitored closely for detachment over a time frame of 2-4 minutes. Once greater than 50% detachment was observed by microscopy, growth medium was applied to the cell culture once more to inactivate the trypsin and aid in the detachment of the remaining cells. The resultant mix of inactivated trypsin, growth medium and detached cells was then centrifuged for 5 minutes at 0.1 relative centrifugal force (rcf) at room temperature. Subsequent to this, the media/trypsin mix was aspirated off, and the cells were either resuspended in fresh growth media and counted, or they were placed in freeze-down media for storage.

If cells were being split for continued culture, the HAECs from one P100 plate were split to new plates containing fresh growth medium with a 1:3 or a 1:4 ratio, whereas HASMCs were split with a 1:2 or 1:3 ratio. At 24 hours after splitting, the cell cultures were washed with PBS to remove any cellular debris from the trypsinization process, and fresh growth medium was applied once more.

2.1.3. Cryopreservation of Cells

Cells undergoing cryopreservation were placed in sterile cryovials and Cryo-SFM (Promocell, Heidelberg, Germany), a serum-free medium containing the cryoprotectants methycellulose and dimethyl sulfoxide (DMSO) was added. The vials

were then placed in a Mr Freeze™ cryo-freezing container, which in turn was placed in a -80°C freezer to produce a gradual reduction in temperature, prior to long-term storage in a liquid nitrogen cryo-freezer unit. If cells were being retrieved from storage, they were placed directly into a water bath at 37°C for 15-30 minutes prior to placement into a tissue culture dish with a minimum of 10 mls of pre-warmed growth media for 24 hours prior to washing with sterile PBS and the application of fresh growth medium.

2.1.4. Quantification of Cell Numbers and Viability

Counting of cell populations was routinely performed during the trypsinization process and at the conclusion of experiments. Counting the cells while they were being grown ensured appropriate seeding densities for the respective cell populations (necessary for healthy growth and function), while counting the cells prior to their use in the experiments avoided variations in baseline cell numbers between the different experimental conditions. Counting the cells at the conclusion of experiments allowed data to be normalized against viable cell count. Cell counting was accomplished using the advanced detection and accurate measurement (ADAM™) cell counter (Digital Bio, Seoul, South Korea). This system utilizes two dyes to measure the number of viable and non-viable cells in a suspended sample. Solution N contains a propidium iodide containing solution that will bind to deoxyribonucleic acid (DNA) and act as a fluorescent dye, but cannot enter viable cells with intact cell membranes, whereas solution T contains both propidium iodide and a solution that disrupts cell membranes. Both solutions are added to separate, fixed volumes (12 µl) of the cell suspension in separate aliquots, with the resultant mix transferred to a glass slide. The glass slide is inserted into the ADAM™ counter (figure 2.1), and solution N identifies non-viable cells, while solution T identifies all cells, with the average cell number and viability data calculated by the image analysis software inherent to the ADAM™ counter. The resultant data is displayed on a digital readout. To ensure that experiments were being

conducted with sufficient numbers of viable cells, a viability of 80% or greater was required when seeding cells to experimental conditions.

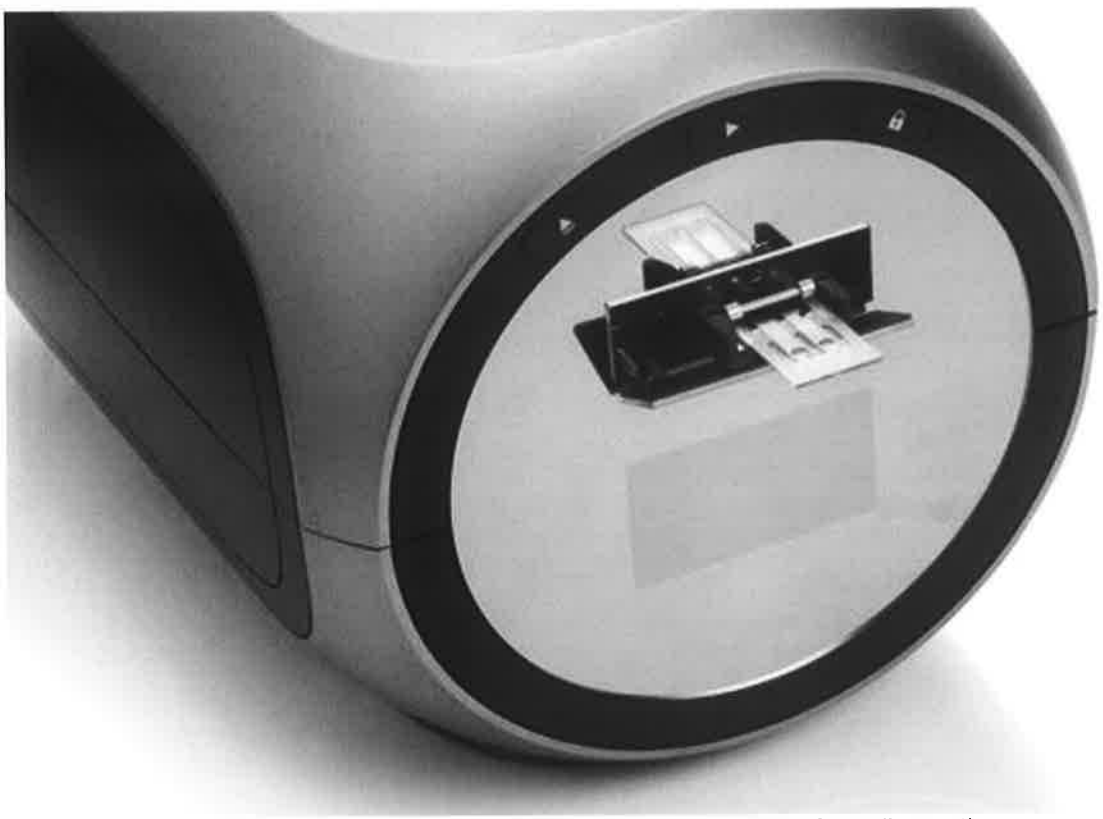

Figure 2.1. Adam™ counter with glass slide inserted in preparation for cell counting.

2.1.5. Standard 6-Well Culture Dish Experiments

The majority of the experiments in Study I, the initial experiments in Study II, and the *in vitro* component of Study III were conducted using standard 6-well culture dishes (Aktiengeselischaft and Company, Numbrecht, Germany). HAECs were seeded at densities of 250000 cells per well, whereas HASMCs were seeded at densities of 150000 cells per well. At confluency, the cultures were washed with sterile PBS, fresh media was applied, and experiments were commenced. Once growth media had been added to the cells, soluble factors (e.g. TNF-α, glucose etc.) could be added as required to produce experimental conditions.

2.1.6. Cyclic Strain Experiments

In addition to the static conditions of the standard 6-well culture dish experiments, Study I included a number of experiments involving the application of increased cyclic strain to HAECs and HASMCs. For these experiments, HAECs and HASMCs were seeded at densities of 350000 and 250000 cells, respectively, to each well of a Bioflex® plate (Dunn Labortechnik GmBH, Ansbach, Germany). Bioflex® plates are 6-well culture dishes with a flexible, ProNectin®-coated silicon membrane at their base, whose shape can be altered via the use of a microprocessor-controlled vacuum (figure 2.2). Stretching of the flexible membrane in this fashion can be utilized to apply physiological equibiaxial strain (0-12.5% strain, 60 cycles per min or 1 Hz, cardiac waveform) to the cells, effectively imitating the periodic circumferential stretching of the arterial wall that results from pulsatile blood flow *in vivo* [208]. In the cyclic strain experiments in Study I, the vacuum that was applied in this fashion to the Bioflex® plates was generated and controlled by the Flexercell Tension Plus FX-4000™ system (Flexercell International, Hillsborough, North Carolina, USA).

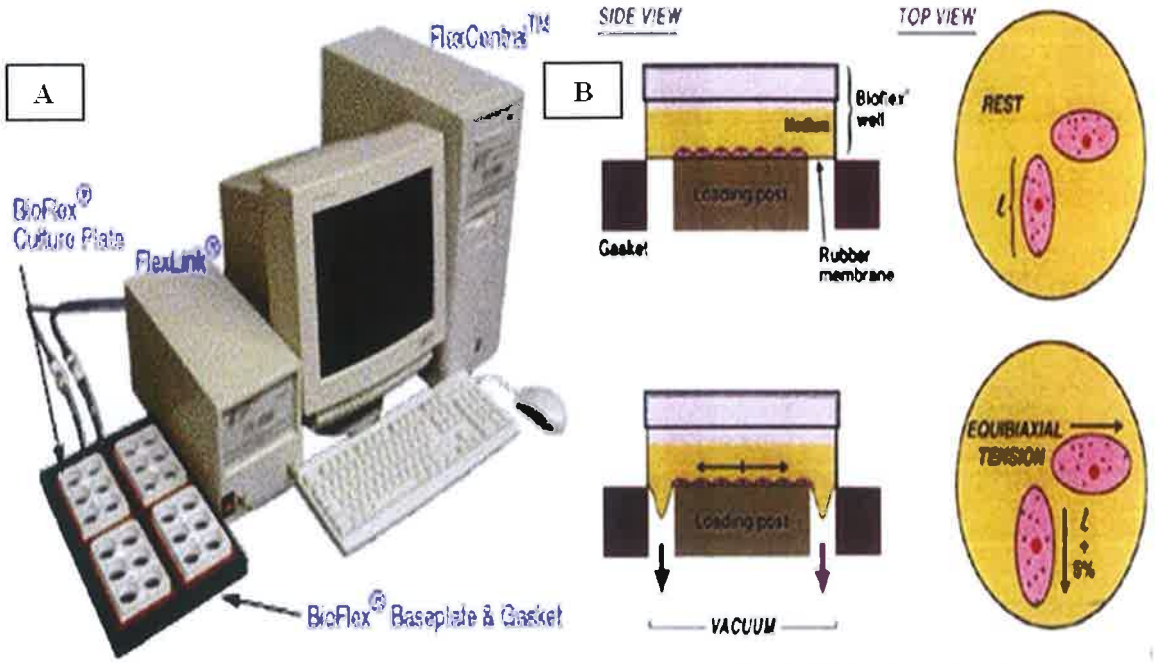

Figure 2.2. A: Flexercell Tension Plus FX-4000™ system with 4 Bioflex® plates inserted into the baseplate and gasket. During experiments the gasket and the Bioflex® plates were maintained in a humidified incubator as previously described. B: Schematic diagrams of the vacuum exerted on the inferior aspect of the flexible membrane, the resultant downward displacement of the membrane, and the strain exerted on the cell populations.

2.1.7. Conditioned Media Experiments

As part of Study II, the putative contribution of HAEC:HASMC paracrine signalling to VC was examined *in vitro*. In essence, these experiments involved culturing HAECs in standard growth media that was subsequently harvested and transferred to reporter HASMC cultures. In this way, paracrine factors secreted by HAECs into the supernatant media (the media in which the cells were cultured) were transferred, along with the media, onto HASMC cultures.

For this series of experiments, HAECs were seeded to transwell culture inserts (Merck Millipore, Massachusetts, USA) at a density of 200000 cells per insert (figure 2.3). Transwell inserts allow the culture of an endothelial monolayer above a permeable membrane (0.4 μm pores), approximating the *in vivo* structure of the endothelial monolayer and the basal lamina in the arterial wall. The inserts are placed into standard 6-well culture dishes containing growth media (figure 2.4), to create separate abluminal (apical) and subluminal (basolateral) compartments. At the conclusion of the experiments, supernatant media can be harvested from either side of the endothelial monolayer. Using transwell inserts in this fashion facilitates the application of experimental factors (e.g. RANKL and TRAIL) to the apical aspect of the endothelial monolayer (the aspect that would be exposed to circulating factors *in vivo*), followed by harvesting of media from the basolateral aspect of the endothelial monolayer (the aspect that would be in close proximity to HASMCs *in vivo*). Thus, those paracrine factors that are secreted by HAECs from their basolateral surface are also harvested. For the experiments performed in Study II, conditioned media was harvested in this fashion and HASMCs seeded in standard 6-well culture dishes were exposed to the HAEC-conditioned media.

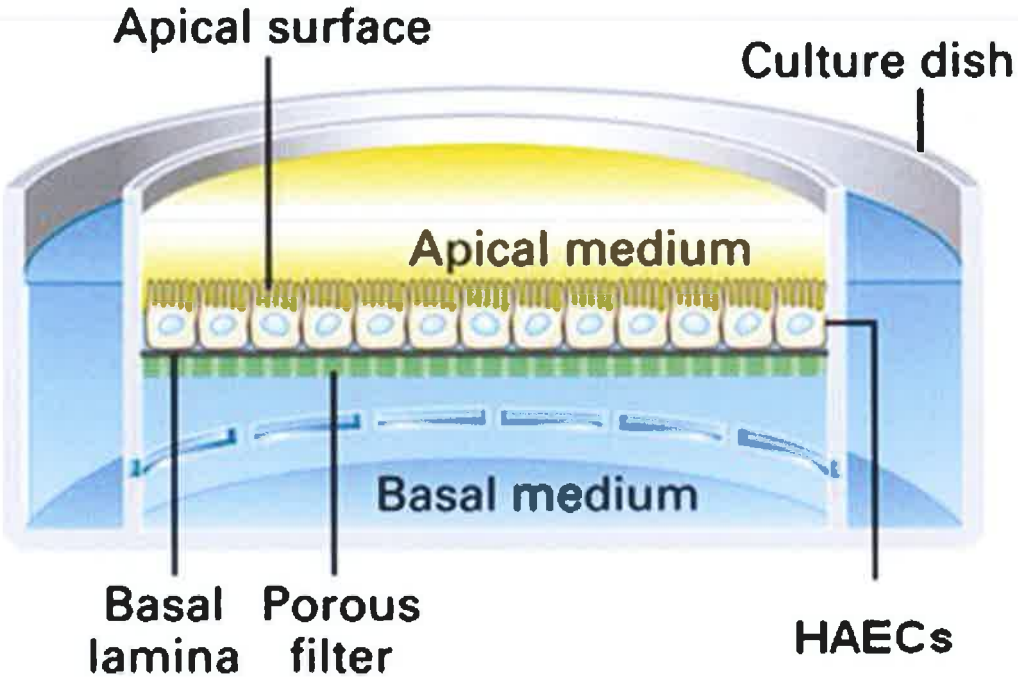

Figure 2.3. Culture dish containing transwell insert. HAECs are grown in a monolayer on a porous membrane, leading to the establishment of apical and basolateral compartments and granting the ability to harvest media from both aspects. HAEC, human aortic endothelial cell.

Figure 2.4. Standard 6-well culture dish with transwell inserts present in bottom left and bottom right wells, and transwell insert demonstrated outside of 6-well dish in the foreground.

2.1.8. CELLMAX® DUO experiments

2.1.8.1. Introduction

The CELLMAX® DUO (Spectrum laboratories, California, USA) is an artificial capillary system that permits the co-culture of ECs and SMCs in a manner similar to how these cells exist and communicate with each other within the vessel wall [209]. In essence, ECs are grown along the inside (lumen) of artificial capillaries, whilst SMCs are grown on the outside of these capillaries, within the extracapillary space (ECS), as seen in figure 2.5.

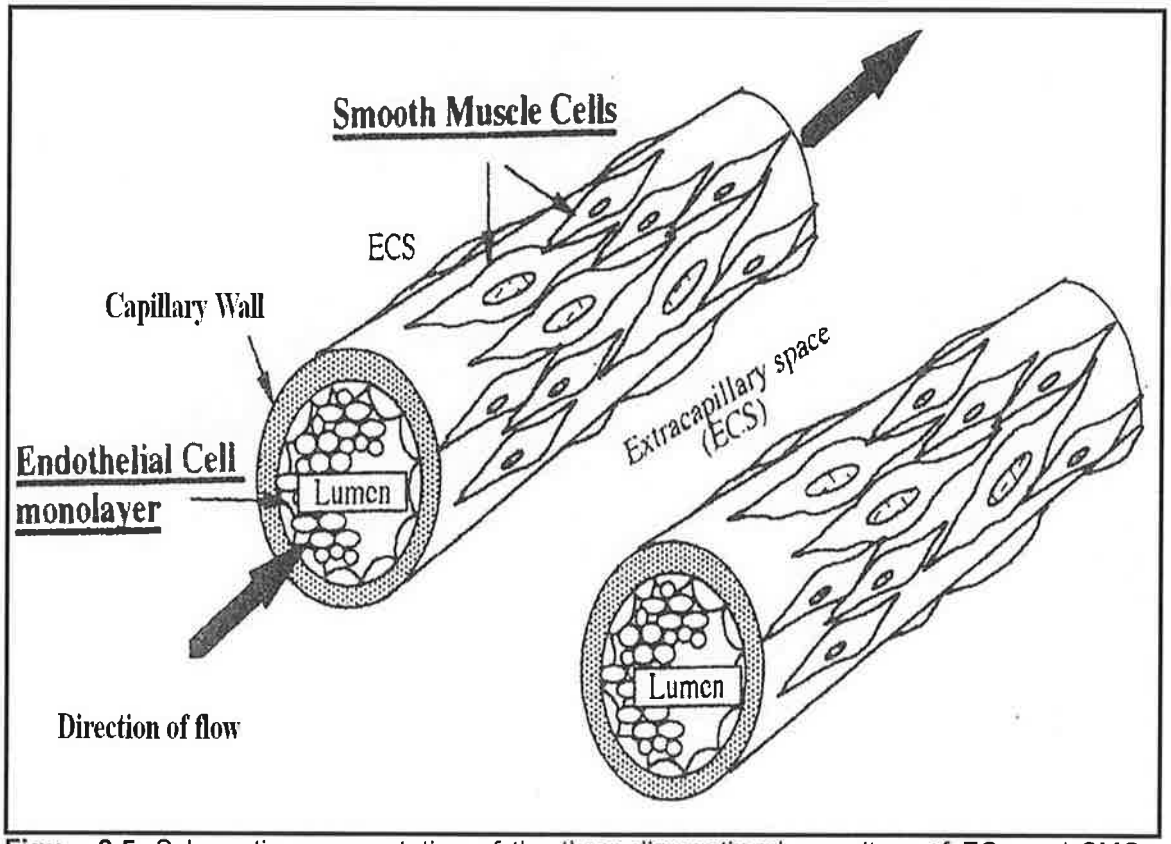

Figure 2.5. Schematic representation of the three-dimenstional co-culture of ECs and SMCs within the capillary bundles of the bioreactor. ECs grow in a monolayer that lines the lumen of the artifical capillaries, while SMCs grow in the ECS surrounding the capillaries. Media flows through the capillary in the direction indicated by the black arrows. EC, endothelial cell; ECS, extracapillary space. Adapted and reproduced with permission from Redmond *et al.* [209].

This approach simulates the three-dimensional relationship of these two cell populations *in vivo*. The walls of the artificial capillaries are semi-permeable, allowing the exchange of paracrine signals between ECs and SMCs, an aspect of *in vivo*

physiology that is relevant to both healthy cell function and, if dysregulated, numerous disease states including atherosclerosis [210,211]. Multiples capillaries of this nature (bundles), sharing a common ECS, make up a single bioreactor unit. These bioreactor units can be connected to a positive pressure displacement pumping system. The resultant system leads to a perfusion of oxygenated growth media through the capillaries of the bioreactor in a manner similar to blood circulating within the vasculature (figure 2.6). In this fashion, hemodynamic forces (e.g. laminar shear stress) exerted on the EC monolayer *in vivo* are reproduced in a precisely controlled fashion within the artificial capillaries.

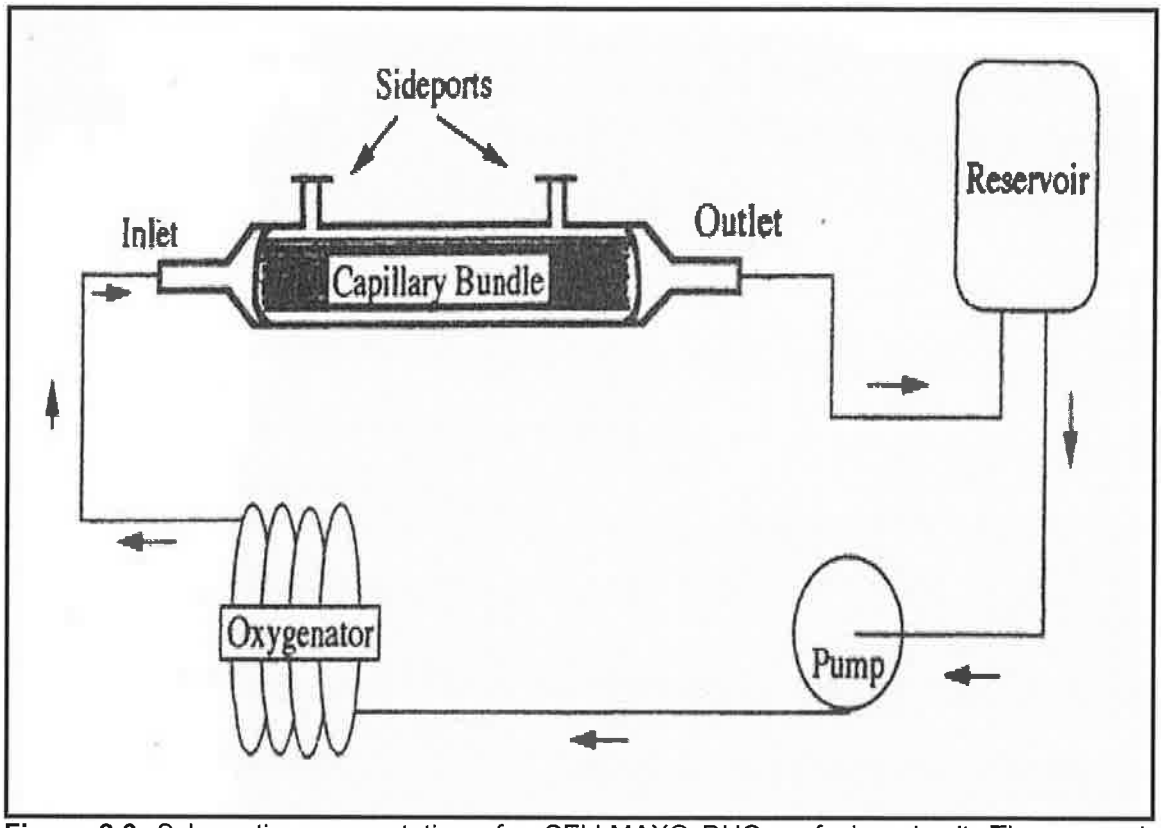

Figure 2.6. Schematic representation of a CELLMAX® DUO perfusing circuit. The reservoir contains growth media, and a displacement pump produces a positive pressure that induces the media to flow through the system. The direction of flow is indicated by the arrows. Media is oxygenated as it passes through a coil of tubules that allow oxygen exchange (oxygenator), prior to perfusion through the capillary bundles of the bioreactor unit. After bringing oxygen and nutrients to the ECs lining the luminal space, and, via the semipermeable membrane, the SMCs in the ECS, the media returns to the reservoir. Sideports grant access to the ECS as required. EC, endothelial cell; ECS, extracapillary space; SMC, smooth muscle cell. Adapted and reproduced with permission from Redmond *et al.* [209]

With regards to generating data during experiments, a number of ports provide access to both the luminal space within the capillaries and the ECS, allowing the harvesting of media from both spaces during an experiment and the harvesting of the ECs and SMCs at the conclusion of the experiment.

Ultimately, by incorporating numerous aspects of in vivo arterial physiology, the CELLMAX® DUO is designed to produce data that has increased clinical applicability, especially when compared to monocultures performed under static (no hemodynamic flow) conditions [209,212,213].

2.1.8.2. Initial Set-up of CELLMAX® DUO

The components of the CELLMAX® DUO can be seen separately in figure 2.7 and assembled in figure 2.8. Once the reservoir, gas permeable tubing and bioreactor unit were connected, the various components of the CELLMAX® DUO became one sealed, perfusing circuit. Procedures that involved accessing this circuit (e.g. to allow HAEC/HASMC insertion, replenishment of media in the reservoir, or harvesting of media samples and/or cells from the reservoir and the ECS) were performed inside the laminar flow cabinet, utilizing a sterile technique with frequent applications of 70% industrial methylated spirit (IMS, Sigma-Aldrich, Dorset, UK) to the system. At all other times, the CELLMAX® DUO system was maintained within a dedicated humidified incubator at 37°C and 5% CO_2. The bioreactor units and the tubing systems were not reusable, and were disposed of at the conclusion of experiments. The media reservoir and tubing were reusable, and were autoclaved prior to each use. The capillaries of the bioreactor units used during the experiments were composed of polypropylene coated with ProNectin®. The pores in the capillary wall were 0.2 µm in maximal diameter. The available luminal surface area in one bioreactor was 100 cm^2, and the ECS volume was 1.5 mls.

Figure 2.7. A: Base of CELLMAX® DUO system with attached control unit that alows regulation of the rate of flow of media through the circuit. B: Pump unit with latch open and white teflon bar visible. Tubing is placed against the teflon bar and the hatch is closed. The pump unit pushes the teflon bar against the rubber tubing and media within the tubing is displaced, setting up a flow of media within the circuit. C: Tubing system that connects the media reservoir to the bioreactor unit. The thick yellow tube is placed within the pump unit. The coiled tubes facillitate oxygenation of the flowing media. D: Bioreactor unit containing bundle of artifical capillaries. Two sets of ports can be seen. The ports extending perpendicular to the bioreactor unit allows access to the extracellular space. The ports at either end of the unit allow access to the luminal space. E: Open bioreactor unit demonstrating bundle of capillaries.

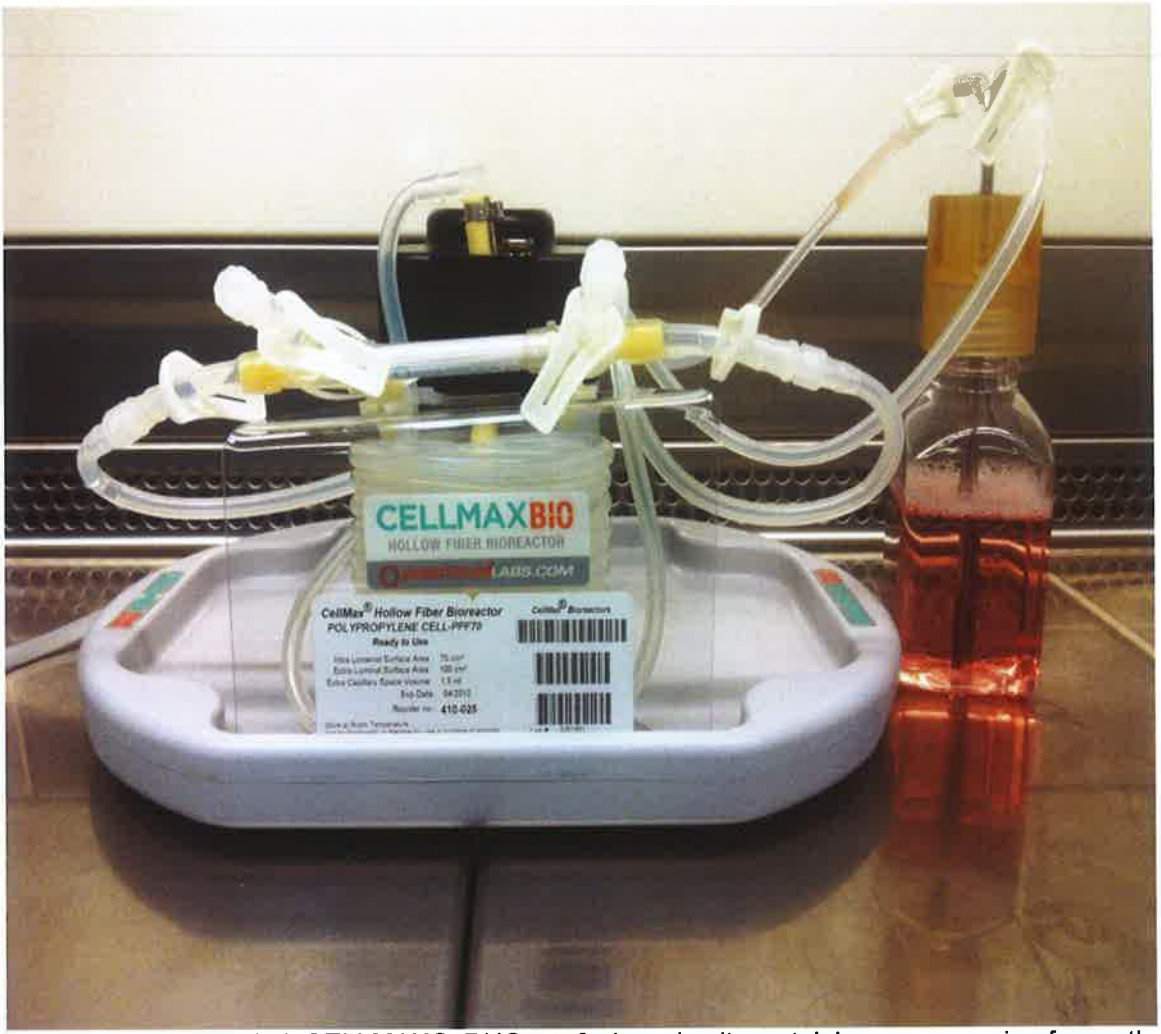

Figure 2.8. Assembled CELLMAX® DUO perfusing circuit containing a reservoir of growth media, colied tubing to facilitate oxygenation of media, a length of thick rubber tubing fixed against the teflon bar by the closed hatch of the pump unit, and the bioreactor unit.

As both HAECs and HASMCs were present within the CELLMAX® DUO for the experiments in Study II, and only one growth media could be used within the system at any given time, a mix of HAEC and HASMC growth media, in a 1:1 ratio, was utilized for the CELLMAX® DUO experiments, in order to nourish both cell populations.

Prior to cell inoculation into the bioreactor unit, the perfusing circuit was set up and the 1:1 media mix was allowed to circulate for a minimum of 3 days equilibration. During this time period, the media in the reservoir and the media in the ECS were changed at least once. These steps were performed to determine if any leaks were present in the perfusing circuit, and to ensure contamination was not present before cells were added

to the system. Air bubbles, if present, were manipulated through the tubing system until they entered the reservoir.

When establishing the co-culture model, HASMCs were inoculated into the system first, as the growth rate of these cells is slower than that of HAECs. In essence, HASMCs were trypsinized off P100 plates, centrifuged as previously described, and resuspended in growth media in a 50 ml tube. Immediately prior to the inoculation of HASMCs, media flow through the perfusing circuit was halted. The suspension of HASMCs was then introduced into the ECS through the appropriate access port. In keeping with the methodology of Redmond *et al.*, each bioreactor unit was inoculated with $1x10^7$ HASMCs [209]. Once all HASMCs were inoculated into the ECS, the flow of media was recommenced. HASMCs were then allowed to adhere and grow within the ECS of the bioreactor for a minimum of 3 weeks at a media flow rate of 20 ml/minute. At the end of this time, HAECs were inoculated into the luminal space. To begin with, HAECs were trypsinized and suspended in a 50 ml tube (in a similar fashion to HASMCs). Media flow was halted, and the suspension of HAECs was inserted into the luminal space of the capillaries, with an ECS access port opened to allow gentle ultrafiltration of the HAEC suspension across the capillary wall, leaving HAECs pressed against the lumenal wall and becoming adherent as early as possible. Each bioreactor unit was inoculated with $2.5x10^7$ cells. Media flow was halted for one hour while HAECs became sufficiently adherent to the ProNectin®-coated wall. During this time, fresh media was gently infused into the ECS to ensure continued cell viability. Media flow was then recommenced at the 5 ml/minute for a minimum of 24 hours. HAECs were allowed to proliferate over the intralumenal capillary walls for a minimum of 2 weeks prior to the establishment of any experimental conditions. During experiments, the flow rate was adjusted to produce physiological levels of laminar shear stress (the frictional

force exerted by blood flow as it 'drags' across the endothelial surface), at 10 dynes/cm^2 [209,214].

2.1.8.3. Maintenance of Co-Cultures Within the CELLMAX® DUO

As the cell cultures could not be visualised once inoculated into the bioreactor unit, data on the metabolic status and proliferation rate of the inoculated HAECs and HASMCs were gathered via daily measurements of glucose consumption and lactate production by both cell populations. The ratio of glucose consumption to lactate production was directly related to the metabolic status of the cells, and equimolar depletion of glucose with concomitant production of lactate was indicative of a healthy state of metabolism. Proliferation of the inoculated cells was reflected in an overall increase in both parameters. Media was replaced whenever its initial glucose concentration was reduced by 50%.

To measure these parameters, 250 µl was harvested from the media reservoir each day with glucose and lactate measured immediately using an YSI 2300 STAT Plus glucose and lactate analyzer (YSI Incorporated Life Sciences, Ohio, USA, figure 2.9), which was calibrated against glucose (2.5 and 5 mmol/l standards) and lactate (2.5 and 5 mmol/l) standards on a daily basis [215].

Once both HASMC and HAEC populations were inoculated, and stable rates of glucose consumption and lactate production for the bioreactor unit were demonstrated, the bioreactor unit was ready for experimental conditions. The total time required for this process varied depending on cell proliferation rates within the bioreactor unit, but averaged between 5.5 and 6.5 weeks.

Figure 2.9. YSI 2300 STAT Plus glucose and lactate analyzer. An automated sampler aspirates 25 µl of liquid, and an enzyme that is specific to the substrate under examination (e.g. glucose) produces hydrogen peroxide if the substrate is present, leading in turn to the generation of a current at a platinum electrode that is proportional to the concentration of the original substrate.

2.1.9. Addition of Soluble Factors to Growth Media

In the standard 6-well culture dish experiments in Study I, the production and release of OPG, RANKL and TRAIL from HAECs and HASMCs under pathological conditions was examined. To this end, soluble factors were added to the growth media to produce a variety of pathological conditions. These factors were typically added at pathophysiological (high concentrations that have been reported *in vivo* in association with disease states) and supraphysiological (concentrations significantly greater than are typically found *in vivo*) concentrations. For TNF-α (Millipore, Massachusettes, USA) this equated to 10 ng/ml and 100 ng/ml concentrations, respectively. Glucose (Sigma-Aldrich, Dorset, UK) was added to the media at concentrations of 15 and 30 mmol/l. Finally, insulin glargine (Sanofi-Aventis, Surrey, UK) was added to the media at 1 nmol/l (equivalent to the upper range of circulating insulin concentrations seen in

insulin-resistant patient populations) and 10 nmol/l concentrations (supraphysiological concentrations) [216,217].

In the standard 6-well culture dish and conditioned media experiments in Study II, the effects of RANKL and TRAIL on HAEC and HASMC populations were examined. To this end, recombinant human RANKL and TRAIL (R&D systems, Minneapolis, USA) were reconstituted in sterile PBS containing 0.1% bovine serum albumin (BSA). Based on the endogenous production of OPG by HAECs and HASMCs reported in Study I, RANKL and TRAIL were added to the growth media to achieve concentrations of 2.5 ng/ml for HAEC cultures, and 50 ng/ml for HASMC cultures. These concentrations ensured that RANKL and TRAIL would be added in sufficient amounts to these cell cultures to overcome the blocking actions of endogenously produced OPG. A neutralizing polyclonal antibody to OPG was also sourced from R&D systems, and was reconstituted in sterile PBS. It was added to growth media to achieve concentrations of 2.5 µg/ml for HASMC cultures. The concentration this antibody requires to neutralize 50% of the activity of OPG has previously been established as 0.25-0.7µg/ml (in the presence of 1 µg/ml of TRAIL) [218]. At the conclusion of the conditioned media experiments, noggin (R&D systems) was added to growth media to achieve a concentration of 2.5 µg/ml [219]. Noggin is a BMP-binding protein that antagonizes the effects of BMP signalling, and was reconstituted in sterile PBS containing 0.1% BSA. Finally, RANKL was also utilized in the CELLMAX® DUO experiments. As large volumes of media (250 mls) were used to perfuse this system, raising the concentrations of RANKL throughout the entire perfusing circuit was not practical. Instead, the media flow was halted twice a day, and a 7 ml volume of growth media containing RANKL at a concentration of 50 ng/ml was infused into the intralumenal space of the bioreactor units and allowed to exert its effects on the HAEC monolayer for 20 minutes before the media flow was recommenced. CELLMAX® DUO

experiments acting as a control for this approach also had their media flow halted in this fashion, but the 7 mls of growth media infused did not contain any RANKL.

In the *in vitro* component of Study III, insulin (insulin glargine) and liraglutide (a GLP-1 analogue produced by Novo Nordisk, Bagsvaerd, Denmark) were added to standard 6-well culture dishes and conditioned media experiments. Insulin was added to the growth media to produce concentrations of 1 nmol/l and 10 nmol/l, whereas liraglutide was added to produce concentrations of 30 nmol/l (equivalent to concentrations reported in the LEAD-6 study by Buse *et al.*) and 300 nmol/l (supraphysiological concentrations) [220].

2.1.10. Harvesting of Samples and Measurement of In Vitro Endpoints

At the conclusion of the *in vitro* experiments performed in this thesis, samples were harvested and a variety of endpoints were measured. These endpoints included a number of enzyme-linked immunosorbent assays (ELISAs) performed on the supernatant media and cell lysates, a colorimetric kinetic assay to determine ALP activity in the supernatant media, the harvesting of mRNA from HAECs and HASMCS for subsequent complementary DNA (cDNA) transcription, and quantitative assessment of this cDNA by quantitative real-time polymerase chain reaction (qRT-PCR). An ELx800 mircoplate reader (Biotek, Vermont, USA) was used for the final optical density (OD) analysis of all the assays performed ,and an Applied Biosystems 7900HT Fast RealTime PCR system was used for qRT-PCR.

2.1.10.1. Assay Overview

ELISA was used to measure the concentrations of a number of proteins in the supernatant media and cell lysate samples generated in Studies I, II and III. With this form of ELISA, the antigen of interest in the sample (e.g. OPG in media supernatant) is first immobilized on a 96-well plate by a capture antibody. A detect antibody is then

added to the plate, which binds to the captured antigen. The detect antibody is then linked to an enzyme (peroxide-labelled streptavidin), and in the final step of the assay a substrate for this enzyme is added, producing a colour change related to the antigen concentration (figure 2.10). This colour change is fixed by the addition of an acidic stop solution, and the intensity of the colour change is assessed via measurement of the OD of each well of the 96-well plate. Between each step in the assay process the plate is washed with a mild detergent to remove any unbound proteins.

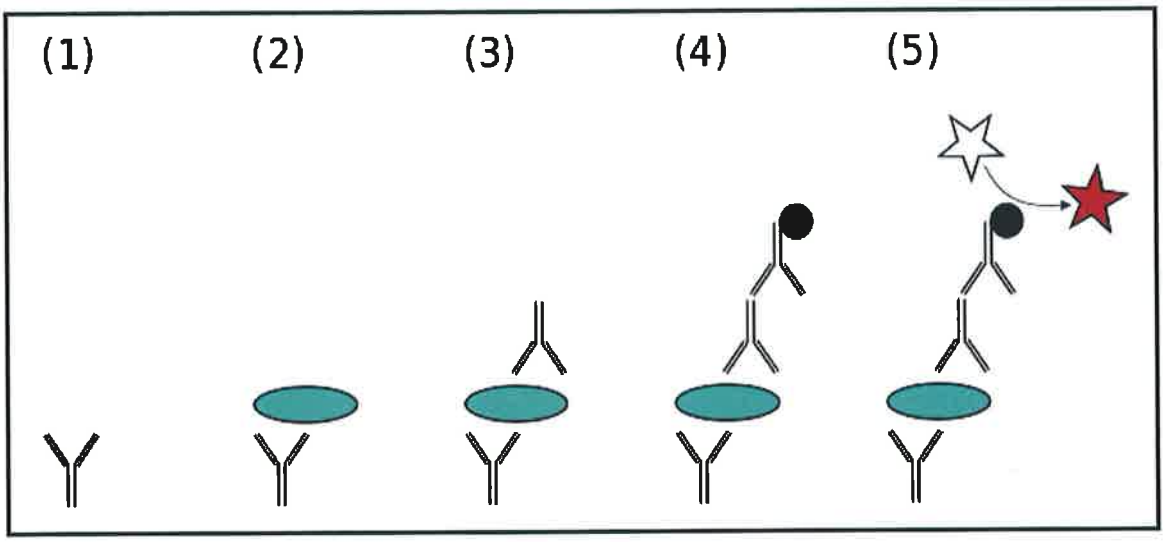

Figure 2.10. Schematic representation of sandwich enzyme-linked immunosorbent assay method. 1: Capture antibody specific to the antigen/protein of interest is present in a 96-well plate. 2: Samples are added and if the protein of interest is present it becomes bound to the capture antibody. 3: A detect antibody is then added to the plate, which binds to any capture antibody-protein complexes present. 4: An enzyme-linked secondary antibody is added, which binds to any capture antibody-protein-detect antibody complexes present. 5: A substrate for the enzyme is added, producing a colour change that is proportional to the quantity of the protein of interest in the sample. Adapted and reproduced with permission from Mr Jeffrey Vinocur.

To quantify ALP activity in samples, a colorimetric kinetic assay kit was utilized (Qunatichrom™ Kit, BioAssay Systems, California, USA). The basic principle of this assay is that ALP, if present, will hydrolyze *p*-Nitrophenyl phosphate (pNPP, a colourless solution) to *p*-nitrophenyl (a yellow coloured solution) and phosphate. By adding samples to pNPP in a 96-well plate, the emergence of a yellow colour change can be measured with a microplate reader (405 nm) at baseline and again at 4 minutes [221]. The colour change over this time period is compared to distilled water (no

inherent ALP activity) and tartrazine (coloured solution with a fixed OD), and the ALP activity (IU/l) is determined via the equation in figure 2.11.

$$= \frac{(OD_{SAMPLE\ t} - OD_{SAMPLE\ 0}) \cdot \text{Reaction Vol}}{(OD_{CALIBRATOR} - OD_{H2O}) \cdot \text{Sample Vol} \cdot t} \times 35.3$$

Figure 2.11. Equation for the calculation of ALP activity in a sample. OD sample 0, OD sample t, OD sample calibrator and OD sample H_2O are the mean 405 nm OD values for the sample at 0 minutes, the sample at 4 minutes, the calibrator at 0 minutes, and distilled water at 0 minutes. The reaction volume is 200 µl. The sample volume is 50 µl. *t* is the time in minutes between the baseline and second readings (4 minutes). ALP, alkaline phosphatase; H_2O, water; OD, optical density.

2.1.10.2. Sample Harvesting and Assay Performance

ELISA was used to measure OPG, RANKL, TRAIL, BMP-2 and BMP-4 in the media supernatant of HAECs and HASMCS, whilst OPG, RANKL and TRAIL were also measured in HAEC- and HASMC-derived cell lysates. ALP was measured by Quantichrom™ in media supernatant samples only.

With regards to the harvesting of media supernatants from HAEC and HASMC cultures; at the conclusion of experiments the culture media was aspirated off each well of the 6-well culture dish (or Bioflex® plate), spun at 100 revolutions per minute (rpm) for 5 minutes at 4°C to remove cellular debris, and the supernatant was stored at -80°C for subsequent ELISA analysis. Cell cultures were then washed with PBS, trypsinized and suspended as previously described, and a cell count was obtained with the ADAM™ counter (to allow for normalization of the ELISA results for each well by the number of cells in that well). With regards to the quantification of these proteins in the CELLMAX® DUO experiments, media was harvested directly from the reservoir on each day of a CELLMAX® DUO experiment, and from the ECS at the conclusion of the experiment. This allowed quantification of intralumenal protein concentrations and ALP activity throughout the experiment, and quantification of these factors within the ECS at

the conclusion of the experiment, respectively. Results from the CELLMAX® DUO were corrected for the initial cell number inoculated.

With regards to the harvesting of cell lysates, this was accomplished on ice (<4°C) [222]. Culture medium was removed and cells were washed three times in PBS solution. Following complete aspiration of PBS, radioimmunoprecipitation assay (RIPA) lysis buffer (64mM HEPES, 192 mM NaCl,1.28% Triton X-100, 0.64% w/v sodium deoxycholate, 0.128% w/v sodium dodecyl sufate/ SDS, supplemented with 0.5M sodium fluoride, 0.5 M ethylenediaminetetracetic acid/ EDTA, 0.1 M sodium phosphate, 10 mM sodium orthovanadate, and a 1x protease and phosphatase inhibitor cocktail) was added to the cells, which were then harvested using a cell scraper. The resultant mix was transferred into a pre-chilled micro-centrifuge tube, and continuous rotation applied for 1 hour at 4°C. Centrifugation at 10000 rpm for 20 minutes at 4°C was then utilized to sediment any Triton-insoluble material. Lysates were then transferred into fresh tubes and stored at -80°C. In addition to ELISA for OPG, RANKL and TRAIL, cell lysates were also assessed for protein concentration with a bicinchoninic acid (BCA) assay [223], to allow for normalization of ELISA results for each cell lysate based on the quantity of protein in that lysate). Each sample was assayed in triplicate on a 96-well plate, the OD of which was subsequently read at 560 nm using a microplate reader.

For the quantification of OPG in the harvested samples, the OPG Duoset kit (R&D systems, Minneapolis, USA) was utilized. This is a sandwich ELISA that has been optimized for cell culture supernatants, but has also been used in the Tromsø for the measurement of circulating concentrations of OPG *in vivo*, and by Janssens *et al.* for measurement of OPG in cell lysates [224,225]. This assay measures total OPG (including OPG bound to RANKL and/or TRAIL, along with unbound OPG). The lower

limit of the assay is 62.5 pg/ml. Initially, each well in the ELISA plates were coated with a capture antibody at a concentration of 2 µg/ml and allowed to sit overnight at room temperature. Subsequently, the plate was subjected to a thorough cleaning with wash buffer (0.05% Tween® in PBS) before reagent dilutent (1% BSA in PBS) was placed into the wells for 1 hour, followed by another wash buffer cycle. Standards and samples were then added to the wells in duplicate, and the plate was allowed to sit for 2 hours at room temperature before underoing another wash buffer cycle, followed by addition of detection antibody at a concentration of 200 ng/ml, another 2 hours at room temperature, and another wash buffer cycle. Streptavidin horseradish-peroxidase at 200 ng/ml was then added to the wells, followed by a 20 minute period at room temperature and out of direct light. After a final wash buffer cycle a 1:1 mixture of H_2O_2 and tetremethylbenzidine was added to each well, and the OD of each well was determined using a microplate reader (set to 450 nm, with wavelength correction measured at 540 nm) after another 20 minutes. A 10x dilution of all harvested supernatant media samples from HASMCs proved necessary, as OPG concentrations from this cell population were significantly above the upper limit of the standard curve. The standard curve is illustrated in figure 2.12.

In contrast to OPG, which is relatively easy to detect and quantify, a number of groups have reported difficulties when measuring RANKL in serum samples and cell culture supernatants. These difficulties have stemmed, at least in part, from the fact that RANKL can exist in both bound (to OPG and RANK) and unbound forms, and many ELISA kits do not clarify which form they measure, or whether the performance of the assay is affected by high concentrations of OPG. With these difficulties in mind, I utilized three specific sandwich ELISA kits to measure RANKL in my samples. These included the RANKL Duoset (R&D systems, Minneapolis, USA), the ampli-sRANKL assay kit (Biomedica, Vienna, Austria), and the sRANKL assay kit (Biovendor,

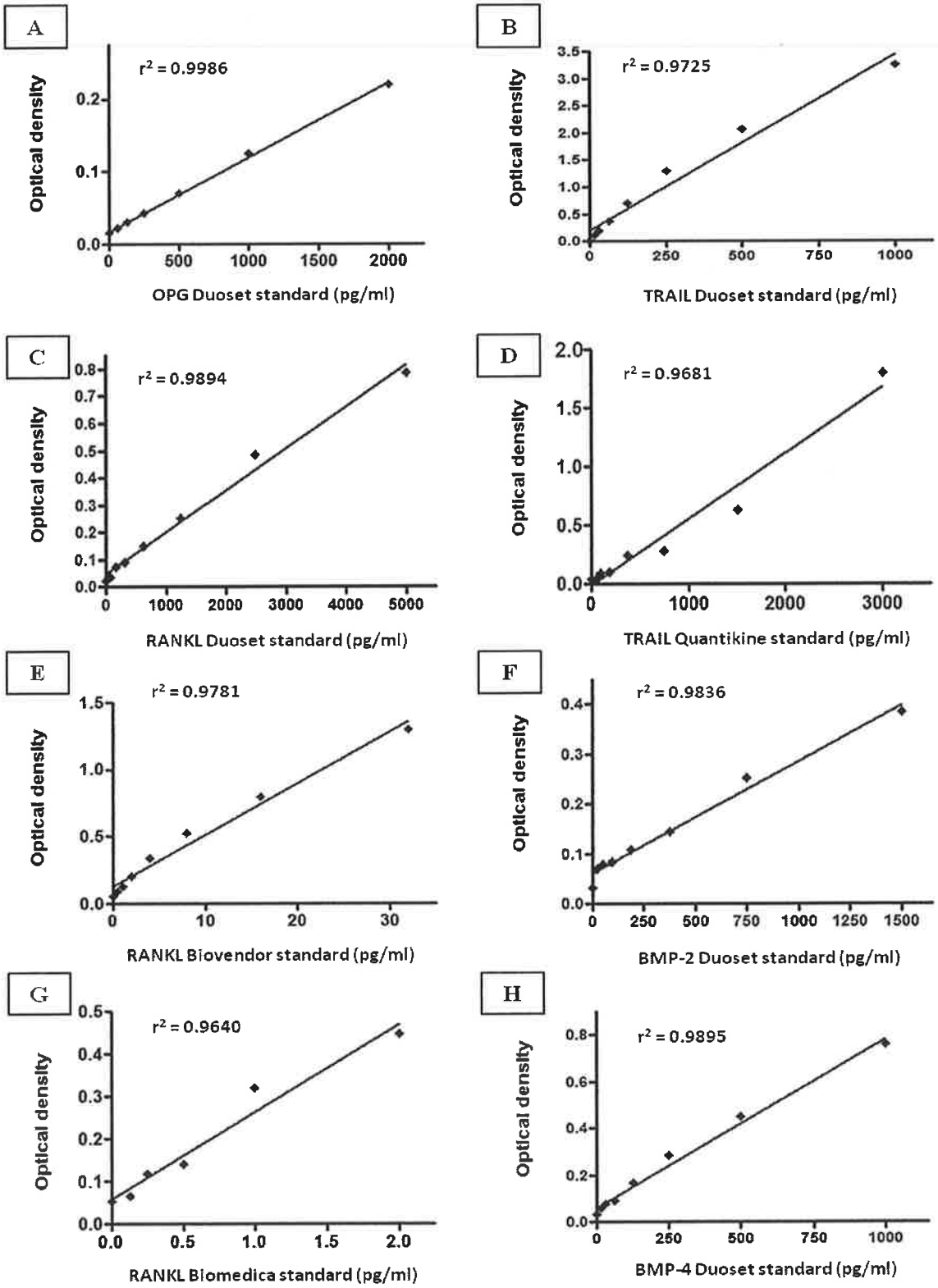

Figure 2.12. Standard curves generated from reading the OD of A: the OPG Duoset assay, B: the TRAIL Duoset assay, C: the RANKL Duoset assay, D: the TRAIL Quantikine assay, E: the RANKL Biovendor assay, F: the BMP-2 Duoset assay, G: the RANKL Biomedica assay, and H: the BMP-4 Duoset assay. Correlation coefficient (r^2) was established via linear regression analysis. All samples were assayed in duplicate. BMP 2/4, bone morphogenetic protein 2/4; OD, optical density; OPG, osteoprotegerin, RANKL; receptor activator of nuclear factor kappa-beta ligand, TRAIL; tumour necrosis factor-related apoptosis-inducing ligand.

Heidelberg, Germany). Of these assay kits, the Duoset and Biomedica ELISAs have been optimized for serum and cell culture supernatants, and the Biovendor assay has been optimized for serum samples (but has also been used for cell lysates). Ultimately, the use of multiple assays in this fashion was designed to ensure that both total and free RANKL, if present in significant amounts in samples, would be identified and quantified accurately.

The RANKL Duoset assay measures total RANKL (including RANKL bound to OPG and/or RANK, along with unbound RANKL), and its lower limit of detection is 78.1 pg/ml. When performing this assay a similar approach to that adopted for the OPG Duoset assay was utilized, albeit with an initial capture antibody concentration of 1 µg/ml, and a detection antibody concentration of 50 ng/ml. The OD measurements were the same as that for OPG, namely 450 nm with a wavelength correction measurement of 540 nm. In contrast to the OPG Duoset, however, no diluation of samples was necessary. The Biomedica ampli-sRANKL assay measures only free soluble RANKL (unbound to OPG or RANK), and it's lower limit of detection is 1.6 pg/ml. With this assay, the plate was provided already preincubated with capture antibody. Samples and standards were added in duplicate to the wells on this plate, followed by the addition of 100 µl of premade biotin labelled anti sRANKL antibody to each well. Plates were allowed to sit at 2-8 °C overnight, then were washed with wash buffer prior to the addition of 200 µl of premade streptavidin horseradish peroxidase. Plates were then allowed to sit at room temperature for 1 hour, prior to another wash with washbuffer. At this point 200 µl of substrate solution was added and the plates allowed to incubate in the dark for 30 minutes, prior to the addition of 50 µl of stop solution. The OD of the wells were measured using a microplate reader at 450 nm with a wavelength correction measurement at 620 nm. Finally, the Biovendor sRANKL assay measures total soluble RANKL (bound to OPG along with unbound), and it's

lower limit is 0.4 pmol/l (8 pg/ml). The assay plate in this kit was also preincubated with capture antibody, and the assay procedure commenced with the addition of standards and samples in duplicate into the wells of this plate. Standards and samples were diluted 100x with dilution buffer immediately prior to being pipetted into their respective wells. The assay plate was then incubated at 2-8 °C for 20 hours on an orbital microplate shaker at 300 rpm, after which it was washed with wash buffer and 100 µl of premade biotin labelled antibody added to each well. The plate was then incubated for 1 hour at room temperature on the microplate shaker at 300 rpm before another wash with wash buffer. Premade streptavidin (100 µl) was added to each well, and the plate was subjected to another hour at room temperature on the microplate shaker at 300 rpm. After another wash with wash buffer, 100 µl of substrate solution was added to each well, and the plate incubated at room tempearature (no shaking) out of direct sunlight, for 25 minutes. After addition of 100 µl of stop solution the optical densities were read at 450 nm with a wavelength correction measurement of 630 nm. The standard curves generated for all 3 RANKL assay kits are illustrated in figure 2.12.

With regards to TRAIL, two different sandwich ELISAs were utilized; the TRAIL Duoset and the TRAIL Quantikine. Both assays are manufactured by R&D systems (Minneapolis, USA), both detect total TRAIL (including TRAIL bound to OPG, along with unbound), and neither are subject to interference from the presence of high concentrations of OPG or RANKL. As high concentrations of TRAIL are found in saliva, a face mask was utilized through the performance of both of these assays. With regards to the performance of tha assays, the TRAIL Duoset was performed in a similar fashion to the OPG and RANKL Duoset assay kits. The capture antibody concentration in the TRAIL Duoset was 2 µg/ml, and that of the detect antibody was 200 ng/ml. No dilution of samples proved necessary, and the OD measurements were, once again, 450 nm with a correction measurement of 540 nm. The TRAIL Quantikine

assay included an assay plate that was preincubated with capture antibody to TRAIL, and the assay began with the addition of 100 µl of assay dilutent to each well. This was followed by the addition of 50 µl of standards or samples in duplicate to each well, after which the plate was incubated for 2 hours at room temperature on an orbital microplate shaker at 450 rpm. The plate was then washed with wash buffer, before the addition of 200 µl of TRAIL conjugate (21 ml of detect antibody for TRAIL conjugated to horseradish peroxidase) to each well. The plate was then placed back on the shaker at 450 rpm at room temperature for another 2 hours, followed by an additional wash with wash buffer, and the addition of 200 µl of substrate solution. The plate was then incubated for 30 minutes at room temperature out of sunlight before 50 µl of stop soluation was added to each well. The OD of each well was read at 450 nm, with wavelength correction measurements at 540 nm. The standard curves for the TRAIL assay kits utilized are illustrated in figure 2.12.

The primary difference between the two TRAIL assays utilized is that the Duoset was developed more recently and is specifically optimized for cell culture supernatants, while the Quantikine has a broader range of applications, having been used for the analysis of saliva, serum samples, cell culture supernatants, and cell lysates previously. The lower limit of detection for the Duoset was 23.4 pg/ml, while the lower limit for the Quantikine kit was 2.86 pg/ml. Once again, the use of two assays with different optimizations was designed to ensure the proper identification and quantification of any TRAIL present in samples.

Duoset assays from R&D were also utilized for the measurement of BMP-2 and BMP-4 in the media supernatants from HAECs and HASMCs. Both of these assays have previously been optimized for use in cell culture supernatants. The lower limit of detection for the BMP-2 assay was 46.9 pg/ml, whereas the lower limit of detection for

the BMP-4 assays was 15.6 pg/ml. Both of these assays utilized a similar approach to that adopted for the OPG and RANKL Duoset assays, including the OD wavelengths measured. Both the capture and detect antibody concentrations used in the BMP-2 assay were 1 µg/ml, with respective concentrations of of 2 µg/ml and 1 µg/ml used in the BMP-4 assay. As before, the standard curves for both of these assays are illustrated in figure 2.12.

With regards to quality control, it should be noted that all samples were assayed in duplicate, that the average coefficient of variation (CV) for these duplicate samples in the ELISA and Quantichrom™ assays was <5%, and that as noted previously, all ELISA OD readings were subjected to wavelength correction to account for optical imperfections in the plate.

2.1.10.3. mRNA Harvesting, cDNA Transcription, and PCR

2.1.10.3.1. mRNA Harvesting

Prior to the sampling or processing of mRNA samples, RNase-away spray was applied to equipment and surfaces, appropriate gloves were utilized, and pipette tips, eppendorfs, and PBS were autoclaved [226]. To extract the ribonucleic acid (RNA) at the conclusion of standard 6-well culture dish and conditioned media experiments, cell cultures were first washed with autoclaved PBS, this was then aspirated off, and Trizol® (Invitrogen, Groningen, The Netherlands) was added to disrupt cell membranes and dissolve intracellular structures while maintaining RNA integrity, following the techniques described by Chomczynski *et al.* [227]. A cell scraper was used to remove the cellular material completely from the culture plate, and samples were incubated at room temperature for 5 minutes. Each ml of Trizol® generated in this fashion contained the RNA from two wells on a 6-well culture dish, and had a final volume of 1ml. With regards to mRNA harvesting from the CELLMAX® Duo, at the conclusion of the

experiment trypsin (1x) was inserted into the ECS, and at 5 and 10 minutes media was flushed through the ECS to remove the detached HASMCs, followed by the addition of trypsin (2.5x) to the intralumenal space, with flushing at 5 and 10 minutes to remove detached HAECs. Both of these cell populations were centrifuged at 0.1 rcf for 5 minutes, the supernatant media was aspirated off, and Trizol® was added directly to the cell populations, followed by vortexing. Each CELLMAX® DUO experiment generated 1 ml of Trizol® with HAEC mRNA, and 1 ml of Trizol® with HASMC mRNA.

To each ml of Trizol® generated, chloroform (0.1ml) was added, and samples were vortexed for 15 seconds, incubated for 15 minutes at room temperature, then centrifuged at 9000 rpm for 15 minutes at 4°C. The colourless supernatants (containing RNA) were then carefully transferred to new eppendorf tubes. Isopropanol (0.5 ml) was added to each tube, inducing a precipitation of RNA out of solution as the samples were inverted 10 times and incubated for 10 minutes at room temperature. Samples were then centrifuged at 9000 rpm for 10 minutes at 4°C to produce an RNA pellet. The supernatants were aspirated off, and the pellet was resuspended in 1 ml of 75% ethanol, vortexed, and centrifuged at 9000 rpm for 5 minutes at 4°C. The supernatants were aspirated off once again, and the final pellet was air-dried for 5-10 minutes before being resuspended in 50 µl of nuclease-free water. The RNA samples were incubated for 10 minutes at 60°C prior to quantification via NanoDrop®, and were stored at -80°C prior to reverse transcription into cDNA.

2.1.10.3.2. Quantification of RNA and DNA with Nanodrop®

Both RNA and DNA samples were quantified with the Nanodrop® ND-1000 Spectrophotometer (Thermo Fischer Scientific, Massachusetts, USA). In brief, a 2 µl sample of either RNA or DNA was placed onto the end of a fibre optic cable, with a second cable then being brought into contact with the liquid sample, leading to the formation of a liquid bridge between the two fibre optic ends. A pulsed xenon flash

lamp was used as the light source, and a spectrometer analyzed the light passing through the sample. In addition to quantifying absolute amounts of RNA and DNA, the Nanodrop® also calculated the purity of the samples by reading the absorbance at 260 nm and 280 nm (figure 2.13). If the RNA samples required additional purification a DNase treatment kit (Sigma-Aldrich, Dorset, UK) was utilized. With this process, the RNA sample was first digested with DNase I (with DNase buffer) over 15 minutes at room temperature, prior to the addition of DNase stop solution and incubation for another 10 minutes at 70°C to denature the DNase.

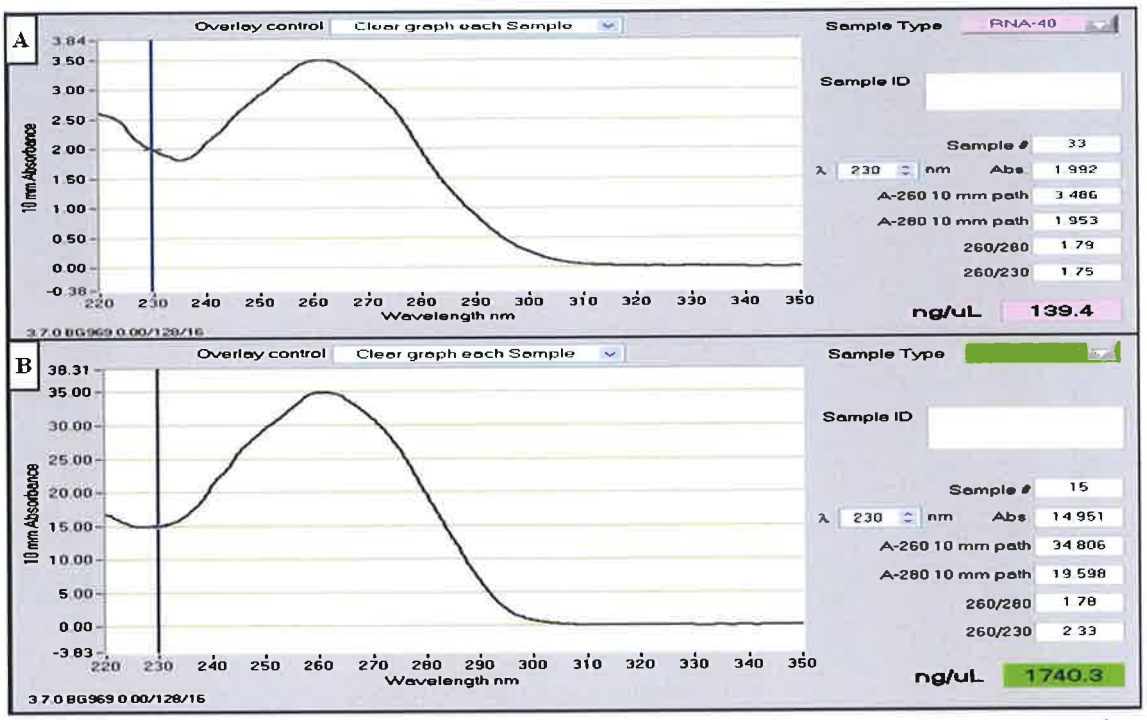

Figure 2.13. Data output from the Nanodrop®. A: RNA concentration. B: DNA concentration. Concentration is displayed in ng/µl, and purity of sample is indicated by the 260/280 and 260/230 ratios. DNA, deoxyribonucleid acid; RNA, ribonucleic acid.

2.1.10.3.3. cDNA Synthesis

In this technique, mRNA, as quantified with Nanodrop®, was transcribed into cDNA via the use of a high capacity cDNA reverse transcription kit (Applied Biosystems, California, USA). 10 µl of a sample containing 1000 ng of mRNA was added to the following reagents; 2 µl of reverse transcriptase (RT) buffer (10x), 0.8 µl of deoxynucleotide (dNTP) mix (100 mM), 2 µl of random primers (10x), 1 µl of multiscribe RT, and 4.2 µl of nuclease free water. The final volume of 20 µl was spun briefly, then

placed in a PCR machine at 25°C for 10 minutes, 37°C for 120 minutes, and 85°C for 5 minutes. Nanodrop® was utilized as described above to quantify the resultant cDNA samples.

2.1.10.3.4. PCR and qRT-PCR

Primers for OPG, RANKL and TRAIL were generated against sequences identified in the nucleotide database provided online by the National Centre for Biotechnology Information (NCBI). Primer candidates were optimized in terms of size, melting temperatures and guanine-cytosine content using Primer3 software, and checked for risk of hairpin formation and self-folding on OligoCalculator software. The final primer sets were ordered from Eurofins (Eurofins, Dublin, Ireland).

Standard PCR was utilized to test and optimize the primers in the laboratory. In brief, 1 µl of forward and 1 µl of reverse primers were added to 1 µl of a template cDNA sample, 2.5 µl of reaction buffer (10x), 2 µl of dNTP (10 mM), 1.5 µl of $MgCl_2$ (25 mM), 15.75 µl of nuclease-free water, and 0.125 µl of Taq polymerase. Samples were then subjected to cycles of denaturation and annealing in a PCR machine to allow DNA amplification to proceed. To rule out DNA contamination of the mRNA samples, negative controls (samples lacking any reverse transcriptase, and samples without any RNA added) were run with each primer set. The DNA products of the various primer sets were then analyzed via gel analysis. Agarose gel (1 g) was dissolved in 100 ml 1x TAE buffer (40 mM Tris-acetate at pH of 8.2 mixed with 1 mM of EDTA) and the solution was heated until clear, then allowed to cool to approximately 60°C prior to the addition of 10 µl SYBR Safe (Invitrogen, Groningen, The Netherlands). The resultant mix was poured into a casting rig, a comb was utilized to generate wells, and once the mix had completely cooled the chamber was filled with 1x TAE and the comb was removed. An appropriately sized DNA ladder was added to the first well, 10 µl of each DNA sample from the PCR run was added to the other wells, and the gel was then run

at 100 V for 1 hour. Samples were then visualized with the transilluminator setting on a G:Box (Syngene, Cambridge, UK) to confirm predicted band sizes for each primer pair employed. The final sequences for the S18, OPG, RANKL, TRAIL, Runx2, BSP and ALP primers, along with their size and optimum annealing temperatures, are listed in table 2.1.

Table 2.1. Primer sequences, size of product and optimal annealing temperatures for the S18, OPG, RANKL, TRAIL, Runx2, BSP and ALP primer sets utilized.

Gene	*Primer sequence*	*Annealing temperature (°C)*	*Product size (bp)*
S18	Forward: 5'-CAGCCACCCGAGATTGAGCA-3'	62	250
	Reverse: 5'-TAGTAGCGACGGGCGGTGTG-3'		
OPG	Forward: 5'-GGCAACACAGCTCACAAGAA-3'	58	241
	Reverse: 5'-CTGGGTTTGCATGCCTTTAT-3'		
RANKL	Forward: 5'-AGAGCGCAGATGGATCCTAA-3'	58	180
	Reserve: 5'-TTCCTTTTGCACAGCTCCTT-3'		
TRAIL	Forward: 5'-TTCACAGTGCTCCTGCAGTC-3'	60	170
	Reserve: 5'-ACGGAGTTGCCACTTGACTT-3'		
Runx2	Forward: 5'-GGTACCAGATGGGACTGTGG-3'	59	315
	Reverse: 5'-GAGGCGGTCAGAGAACAAAC-3'		
BSP	Forward: 5'- TCAGCATTTTGGGAATGGCC-3'	61	567
	Reverse: 5'- GAGGTTGTTGTCTTCGAGGT-3'		
ALP	Forward: 5'- GCCTGGCTACAAGGTGGTG-3'	58	293
	Reverse: 5'- GGCCAGAGCGAGCAGC-3'		

ALP, alkaline phosphatase; Bp, base pairs; BSP, bone sialoprotein; °C, Celsius; OPG, osteoprotegerin; RANKL, receptor activator of nuclear factor kappa-beta ligand; Runx2, runt-related transcription factor 2; TRAIL, tumor necrosis factor-related apoptosis-inducing ligand.

Once the primer sets were optimized, they were employed in qRT-PCR. The basic mechanism underlying qRT-PCR is as follows: if one mRNA sample has a lower level of OPG mRNA when compared to a second mRNA sample, then this difference will be maintained when the two mRNA samples are transcribed into cDNA. When the two cDNA samples are then subjected to qRT-PCR with primers for OPG (with the

amplification of DNA being monitored at the end of each PCR cycle in real time) the original difference between the samples will manifest itself as the first sample taking longer to reach an amplification threshold in comparison to the second. This difference can be quantified to allow comparison of mRNA levels between experimental conditions (figure 2.14).

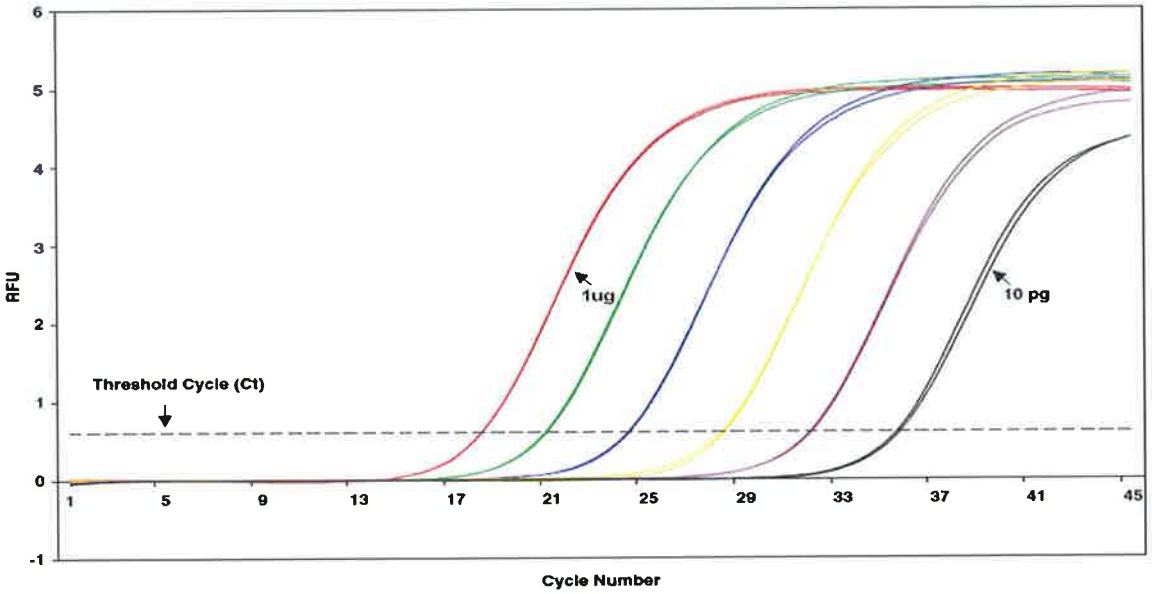

Figure 2.14. Illustration of principles of qRT-PCR. Cycles of denaturation and annealing are numbered on the x-axis. The RFU values, as read by laser, are displayed on the y-axis. The coloured lines indicate human placental cDNA samples that have undergone serial dilution (decreasing concentration from left to right), and are being amplified by primers for GAPDH. The red line (labelled as 1 ug) is from the sample with the highest concentration of cDNA, and it has been amplified at an earlier timepoint (cycle) than the other samples. The black line (labelled as 10 pg) is from the sample with the lowest concentration of cDNA, and it has been amplified at the latest timepoint (cycle). The threshold cycle (Ct) is the number of cycles each sample requires before the flourescence from its cDNA amplicification exceeds the background flourescence. cDNA, complimentatry deoxyribonucleic cid; Ct, threshold cycle; qRT-PCR, quantitative real-time polymerase chain reaction; RFU, relative flourescence units. Image provided by Affymetric.

To perform qRT-PCR, cDNA samples generated were mixed with the primer sets for the gene under examination (e.g. OPG) along with SYBR Green Master (Rox), from Roche Diagnostics (Basel, Switzerland). SYBR Green Master (Rox) contains SYBR Green I, a dye that fluoresces when bound to double-stranded DNA, TaqDNA polymerase, nucleotides, and a passive reference dye (Rox). The mix of SYBR Green Master (Rox), cDNA and primers was as follows; 1 µl of forward primer, 1 µl of reverse primer (both at 10 µM concentrations), 2 µl of cDNA at 500 ng/µl, 12 µl of SYBR Green

Master (Rox) and 9 µl of water. With a final volume of 25 µl, this mix filled one well of a 96-well qRT-PCR plate. This mix was then subjected to repeated cycles of denaturing and annealing in the Applied Biosystems 7900HT Fast RT-PCR machine. Samples were denatured at 95°C for 10 minutes, followed by 45 cycles of 95°C for 15 seconds alternating with a primer-specific temperature (57-62°C) for 1 minute. At the end of each cycle a laser read the fluorescence generated by the SYBR Green I binding to DNA, and in this manner the amount of DNA product formed during each PCR cycle was quantified and graphically visualized in real time. The differences in time to amplification were analyzed via the comparative Ct method (ΔΔCt), as first described by Livak *et al.* [228].

With regards to quality control and normalization procedures, all samples were analyzed in triplicate. S18, a housekeeping gene that was not affected by the experimental conditions in question was routinely employed to normalize cDNA quantity between samples. Furthermore, the use of the passive reference dye Rox allowed the SYBR Green I fluorescence to be normalized for non-PCR-related fluctuations between wells. Finally, melt-curve analysis was carried out to ensure single product formation and to assess for non-specific binding and primer-dimer formation.

2.1.11. In Vitro Statistical Analysis

Data from the *in vitro* experiments were analyzed using GraphPad Prism version 4.03 (Graphpad software, California, USA). Data are expressed in mean ± standard error of the mean (SEM). Unless otherwise indicated all experiments were conducted to n=18. Statistical comparisons between controls versus treated groups were made by analysis of variance (ANOVA) in conjunction with a Dunnett's post-hoc test for multiple comparisons. Student' s unpaired *t*-test was employed for pair-wise comparisons. A value of $p<0.05$ was considered significant.

2.2. *In Vivo* Experiment

2.2.1. Introduction

In the *in vivo* component of Study III of the present thesis, patients with type 2 diabetes who were; a) remaining on oral diabetes medications, b) commencing add-on therapy in the form of liraglutide therapy or c) commencing add-on therapy in the form of insulin were recruited into a prospective, observational study. These patients had blood tests, anthropometric measurements, and CT scans of their coronary arteries at the beginning and end of the study. The hypothesis of this study was that treatment with insulin would accelerate CAC in these patients, whereas treatment with liraglutide would have either a neutral or inhibitory effect on CAC. Accordingly, the primary endpoint of the study was the progression in CAC score of these patients over the timeframe studied (16 months), stratified by whether the patients had remained on oral diabetes medications (control group), whether they had commenced liraglutide, or whether they had commenced insulin.

2.2.2. Ethical Approval and Study Design

This was a multi-centre prospective observational study conducted between 2011 and 2013 in Beaumont Hospital (Beaumont, Dublin, Ireland), James Connolly Memorial Hospital (Blanchardstown, Dublin, Ireland), and the Sports Surgery Clinic (Santry, Dublin, Ireland). Patients were recruited from Beaumont and Connolly hospitals, and the CAC scans were performed and analyzed in the Sports Surgery Clinic. Ethics approval was sought and received from the local ethics committees in all three centres, and included approval for the transfer of coded patient information and blood samples between the centres.

It must be noted that this was an observational study only. All diabetes treatment decisions were made by the patient's diabetes team, and no diabetes treatment

regimes were altered due to the patient's participation in this study. This study, therefore, was not a randomized control trial of a medical product. Instead, patients were recruited if their diabetes team had made a decision regarding their diabetes treatment that rendered them eligible for entry into the study. Equally, if further treatment decisions rendered them ineligible for continued participation in the study, they were removed from the study and their data were not included in the final analysis. As such, this research was defined as a multicentre, prospective observational trial.

2.2.3. Inclusion and Exclusion Criteria

Inclusion criteria for this study included the following; a) confirmed T2DM (diagnosis made by primary diabetes team) for at least 6 months prior to recruitment, and b) To be eligible for the control group, it was necessary for patients to be on metformin ± sulphonylurea therapy for at least 6 months. To be eligible for the liraglutide or insulin arms, it was necessary for patients to have been on metformin ± sulphonylurea for at least 6 months in addition to having been referred to the local diabetes centre for the commencement of liraglutide or basal insulin (± bolus insulin).

Exclusion criteria for this study included the following; a) age less than 30 years, b) pregnancy, breastfeeding, or women of childbearing potential (unacceptable radiation exposure risk), c) stroke or myocardial infarction in the preceding 6 months (known to cause acute fluctuations in circulating OPG and RANKL concentrations), d) eGFR < 60 ml/min/1.73m^2 (ESRF exerts significant effects on multiple aspects of VC which could confound any potential medication effect, e) active malignancy, f) treatment with medications known to interfere with circulating OPG concentrations and/or alter bone metabolism including denosumab, thiazolideinediones, DPP-IV inhibitors, acarbose, glinides, strontium or calcitonin within the preceding 6 months, or at any point, g) fracture within the preceding 6 months (known to affect circulating OPG concentrations), and h) unable to read or give informed consent.

2.2.4. Patient Recruitment and Participation in the Study

An overview of the study protocol is illustrated in figure 2.15. Patients who met the inclusion and exclusion criteria were identified and recruited from the diabetes clinics in Beaumont and Connolly Hospitals. If patients were agreeable in clinic, they were provided with an information leaflet on the details of the study and their participation in it. After a minimum of 1 week to allow patients to consider the study, they were contacted by phone, and if they agreed to enter the study, a time and date was set for the patient to attend the diabetes day centre (DDC) in their respective hospital. At this meeting any remaining questions were answered, eligibility criteria were reviewed, and voluntary informed consent was obtained. A separate information leaflet was dispatched to the patient's general practitioner. Patients were then scheduled for a morning visit to the DDC for fasting blood tests and anthropometric measurements, and a CAC CT scan was scheduled in the Sports Surgery Clinic. In the case of patients who were due to commence liraglutide or insulin, these visits were conducted within the 2 weeks immediately prior to starting these medications.

During the study, patients were contacted every 6 months by phone to determine if they continued to meet the inclusion and exclusion criteria for the study, and to answer any queries that they had regarding the study. If it appeared that any of the exclusion criteria had been met during these contacts, the patient in question was invited back to the DDC for another meeting, and upon confirmation that an exclusion criteria had been met the patient's participation in the study ceased. At the conclusion of the study timeframe, patients were scheduled to re-attend their DDC, at which point fasting blood tests and anthropometric measurements were repeated, and a second CAC CT scan was scheduled. At this point they ceased to participate in the study. At all points throughout the study the patients remained under the care of their diabetes team, who continued to follow them up upon completion of the study.

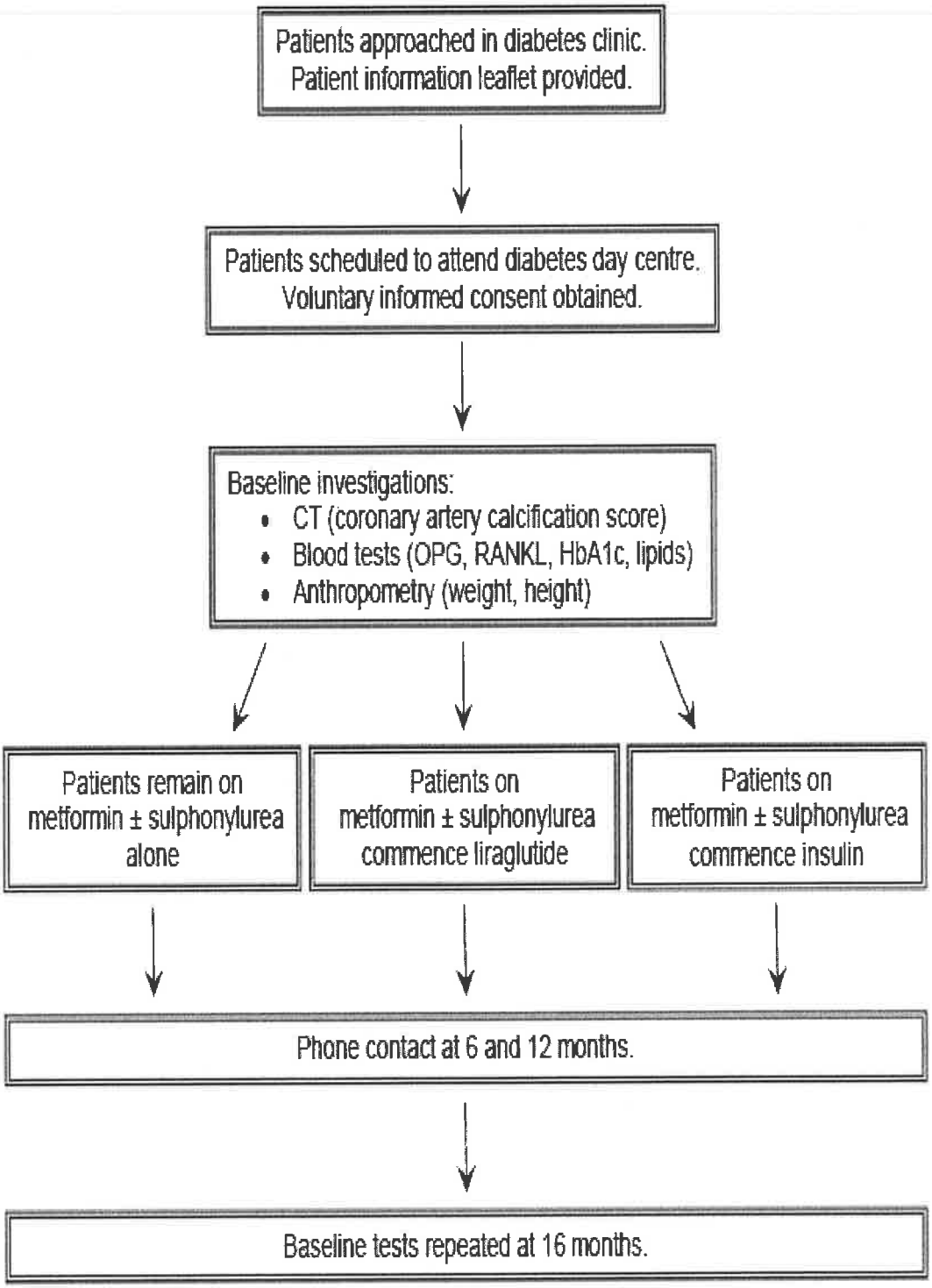

Figure 2.15. Flowchart of patient recruitment, baseline investigations and stratification into groups based on treatment regime (determined by patient's diabetes team), and follow-up until the baseline tests were repeated at the conclusion of the study.

2.2.5. Sample Collection and Measurement of In Vivo Endpoints

2.2.5.1. Anthropometric Measurements and Demographic Information

During their visits to the DDC at the beginning and end of the study, all patients had their height and weight measured, and their body-mass index (BMI) calculated. A proforma was also completed during these visits that included details of their age, gender, ethnicity, duration of diabetes, current medications (including dosages), and a comprehensive past medical history.

2.2.5.2. Blood Tests

At the beginning and end of the study period patients provided blood samples to the investigators. Blood tests were taken in the DDC with the patients fasting from midnight the night before, using a sterile technique, between 8 and 10 am. Blood samples were sent to measure renal function, lipid profiles, glycated hemoglobin A1c (HbA1c), and calcium levels (corrected for albumin) using standard laboratory techniques. eGFR was calculated with the modified diet in renal disease (MDRD) formula [229]. The remaining whole blood samples were processed to serum as follows; samples were allowed to sit at 4°C for a minimum of 30 minutes to allow clotting to occur. Samples were then centrifuged for 20 minutes at 3000 rpm, at which point the serum was aspirated off and placed in coded aliquots for storage at -80°C. ELISA was used to measure the concentrations of OPG, RANKL and TRAIL in these samples within 6 months of collection. Repeated freeze-thaw cycles of the samples were avoided. Duoset ELISA kits from R&D were utilized for this purpose.

2.2.5.3. CAC CT Scans

The CAC CT scans in this study were performed in the Radiology Department of the Sports Surgery Clinic (Santry, Dublin). The radiographers and radiologists who performed and interpreted the scan were blinded to the treatment status of the patient

(control versus liraglutide versus insulin). A GE Lightspeed VCT 64 slice CT scanner (GE Healthcare, Connecticut, USA) was used to image the coronary arteries of the patients (figure 2.16). As the goal of the imaging was to quantify calcification burden only, contrast was not administered during these scans, and no intravenous cannulation was required. Patients were instructed not to exercise or smoke for 4 hours prior to the procedure. The patient was connected to an electrocardiogram monitor, which in turn was connected to the CT scanner, allowing imaging to be timed with the cardiac cycle. The entire time taken to prepare and scan the patient was typically under 30 minutes. The resultant scans were analyzed according to the Agatson scoring system, and the coded scores were returned to the study investigators [73].

Figure 2.16. The GE Lightspeed VCT 64 slice CT scanner. The 64 rows of detectors enable this CT scanner to obtain submillimeter resolution of the coronary arteries within 4-5 heartbeats. Image provided by GE Healthcare.

2.2.6. In Vivo Statistical Analysis

Data from the *in vivo* study was analyzed using statistical package for the social sciences (SPSS) version 16 (SPSS Incorporated, Chicago, USA). Data are reported as

means ± SEM or media (25th centile - 75th centile) as appropriate. Differences between groups at baseline were assessed using one-way ANOVA or Chi-squared test, as appropriate. Differences in study variables from baseline to study completion were analyzed using a paired t-test or Wilcoxon rank test, as appropriate. To test whether exposure to liraglutide or insulin influenced the observed changes in study variables (treatment effect) over the duration of the study, an analysis of covariance (ANCOVA) was performed, utilizing the baseline value as the primary confounding variable, on the follow-up values for each variable. If a significant treatment effect was observed, Bonferroni post-hoc tests were employed to perform pairwise comparisons of the effect between the three treatment groups. To control for the differences between the groups at baseline, the analysis was repeated in a number of models in which baseline differences were added in a step-fashion. A $p<0.05$ was taken as indicative of statistical significance.

Chapter 3 - Production and Release of OPG, RANKL and TRAIL from HAECs and HASMCs

3.1. Introduction

The goal of Study I of the present thesis was to characterise the production and secretion of OPG, RANKL and TRAIL from HAECs and HASMCs *in vitro*. This assessment was performed a) under basal conditions and b) under pathological conditions associated with the development of VC.

Previous studies have indicated that OPG is released from ECs and SMCs in large quantities. These studies, however, varied significantly in terms of the EC/SMC populations utilized (e.g. murine versus human, aortic versus umbilical), the methods by which OPG was measured (e.g. ELISAs versus western blot), and whether the cell populations were exposed to basal or pathological conditions [39,138,144,230,231]. As such, I surmised that the heterogeneous data generated by these studies merited confirmation and extrapolation in a single series of experiments on HAECs and HASMCs, with measurement of both protein release and mRNA levels, and involving exposure to both basal and pathological conditions.

With regards to RANKL and TRAIL, the data have been conflicting regarding the source of these proteins within the vascular wall. Both RANKL and TRAIL have been identified in atherosclerotic, calcified arteries *in vivo*, but it is unclear if their origin is vascular (e.g. ECs and SMCs) or immune (e.g. lymphoctes and monocytes) in nature [144,148,179,180,232,233]. Study I, therefore, included a comprehensive assessment of the production and release of RANKL and TRAIL from HAECs and HASMCs, to determine whether these cell populations produce significant amounts of either protein.

The pathological conditions assessed in this study were a representative sample of the known promoters of VC, including inflammation (as may be found in atherosclerosis),

hyperglycemia and hyperinsulinemia (as may be found in T2DM), and cyclic strain (the circumferential stretching of the vascular wall deriving from pulsatile blood flow and pulse pressure), a hemodynamic force that can exert both pro and anti-atherogenic effects within the vasculature in an amplitude-, frequency- and location-dependent manner [46,234-238]. To ensure that the *in vitro* data generated in these experiemnts would complement the clinical data generated in Study III, the insulin analogue glargine was used in place of human insulin. In addition to confirming and expanding upon previous research findings in this area, Study I represents, to the best of my knowledge, the first assessment of the effects of an insulin analogue (as opposed to native insulin) on the OPG/RANKL/TRAIL system in vascular cells, despite the widespread use of insulin analogues in the treatment of diabetes. Furthermore, Study I represents the first assessment of the effects of cyclic strain upon this system.

As a final point, the present study was also performed to provide baseline data on the OPG/RANKL/TRAIL system when HAECs and HASMCs were assessed separately prior to the commencement of the conditioned media and co-culture experiments of Study II.

3.2. Experiments and Results

HAECs and HASMCs were grown (figure 3.1) in Promocell growth media with supplements as previously described and seeded to either 6-well plates (for the addition of TNF-α, glucose or insulin) or Bioflex® plates for cyclic strain experiments. At confluency, the cell cultures were washed, fresh growth media with supplements was added, and the experimental conditions were initiated. To quantify and characterise the basal release of OPG, RANKL and TRAIL from HAECs and HASMCs, the supernatant media was harvested from cell cultures after 24, 48 and 72 hours under basal conditions and subjected to ELISA. To quantify the effects of TNF-α, glucose, insulin

glargine and cyclic strain on the release of OPG, RANKL and TRAIL, the supernatant media was harvested from cell cultures after 72 hours of exposure to these conditions and also subjected to ELISA. With regards to the mRNA levels for OPG, RANKL or TRAIL in HAECs and HASMCs, this endpoint was also harvested from cell cultures after 72 hours of exposure to either basal or pathological conditions. Finally, concentrations of OPG, RANKL and TRAIL in cell lysates from HAECs and HASMCs were measured by ELISA after 24 hours under basal conditions.

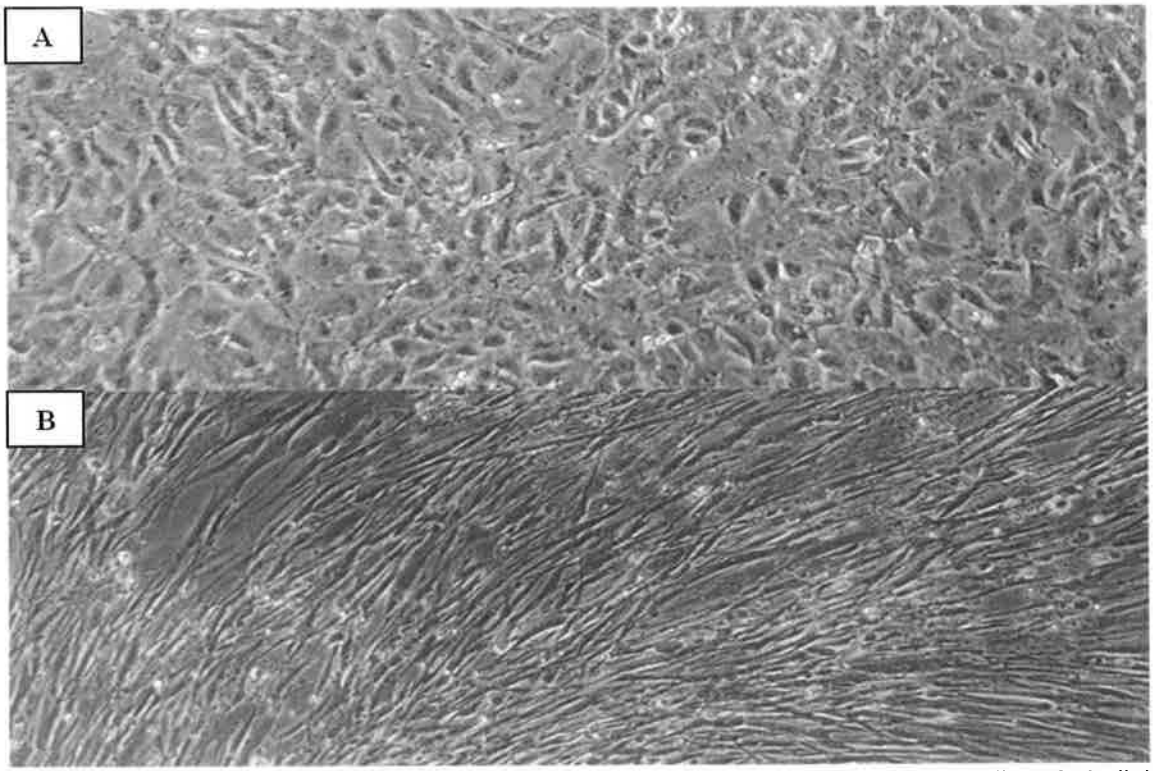

Figure 3.1. A: HAECs were isolated from the aorta and cultured with Promocell endothelial growth media MV. HAECs at passage number 5 can be seen in this figure demonstrating the characteristic cobblestone morphology thay assume when cultured under static conditions. B: HASMCs were isolated from the aorta and cultured with Promocell smooth muscle growth media. HASMCs at passage 6 can be seen in this figure demonstraing the characteristic parallel growth patterns they assume when cultured inder static conditions. Images were taken using the Nikon eclipse TS100 microscope. HAEC, human aortic endothelial cell, HASMC, human aortic smooth muscle cell.

3.2.1. Production and Release of OPG, RANKL and TRAIL from HAECs

Upon examination of the release of OPG under basal conditions, HAECs were noted to release OPG into the supernatant media, achieving concentrations of 24.5±1.4 pg/10000 cells after 72 hours in culture (figure 3.2). This equated to absolute concentrations of 83.7±6.1 pg/ml in the supernatant media. Exposure of HAECs to

TNF-α increased the release of OPG in a dose dependent manner, as did the addition of insulin glargine. Increasing concentrations of glucose also increased OPG release (up to a maximum of 15 mmol/l), but to a lesser degree than insulin glargine or TNF-α. Cyclic strain at 5% had no significant effect on OPG release (figure 3.3).

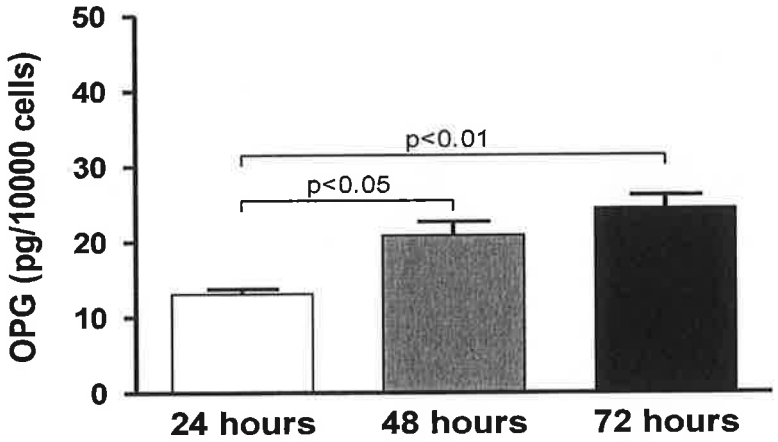

Figure 3.2. Concentrations of OPG when measured by ELISA in the supernatant media of HAECs after 24, 48 and 72 hours under basal conditions, displayed in pg/10000 cells following correction for viable HAEC population. Data are given as mean±SEM. There was no detectable OPG in the growth media prior to conditioning by HAECs. n=18 for each time-point. ELISA, enzyme-linked immunosorbent assay; HAEC, human aortic endothelial cell; OPG; osteoprotegerin; SEM, standard error of the mean.

On examination of the release of RANKL and TRAIL into the supernatant media, no significant concentrations of either free, bound, or total RANKL or TRAIL were detected on any of the assays utilized, under both basal conditions, and following the addition of TNF-α, glucose, insulin glargine or cyclic strain. To ensure these negative results were not caused by any factors within the supernatant media interfering with the performance of the assay, RANKL and TRAIL standards were mixed in equal volume with a sample of the supernatant media and subject to analysis, whereupon no interference of this nature was noted.

The presence and concentration of OPG, RANKL and TRAIL was also measured in HAEC whole cell protein lysates, and a similar picture to that of the supernatant media was observed. Whilst OPG presence was demonstrated at significant concentrations

within HAEC lysates at baseline (816±41 pg/mg cell protein, n=12), approximately 20 times the concentration of OPG within the supernatant media, no significant concentrations of RANKL or TRAIL were detected.

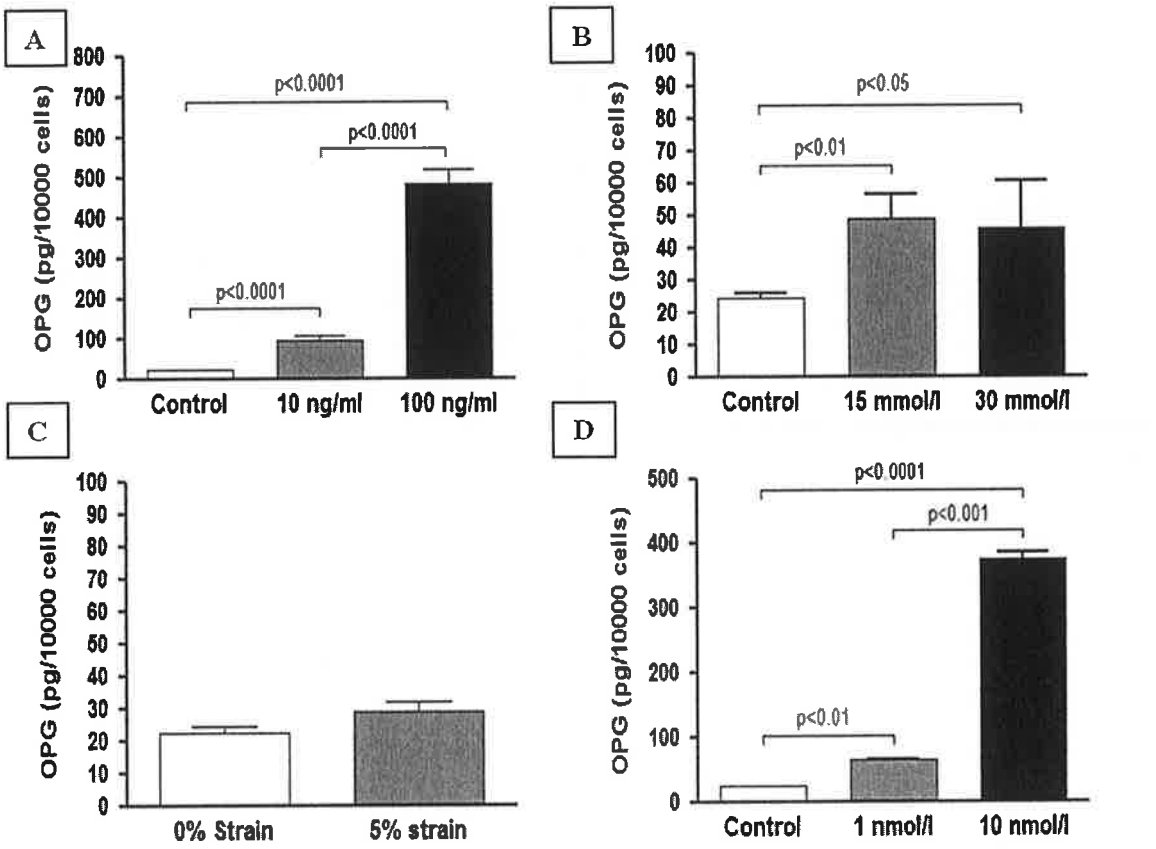

Figure 3.3. Concentrations of OPG when measured by ELISA in the supernatant media of HAECs after 72 hours of exposure to A: TNF-α (at 10 ng/ml and 100 ng/ml), B: glucose (at 15 mmol/l and 30 mmol/l concentrations), C: cyclic strain (5%), and D: insulin glargine (concentrations of 1 nmol/l and 10 nmol/l), displayed in pg/10000 cells following correction for viable HAEC population. Data are given as mean±SEM. n=12 for cyclic strain experiments, n=18 for all other experiments. ELISA, enzyme-linked immunosorbent assay; HAEC, human aortic endothelial cell; OPG; osteoprotegerin; SEM, standard error of the mean; TNF-α, tumor necrosis factor alpha.

Using the techniques described in chapter 2, mRNA samples were harvested and processed into cDNA. Using the selected primers for S18, OPG, RANKL and TRAIL, mRNA samples underwent RT-PCR and qRT-PCR. Bands of correct predicted size were produced from HAEC and HASMC samples for all 4 genes of interest, confirming mRNA expression of each of these genes in the 2 cell populations (figure 3.4). A melt-curve analysis of each primer set showed no evidence of primer self-dimerization or any significant deficits in specificity. The use of qRT-PCR to quantify differences in

mRNA levels between samples is illustrated in figure 3.5. The effects of TNF-α, glucose, insulin glargine and cyclic strain on OPG, RANKL and TRAIL mRNA levels can be seen in figure 3.6. TNF-α at pathophysiological concentrations increased the concentration of OPG mRNA, but at supraphysiological levels had the opposite effect. 5% cyclic strain also down-regulated OPG mRNA, as did insulin glargine at both pathophysiological and supraphysiological concentrations. Interestingly, hyperglycemia did not exert any demonstrable effects. With regards to both RANKL and TRAIL, mRNA concentrations of both of these targets were reduced by TNF-α, cyclic strain and insulin glargrine, whereas, once again, glucose did not exhibit any demonstrable effects.

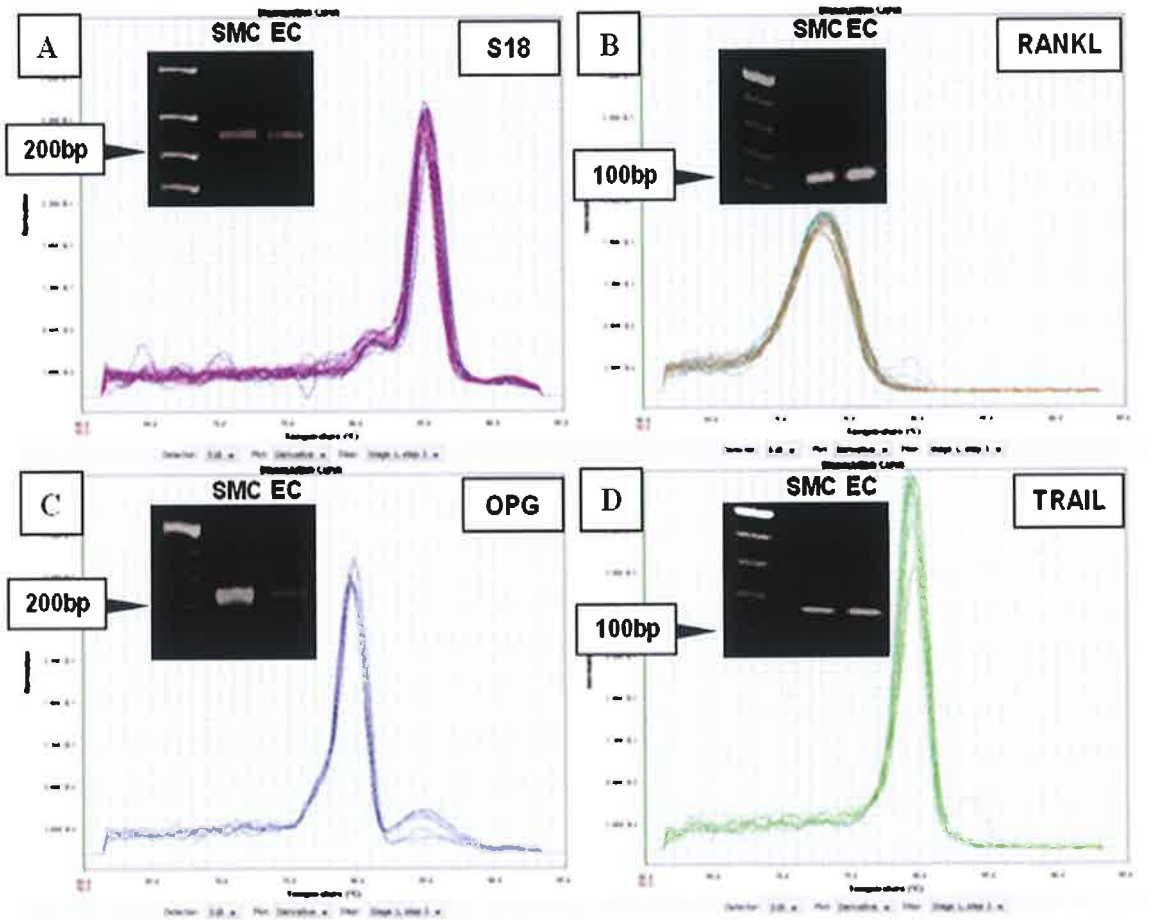

Figure 3.4. Melt curve analysis carried out on Study I primers to determine specificity. Inserts demonstrate representative bands produced by respective primers on qRT-PCR with HAEC and HASMC cDNA, confirming mRNA expression of these genes in the two cell populations. A: S18 primers. B: RANKL primers. C: OPG primers. D: TRAIL primers. Bp, base pair; cDNA, complimentary deoxyribonucleic acid; EC, endothelial cell; HAEC, human aortic endothelial cell; HASMC, human aortic smooth muscle cell; OPG, osteoprotegerin; RANKL, receptor activator of nuclear factor kappa-beta ligand; qRT-PCR, quantitative real-time polymerase chain reaction; SMC, smooth muscle cell; TRAIL, tumor necrosis factor-related apoptosis-inducing ligand.

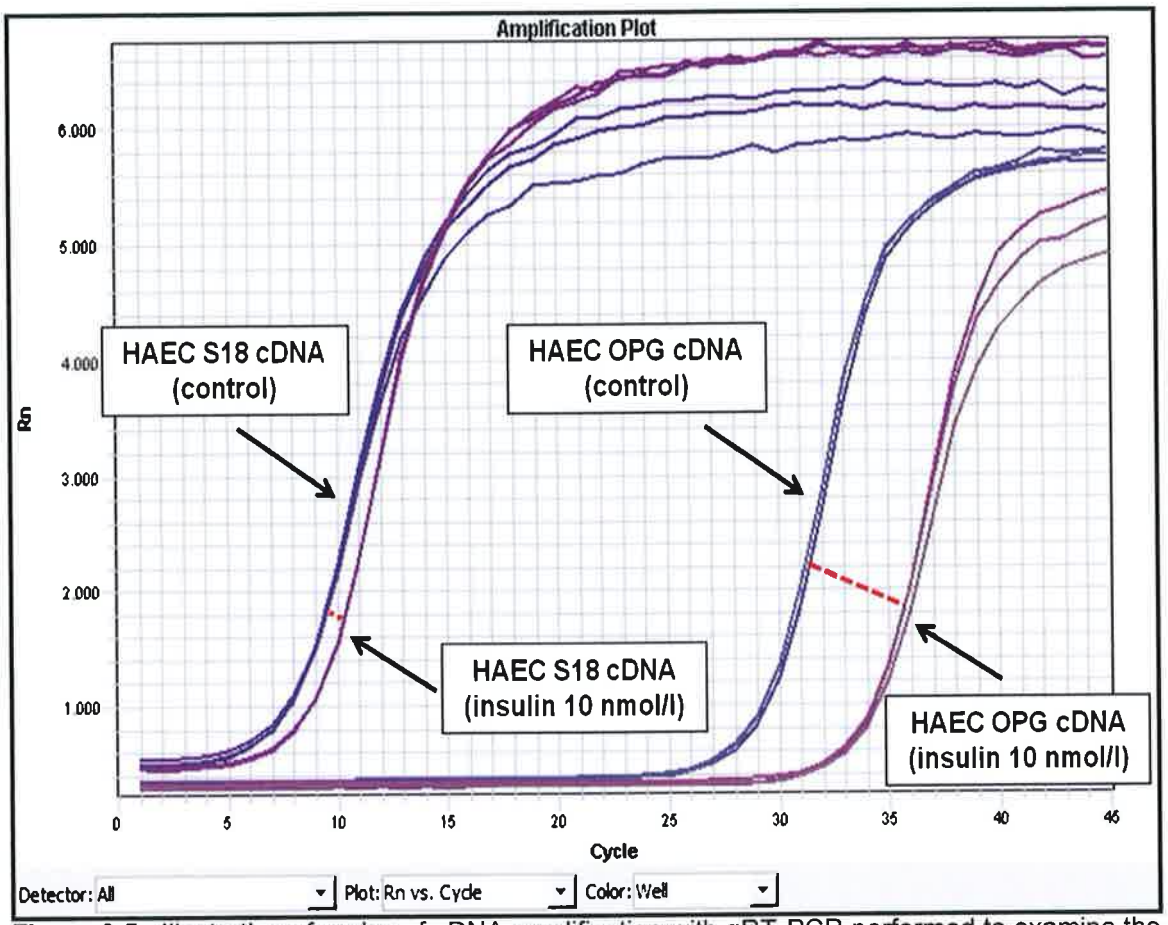

Figure 3.5. Illustration of cycles of cDNA amplification with qRT-PCR performed to examine the effects of insulin glargine on OPG mRNA levels in HAECs. Blue lines indicate control HAEC samples, purple samples indicate HAEC samples exposed to insulin glargine at 10 nmol/l. Rox was utilized to normalize non-PCR-related flourescence fluctuations between wells. S18 cDNA served as a housekeeping control for the quantity of cDNA between samples, and can be seen to amplify in the control and insulin glargine-exposed samples at a relatively early point in the cycles of denaturation and annealing (labelled), whereas the OPG cDNA amplified at a later point (labelled). Red dashed lines illustrate that while S18 cDNA from the control and insulin glargine-treated samples amplified within a cycle of each other, the OPG cDNA from the insulin glargine-treated samples amplified significantly later in comparison to the OPG cDNA from the controls. This indicates a significantly lesser quantity of OPG cDNA (and hence mRNA) in the insulin glargine-treated samples. cDNA, complimentary deoxyribonucleic acid; HAEC, human aortic endothelial cells; mRNA, messenger ribonucleic acid; OPG, osteoprotegerin; PCR, polymerase chain reaction; qRT-PCR, quantitative real-time polymerase chain reaction; Rn, normalized reported signal.

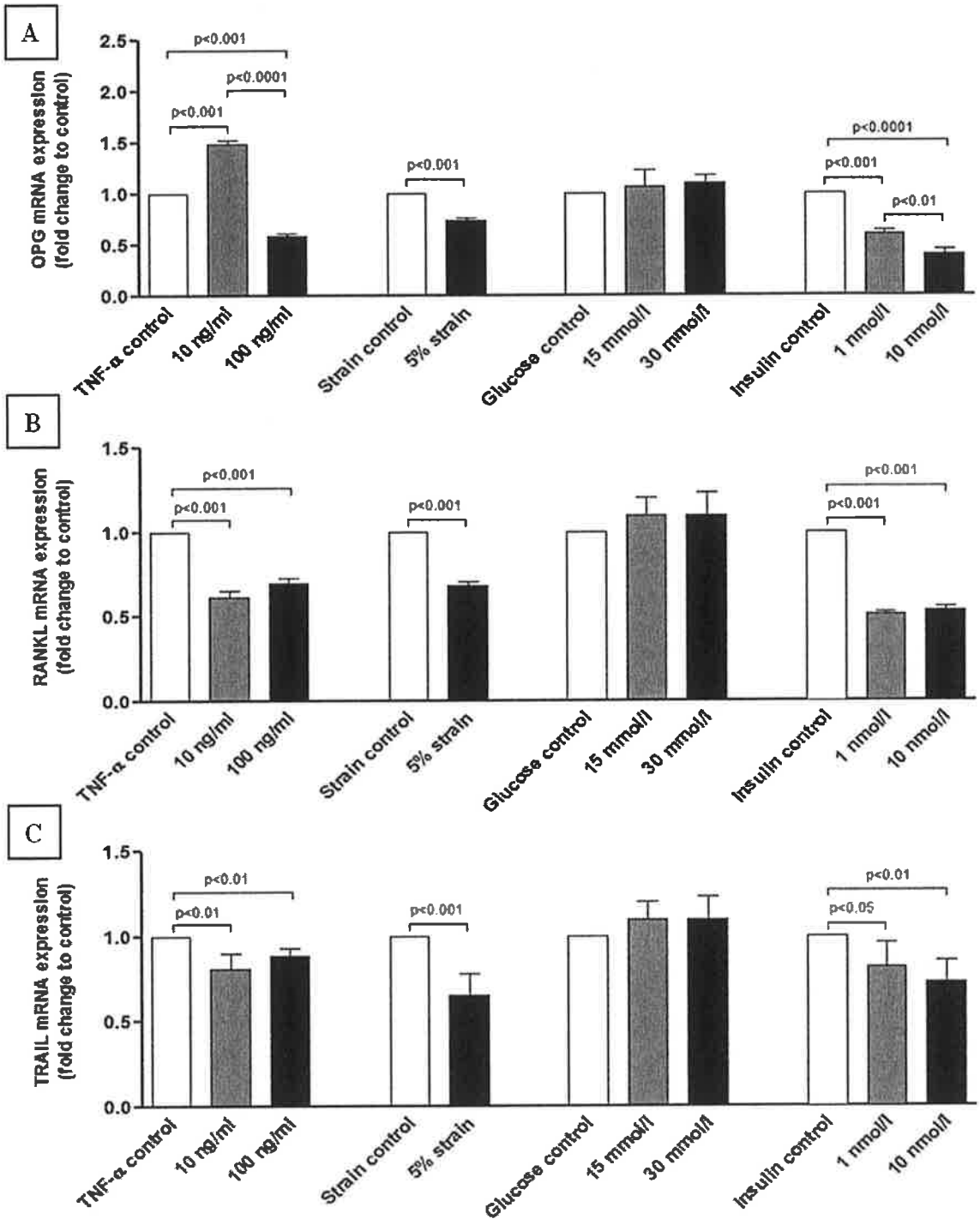

Figure 3.6. Effects, on HAECs, of 72 hours of exposure to TNF-α (10 ng/ml and 100 ng/ml), cyclic strain (0 and 5%), glucose (15 mmol/l and 30 mmol/l) and insulin glargine (1 nmol/l and 10 nmol/l) on A: levels of OPG, B: RANKL, and C: TRAIL mRNA. mRNA differences are expressed as the fold change in mRNA levels relative to control. Data are given as mean±SEM. During the qRT-PCR, S18 was utilized to normalize differences in total cDNA quantity between samples, and Rox was utilized to normalize non-PCR-related flourescence fluctuations between wells. n=12 for cyclic strain experiments, n=18 for all other experiments. cDNA, complimentary deoxyribonucleic acid; HAEC, human aortic endothelial cell; mRNA, messenger ribonucleic acid; OPG, osteoprotegerin; RANKL, receptor activator of nuclear factor kappa-beta ligand; SEM, standard error of the mean; TNF-α, tumor necrosis factor alpha; TRAIL, tumor necrosis factor-related apoptosis-inducing ligand.

3.2.2. Production and Release of OPG, RANKL and TRAIL from HASMCs

With regards to the release of OPG from HASMCs under basal conditions (figure 3.7), these cells were noted to release large quantities of OPG into the supernatant media when measured by ELISA, with OPG concentrations of 11910±1409 pg/10000 cells (absolute concentrations of 32562±2262 pg/ml) after 72 hours in culture (in comparison, high circulating concentrations of OPG in humans, using the Duoset ELISA, would be approximately 1000 pg/ml [239]). TNF-α increased the release of OPG from HASMCs into the supernatant media in a dose-dependent fashion, and 10% cyclic strain also caused a significant increase in OPG release. Hyperglycemia (15 mmol/l or 30 mmol/l) did not affect OPG release, but insulin glargine completely blocked OPG release at both pathophysiological and supraphysiological concentrations (figure 3.8).

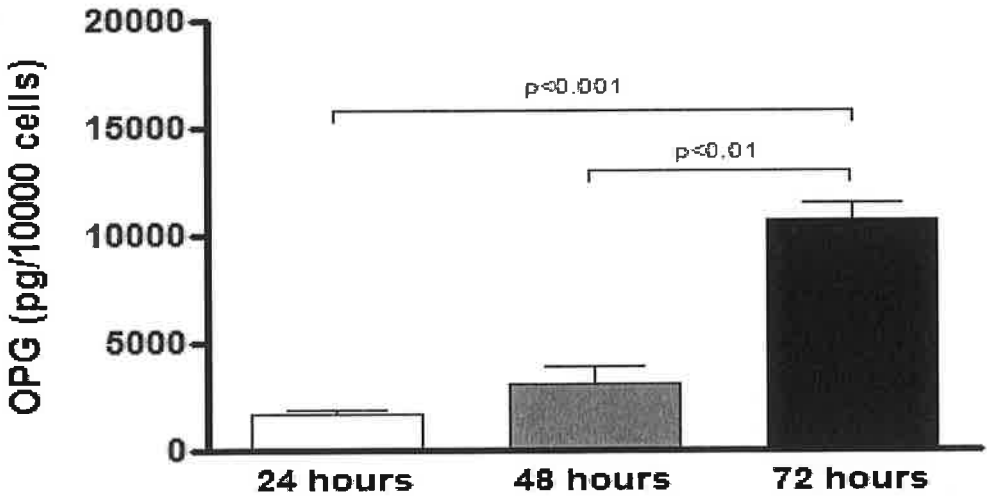

Figure 3.7. Concentrations of OPG when measured by ELISA in the supernatant media of HASMCs after 24, 48 and 72 hours under basal conditions, displayed in pg/10000 cells following correction for viable HASMC population. Data are given as mean±SEM. There was no detectable OPG in the growth media prior to exposure to HASMCs. n=18 for each time point. ELISA, enzyme-linked immunosorbent assay; HASMC, human aortic smooth muscle cell; OPG, osteoprotegerin; SEM, standard error of the mean.

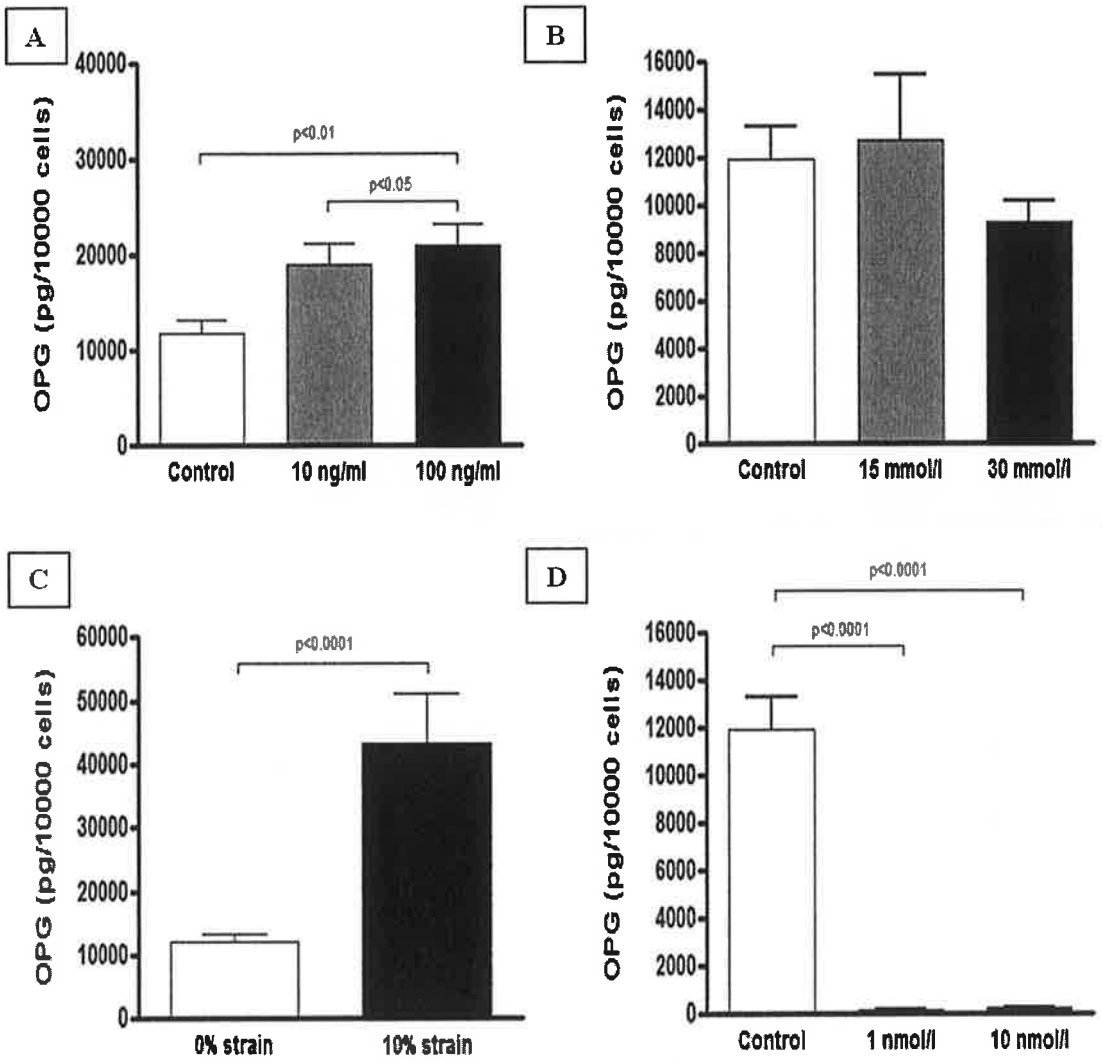

Figure 3.8. Concentrations of OPG when measured by ELISA in the supernatant media of HASMCs after 72 hours of exposure to A: TNF-α (at 10 ng/ml and 100 ng/ml), B: glucose (at 15 mmol/l and 30 mmol/l concentrations), C: cyclic strain (10%, bottom), and D: insulin glargine (concentrations of 1 nmol/l and 10 nmol/l, bottom right), displayed in pg/10000 cells following correction for viable HASMC population. Data are given as mean±SEM. Insulin exposure was associated with a large decrease in OPG to concentrations of 201±27 pg/10000 cells (1 nmol/l insulin) and 282±13 pg/10000 cells (10 nmol/l insulin). n=18 for all experiments. ELISA, enzyme-linked immunosorbent assay; HASMC, human aortic smooth muscle cell; OPG; osteoprotegerin; SEM, standard error of the mean; TNF-α, tumor necrosis factor alpha.

With regards to the release of RANKL and TRAIL into the supernatant media, and in a similar fashion to the HAEC experiments, no significant concentrations of either free, bound, or total RANKL or TRAIL were detected on any of the ELISA assays utilized, under both basal conditions and following the addition of TNF-α, glucose, insulin glargine or 10% cyclic strain. To ensure that there was no interference from endogenous OPG production, or any other factors in the supernatant media, RANKL

and TRAIL standards were mixed with equal volumes of the supernatant media and subjected to ELISA, and no interference of this nature was noted. With regards to the HASMC whole cell protein lysates (harvested at 24 hours), high concentrations of OPG (55386±15324 pg/mg cell protein, n=10) were detected. As with supernatant media samples, however, no significant concentrations of either RANKL or TRAIL were detected in the lysates.

The effects of TNF-α, glucose, insulin glargine and 10% cyclic strain on levels of OPG, RANKL and TRAIL mRNA in HASMCs are reported in figure 3.9. Exposure to TNF-α was associated with an increase in OPG mRNA levels at both pathophysiological and supraphysiological concentrations. Furthermore, and in contrast to HAECs, an increase in the levels of both RANKL and TRAIL mRNA was seen with supraphysiological concentrations of TNF-α. Cyclic strain at 10% was associated with a reduction in OPG mRNA levels, increased RANKL mRNA concentrations, and was not associated with any significant effect on levels of TRAIL mRNA. No significant changes in the levels of OPG, RANKL or TRAIL mRNA were seen with glucose at 15 mmol/l or 30 mmol/l. Finally, exposure to insulin glargine was associated with a significant decrease in the levels of OPG mRNA (at both pathophysiological and supraphysiological concentrations) along with a significant increase in the levels of RANKL mRNA at (supraphysiological concentrations). Exposure to insulin glargine was not associated with any significant changes in levels of TRAIL mRNA.

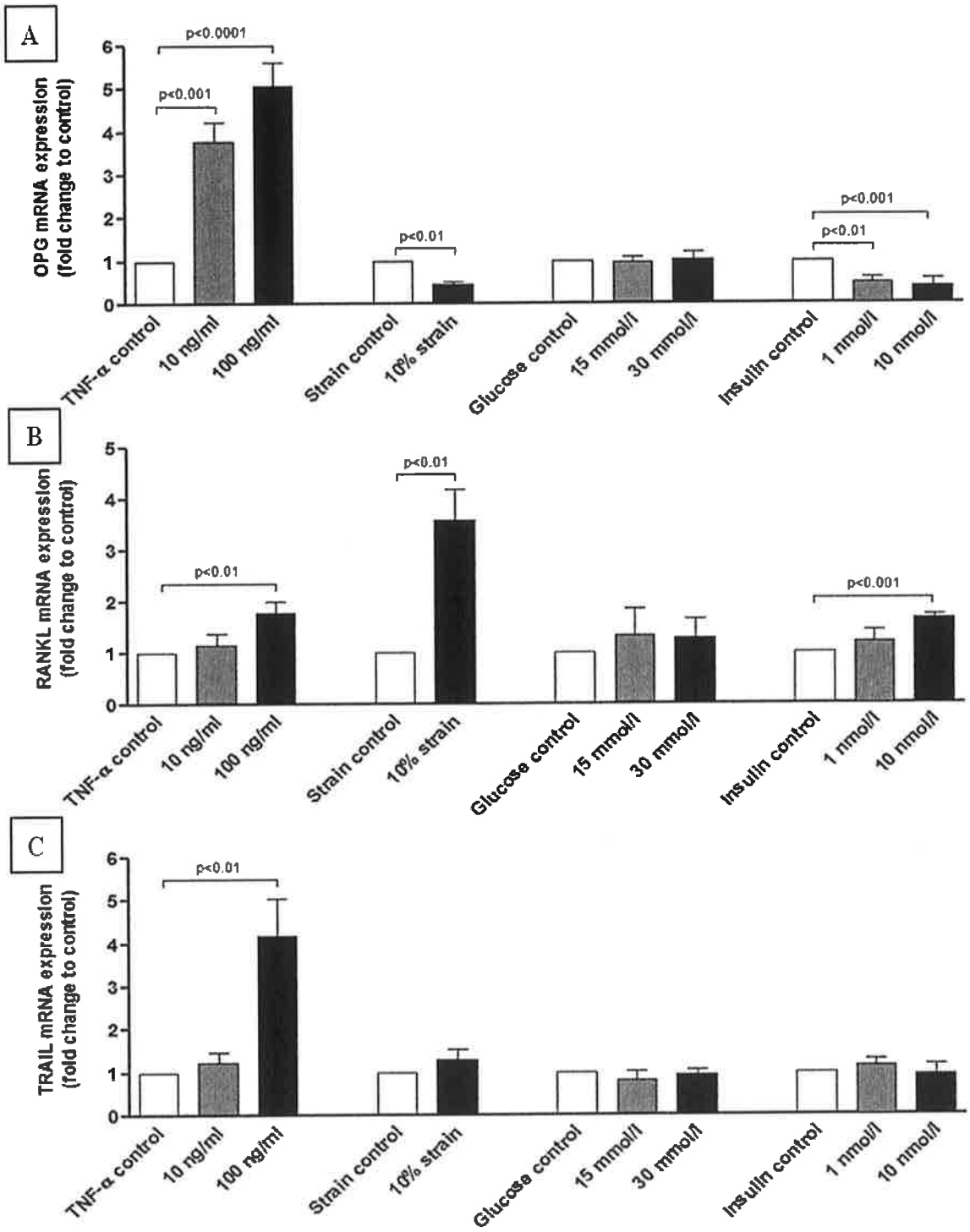

Figure 3.9. Effects, on HASMCs, of 72 hours of exposure to TNF-α (10 ng/ml and 100 ng/ml), cyclic strain (0 and 10%), glucose (15 mmol/l and 30 mmol/l) and insulin glargine (1 nmol/l and 10 nmol/l) on A: levels of OPG, B: RANKL, and C: TRAIL mRNA. mRNA differences are expressed as the fold change in mRNA levels relative to control. Data are given as mean±SEM. During the qRT-PCR, S18 was utilized to normalize differences in total cDNA quantity between samples, and Rox was utilized to normalize non-PCR-related flourescence fluctuations between wells. n=18 for all experiments. cDNA, complimentary deoxyribonucleic acid; HASMC, human aortic smooth muscle cell; mRNA, messenger ribonucleic acid; OPG, osteoprotegerin; qRT-PCR, quantitative real-time polymerase chain reaction; RANKL, receptor activator of nuclear factor kappa-beta ligand; TNF-α, tumor necrosis factor alpha; TRAIL, tumor necrosis factor-related apoptosis-inducing ligand.

3.3. Discussion

In Study I, I characterized the production and release of OPG, RANKL and TRAIL *in vitro*, from HAECs and HASMCs under basal and pathological conditions, the latter including hyperinsulinemia, hyperglycemia, high concentrations of TNF-α, and cyclic strain. All of these experimental conditions have been associated with aspects of both diffuse and localized atherosclerosis and VC of the aorta *in vivo*, and the aorta is recognized as a vascular bed that is prone to calcification [28,46,234-238]. Previous characterizations of OPG and its ligands within the vasculature have typically focused on one vascular cell population in isolation, often harvested from sites that have not been linked to VC *in vivo* (such as the umbilical vein), and have tested a limited range of experimental conditions [28,116,138,187,230,231]. Study I, therefore, represents the first comprehensive assessment of the OPG/RANKL/TRAIL system to incorporate both human endothelial and smooth muscle vascular cell populations, harvested from a vascular site of clinical relevance, and tested with inflammatory, hyperglycemic, hyperinsulinemic and strain conditions. Furthermore, as noted previously, data regarding the effects of both insulin glargine and cyclic strain on this system in vascular cells is highly novel, with neither of these relevant stimuli studied with regards to their effects on OPG and its ligands in vascular cells to date.

3.3.1. Production and Release of OPG, RANKL and TRAIL by HAECs

3.3.1.1. OPG

Upon assessment of OPG concentrations in supernatant media samples, as measured by ELISA, HAECs were noted to release detectable amounts of OPG under basal conditions. This release of OPG increased dose-dependently following exposure to TNF-α and insulin. Exposure to glucose was associated with a more modest, albeit significant, increase. Cyclic strain at 5% had no effect on OPG release from HAECs. OPG was also detected in HAEC whole cell protein lysates under basal conditions.

With regards to mRNA, transcripts for OPG, RANKL and TRAIL were demonstrated in HAECs. Consistent with the ELISA data, an increase in the levels of OPG mRNA was observed with TNF-α at 10 ng/ml concentrations, although a decrease was noted at 100 ng/ml concentrations. Interestingly, the mRNA data on the effects of glucose, insulin and cyclic strain also showed a divergence from the ELISA results, as glucose did not affect mRNA levels of OPG, whereas both cyclic strain and insulin were associated with a decrease in levels of OPG mRNA.

3.3.1.1.1. TNF-α and OPG Secretion from HAECs

As the first study to examine the effects of multiple pathological stimuli on the OPG/RANKL/TRAIL system in a human vascular cell population with a high relevance to VC in clinical practice, Study I adds significantly to the evidence base in this area of vascular research. With regards to OPG production and release under basal conditions and following exposure to TNF-α, while Collins-Osdoby *et al.* previously reported the presence of mRNA transcripts for OPG in ECs (which increased following exposure to TNF-α), the cells utilized in these experiments were human dermal microvascular ECs, which function in a different micro- and macroenvironment in comparison to ECs in medium and large arteries. Furthermore, this group did not confirm whether these mRNA changes correlated with changes in OPG protein production and secretion [138]. Equally, while Malyankar *et al* used Western blot to demonstrate OPG release from rat aortic ECs, their results were limited by the use of a non-human cell populations, nor did they assess the effects of TNF-α on this system [230]. Finally, while Oleson *et al.* Zannettino *et al. and* Secchiero *et al.* reported that OPG was released by human ECs, and that this release was increased following exposure to both TNF-α and interleukin-one beta, these experiments were conducted in HUVEC populations [144,230,231]. As described by Bouis et al, HUVECs and HAECs differ in several respects [240], and, prior to the results of Study I, it was unclear whether these

differences extended to aspects of OPG production and release in ECs from a vascular region prone to calcification.

3.3.1.1.2. Insulin glargine, glucose and OPG Secretion from HAECs

In comparison to TNF-α, there are limited data on the effects of insulin and glucose on OPG production and release from ECs, with only one previous paper examining these variables on a human vascular cell population, published by Secchiero *et al.* [231]. In contrast to my own findings that insulin glargine and glucose increased OPG release by HAECs, this group reported no effects on OPG release following exposure of HUVECs to glucose (30 mmol/l) and insulin (1 µmol/l). In addition to the afore-mentioned differences between HUVECs and HAECs, there are a number of other potential explanations for the discrepancies between their results and my own. Firstly, their study utilized insulin at significantly higher concentrations than would be encountered by ECs *in vivo*, which limits, to a degree, the clinical applicability of their data, and was an approach I avoided with the use of physiologically relevant concentrations. It is possible, therefore, that the high concentrations of insulin utilized in their study accounted for the discrepant results. It is also noteworthy that I utilized insulin glargine in my experiments. As specified previously, insulin glargine is a modified form of insulin optimized for subcutaneous delivery and subsequent stability within the circulation, and one which may also activate the growth hormone receptor on ECs. The decision to use an insulin analogue in the present thesis allowed me to examine the effects of a medication that is administered worldwide to the diabetes population, and one which was not studied in this setting previously. Furthermore, studying insulin glargine and vascular cells ensured that my *in vitro* work correlated with the clinical data in Study III. Nonetheless, I cannot exclude the possibility that the use of insulin glargine may have led to discrepancies between my data and those generated by studies using native insulin, and further research comparing the effects of

the ever-increasing number of insulin analogues available against human insulin will be necessary to examine this issue in more detail.

3.3.1.1.3. Cyclic strain and OPG Secretion from HAECs

Cyclic strain is the repetitive circumferential stretching of the vessel wall in synchronization with the cardiac cycle. Mechanical distension of this nature, when physiological, can exert protective, anti-atherogenic effects on the vasculature. When dysregulated, however, cyclic strain can promote endothelial dysfunction and has been associated with atherosclerosis and hypertension [208,235]. To the best of my knowledge, the effects of cyclic strain on the OPG/RANKL/TRAIL system in HAECs have not been studied previously, and as such the data generated in Study are entirely novel. In the present study we noted that OPG secretion from HAECs did not alter under conditions of increased cyclic statin. As this is a naescent area of research, it is not possible to draw definitive conclusions regarding this lack of interaction. As the levels of cyclic strain established in Study 1 would typically be associated with an atheroprotective effect, however, it may be hypothesized that the secretion of OPG is not altered when a cell is exposed to 'healthier' conditions. In such a state, it is possible that the increased activity of VC inhibitors may not be required.

3.3.1.1.4. OPG Secretion from HAECs as a Response to Inflammation

On reviewing the Study I data on OPG secretion from HAECs, I hypothesize that OPG secretion from HAECs occurs as part of the response of these cells to injury and inflammation. In addition to my own data, this hypothesis is also based upon the observation of Zannettino *et al.* that pre-formed stores of OPG co-localize with vWF within Weibel-Palade bodies in ECs (figure 3.10), and these two proteins are rapidly co-secreted by ECs as part of the immediate response to inflammatory stimuli [144]. In keeping with this theory, I observed the highest rates of OPG release following exposure to high concentrations of TNF-α, while hyperglycemia is a recognized

promoter of endothelial dysfunction that increases ROS production and upregulates pro-inflammatory genes in ECs [241]. Equally, while insulin is not generally considered a pro-inflammatory mediator, sustained levels of hyperinsulinemia have been reported to exert pro-inflammatory and pro-atherogenic effects on ECs, and may also explain the observed release of OPG as a response to injury [242]. It is notable, within the context of this theory, that the application of 5% cyclic strain was not associated with any release of OPG. At 5%, the level of cyclic strain applied to HAECs in Study I was within the physiological range of the aorta *in vivo*, and therefore differs from the other experimental conditions in that it would not be expected to exert pro-inflammatory effects [208].

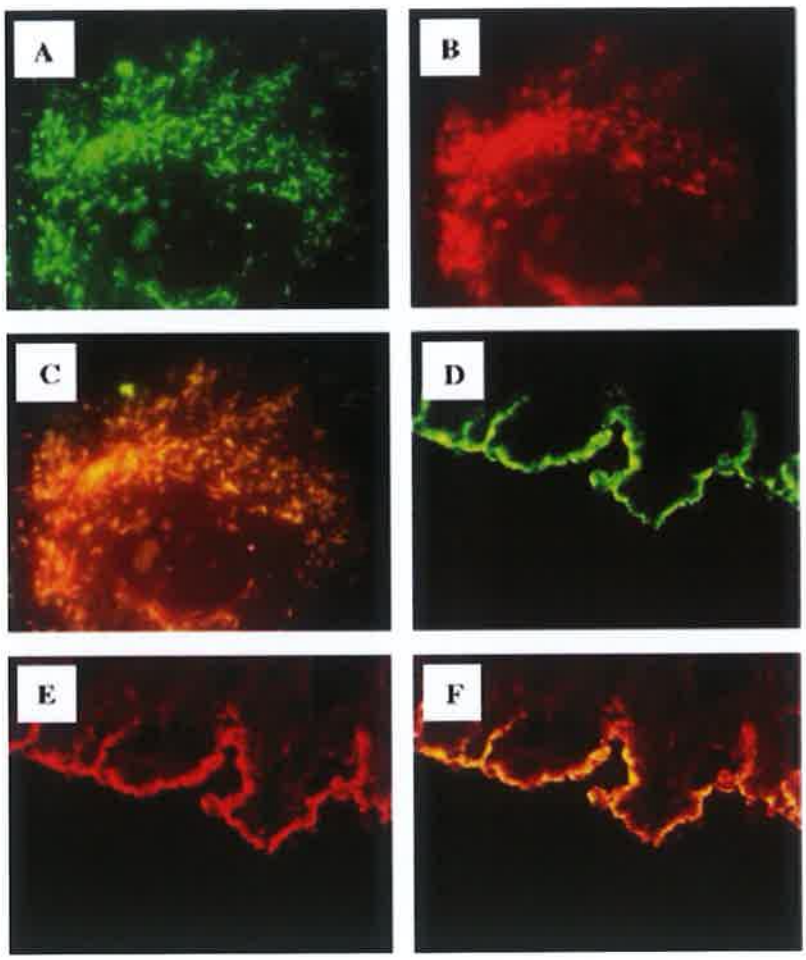

Figure 3.10. Co-localization of OPG with vWF in WPB of ECs, illustrated by dual-colour in-situ immunofluorescence . OPG is stained green (panels A and D). vWF is stained red (panels B and E). Merged images are presented in panels C and F. EC, endothelial cell; OPG, osteoprotegerin, vWF, von Willebrand factor; WPB, Weibel-Palade body. Reproduced with permission from Zannettoni *et al.* [144].

3.3.1.1.5. HAEC OPG mRNA Responses

In Study I, an interesting divergence between OPG release and the levels of OPG mRNA was demonstrated in response to the majority of the experimental conditions. It is important to note, in this context, that transcriptional pathways (DNA copied to RNA) and protein release pathways are often distinct from one another in cells, exhibiting divergent responses to the same stimuli [243,244]. As such, while the release of pre-formed OPG by ECs may occur as part of the immediate EC response to inflammation, as a marker of endothelial dysfunction, the concurrent decrease in OPG synthesis may reflect the phenotypic switching of the EC to an 'activated state', with increased pro-inflammatory gene expression and a shift away from basal levels of protein production. The response of HAECs to 100 ng/ml TNF-α in my own results, for example, involved a significant release of OPG into the media supernatant, while at the same time levels of OPG mRNA were reduced. These findings suggest that sustained stimulation of this nature, while causing an immediate release of pre-formed OPG by ECs, may in the longer term be associated with a reduction in OPG production. In a similar manner, insulin was noted to induce a significant reduction in levels of OPG mRNA, suggesting that sustained release of OPG by ECs in response to insulin is unlikely (in keeping with effects of insulin on HASMCs), and hyperglycemia only affected OPG release, with no effects on levels of OPG mRNA observed. As this is the first study to examine the effects of cyclic strain on OPG production and release by ECs, understanding why cyclic strain at 5% was associated with reduced levels of OPG mRNA without affecting OPG release will require additional research. The significant effect that cyclic strain exerted on OPG gene expression, however, suggests that this gene is mechanosensitive, and that OPG may be relevant to hemodynamic remodeling processes within the vessel wall. Ultimately, I hypothesize that while the immediate release of OPG is relevant to the HAEC response to injury and inflammation, sustained

stimuli of this nature appear to down-regulate production of this protein,possibly as part of a longer-term phenotypic alteration of this cell population.

3.3.1.2. RANKL and TRAIL

With regards to RANKL and TRAIL, a significant and novel finding of Study I is that these proteins were not produced in detectable amounts from HAECs under either basal or pathological conditions. As described in chapter 2, multiple ELISAs, with lower limits in the pg and pmol range, and which captured both free and bound forms of RANKL and TRAIL, were used to test for these two proteins. Of these assays, it should also be noted that the Duoset kits for RANKL and TRAIL were subsequently employed to test serum samples in Study III, and detected both RANKL and TRAIL in these samples with a high degree of reproducibility. Finally, as membrane-bound forms of both RANKL and TRAIL are known to exist [29], whole cell protein lysates were assessed in addition to supernatant media samples. Despite this approach, however, and in contrast to OPG, there was no evidence of the production or release of RANKL or TRAIL protein by HAECs. mRNA transcripts were observed for both proteins, and levels of RANKL and TRAIL mRNA were noted to decrease in response to TNF-α, 5% cyclic strain, and insulin, but these findings were not reflected at the protein level, and so are likely to be of limited clinical significance.

3.3.1.2.1. RANKL and HAECs

As indicated previously, there are conflicting published data on the production of RANKL within the vasculature. In their assessment of human microvascular ECs, Collins-Osdoby *et al* also reported the presence of mRNA transcripts for RANKL, and that when assessed by immunostaining, an increase in the production of RANKL protein was observed following exposure to TNF-α [138]. When HUVECs were assessed by Zannettino *et al* in a similar fashion, however, no evidence of RANKL mRNA or protein was detected, which they suggested was due to differences between

microvascular EC and HUVEC cell populations [144]. Interestingly, a separate study by Ishida et al reported that both RANKL mRNA and protein were produced by HUVECs when stimulated by transforming growth factor beta [245]. With regards to HAECs, Osako *et al* reported RANKL transcripts, and faint RANKL protein expression when assessed by Western blot, but did not attempt to describe the absolute concentrations of RANKL in their cell cultures [38].

Combining these findings with my own data on HAECs, which included a quantitative assessment of RANKL protein, it appears likely that with regards to HAECs, RANKL mRNA may be expressed, but this does not appear to be translated into protein in significant amounts. Divergences between mRNA expression and the detection of protein within the cell have previously been reported, and potential explanations for findings of this nature include low levels of protein expression (potentially below the sensitivity limit of the ELISA in question), sample processing (less likely to be a factor in my results given the abundant detection of OPG) and actual biological differences between transcript and protein abundance due to tight regulation of the translational process [246-248]. Ultimately, while my results suggests that HAECs may be capable of producing RANKL protein, they were not observed to produce detectable amounts under basal conditions, or in response to TNF-α, glucose, insulin, or 5% cyclic strain.

3.3.1.2.2. TRAIL and HAECs

While RANKL has previously been characterized as a protein that is difficult to measure accurately [249,250], no similar concerns have been recorded regarding the measurement of TRAIL in media and cell lysate samples. Indeed, the Quantikine assay utilized in Study I has been utilized successfully in all of these settings in the published literature [251-253]. With regards to my own data on TRAIL and HAECs, my results agree with those of Gochuico *et al* and Secchiero *et al*, both of whom reported an absence of TRAIL in HUVECs [231,254]. They are not consistent, however, with data

from Pritzker *et al,* who demonstrated both TRAIL mRNA and protein (detected via immunoprecipitation) in human microvascular endothelial cells, and Spierings *et al* who reported the presence of TRAIL by immunohistochemistry within pulmonary arteries (but not elsewhere in the vasculature) [255,256]. One explanation for these conflicting results, as suggested by Spierings *et al*, is that the expression of TRAIL within the vasculature is relatively specific to the tissue and cell population under assessment. Therefore, while I report an absence of TRAIL protein in my series of experiments, these results may have limited applicability outside of the HAEC population. Finally, and with regards to both RANKL and TRAIL, it remains possible that both proteins were present in concentrations below the lower limits of the assays utilized. At these concentrations, however, I speculate that neither protein would be likely to exert biologically significant effects in this setting, given the presence of OPG in significantly greater amounts.

3.3.1.3. Summary of HAEC Results

Of the data generated in the HAEC component of Study I, a number of results are of particular interest. I report that HAECs produce and release OPG, albeit at low concentrations relative to HASMCs (reviewed in the following section), that this production is increased by TNF-α, glucose and insulin glargine, and that I hypothesize the release of OPG in this fashion may occur as part of the immediate response to vascular injury. A discrepancy between protein secretion and mRNA expression was noted in response to these injurious stimuli, suggesting that the increased secretion of OPG in response to vascular injury/inflammation may not be sustained in the longer term. With relevance to Study II, HAECs do not produce detectable amounts of RANKL or TRAIL protein and are therefore unlikely to be the source of RANKL and TRAIL demonstrated in atherosclerotic and calcified lesions *in vivo [179,180,232].*

In the context of T2DM, the results of Study I offer additional insights into the relationship between OPG and this clinical condition. It has previously been reported that cicrulating OPG concentrations are higher in T2DM when compared to euglycemic controls, with varying theories as to the cause of this phenomenon. Although I report that HASMCs secrete significantly greater concentrations of OPG than HAECs (reviewed in the following section), the large surface area lined by ECs within the human vasculature, coupled with their immediate proximity to circulating blood, suggest that HAECs could be responsible for a a large amount, if not the majority, of the OPG circulating in the bloodstream. The observation that T2DM is a pro-inflammatory condition coupled with the increased OPG secretion from HAECs in Study I in response to inflammatory and injurious stimuli, suggests that HAECs may be the source of the excess circulating OPG in this clinical condition.

3.3.2. Production and Release of OPG, RANKL and TRAIL by HASMCs

3.3.2.1. OPG

Using a similar approach to that adopted for HAECs, the production and release of OPG and its ligands by HASMCs was characterized in the second part of Study I. With regards to OPG, when supernatant media from HASMCs was subjected to ELISA, significant amounts of OPG were detected under basal conditions. These concentrations were two orders of magnitude greater than those generated by HAECs, and were approximately 30 times greater than circulating concentrations of OPG reported with the same assay [239]. Exposure to TNF-α was associated with an increase in OPG release, as was exposure to cyclic strain at 10% (physiological level for SMCs) [257], whereas a near complete reduction in OPG release was observed upon exposure of these cells to insulin. Hyperglycemia was not associated with any change in OPG release. In contrast to the data on HAECs, a high degree of consistency was noted between the expression of OPG mRNA and the release of OPG

protein. Specifically, the dose-dependent increase in OPG release with TNF-α was reflected by increased mRNA levels, the reduction in OPG release associated with insulin was reflected by decreased mRNA levels, and exposure to hyperglycemia had no effect at the level of mRNA or protein. A discrepancy was noted, however, with cyclic strain, which was associated with an increase in the release of OPG protein, but a reduction in levels of OPG mRNA.

As with the data generated on HAECs, this component of Study I involved a number of novel approachs and findings with regards to OPG/RANKL/TRAIL research and vascular cells. In the context of the OPG system, the effects of insulin glargine and cyclic statin on HASMCs had not been assessed previously. Indeed, the only publications that are immediately relevant to cyclic strain and OPG are from orthodontic journals, in which application of cyclic strain has been associated with increased levels of OPG mRNA, along with increased secretion of OPG, from fibroblast-like cells in the peridontal ligament [258,259]. My data, the first on OPG and cyclic strain in HASMCs, report similar findings in terms of cyclic strain increasing the secretion of OPG, but divergent results with regards to its effects on levels of OPG mRNA. While further research will be necessary to explore these preliminary findings in greater detail, these data, in addition to prior observations on cyclic strain and HAECs, strongly suggest a mechanosensitive nature to OPG within the vasculature. With regards to the effects of TNF-α, glucose, and native insulin, however, both Oleson *et al.* and Nguyen *et al.* have previously reported on the production of OPG by HASMCs in response to these stimuli, with similar findings to my own in that TNF-α increased the production and secretion of OPG, while insulin downregulated the production and release of this protein [39,116,260].

3.3.2.1.1. The Role of OPG in HASMCs Compared to HAECs

An interpretation of the data generated on OPG and HASMCs in Study I is perhaps best performed by contrasting these results against those of the HAEC population, with significant differences immediately apparent. In HASMCs, OPG is stored within the golgi apparatus, and has not been shown, at least to date, to co-localize with any other proteins of note [261]. In my experiments, the basal release of OPG by HASMCs was two orders of magnitude greater than that of HAECs, and resulted in concentrations of OPG in the immediate SMC environment that were 30 times higher than circulating levels. Furthermore, I report that, with the exception of cyclic strain, changes in the release of OPG by HASMCs were accompanied by similar changes in mRNA expression, without the divergence between immediate protein release and long-term production seen with HAECs. Taken together, these findings suggest that the dynamics of OPG production and release by HASMCs differ significantly to those of HAECs. Indeed, based on my data, I hypothesize that the roles (and regulation) of OPG may differ between EC and SMC settings, and that while EC-derived OPG may be involved in thrombus formation via its interaction with vWF [144] in the acute setting of a vascular insult, the basal production of OPG by SMCs may instead participate in chronic processes within the vascular wall, such as the inhibition of VC.

3.3.2.1.2. OPG as an inhibitor of VC in HASMCs under Injurious Conditions

With regards to the effects of the experimental conditions on OPG release by HASMCs, these are perhaps best considered within the context of the findings of Study II, in which I report that RANKL, albeit in an indirect fashion, promoted osteoblastic activity in HASMCs. Given that OPG blocks the actions of RANKL, that RANKL has been reported in sites of inflammation (such as atherosclerotic plaques) *in vivo*, and that TNF-α has been shown to directly induce osteoblastic activity in SMCs, the increased production of OPG by HASMCs in response to TNF-α may represent a compensatory mechanism designed to oppose VC. Equally, in this context, the

possibility that an insulin-induced decrease in OPG may facilitate RANKL-induced calcification becomes apparent, and my subsequent findings in this regard are discussed in the next chapter.

3.3.2.2. RANKL and TRAIL

The finding that HASMCs do not produce detectable amounts of RANKL and TRAIL, despite a comprehensive approach to test for either protein, in both free and bound states, is a significant and novel finding of Study I. An absence of both of these proteins was noted on all the ELISAs employed, under basal and experimental conditions, and in the supernatant media and whole cell protein lysate samples. Once again, I note that the Duoset assay kits subsequently proved themselves capable of measuring RANKL and TRAIL in serum samples in Study III, and that various quality controls (including testing for assay interference from endogenous OPG and any other factors within the supernatant media) were performed and failed to identify any interferences with the ELISA methodology employed. Thus, while mRNA transcripts for both proteins were identified, and mRNA changes on RT-PCR were observed, I report that these findings did not translate into detectable concentrations of protein.

In terms of the published literature on RANKL and TRAIL expression by SMCs, the closest experimental approach to my own was performed by Nguyen *et al.*, who measured the concentrations of RANKL and TRAIL in the supernatant media of HASMCs by ELISA [260]. While this group reported similar findings to my own in that there was an absence of free RANKL or TRAIL, they did report the presence of both of these proteins, in relatively low concentrations, bound to endogenous OPG. It should be noted, however, that a novel ELISA protocol, generated *de novo* by this group for this study, was utilized, and that no data on the validity of this ELISA protocol was provided. This is particularly relevant as OPG, RANKL and TRAIL can, due to their interlinked nature and propensity for dimer and trimer formation, lead to false positives

on ELISA [249,250]. This ELISA has not been used in subsequent research by this group, making it difficult to confirm the accuracy of the initial results. As such, it is possible that methodological differences may account for the discrepancies between this study and my own. Finally, and as with HAECs, it remains possible that both RANKL and TRAIL protein were present in HASMC samples, but at concentrations below the lower limit of the assays utilized, and as such my results do not necessarily contradict those of groups who used different methods of analysis such as Western blot. At these concentrations, however, I submit that neither protein would be likely to exert biologically significant effects in this setting, given the continuous secretion of high concentrations of OPG by HASMCs.

3.3.2.3. Summary of HASMC Results

Of the data generated in the HASMC component of Study I, a number of results are of particular relevance. I report that HASMCs produce and release large quantities of OPG under basal conditions, a phenomenon that is upregulated by TNF-α and 10% cyclic strain, and I hypothesize that OPG may fulfill different functions (and be subject to different forms of regulation) in SMC and EC populations. With relevance to Study II, HASMCs do not produce detectable amounts of RANKL or TRAIL, and, in a similar manner to HAECs, are therefore unlikely to be the source of RANKL and TRAIL demonstrated in atherosclerotic and calcified lesions *in vivo* [179,180,232]. Although outside the scope of this thesis, cells of the immune system such as t-lymphocytes and macrophage-monocytes have been proposed as alternative sources of RANKL and TRAIL in the setting of atherosclerosis *in vivo*, and the data from Study I indicates that these possibilities merits further investigation [233,262]. Finally, and with relevance to Study III, exposure to insulin glargine, at concentrations equal to those encountered *in vivo* in insulin resistant individuals, was associated with a highly significant decrease in OPG production and release from HASMCs. These findings are of particular interest to the context of T2DM, as these patients are often exposed to an excess of endogenous

insulin early in the course of their condition and exogenous insulin as a treatment option in later years. The downregulation of OPG, a putative inhibitor of VC, by insulin glargine suggests a potential role for insulin in the promotion of VC, a concept that is explored in greater detail in chapter 5.

With regards to Studies II and III, is clear from the results of Study I that both HAECs and HASMC populations release OPG into the supernatant media under basal conditions, with the concentrations of OPG released by HASMCs up to two orders of magnitude greater than those released by HAECs. Whilst both cell types clearly demonstrated mRNA levels for all three targets (OPG, RANKL and TRAIL), RANKL and TRAIL protein were not detected within their supernatant media or lysates. Overall these data strongly suggest that the high concentrations of RANKL and TRAIL reported in areas of VC *in vivo* do not originate from ECs or SMCs [179,180,232,233]. Regardless of their origin, however, as RANKL and TRAIL do exist in these areas *in vivo,* it remains possible that OPG may function as an inhibitor of VC by blocking their actions. In Study II of the present thesis, therefore, RANKL and TRAIL are administered to these vascular cell populations, in quantities that overwhelm the neutralizing capabilities of endogenous OPG, and their effects on VC are assessed in detail.

Chapter 4 - The Effects of RANKL and TRAIL on Calcifying Activity in HAECs and HASMCs

4.1. Introduction

The goals of Study II of the present thesis were; a) to assess the effects of RANKL and TRAIL on the emergence of osteoblastic activity in HASMCs in monoculture experiments, b) to examine the putative contribution of HAEC:HASMC paracrine signalling to VC via conditioned media experiments, and c) to test the findings of the monoculture and conditioned media experiments within a co-culture model that simulates various aspects of the *in vivo* state.

As noted previously, the data on the effect of RANKL and TRAIL on the emergence of osteoblastic activity in VSMCs are conflicting. This may be due, at least in part, to the use of hypercalcemic and hyperphosphatemic growth media in many of these experiments (used to generate *in vitro* environment conducive to calcium deposition, but also significant confounding factors if the effects of RANKL and/or TRAIL on VSMCs are to be assessed in isolation) [263-265]. Equally, the endpoint of calcium deposition has been criticized as having low reproducibility between cells from different donors [186]. Finally, the endogenous production of significant quantities of OPG from VSMCs was not always accounted for in the *in vitro* studies on this system [266-268]. Accordingly, in the experiments that comprise Study II, Promocell endothelial and smooth muscle growth media were utilized as previously described in chapter 2, with either calcium or phosphate supplementation. Based on the data generated in Study I, HAECs and HASMCs were exposed to concentrations of RANKL and TRAIL that were deemed sufficient to overcome the blocking effects of endogenous OPG production. Furthermore, two separate approaches to the measurement of osteoblastic activity in HASMCs were adopted; the measurement of ALP activity (increased ALP production and activity is recognised as a critical marker of osteoblastic differentiation and activity) in the supernatant media [89,265], and the measurement of levels of Runx2, BSP and ALP mRNA.

With regards to the paracrine relationship between HAECs and HASMCs, Osako *et al.* previously reported that RANKL increased the production of BMP-2 by ECs, producing conditioned media which induced osteoblastic changes in VSMCs [38]. These experiments, however, were limited in that the only paracrine signal to be measured was BMP-2 (whereas the osteoblastic changes observed in VSMCs could also have been induced by BMP-4, which ECs have previously been shown to produce). Furthermore, the effects of TRAIL were not measured, and the authors only measured mRNA levels as markers of osteoblastic activity, with no assessment of the production of proteins such as ALP. Study II, therefore, contained a number of conditioned media experiments in which this putative paracrine relationship is explored in greater detail, incorporating the measurement of BMP-4, an assessment of the effects of TRAIL, and the measurement of ALP activity as well as levels of osteoblastic mRNA.

In the final component of Study II, the initial conclusions generated by the monoculture and conditioned media experiments were tested in the CELLMAX® DUO perfused capillary co-culture system. In this way, the comparability, to the *in vivo* state, of the results generated by Study II regarding OPG, RANKL, TRAIL and paracrine signalling between HAECs and HASMCs was tested in a model of the vascular wall that incorporates; a) both of these cell populations present as a co-culture, b) capillaries that reproduce the three-dimensional structure and semi-permeability of the vascular wall, and c) the circulation of growth media through the capillary lumens to impart physiological levels of hemodynamic shear stress on the HAEC monolayer.

4.2. Experiments and Results

4.2.1. The Effects of RANKL and TRAIL on Osteoblastic Activity in HASMCs

With regards to the assessment of the effects of RANKL and TRAIL on osteoblastic activity in HASMCs, HASMCs were grown in Promocell media with growth

supplements as previously described and seeded to 6-well plates. RANKL and TRAIL were added to the HASMC supernatant media to achieve 50 ng/ml concentrations. It should be noted that the concentrations of RANKL and TRAIL added to the HASMCs in this series of monoculture experiments exceeded the maximum concentrations of OPG observed with this cell population in Study I (absolute concentrations of 32.6±2.6 ng/ml after 72 hours in culture). At 72 hours, the supernatant media was harvested, ALP activity was measured with the Quantichrom™ assay, and HASMC mRNA was harvested to facilitate measurement of levels of Runx2, BSP and ALP mRNA. OPG concentrations in the supernatant media were also measured by ELISA (Duoset assay) at 72 hours (in order to confirm RANKL and TRAIL treatment concentrations were, in fact, in excess of OPG). To further ensure effective exposure of HASMCs to RANKL and TRAIL, the initial experiments were repeated in the presence of an OPG neutralizing antibody (added at 2.5 µg/ml).

With regards to the effects of RANKL on the production of ALP by HASMCs (using the Quantichrom™ assay, no increase in ALP activity was observed in the supernatant media of HASMCs following exposure to RANKL (an excess of RANKL to OPG was noted to have been established, with absolute concentrations of OPG of 29.9±2.0 ng/ml in the supernatant media at 72 hours). Furthermore, no increase in ALP activity was noted when HASMCs were exposed to both RANKL and the neutralizing antibody to OPG (figure 4.1). Upon examination of the effects of TRAIL on the production of ALP by HASMCs, no increase in ALP activity was observed in the supernatant media of HASMCs following exposure to TRAIL (an excess of TRAIL to OPG was also established in this series of experiments, with absolute concentrations of OPG of 25.4±3.2 ng/ml in the supernatant media at 72 hours). In a similar fashion to RANKL, no increase in ALP activity was noted when HASMCs were exposed to both TRAIL and the neutralizing antibody to OPG (figure 4.1).

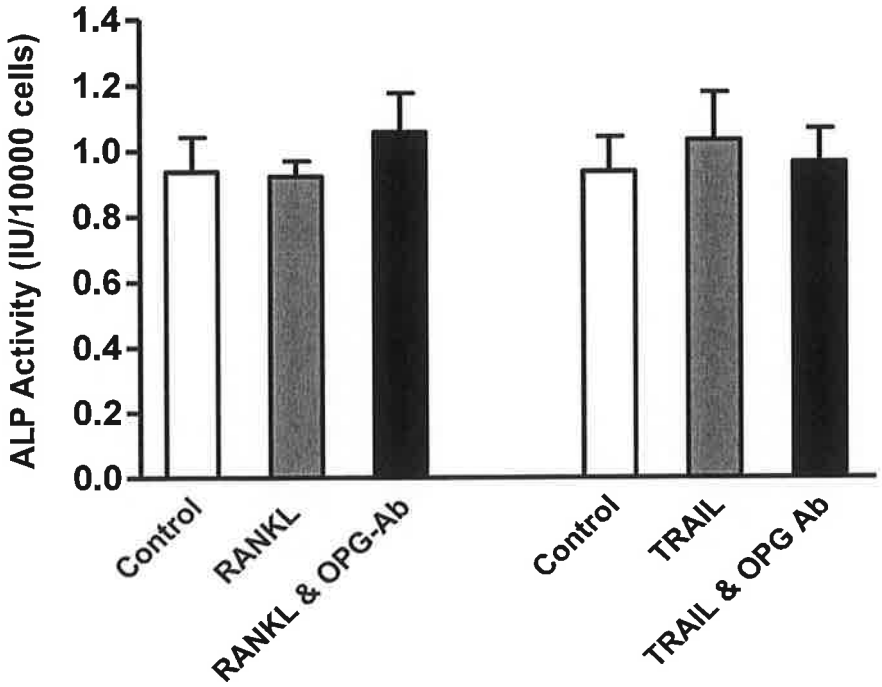

Figure 4.1. ALP activity when measured by Quantichrom™ in the supernatant media of HASMCs after 72 hours of separate exposure to RANKL (50 ng/ml) and TRAIL (50 ng/ml), in the absence and presence of OPG neutralizing antibody (2.5µg/ml). ALP activity is displayed in IU per 10000 cells following correction for viable HASMC population. Data are given as mean±SEM. n=18 for all experiments. ALP, alkaline phosphatase; HASMC, human aortic smooth muscle cell; OPG, osteoprotegerin; OPG-Ab, neutralizing antibody to osteoprotegerin; RANKL, receptor activator of nucelar factor kappa-beta ligand; SEM, standard error of the mean; TRAIL, tumor necrosis factor-related apoptosis-inducing ligand.

Using the techniques described in chapter 2, mRNA samples were harvested and processed into cDNA. Using the selected primers for S18, Runx2, BSP and ALP, mRNA samples underwent RT-PCR and qRT-PCR. Bands of appropriate size were produced from HASMC samples for all 4 genes of interest, indicating mRNA expression of each of these genes in the HASMC cell population. A melt-curve analysis of each primer set confirmed lack of primer-dimer formation or any significant deficits in specificity (figure 4.2). The effects of RANKL, RANKL + neutralizing antibody to OPG, TRAIL and TRAIL + neutralizing antibody to OPG on Runx2, BSP and ALP mRNA levels in HASMCs are illustrated in figure 4.3. No increases in the respective mRNA levels were observed.

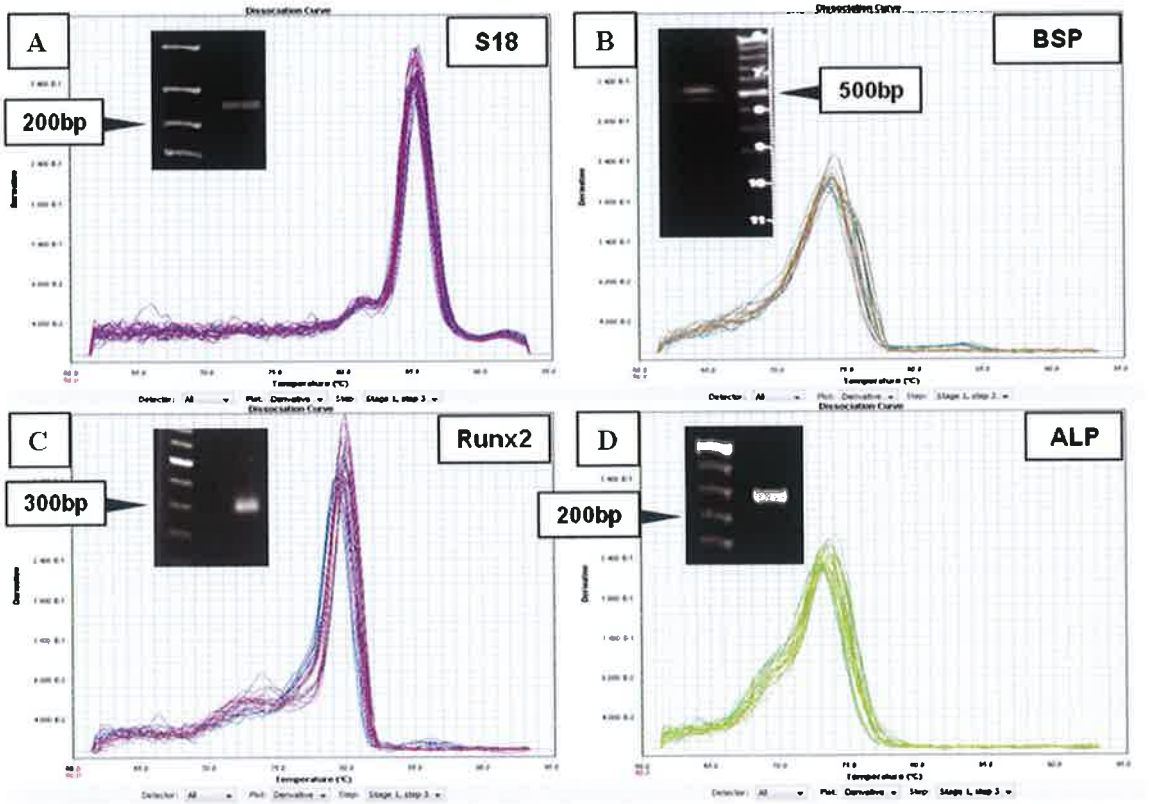

Figure 4.2. Melt curve analysis carried out on Study II and Study III primers to determine specificity. Inserts demonstrate bands produced by respective primers on RT-PCR with HASMC cDNA, confirming mRNA expression of these genes in this cell population. A: S18 primers. B: BSP primers. C: Runx2 primers. D: ALP primers. ALP, alkaline phosphatase; bp, base pair; BSP, bone sialoprotein protein; HASMC, human aortic smooth muscle cell; mRNA, messenger ribonucleic acid; RT-PCR, reat-time polymerase chain reaction; Runx2, runt-related transcription factor 2. Bands are representative.

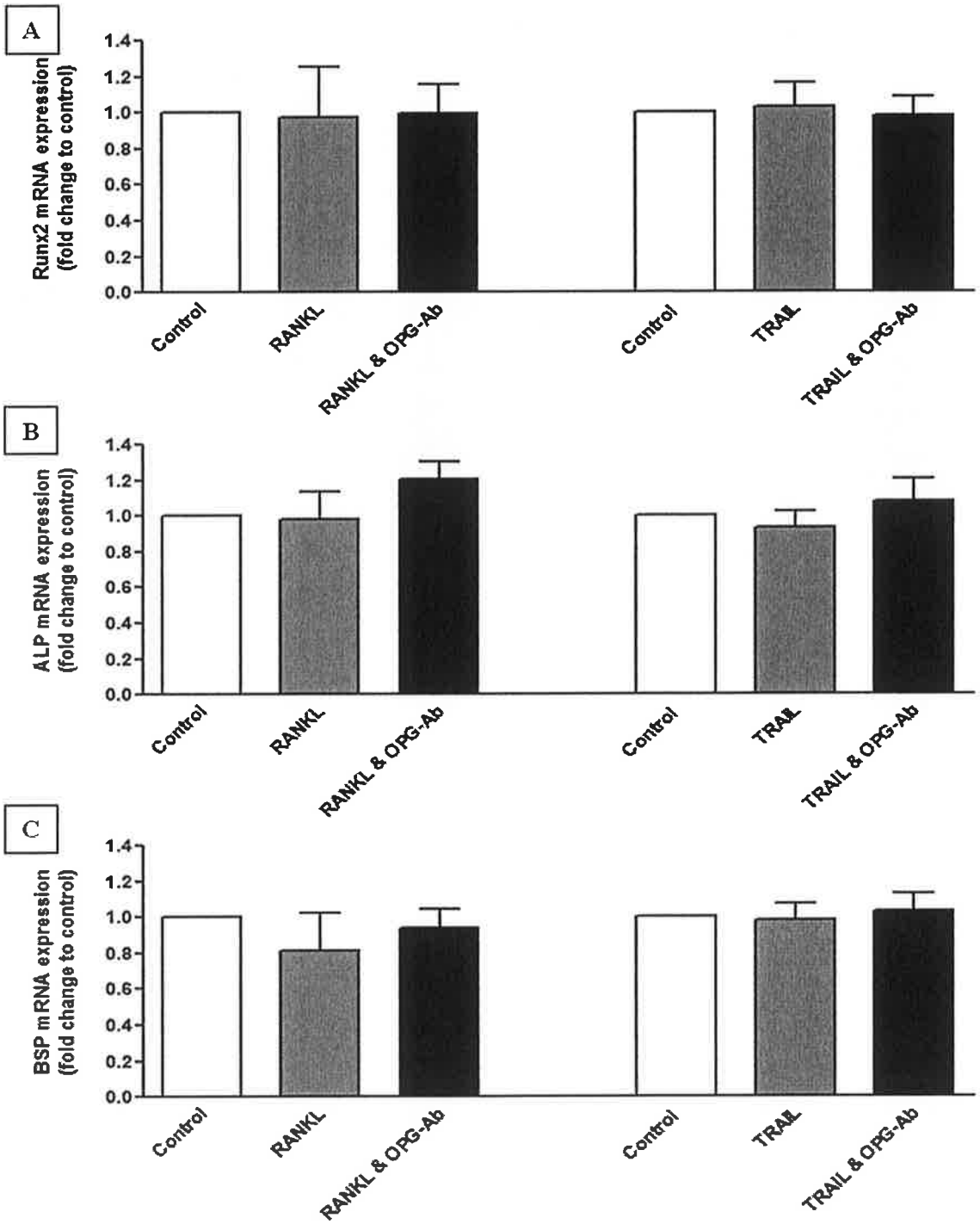

Figure 4.3. Effects, on HASMCs, of 72 hours of exposure to RANKL (50 ng/ml), RANKL (50 ng/ml) + OPG neutralizing antibody (2.5 µg/ml), TRAIL (50 ng/ml) and TRAIL (50 ng/ml) + OPG neutralizing antibody (2.5 µg/ml) on levels of Runx2 (top), ALP (middle) and BSP (bottom) mRNA. mRNA differences are expressed as the fold change in mRNA levels relative to control. Data are given as mean±SEM. During the qRT-PCR, S18 was utilized to normalize differences in total cDNA quantity between samples. n=18 for all experiments. ALP, alkaline phosphatase; BSP, bone sialoprotein protein; HASMC, human aortic smooth muscle cell; mRNA, messenger ribonucleic acid; OPG-Ab, neutralizing antibody to osteoprotegerin; qRT-PCR, quantitative reat-time polymerase chain reaction; RANKL, receptor activator of nuclear factor kappa-beta ligand; Runx2, runt-related transcription factor 2; SEM, standard error of the mean; TRAIL, tumor necrosis factor-related apoptosis-inducing ligand.

4.2.2. The Role of HAEC:HASMC Paracrine Signaling in VC and the Effects of RANKL and TRAIL on This Relationship

HAECs were seeded to transwell inserts, and, at confluency, RANKL and TRAIL were added to the supernatant media within the abluminal space to produce concentrations of 5 ng/ml (absolute concentrations of OPG observed with this cell population in Study I were 0.08±.006 ng/ml). After 72 hours of culture under these conditions, the supernatant media from the subluminal or basolateral aspect of the HAEC monolayer was harvested (HAEC-conditioned media). 750 µl of this media was subjected to analysis by Quantichrom™ (for ALP activity) and ELISA (concentrations of BMP-2 and BMP-4), and the remaining 3250 µl was applied to confluent "reporter" HASMC cultures. After the HASMC cultures had been exposed to the HAEC-conditioned media for 72 hours, the supernatant media from the HASMC cultures was harvested and tested for ALP activity, whilst HASMC mRNA was also harvested to allow measurement of Runx2, BSP and ALP mRNA. The initial experiments were then repeated with the addition of noggin (blocks the actions of BMP-2 and BMP-4, added to achieve a concentration of 2.5 µg/ml) to the HAEC-conditioned media prior to its transfer to the HASMC cultures.

With regards to the release of BMP-2 and BMP-4 by HAECs, these cells were noted to release significant concentrations of both BMP proteins into the supernatant media. Higher concentrations of BMP-2, but not BMP-4, were released by HAECs exposed to RANKL. TRAIL did not affect the release of either BMP protein from HAECs. With regards to HASMCs, stored supernatant media samples from the monocultures of HASMCs exposed to RANKL and TRAIL were thawed to allow measurement of BMP-2 and BMP-4. Upon doing so, BMP-2 and BMP-4 were also detected in the supernatant media of HASMCs under basal conditions, but at an order of magnitude lower than the

supernatant media of HAECs. RANKL and TRAIL did not affect the release of either BMP protein from HASMCs. (figure 4.4).

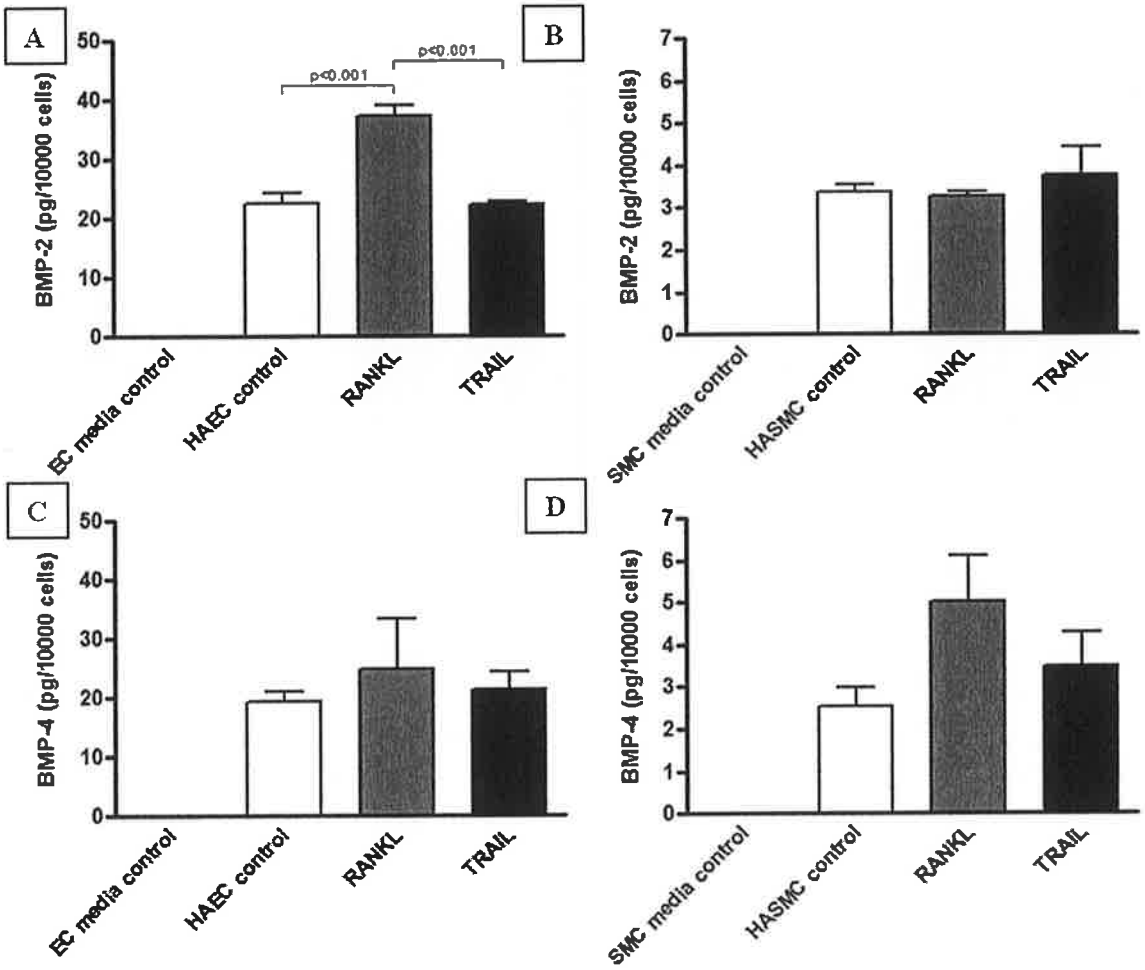

Figure 4.4. Concentrations of BMP-2 (A&B) and BMP-4 (C&D) when measured by ELISA in the supernatant media of monocultures of HAECs (A&C) and HASMCs (B&D) after 72 hours of exposure to RANKL (5 ng/ml added to HAEC cultures, 50 ng/ml added to HASMC cultures), and TRAIL (5 ng/ml added to HAEC cultures, 50 ng/ml added to HASMC cultures). BMP-2 and BMP-4 concentrations are displayed in pg per 10000 cells following correction for viable HAEC/HASMC populations. Data are given as mean±SEM. n=12 for HASMC experiments. n=18 for HAEC experiments. BMP-2, bone morphogenetic protein 2; BMP-4, bone morphogenetic protein 4; EC, endothelial cell; ELISA, enzyme-linked immunosorbent assay; HAEC, human aortic endothelial cell; HASMC, human aortic smooth muscle cell; RANKL, receptor activator of nucelar factor kappa-beta ligand; SEM, standard error of the mean; SMC, smooth muscle cell; TRAIL, tumor necrosis factor-related apoptosis-inducing ligand.

With regards to experiments where HAEC conditioned-media was applied to reporter HASMC populations, I employed the following terminology for the conditioned-media being transferred; HAEC-conditioned media harvested from HAECs under basal conditions was termed HCMB, whereas HAEC-conditioned media from HAECs exposed to RANKL and TRAIL was termed HCMR and HCMT, respectively.

With regards to the effect of HAEC-conditioned media on osteoblastic activity in HASMCs, exposure of HASMCs to HCMB led to a significant increase in ALP activity when compared to controls (HASMCs that were not exposed to HAEC-conditioned media). ALP activity in the supernatant media of HASMCs was observed to be higher again following exposure to HCMR, but not HCMT. Preincubation of HAEC-conditioned media samples with noggin was associated with a significant reduction of ALP activity in the supernatant media of HASMCs, and completely abrogated the increased ALP activity observed with HCMR. Despite the addition of noggin, however, ALP activity remained higher in HASMCs exposed to HAEC-conditioned media than in control samples (figure 4.5). There was no detectable ALP activity in the custom Promocell HAEC and HASMC growth media, or in the HAEC-conditioned medias (HCMB, HCMR and HCMT).

When mRNA samples were subjected to analysis, increased levels of Runx2 and ALP mRNA were observed in HASMCs following exposure to HCMB, HCMR, and HCMT, with highest levels noted for RANKL (HCMR) treatments, when compared to mRNA levels in HASMCs cultured in unconditioned growth medium. The addition of noggin to each of the HAEC-conditioned media fractions (HCMB, HCMR and HCMT) was associated with a significant reduction in Runx2 and ALP mRNA levels. No change in BSP mRNA levels were observed under any of the experimental conditions tested (figure 4.6).

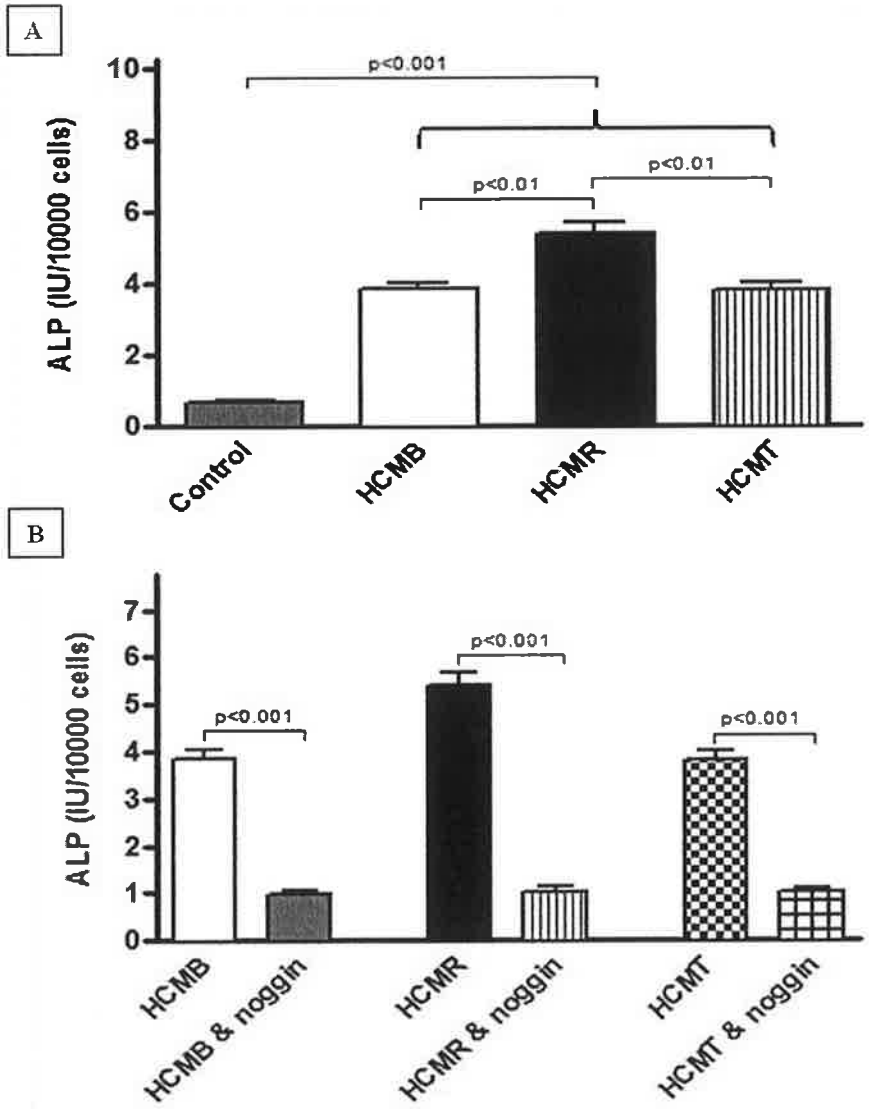

Figure 4.5. ALP activity when measured by Quantichrom™ in the supernatant media of HASMCs after 72 hours of exposure to Promoell smooth muscle growth media 2, and HCMB, HCMR and HCMT (with and without noggin at 2.5 µg/ml). ALP activity is displayed in IU per 10000 cells following correction for viable HASMC populations. Data are given as mean±SEM. A: ALP activity in supernatant media of HASMCs following exposure to Promocell smooth muscle growth media 2 (control), HCMB, HCMR and HMCT. B: ALP activity in supernatant media of HASMCs following exposure to the three HAEC-conditioned media fractions, HCMB, HCMR and HCMT, in the presence and absence of noggin. n=18 for all experiments. HASMC, human aortic smooth muscle cell; HCMB, supernatant media from human aortic endothelial cells under basal conditions; HCMR, supernatant media from human aortic endothelial cells exposed to receptor activator of nuclear factor kappa-beta ligand (5 ng/ml); HCMT, supernatant media from human aortic endothelial cells exposed to tumor necrosis factor-related apoptosis-inducing ligand (5 ng/ml); SEM, standard error of the mean.

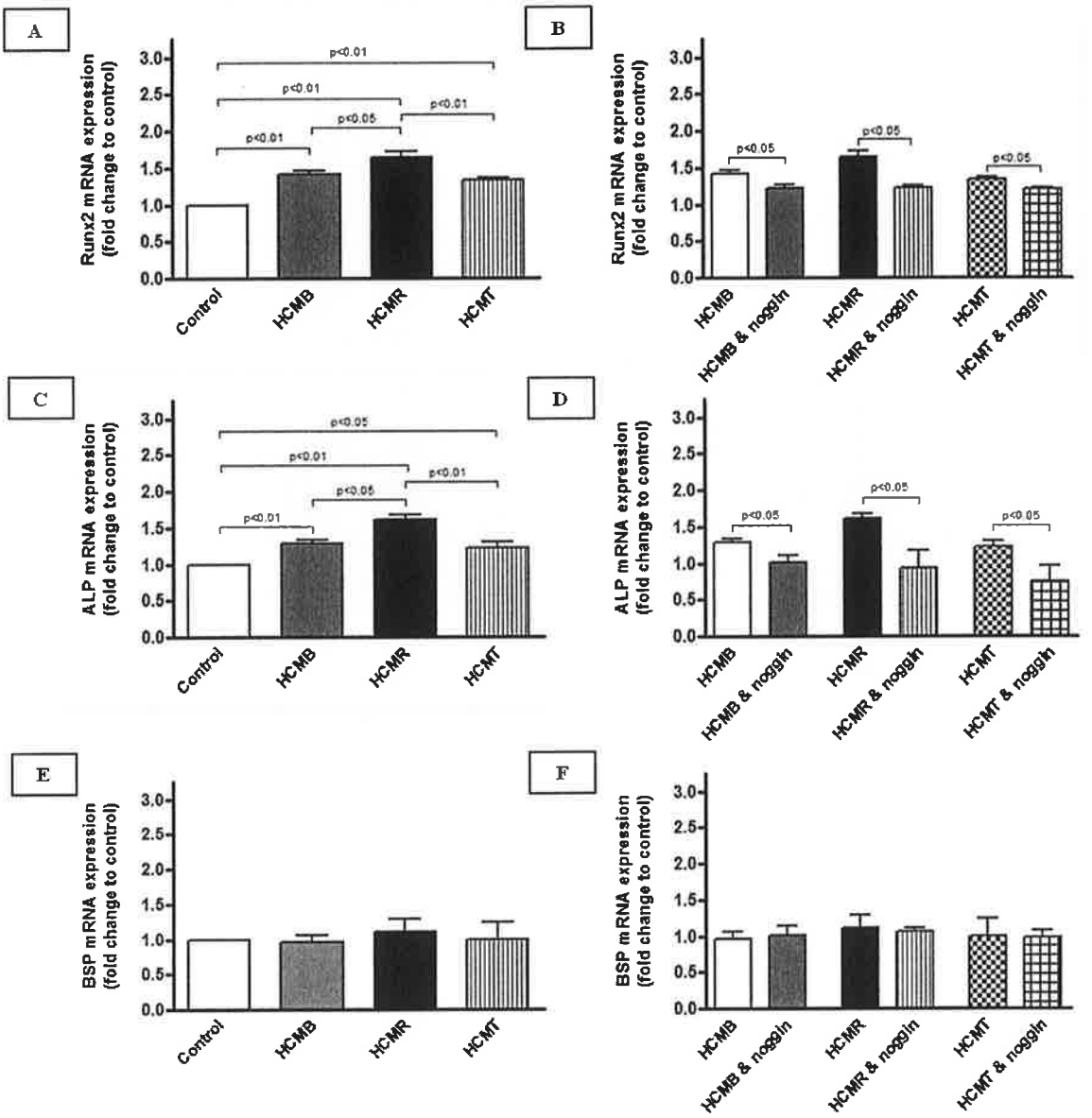

Figure 4.6. Effects, on HASMCs, of 72 hours of exposure to Promoell smooth muscle growth media 2, HCMB, HCMR and HCMT (A, C&E), with and without noggin at 2.5 µg/ml (B, D&F) on levels of Runx2 (A&B), ALP (C&D) and BSP (E&F) mRNA. mRNA differences are expressed as the fold change in mRNA levels relative to control. Data are given as mean±SEM. During the qRT-PCR, S18 was utilized to normalize differences in total cDNA quantity between samples, and Rox was utilized to normalize non-PCR-related flourescence fluctuations between wells. n=18 for all experiments. ALP, alkaline phosphatase; BSP, bone sialoprotein; cDNA. complimentary deoxyribonucleic acid; HASMC, human aortic smooth muscle cell; HCMB, supernatant media from human aortic endothelial cells under basal conditions; HCMR, supernatant media from human aortic endothelial cells exposed to receptor activator of nuclear factor kappa-beta ligand (5 ng/ml); HCMT, supernatant media from human aortic endothelial cells exposed to tumor necrosis factor-related apoptosis-inducing ligand (5 ng/ml); mRNA, messenger ribonucleic acid; qRT-PCR, quantitative reat-time polymerase chain reaction; Runx2, runt-related transcription factor 2; SEM, standard error of the mean.

4.2.3. The Effect of RANKL on Osteoblastic Activity in HASMCs Maintained in Co-Culture with HAECs in the CELLMAX® DUO.

The CELLMAX® DUO system, containing a HAEC:HASMC co-culture subjected to physiological levels shear stress at 10 dynes/cm^2, was established as described in chapter 2, and a 1:1 mix of custom endothelial growth media MV (catalogue number c-22120) and smooth muscle growth media 2 (catalogue number c-22162) was utilized to perfuse the co-culture [209]. Importantly, the effects of this mixed media preparation were assessed on monocultures of HAECs and HASMCs prior to its use in the CELLMAX® DUO co-culture experiments, with normal morphology and viability noted for both cell populations (figure 4.7). During co-culture set-up, samples were routinely harvested from the reservoir of each CELLMAX® DUO system on a daily basis, and glucose and lactate concentrations measured. During the experiments, RANKL was added to the intralumenal space of the bioreactor unit to achieve concentrations of 50 ng/ml twice a day. After 72 hours, the supernatant media in the extracapillary space (ECS, where HASMCs are seeded) and the reservoir media flowing through the intralumenal space (ILS, where the HAECs are seeded) were harvested and subjected to analysis via Quantichrom™ (ALP) and ELISA (RANKL, BMP-2 and BMP-4). Both HAECs and HASMCs were ultimately recovered from the bioreactor unit and total mRNA was harvested to allow measurement of levels of Runx2, BSP and ALP gene expression.

The metabolism of glucose and production of lactate in each of the CELLMAX® DUO experiments are illustrated in figure 4.8 and figure 4.9. Stable equimolar depletion of glucose with concomitant production of lactate was established in all cases prior to treatment with RANKL. Both RANKL and OPG concentrations were routinely measured in the media reservoirs of each CELLMAX® DUO system at the conclusion of each

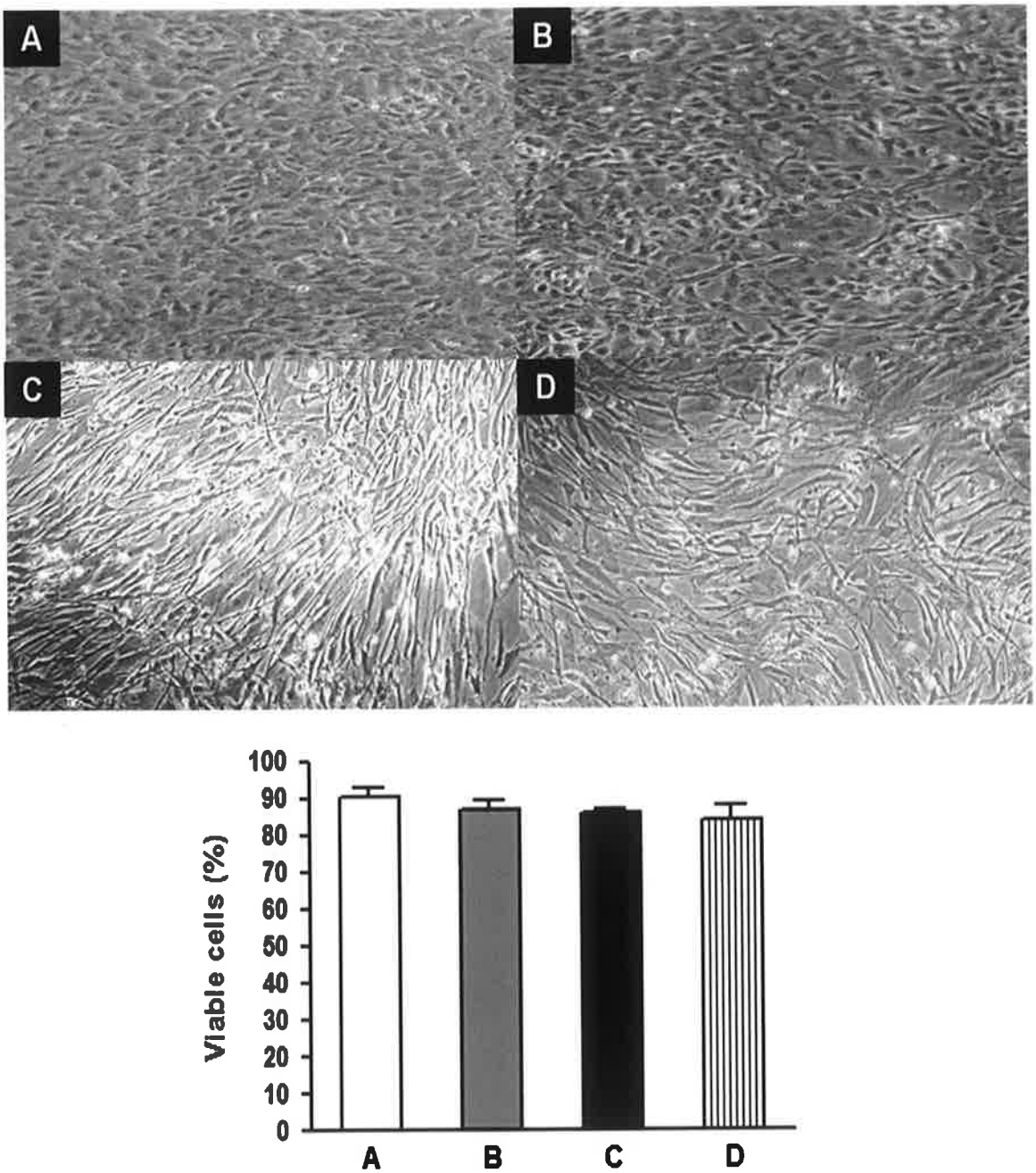

Figure 4.7. Morphology and viability of HAEC and HASMCs when cultured in the mixed media utilized in the CELLMAX® DUO experiments in Study II. Viability expressed as the percentage of viable cells in the entire cell population, measured with the Adam™ counter after 5 days in culture. Viabilty data are given as mean±SEM. A: HAECs at passage number 6, cultured with Promocell endothelial growth media MV and demonstrating characteristic cobblestone morphology. B: HAECs at passage number 6, cultured with a mix of Promocell endothelial growth media and Promocell smooth muscle growth media 2 in a 1:1 ratio and demonstrating similar morphology to A. C: HASMCs at passage number 4, cultured with Promocell smooth muscle growth media 2 demonstrating characteristic parallel growth patterns. D: HASMCs at passage number 5, cultured with a mix of Promocell endothelial growth media and Promocell smooth muscle growth media 2 in a 1:1 ratio and demonstrating similar morphology to C. Images were taken using the Nikon eclipse TS100 microscope. n=6 for each assessment of viability. HAEC, human aortic endothelial cell; HASMC, human aortic smooth muscle cell; SEM, standard error of the mean.

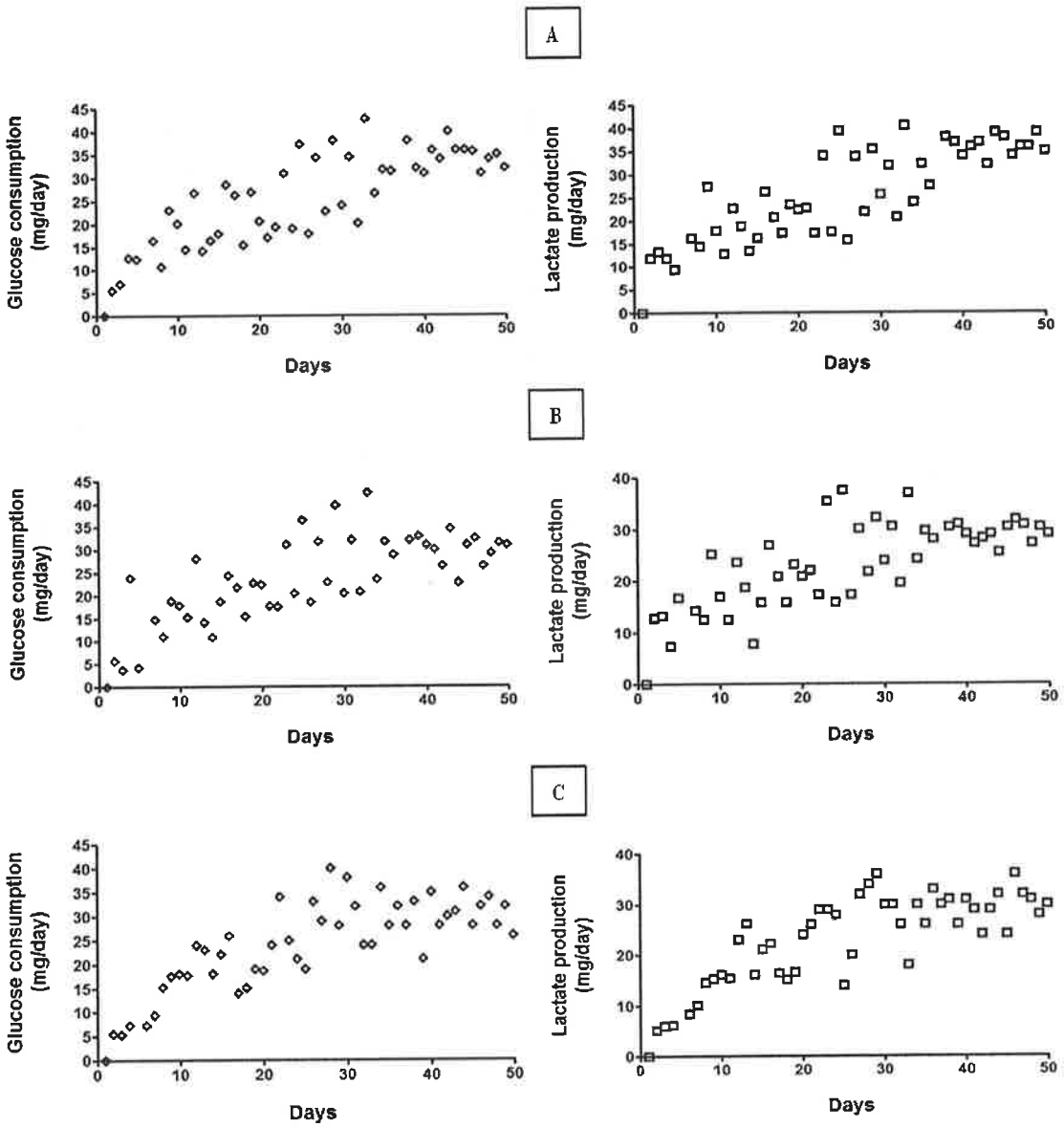

Figure 4.8. Paired glucose consumption (mg/day) and lactate production (mg/day) in the 3 (A,B & C) control CELLMAX® DUO units established in study II. Samples were harvested from the media reservoirs and measured with the YSI 2300 STAT Plus glucose and lactate analyzer. Glucose consumption and lactacte production rates were corrected for the periodic replacement of media in the reservoirs (performed whenever glucose concentrations in the circulating growth media dropped by 50% or more from the previous time growth media was replaced). HASMCs ($1x10^7$) were inoculated into the ECS at day 0. HAECs ($2.5x10^7$) were inoculated into the ILS at day 20. Experimental conditions were commenced on day 45. ECS, extracapillary space; ILS, intra-lumenal space; HAEC, human aortic endothelial cell; HASMC, human aortic smooth muscle cell; RANKL, receptor activator of nuclear factor kappa-beta ligand.

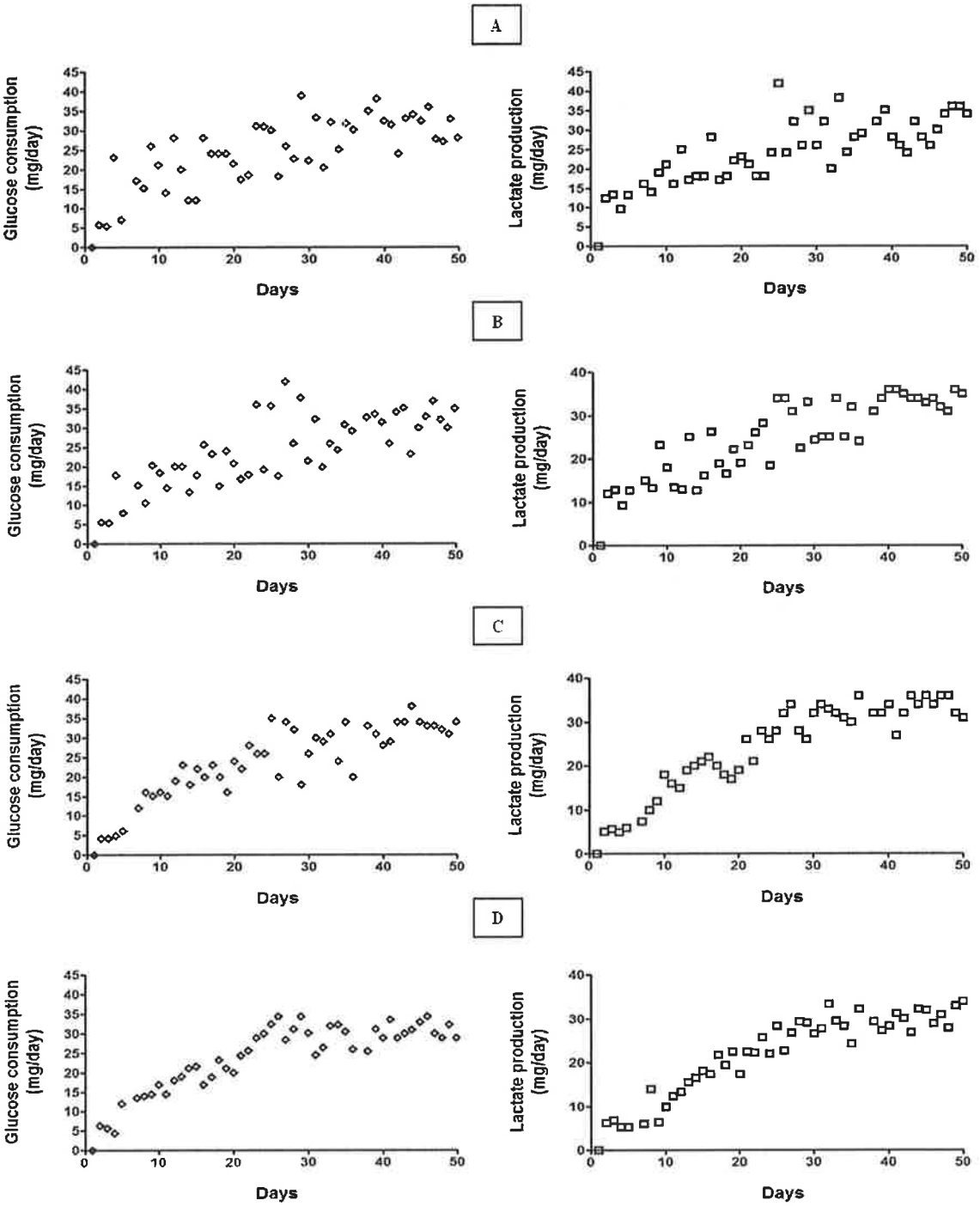

Figure 4.9. Paired glucose consumption (mg/day) and lactate production (mg/day) in the 4 (A,B,C & D) active (treatment with RANKL) CELLMAX® DUO experiments units established in study II. Samples were harvested from the media reservoirs and measured with the YSI 2300 STAT Plus glucose and lactate analyzer. Glucose consumption and lactacte production rates were corrected for the periodic replacement of media in the reservoirs (performed whenever glucose concentrations in the circulating growth media dropped by 50% or more from the previous time growth media was replaced). HASMCs ($1x10^7$) were inoculated into the ECS at day 0. HAECs ($2.5x10^7$) were inoculated into the ILS at day 20. Experimental conditions were commenced on day 45. ECS, extracapillary space; ILS, intra-lumenal space; HAEC, human aortic endothelial cell; HASMC, human aortic smooth muscle cell; RANKL, receptor activator of nuclear factor kappa-beta ligand.

experiment (figure 4.10), and demonstrate that a) there was no RANKL present in the untreated CELLMAX® DUO systems that acted as controls and b) there was an excess of RANKL relative to OPG circulating through the treated CELLMAX® DUO systems. With regards to effects of RANKL on the osteoblastic activity of HASMCs within the ECS, the exposure of intralumenal HAECs to RANKL was associated with increased concentrations of BMP-2, as well as increased ALP activity, within media harvested from the ECS, but not from the intralumenal space, when compared to controls (figure 4.11 and figure 4.12). There were no significant changes in BMP-4 concentrations under the experimental conditions. Exposure to RANKL was also associated with significant increases in levels of Runx2 and ALP (but not BSP) mRNA compared to controls (figure 4.13).

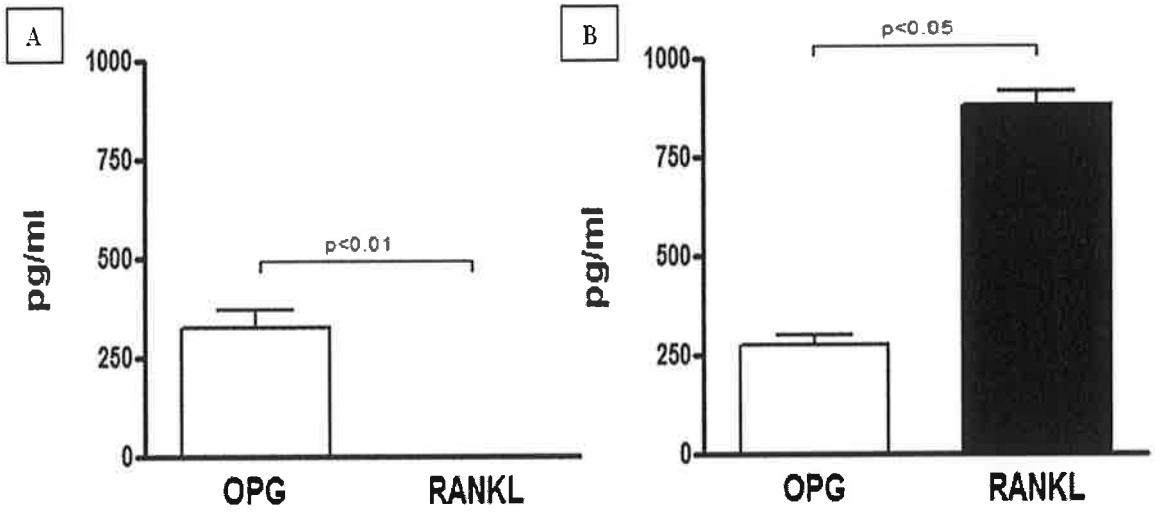

Figure 4.10. Concentrations of OPG and RANKL, as tested by Duoset assay, in samples harvested from media reservoirs of CELLMAX® DUO systems at the conclusion of the 72 hour experiments (media was a custom mix of Promocell growth media). A: media harvested from control experiments which were not exposed to RANKL (n=3). B: media harvested from active experiments in which RANKL was added to the ILS of the bioreactor at 50 ng/ml twice a day for the duration of the 72 hour experiments (n=4). OPG and RANKL concentrations are displayed in pg/ml, as the process of retrieving the cell populations from the bioreactors adversely affected viability data, and the CELLMAX® DUO experiments were matched for circulating media volume and cell numbers inoculated. Data are given as mean±SEM. ILS, intralumenal space; RANKL, receptor activator of nucelar factor kappa-beta ligand; SEM, standard error of the mean.

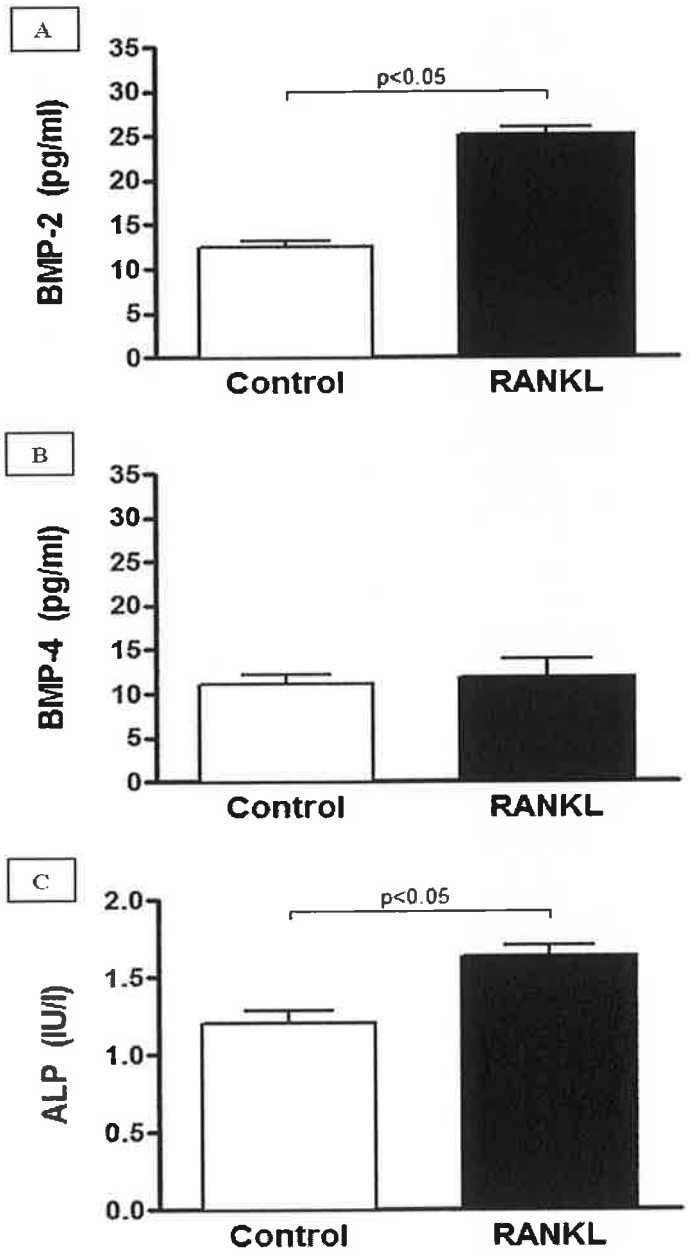

Figure 4.11. BMP-2/4 concentrations (as measured by Duoset assay) and ALP activity (as measured by Quantichrom™ assay) in samples harvested from the ECS at the conclusion of the CELLMAX® DUO experiments. ALP activity is displayed in IU/l, and BMP-2/4 concentrations are displayed in pg/ml. A: BMP-2 concentrations in ECS from control and active experiments. B: BMP-4 concentrations in ECS from control and active experiments. C: ALP activity in ECS from control and active experiements. Data are presented as mean±SEM. n=3 for control conditions. n=4 for active experiments (treatment with RANKL). ALP, alkaline phosphatase; BMP-2/4, bone morphogenetic protein 2/4; ECS, extracapillary space. RANKL, receptor activator of nuclear factor kappa-beta ligand; SEM, standard error of the mean.

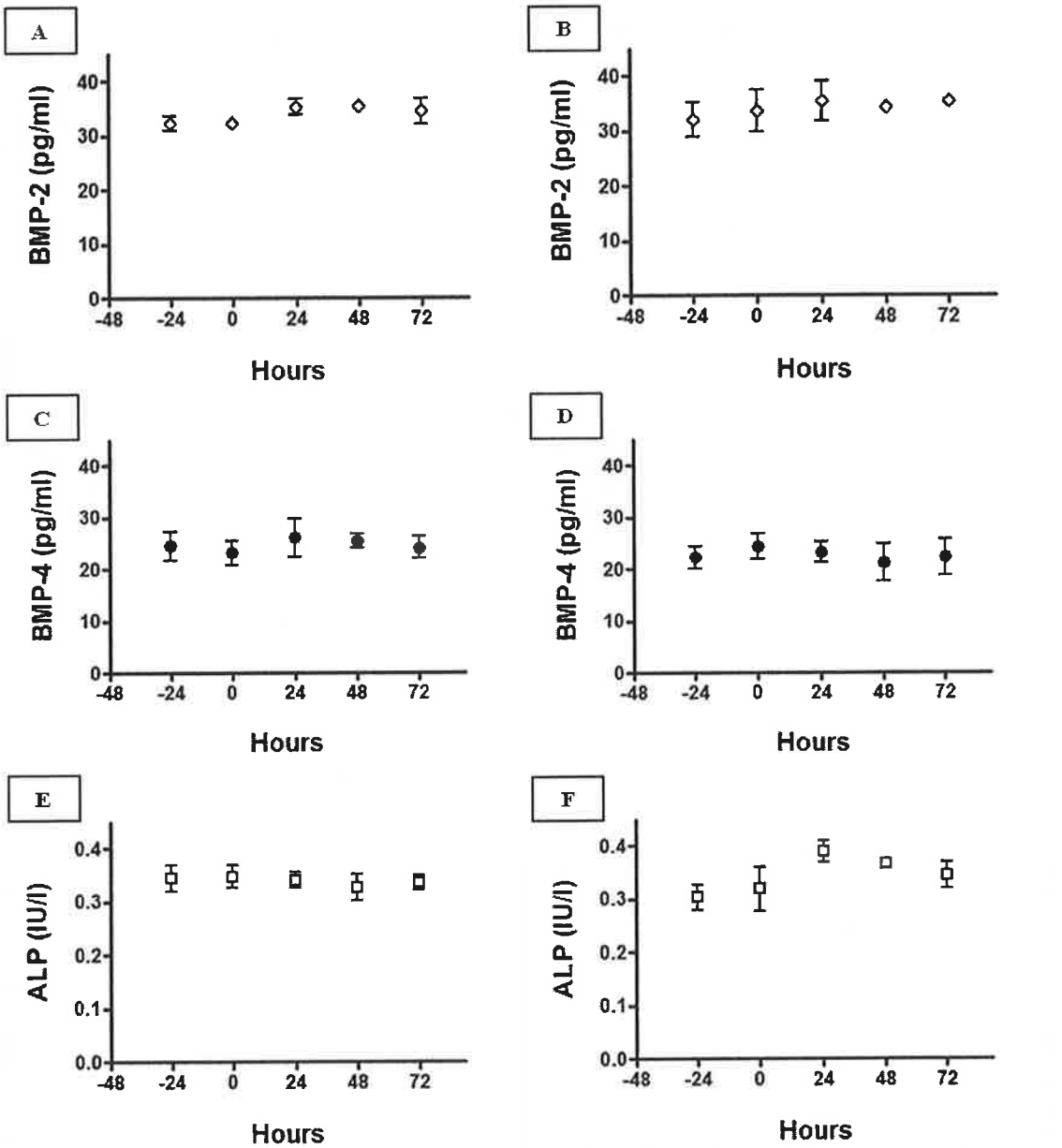

Figure 4.12. BMP-2/4 concentrations (as measured by Duoset assay) and ALP activity (as measured by Quantichrom™ assay) in intralumenal samples (harvested from media reservoirs) during CELLMAX® DUO experiments. Samples were harvested 24 hours prior to commencement of the experiment, and on a daily basis throughout the experiments. ALP activity is displayed in IU/l and BMP-2/4 concentrations are displayed in pg/ml. A: BMP-2 concentration in control experiments. B: BMP-2 concentration in active experiments. C: BMP-4 concentrations in control experiments. D: BMP-2 concentrations in active experiments. E: ALP activity in control experiments. F: ALP activity in active experiments. Data are presented as mean±SEM. n=3 for control experiments.n=4 for active experiments (treatment with RANKL). ALP, alkaline phosphatase; BMP-2/4, bone morphogenetic protein 2/4; ILS, intralumenal space; RANKL, receptor activator of nuclear factor kappa-beta ligand; SEM, standard error of the mean.

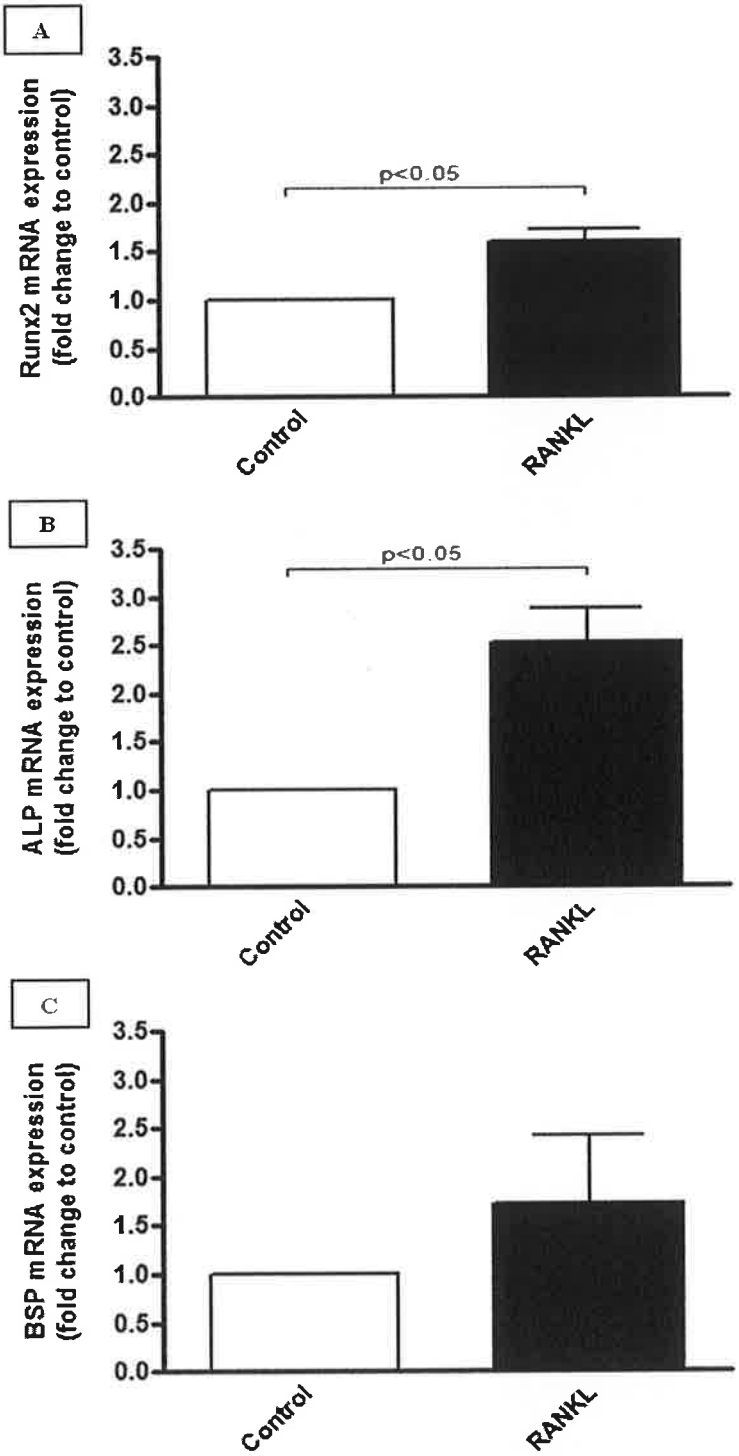

Figure 4.13. Levels of Runx2, ALP and BSP mRNA in HASMCs following 72 hours of co-culture with HAECs in the CELLMAX® DUO system, with or without twice daily exposure to RANKL at 50 ng/ml. mRNA differences are expressed as the fold change in mRNA levels relative to untreated control. Data are given as mean±SEM. During the qRT-PCR, S18 was utilized to normalize differences in total cDNA quantity between samples, and Rox was utilized to normalize non-PCR-related flourescence fluctuations between wells. A: Runx2 mRNA. B: ALP mRNA. C: BSP mRNA. n=3 for control experiments. n=4 for active experiments (treatment with RANKL). ALP, alkaline phosphatase; BSP, bone sialoprotein; cDNA, complimentary deoxyribonucleic acid; HAEC, human aortic endothelial cell; HASMC, human aortic smooth muscle cell; mRNA, messenger ribonucleic acid; PCR, polymerase chain reaction; qRT-PCR, quantitative reat-time polymerase chain reaction; Runx2, runt-related transcription factor 2; SEM, standard error of the mean.

4.3. Discussion

In Study II, I examined the effects of RANKL and TRAIL on the emergence of osteoblastic activity in HASMCs in three separate but inter-linked settings; (a) monocultures of HAECs and HASMCs, (b) conditioned media experiments in which HAEC-conditioned media was transferred onto reporter HASMC populations, and (c) HAEC/HASMC co-cultures within perfused artificial capillary systems. In the first component of Study II, I performed an examination of the direct effects of RANKL and TRAIL upon the emergence of osteoblastic activity in HASMCs. In the second component, communication between HAECs and HASMCs was assessed, with an examination of the paracrine signals produced by HAECs that can induce osteoblastic change in HASMCs, as well as the effects of RANKL and TRAIL on the production of these signals. In the third and final component of Study II, and in order to increase the comparability of these results to the *in vivo* state, the observations from the monoculture and conditioned-media experiments were tested in an artificial capillary system that simulates the structural and hemodynamic aspects of the vasculature [209]. To the best of my knowledge, these studies represent the first time that VC has been studied in a model of this nature. With this stepwise approach, Study II was designed to a) amalgamate and b) expand significantly upon the previous research in this area, with the ultimate aim of generating both data and hypotheses that will aid the design of future clinical studies into VC.

4.3.1. The Effects of RANKL and TRAIL on Calcifying Activity in HASMCs

4.3.1.1. RANKL

With regards to the effects of the direct administration of RANKL on osteoblastic activity in HASMCs, the first notable finding of Study II was that there was no evidence that RANKL (at concentrations in excess of endogenous OPG levels, as established by Study I) increased osteoblastic activity within this cell population. To further ensure that

RANKL was able to act on HASMCs unopposed by OPG, the initial experiments were repeated in the presence of an OPG neutralizing antibody, and once again, there was no evidence of osteoblastic change within the HASMC cultures (i.e. no change in ALP activity within the supernatant media, and no change in levels of Runx2, ALP or BSP mRNA levels).

In terms of previous research in this field, one of the seminal papers regarding the role of RANKL and VSMCs in VC was published by Panizo *et al* [183]. In this paper, the authors administered RANKL to rat aortic VSMCs and reported an increase in calcium deposits in the cell cultures exposed to RANKL, accompanied by an increase in ALP, and that this increase appeared to be mediated, at least in part, by a RANKL-dependent increase in BMP-4 production by VSMCs. Furthermore, they reported that knockdown of the RANK receptor by shRNA abrogated this effect, as did co-incubation of the cell cultures with an excess of OPG, indicating that the direct effects of RANKL-RANK binding were responsible for these effects. Although Kaden *et al* had previously described similar effects with RANKL and myofibroblasts in the setting of aortic valve calcification, Panizo's paper represented the first *in vitro* data on RANKL and VSMCs. These results offered a robust explanation as to why the absence of OPG was associated with the development of VC in mouse gene deletion models, why the administration of exogenous OPG reduced VC burden in mice and, ultimately, formed the basis of the prevailing theory regarding RANKL, OPG and VC (i.e. that RANKL promotes osteoblastic change by binding to RANK on VSMCs, and OPG inhibits this process by preventing RANKL from binding to RANK) for a number of years. Since the publication of this study in 2009, however, a significant amount of conflicting data has been presented by other groups in this field. In 2012, Lars Rasmussen's group, reported, in a similar manner to my own findings, that the administration of RANKL and TRAIL to HASMCs was not associated with any change in the accumulation of calcium

by these cells, or on the regulation of genes associated with osteoblastic activity as measured by micro-array [186]. These findings were further supported by data from Tseng *et al.* and Byon *et al.*, both of whom reported no effects when murine aortic SMCs were exposed to RANKL [187,269]. Contrary to these findings, however, and in support of Panizo *et al,* in 2011 Xie *et al.* published *in vivo* data reporting that the production of omentin-1, a cytokine which inhibits the production of RANKL, attenuated VC in OPG knockout mice [185].

While there are a number of potential explanations behind the conflicting evidence in this field of research, including various methodological differences adopted by the groups mentioned above, and the differing origins of the cell populations (e.g. murine versus human), perhaps most important amongst these is the observation that calcium deposition represents, somewhat counter-intuitively, a poor endpoint for studies into osteoblast activity and VC. There are two main issues that have been raised in this regard. The first is that the use of calcium deposition as an endpoint typically involves the use of calcifying media, containing both calcium and phosphate that can be extracted by VSMCs and deposited into the cell culture to be subsequently measured by Von Kossa staining. As noted previously, however, both calcium and phosphate are themselves inducers of osteoblastic activity in VSMCs, and as such may act as significant confounders of experiments addressing this process [263-265]. The second issue with calcification as an endpoint is that the propensity of VSMCs to accumulate and deposit calcium varies significantly between donors. When Oleson *et al* examined rates of calcification in HASMC populations from 7 different donors, for example, they reported marked heterogeneity in the response of these cells to both RANKL and insulin [186]. Finally, and as noted previously, the endogenous production of OPG was not always properly controlled for in studies of this system, raising some doubts as to the effective exposure of the SMCs to RANKL [266-268].

In terms of my own data on RANKL and osteoblastic activity in HASMCs, it is important to note that my experiments were designed to avoid, as much as possible, the confounding factors mentioned above. Phosphate and calcium were not added to my growth media, and instead of calcium deposition as the primary endpoint of my studies, I chose instead a combination of ALP activity (as increased ALP activity is a critical marker of osteoblastic activity) and mRNA expression [89,270]. As such, I examined for HASMC osteoblastic change both intra- and extra-cellularly. HASMCs were obtained from one donor only to ensure homogeneity of the HASMC response to stimuli such as RANKL and insulin. Furthermore, and based on the results of Study I, I accounted for the production of endogenous OPG by HASMCs. With this approach in mind, I report findings that are consistent with the more recent papers in this field, indicating that if RANKL is involved in the emergence of osteoblastic activity in HASMCs, *it does not do so by acting on HASMCs in a direct manner.* Finally, I note (also in contrast to the data presented by Panizo *et al*) that exposure to RANKL was not associated with any change in BMP-2 or BMP-4 concentrations in the media supernatant.

4.3.1.2. TRAIL

In a similar manner to RANKL, exposure to TRAIL was not observed to exert any effects on osteoblastic activity in my HASMC populations. Once again, in addition to adding an excess of TRAIL relative to endogenous OPG, these experiments were repeated with an OPG neutralizing antibody. In both series of experiments, however, osteoblastic activity failed to develop within the HASMC cultures. Furthermore, no changes in the concentrations of BMP-2 or BMP-4 in the media supernatant were observed.

In comparison to RANKL, there is limited evidence regarding the effects of TRAIL on osteoblastic activity and VC. As the actions of TRAIL are blocked by OPG, however,

and the absence of OPG is associated with the development of calcification, it is possible that TRAIL, and not RANKL promotes VC *in vivo* [29,31]. In one of the few previous publications to look specifically at this topic, Chasseraud *et al.* reported that the administration of TRAIL was associated with increased deposition of calcium by HASMCs [189]. These experiments, however, were performed with calcifying media and serum from patients with ESRF, and as such their results may not be applicable outside of this specific setting. Certainly, my own findings with regards to TRAIL are more in keeping with those of Ramsussen's group, who also reported no effect when TRAIL was added to HASMCs [186]. Furthermore, it is with interest that I note the recent paper by Di Bartolo *et al.,* who suggest that TRAIL may actually protect against VC by modulating RANKL expression [190]. While this facet of VC clearly requires further characterization, the weight of evidence (including my own) appears to favor the conclusion that TRAIL does not induce osteoblastic change in HASMCs via any direct effect on this cell population.

4.3.1.3. Summary of RANKL and TRAIL Results

With regards to the initial component of Study II, I report that neither RANKL or TRAIL exert direct effects on HASMCs with regards to osteoblastic activity and VC. Whilst these data are not consistent with early reports on RANKL in particular, they do agree with more recent papers on this topic, and add novel results to this field of research by avoiding the use of calcifying media, omitting calcium deposition as an endpoint, and factoring endogenous production of OPG into the experimental design, ultimately offering data that are relatively free of confounders that have limited previous studies in this area. In summary, and in relation to the putative role of OPG as an inhibitor of VC, this data indicates that if OPG does indeed fulfill this role, then it does not appear to do so via a blockade of the direct actions of RANKL or TRAIL on HASMCS.

4.3.2. The Role of HAEC:HASMC Paracrine Signaling in VC and the Effects of RANKL and TRAIL on This Relationship

In the second component of Study II, I performed conditioned media experiments by culturing HAECs in transwell inserts. At confluency, RANKL and TRAIL were applied to the abluminal (apical) aspect of the HAEC monolayer growing on the inserts for a given treatment period. This technique subsequently allowed us to harvest HAEC-conditioned media from the basolateral side of the endothelial monolayer, effectively simulating *in vivo* conditions in which paracrine factors are secreted from the basolateral aspect of this cell population onto the underlying SMCs. RANKL and TRAIL were then applied to the abluminal aspect of these inserts. When the HAEC-conditioned media from these cultures was then transferred onto reporter HASMC populations, a significant degree of osteoblastic activity was observed, with increases in ALP activity in the HASMC supernatant media along with increased expression of levels of Runx2 and ALP mRNA. Interestingly, exposure of HAECs to RANKL was associated with the highest subsequent levels of osteoblastic activity in the reporter HASMC cultures. When the HAEC-conditioned media was analyzed by ELISA, significant concentrations of BMP-2 and, to a lesser degree, BMP-4, were noted, and exposure of HAECs to RANKL was associated with a significant rise in the concentrations of BMP-2, but not BMP-4. Working on the assumption that BMP-2 represented the paracrine signal by which the HAEC-conditioned media putatively induced osteoblastic activity in HASMCs, I pre-incubated the HAEC conditioned media with noggin (a BMP inhibitor), subsequently abrogating the increased HASMC osteoblastic activity. By contrast, exposure of HAECs to TRAIL was not associated with any increase in osteoblastic activity within reporter HASMC cultures.

While paracrine signaling between EC and SMC populations has been reported as relevant to various aspects of vascular physiology and pathophysiology [210,211], to

the best of my knowledge only one group, Osako *et al,* have examined the influence of this system on VC to any significant degree [38]. In general, the data presented by this group are consistent with my own in that they also reported that a paracrine signal, most likely BMP-2, was produced by HAECs in response to RANKL, and induced osteoblastic change in VSMCs. My own methodological approach differed somewhat from that adopted by this group in that I also assessed the effects of TRAIL on HAEC:HASMC paracrine signaling, and I assessed the roles of both BMP-2 and BMP-4 in this context. Furthermore, their approach involved the use of calcifying media, whereas I utilized standard Promocell growth media as described in chapter 3, which as previously stated, does not contain excess calcium or phosphate. It should be noted, however, that my own approach did have one limitation (also relevant to the experiments involving the CELLMAX® DUO) in that it is possible the hydrocortisone supplement in Promocell endothelial growth factor media MV may have accentuated the osteoblastic activity of HASMCs observed in these experiments. This possibility arises as steroids have been reported to induce calcification *in vitro* [271]. This effect, however, would have been expected to be evident evenly throughout the experiments, and would not account for the increased osteoblastic response following exposure of HAECs to RANKL, nor would it be abrogated by noggin, an inhibitor specific to BMP proteins [272]. Therefore, while I acknowledge and highlight this aspect of my own methodology, I submit that it is unlikely to account for the RANKL-induced osteoblastic effects observed.

Ultimately, I report that the cumulative results of the first and second components of Study II of the present thesis indicate that neither RANKL nor TRAIL affect osteoblastic activity in HASMCs directly, but that RANKL (but not TRAIL) instead promotes VC in an indirect fashion via the upregulation of BMP-2 production by HAECs. This relationship, whose characterization and confirmation are one of the major findings of the present

thesis, describes a theoretical basis by which RANKL may promote VC *in vivo*, and is illustrated in figure 4.14.

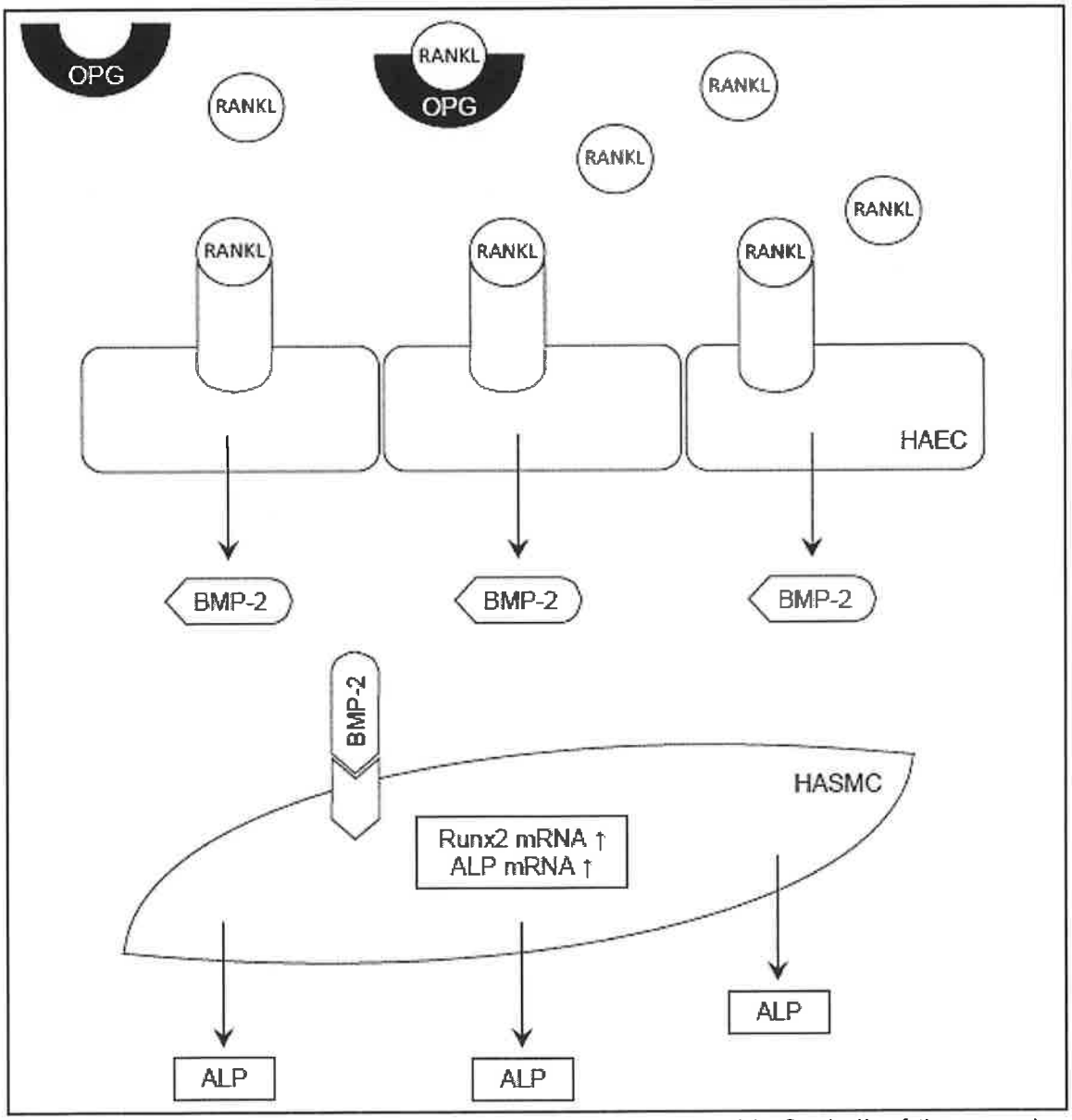

Figure 4.14. Schematic representation, based on data genearted in Study II, of the paracrine relationship between HAECs and HASMCs with regards to osteoblastic activity. RANKL binding to RANK receptors on HAECs can be seen to induce BMP-2 release, which acts in turn on HASMCs to induce osteoblastic change. As a decoy receptor for RANKL, it may be hypothesized that OPG opposes this process. ALP, alkaline phosphatase; BMP-2, bone morphogenetic protein-2; HAEC, human aortic endothelial cell; HASMC, human aortic smooth muscle cell; OPG, osteoprotegerin; RANKL, receptor activator of nuclear factor kappa-beta ligand; Runx2, runt-related transcription factor 2.

4.3.3. The Effect of RANKL on Osteoblastic Activity in HASMCs Maintained in Co-Culture with HAECs in the CELLMAX® DUO Perfused Capillary System.

On reviewing the literature regarding OPG, RANKL, TRAIL and VC, it quickly becomes apparent that there is a significant degree of discrepancy within the evidence base on these ligands and calcification to date. As stated previously, there are a variety of methodological issues that may explain some of these discrepancies, but ultimately, the conflicting data in this area have made it difficult to obtain any useful insights into the role played by OPG and its ligands within the vascular wall *in vivo.* With this in mind, in the final component of Study II of the present thesis I designed and conducted experiments which matched, to the greatest degree possible in the laboratory, the vascular environment *in* vivo, an approach which, to the best of my knowledge, is entirely novel in the field of calcificaion research. Whilst the logistical challenges of establishing and maintaining the CELLMAX® DUO system made it impracticable (with regards to labor, time and cost) for exploring the basic aspects of the OPG system in HAECs and HASMCs, its usefulness instead lay in allowing us to test the principal findings from the monoculture and conditioned media experiments in an approximation of the vascular environment [212,213]. In this way, the concluding experiments of Study II were designed with the goal of progressing the overall evidence base on OPG, RANKL and VC towards closer comparability to the *in vivo* state.

The principal finding of the first two components of Study II was the characterization of the effects of RANKL on HAECs, with the induction of BMP-2 and the subsequent osteoblastic reactions of HASMC cultures. As such, it was this relationship that I tested with the CELLMAX® DUO system. In total, 7 CELLMAX® DUO co-cultures were established, each hosting a co-culture of HAECs and HASMCs, arranged on the inside and outside, respectively, of semi-permeable capillaries that allow an exchange of paracrine signals, with media flowing through the HAEC-lined lumens at flow rates

designed to produce physiological levels of shear stress (10 dynes/cm^2) on the HAEC population. This final aspect of the system is of particular importance, as shear stress has previously been shown by Chiu *et al* to exert both pro-and anti-atherogenic effects, depending on its intensity and location within the vasculature [214,273]. At physiological levels of laminar shear stress, such as were established for these experiments, HAECs tend to assume an anti-atherogenic phenotype, and as such may be assumed to approximate the *in vivo* state more closely than when they are maintained in static cultures [214]. As described in chapter 2, RANKL was added to 2 of these systems on a twice-daily basis, and after 72 hours of exposure of the HAECs to this ligand, the co-cultures were harvested from these CELLMAX® DUO systems and compared to the 2 control systems. Ultimately, therefore, the final experiments of Study II involved the establishment of an artificial vessel wall, with an exposure of the intimal HAECs to RANKL in the circulating media, and a harvesting of the outer medial HASMCs to determine if any osteoblastic change had resulted.

At the conclusion of the CELLMAX® DUO experiments, exposure of HAECs to RANKL within the circulating media was associated with a significant increase in HASMC ALP activity, along with increased expression of levels of Runx2, ALP and BSP mRNA within the HASMC population. Although these experiments may be critiqued as having a relatively small n (n=4 for units exposed to RANKL, n=3 for controls), the large number of cells (>1x10^7 HAECs and HASMCs) maintained within each system, in addition to the approximation of the *in vivo* environment provided by the CELLMAX® DUO, and also the fact that these are the first *in vitro* experiments of their kind in the field of VC, render these observations highly novel and of particular interest to the emerging picture on the actions of RANKL within the vasculature. Encouragingly with regards to previous monoculture and conditioned media experiments within the field,

the results of the CELLMAX® DUO experiments were consistent with what I had observed in the first two parts of Study II.

In conclusion, therefore, the results of Study II describe a pathway whereby RANKL may induce osteoblastic activity, and hence VC, by stimulating BMP-2 release from HAECs (which in turn acts in a paracrine fashion on HASMCs to induce an osteoblastic phenotype). With such a mechanism identified, the role of OPG as a blocker of RANKL becomes of greater relevance to VC. Moreover, when combined with the observations from Study I that insulin reduces OPG release from HASMCs, it may be speculated that insulin, by reducing the release of OPG, facilitates the unopposed action of RANKL within the vascular wall, with increased release of BMP-2 by HAECs leading to increased osteoblastic activity by HASMCs. In Study III, these observations are tested *in vivo*, with a progression from the artifical capillary experiments of the CELLMAX® DUO to the clinical setting of T2DM, and a prospective study on the effects of insulin on calcification of the coronary arteries.

Chapter 5 - The Effect of Insulin Versus Liraglutide on Calcification of the Vasculature *In Vitro* and *In Vivo*

5.1. Introduction

As noted previously, human insulin has been reported to accelerate the calcification of VSMCs in culture [39], although whether insulin analogues such as insulin glargine have a simliar effect is unknown. Furthermore, hyperinsulinemia has been associated with high rates of VC in patients with T2DM, although whether this represents an effect of insulin or of co-morbid conditions such as dyslipidemia is difficult to determine. With this is mind, the goals of Study III of the present thesis were twofold. To begin with, the direct effects of insulin glargine and liraglutide on the emergence of osteoblastic activity in HASMCs were assessed *in vitro*. Subsequently, a prospective, observational study of patients a) remaining on metformin±sulphonylurea only, b) commencing liraglutide or c) commencing insulin analogue therapy was performed to assess the effect of these medications on CAC.

In Study I, insulin glargine was noted to decrease the release of OPG from HASCMs, whilst in Study II it was demonstrated that RANKL (a glycoprotein whose actions are blocked by OPG), was associated with an increased production of BMP-2 by HAECs, which was in turn associated with increased osteoblastic activity in HASMCs. By decreasing the production of OPG by HASMCs, therefore, it is possible that insulin glargine facilitates unchecked RANKL-induced osteoblastic activity and VC. In addition to affecting the activity of OPG and RANKL, however, receptors for insulin (and its analogues) exist on both HAECs and HASMCs, and the possibility of a direct effect by insulin glargine on calcifying activity in these two cell populations, in the absence of RANKL, also merits assessment. Furthermore, and as noted previously, liraglutide is a therapeutic alternative to insulin analogues in certain patients with T2DM, and its effects on osteoblastic activity in HASMCs have not been assessed. The *in vitro* component of Study III, therefore, tested the effects of insulin glargine and liraglutide, in

the absence of RANKL on a) the production of BMP-2 and BMP-4 by HAECs and HASMCs, and b) the emergence of osteoblastic activity in HASMCs.

While VC is a characteristic component of T2DM, hyperinsulinemia is a recognised aspect of T2DM [193], and insulin in various forms has been utilized to treat T2DM since the early part of the 20th century, there is a paucity of data on the effects of insulin analogues on the progression of VC. While Jorgensen *et al.* and Xiang *et al.* have both reported a decrease in circulating OPG concentrations with insulin administration in T1DM and T2DM, VC was not included as an endpoint in these studies [21,117]. To the best of my knowledge, the effects of liraglutide on VC *in vivo* have not been assessed in any significant detail to date. The *in vivo* component of Study III, therefore, followed a group of patients with T2DM as they commenced either liraglutide or insulin analogue therapy, with CAC scores measured prior to commencement of, and again after 16 months of exposure to, these medications.

5.2. Experiments and Results

With regards to the assessment of the effects of insulin glargine and liraglutide on calcifying activity in HAECs and HASMCs, these cell populations were grown in Promocell media with growth supplements as previously described and seeded to 6-well plates. Insulin glargine (1 nmol/l and 10 nmol/l) and liraglutide (30 nmol/l and 300 nmol/l) were added to the supernatant media to achieve pathophysiological (1 nmol/l and 30 nmol/l, respectively) and supraphysiological (10 nmol/l and 300 nmol/l) concentrations. At 72 hours, the supernatant media was harvested from the cell cultures, ALP activity in the supernatant media of HASMCs was measured with the Quantichrom™ assay, BMP-2 and BMP-4 concentrations in the supernatant media of HAECs and HASMCs were measured by ELISA, and HASMC mRNA was harvested to facilitate measurement of mRNA levels for Runx2, BSP and ALP. To determine

whether BMP-2 or BMP-4 signaling were involved in any medication effects observed, the HASMC experiments with insulin glargine and liraglutide were repeated in the presence of noggin (2.5 µg/ml).

In the clinical study, patients with T2DM were recruited as previously described, serum samples were harvested and subjected to ELISA for OPG, RANKL and TRAIL (Duoset assay), the remaining blood tests were performed using standard laboratory techniques, and CAC scores were calculated using MDCT (GE Lightspeed). Patients in the control group remained on metformin ± sulphonylurea, whereas patients in the liraglutide and insulin analogue groups commenced these medications as planned, and the baseline tests were repeated after 16 months. Statistical tests utilized are reported in the respective figures.

5.2.1. The Effects of Insulin Glargine and Liraglutide on Calcifying Activity in HAECs and HASMCs

Quantichrom™ and Duoset assays were performed as previously described in Study II. The effects of 72 hours of exposure to liraglutide on OPG release by HAECs and HASMCs are illustrated in figure 5.1. As shown, exposure to liraglutide was not associated with any significant change in OPG concentrations in either cell population. Upon examination of the effects of insulin glargine on the production of ALP by HASMCs, a significant increase in ALP activity was observed in the supernatant media of HASMCs exposed to insulin glargine at 1 nmol/l and 10 nmol/l (non-dose-dependent) when compared to controls without insulin glargine or liraglutide. Exposure of HASMCs to liraglutide (30 nmol/l and 300 nmol/l) was not associated with any significant change in ALP activity. No change in the concentrations of BMP-2 and BMP-4 in the supernatant media of HASMCs were observed under any experimental conditions, whilst he addition of noggin had no demonstrable effect on ALP activity (figure 5.2).

When mRNA samples were subjected to analysis, dose-dependent increases in levels of Runx2 and ALP mRNA were observed in HASMCs following exposure to insulin glargine at 1 nmol/l, while increased levels of Runx2, ALP and BSP mRNA were observed following exposure to insulin glargine at 10 nmol/l. No changes in target mRNA levels were observed following exposure to liraglutide at 30 nmol/l and 300 nmol/l. The addition of noggin had no demonstrable effect on mRNA levels (figure 5.3).

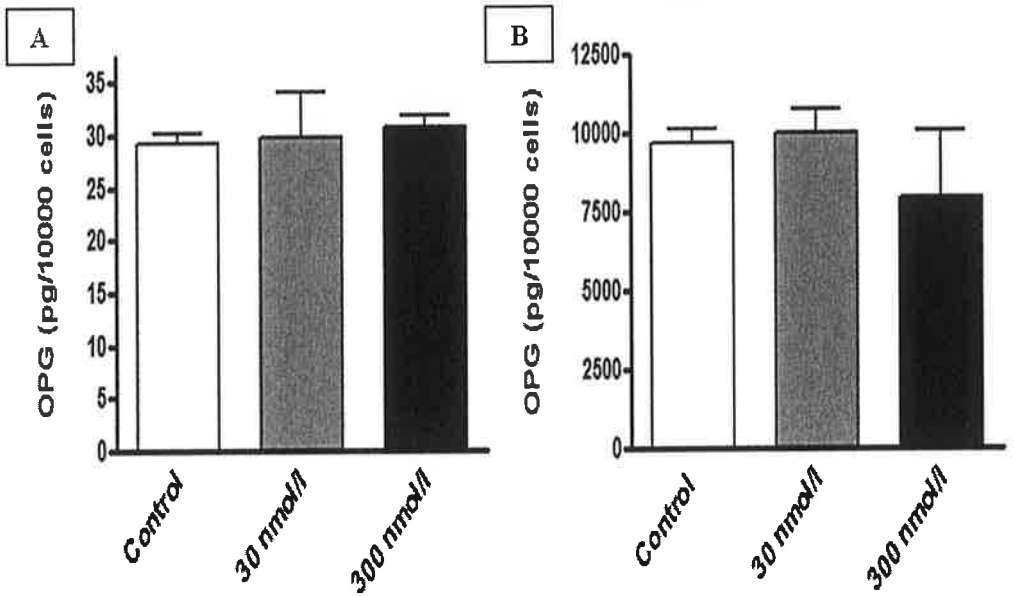

Figure 5.1. OPG concentrations as measured by Duoset assay in supernatant media from A: HAECs, and B: HASMCs exposed to liraglutide (30 nmol/l and 300 nmol/l) for 72 hours. OPG concentrations are displayed in pg per 10000 cells following correction for viable HAEC and HASMC population. Data are given as mean±SEM. n=18 for all experiments. HAEC, human aortic endothelial cell; HASMC, human aortic smooth muscle cell; OPG, osteoprotegerin; SEM, standard error of the mean.

With regards to the effects of insulin glargine and liraglutide on HAECs, increased concentrations of BMP-2 were observed in the supernatant media of HAECs exposed to insulin glargine at 1 nmol/l and 10 nmol/l (non-dose-dependent) and liraglutide at 30 nmol/l and 300 nmol/l (non-dose-dependent). Exposure of HAECs to either insulin glargine or liraglutide was not associated with any change in BMP-4 concentrations in the supernatant media (figure 5.4).

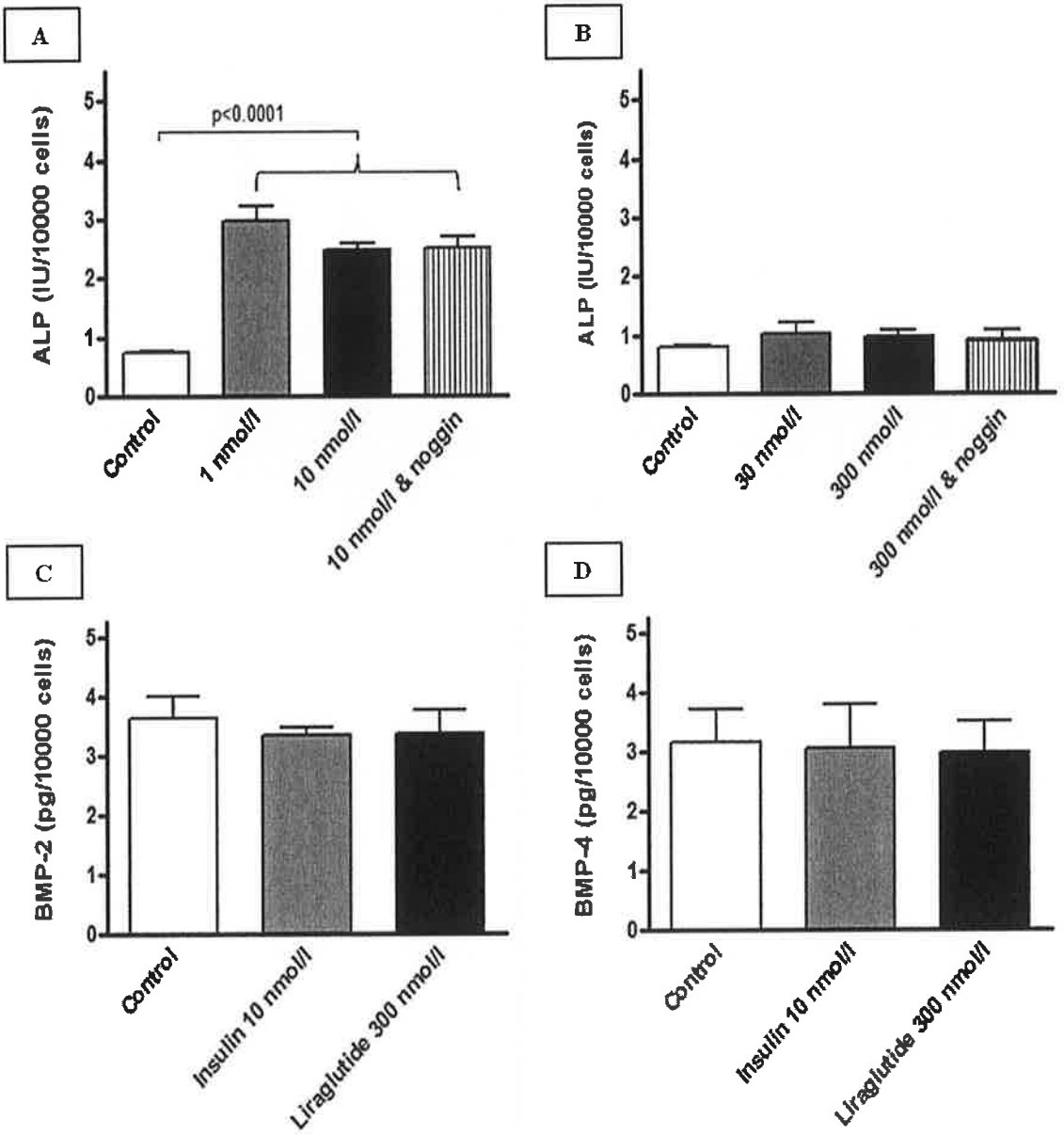

Figure 5.2. ALP activity (as measured by Quantichrom™ assay) and BMP-2/4 concentrations (as measured by Duoset assay) in supernatant media from HASMCs following exposure to insulin glargine or liraglutide. A: ALP activity following exposure to insulin glargine (1 nmol/l and 10 nmol/l ±2.5 µg/ml noggin). B: ALP activity following exposure to liraglutide (30 nmol/l and 300 nmol/l ± 2.5 µg/ml noggin). C: BMP-2 concentrations following exposure to insulin glargine (10 nmol/l) and liraglutide (300 nmol/l). D: BMP-4 concentrations following exposure to insulin glargine (10 nmol/l) and liraglutide (300 nmol/l). ALP activity is displayed in IU per 10000 cells, and BMP-2 and BMP-4 concentrations are displayed in pg per 10000 cells, following correction for viable HASMC population. Data are given as mean±SEM. n=18 for all experiments. ALP, alkaline phosphatase; BMP-2/4, bone morphogenetic protein 2/4; HASMC, human aortic smooth muscle cell; SEM, standard error of the mean.

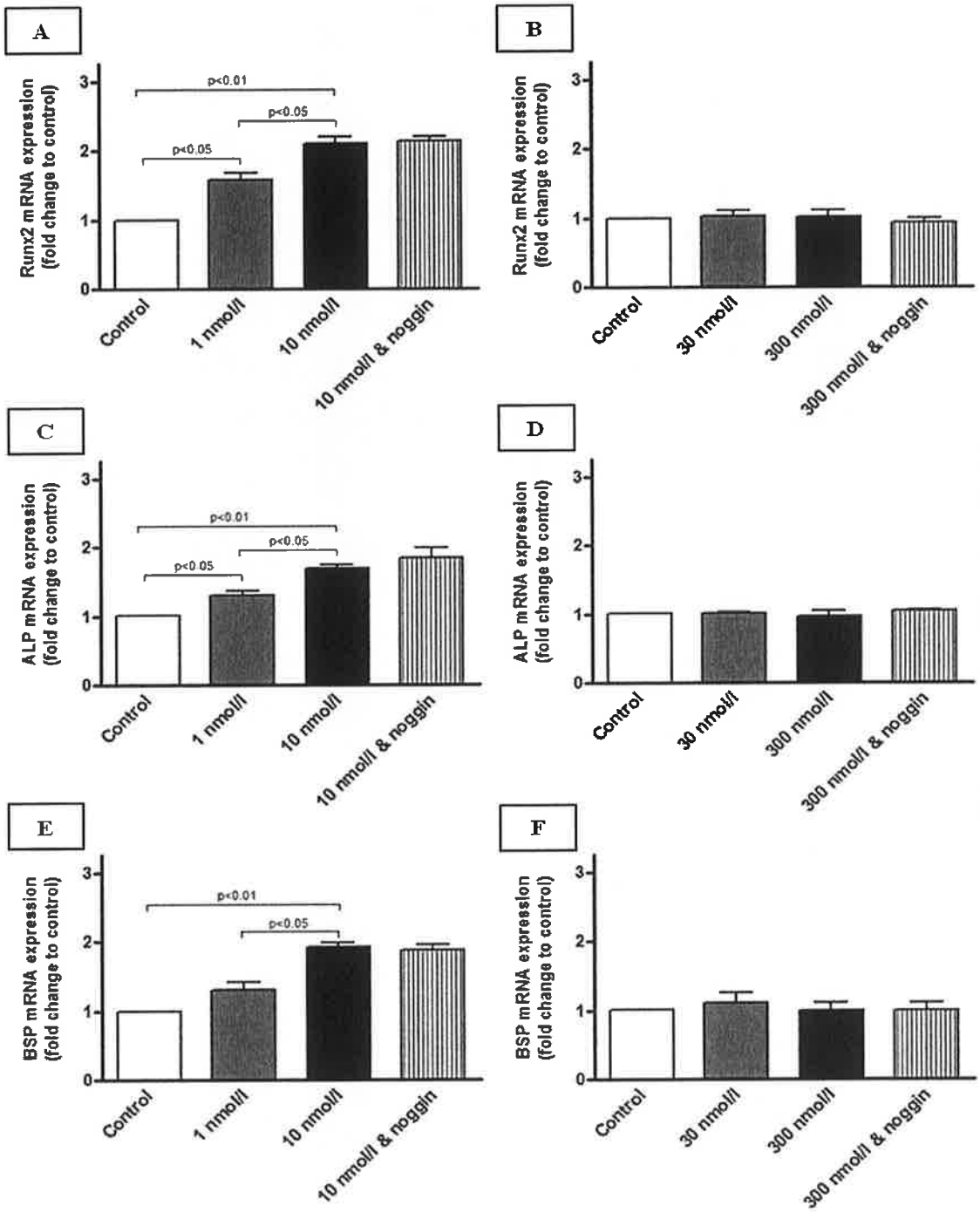

Figure 5.3. Effects, on HASMCs, of 72 hours of exposure to insulin glargine at 1 nmol/l and 10 nmol/l and liraglutide at 30 nmol/l and 300 nmol/l, with and without noggin at 2.5 µg/ml, on levels of Runx2, ALP and BSP mRNA. A: Effect of insulin glargine on levels of Runx2 mRNA. B: Effect of liraglutide on levels of Runx2 mRNA. C: Effect of insulin glargine on levels of ALP mRNA. D: Effect of liraglutide on levels of ALP mRNA. E: Effect of insulin glargine on levels of BSP mRNA. F: Effect of liraglutide on levels of BSP mRNA. mRNA differences are expressed as the fold change in mRNA levels relative to control. Data are given as mean±SEM. During the qRT-PCR, S18 was utilized to normalize differences in total cDNA quantity between samples, and Rox was utilized to normalize non-PCR-related flourescence fluctuations between wells. n=18 for all experiments. ALP, alkaline phosphatase; BSP, bone sialoprotein; cDNA. complimentary deoxyribonucleic acid; HASMC, human aortic smooth muscle cell; mRNA, messenger ribonucleic acid; qRT-PCR, quantitative reat-time polymerase chain reaction; Runx2, runt-related transcription factor 2; SEM, standard error of the mean.

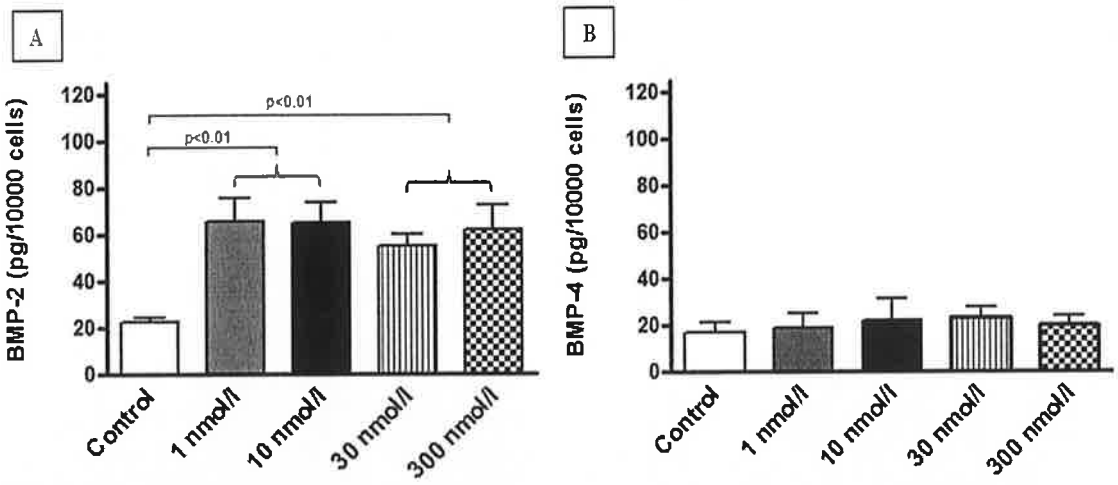

Figure 5.4. BMP concentrations as measured by Duoset assay in supernatant media from HAECs exposed to insulin glargine (1 nmol/l and 10 nmol/l) and liraglutide (30 nmol/l and 300 nmol/l). A: BMP-2 concentrations following exposure to insulin glargine and liraglutide. B: BMP-4 concentrations following exposure to insulin glargine and liraglutide. BMP-2/4 concentrations are displayed in pg per 10000 cells following correction for viable HAEC population. Data are given as mean±SEM. n=18 for all experiments. BMP-2/4, bone morphogenetic protein 2/4; HAEC, human endothelial cell; SEM, standard error of the mean.

5.2.2. The Effects of Insulin Versus Liraglutide on CAC in Patients with T2DM

5.2.2.1. Descriptives

Duoset assays were performed as previously described, with significant colour change noted with serum samples. Data are presented as mean±SEM or median (25% percentile - 75% percentile), as appropriate. Statistical tests utilized are described in figure legends.

5.2.2.2. Recruitment

During the recruitment phase, 110 patients with T2DM who were a) continuing on metformin±sulphonylurea, b) on metformin±sulphonylurea and due to commence liraglutide or c) on metformin±sulphonylurea and due to commence insulin analogue therapy, and who did not meet any exclusion criteria, agreed to enter this observational study. Of the two recruitment sites, 99 patients were recruited and followed-up in Beaumont Hospital, and 11 patients were recruited and followed-up in James Connolly Hospital. Of the population recruited, 7 patients met exclusion criteria (due to changes in their diabetes treatment regime) over the course of the study, and 2 patients

declined to attend for the follow-up visits at the conclusion of the study. Baseline and follow-up data were provided for 101 patients in total, and these data were included in the final analysis.

5.2.2.3. Baseline Characteristics of the Study Population

In table 5.1, the characteristics of the study population, stratified by treatment group, are presented. The mean age (±SEM) of the entire study population was 59.4±1.1 years. 44 patients remained on metformin±sulphonylurea therapy for the duration of the study (metformin group). 32 patients commenced liraglutide and were exposed to this medication, without any concomitant exposure to insulin analogues, for the duration of the study (liraglutide group). 25 patients commenced insulin analogue therapy and were exposed to this medication, without any concomitant exposure to liraglutide, for the duration of the study. Within the insulin analogue group, 22 patients received insulin glargine, and 3 received insulin determir. In addition to the basal insulin analogues, a bolus insulin analogue (insulin aspart) at mealtimes was prescribed for 5 patients over the duration of the study.

With regards to baseline differences between the groups in this observational study, age was higher and eGFR was lower in the metformin group in comparison to the liraglutide group. Sulphonylurea use was also lower in this group than in the liraglutide and insulin analogue groups. Weight and BMI were significantly higher in the liraglutide group than the metformin and insulin analogue groups. Years since diagnosis of diabetes, along with OPG concentrations, were significantly higher in the insulin analogue group than the metformin or liraglutide groups. HbA1c and triglycerides were higher in the liraglutide group than the metformin group, and higher again in the insulin analogue group.

Table 5.1. Clinical characteristics of the study subjects at baseline.

	Metformin	*Liraglutide*	*Insulin*	*p*
Gender male/female; (%)	35/9; 79.5%	21/11; 65.6%	15/10; 60.0%	NS
Age (yrs)	63.8±1.3**	53.6±1.7	59.2±2.3	<0.0005
Metabolic characteristics				
Weight (kg)	89.2 (75.5-96.2)**	109.8 (100.0-121.1)†	90.5 (80.4-113.4)	<0.0005
BMI (kg/m^2)	30.1 (27.5-33.2)**	36.8 (33.3-41.1)	31.4 (29.2-39.1)	<0.0005
HbA1c (mmol/mol)	49 (46-53)**	58 (52-66)††	73 (63-85)‡‡	<0.0005
Total cholesterol (mmol/l)	3.8±0.1	4.1±0.2	4.4±0.2	NS
LDL cholesterol (mmol/l)	1.9±0.1	2.0±0.1	2.2±0.2	NS
HDL cholesterol (mmol/l)	1.16 (1.00-1.34)	1.11 (0.95-1.29)	1.07 (0.93-1.47)	NS
Triglycerides (mmol/l)	1.44 (1.18-2.38)	1.55 (1.21-2.33)	2.12 (1.42-2.86)	<0.05
eGFR (ml/min/1.73m^2)	98±3*	110±4	96±5	<0.05
Calcification data				
OPG (pg/ml)	1080±58	1192±77	1445±106‡	0.005
RANKL (pg/ml)	256 (0-874)	88 (0-544)	47 (0-383)	NS
TRAIL (pg/ml)	242±42	209±65	212±24	NS
Calcium (mmol/l)	2.36±0.01	2.38±0.02	2.39±0.02	NS
CAC score	219 (3-768)	5 (0-150)	354 (3-738)	NS
Medical history				
Years since T2DM dx	4.0 (3.0-6.0)	5.0 (3.0-6.5)	7.0 (4.5-11.0)	<0.05
Smoking (yes/no; %)	9/35; 20.5%	6/26; 17.1%	2/23; 8.0%	NS
IHD (yes/no; %)	3/41; 6.8%	0/32; 0%	3/22; 12.0%	NS
CVA (yes/no; %)	1/43; 2.3%	0/32; 0%	1/24; 4.0%	NS
Statins (yes/no; %)	37/7; 84.1%	27/5; 84.4%	20/5; 80.0%	NS
ACEi/ARB (yes/no; %)	30/14; 68.2%	23/9; 71.9%	18/7; 72.0%	NS
Sulphonylureas (yes/no; %)	4/40; 9.1%*	11/21; 34.4%	12/13; 48.0%‡‡	0.001

Data are given as mean±SEM or median (25% percentile - 75% percentile), as appropriate. Statistical tests used to assess the differences between the study groups are one-way ANOVA or Chi-squared test, as appropriate. *for comparison (Games-Howell post hoc test) between metformin and liraglutide groups, *<0.05, **<0.0005. †for comparison (Games-Howell post hoc test) between liraglutide and insulin groups, †<0.05, ††<0.005. ‡for comparison (Games-Howell post hoc test) between insulin and metformin groups, ‡<0.05, ‡‡<0.005. ACEi, angiotensin converting enzyme inhibitor; ARB, angiotensin receptor blocker; BMI, body mass index; CAC, coronary artery calcification; CVA, cerebrovascular accident; dx, diagnosis; eGFR, estimated glomerular filtration rate, HDL, high-density lipoprotein; HbA1c, glycated hemoglobin A1c; IHD, ischemic heart disease; LDL, low-density lipoprotein; NS, non-significant; OPG, osteoprotegerin; RANKL, receptor activator of nuclear factor kappa-beta ligand; T2DM, type 2 diabetes mellitus; TRAIL, tumor necrosis factor-related apoptosis-inducing ligand.

With regards to an analysis of the variables of interest at baseline (figure 5.5), a significant correlation was noted between CAC score and age across the entire group (Spearman's rank correlation coefficient of 0.48). No significant correlations were noted between CAC score, RANKL, TRAIL and OPG at baseline. Circulating concentrations of OPG were significantly higher in patients with a past history of IHD.

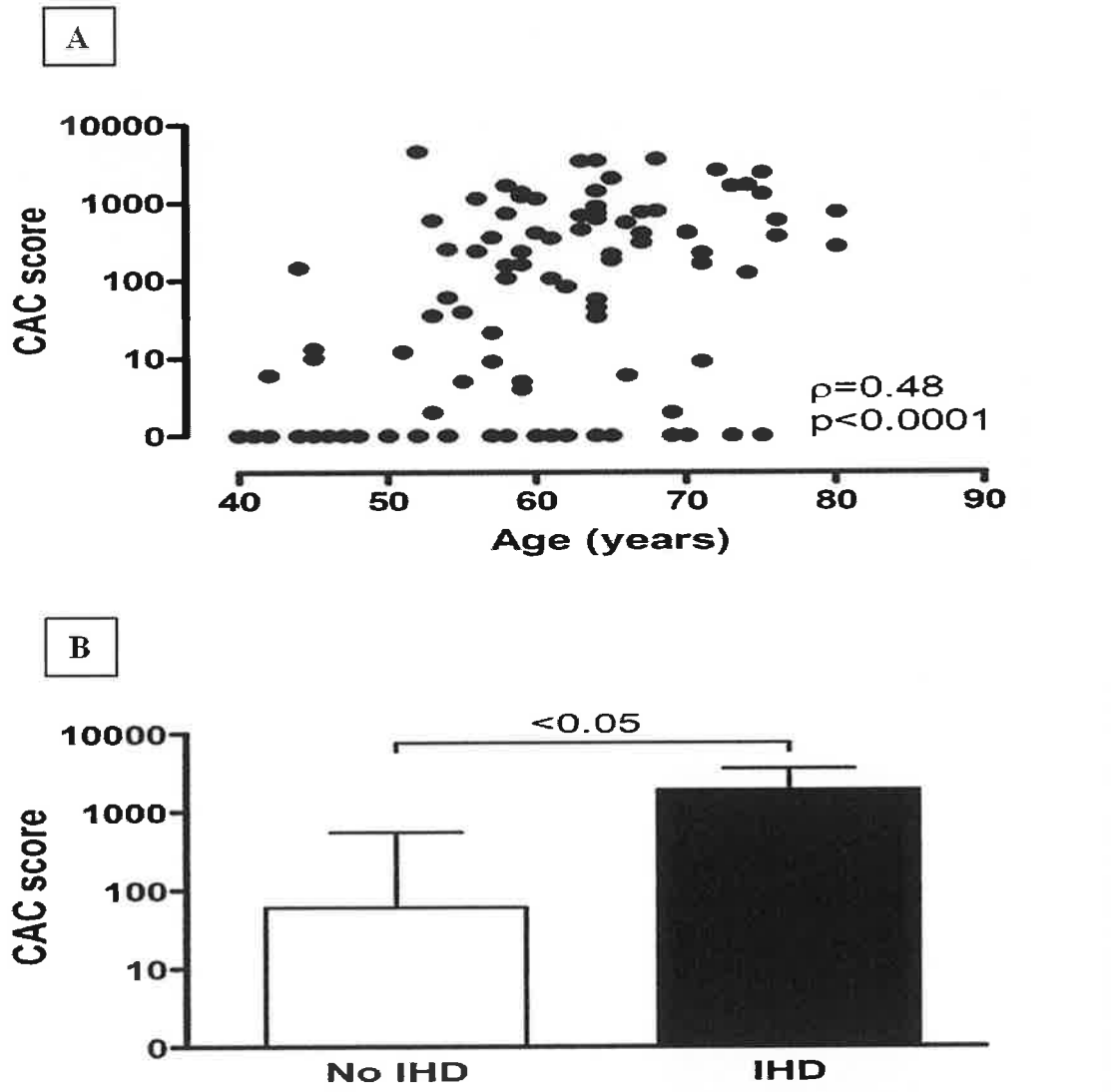

Figure 5.5. Baseline analysis of CAC scores as measured by MDCT. A: CAC scores correlated with age across the entire study population at baseline. B: CAC scores were significantly higher in patients with a history of IHD compared to those without at baseline. Data are given as median (25% percentile - 75% percentile). A non-parametric test (Spearman rank) was used to assess correlation. Difference between the groups was assessed with the Mann Whitney test. CAC, coronary artery calcification; IHD, ischemic heart disease; MDCT, multidetector computed tomography.

5.2.2.4. Change in Baseline Variables over the Duration of the Study

In table 5.2, the changes in baseline variables over the duration of the study, stratified by group, are presented. CAC and OPG, as variables of particular interest, are presented in figure 5.6 and figure 5.7. With regards to the metformin group, no significant change in any of the baseline variables were observed over the duration of the study. With regards to the liraglutide group, significant reductions in weight, HbA1c and triglycerides were observed over the duration of the study. With regards to the insulin analogue group, CAC score was observed to increase significantly, while OPG and HbA1c decreased significantly, over the study timeframe.

Table 5.2. Change in baseline variables over the duration of the study.

	Metformin	*Liraglutide*	*Insulin*
Metabolic characteristics			
Weight (kg)	-0.31±0.8	-2.9±1.0†	+0.2±0.7
BMI (kg/m^2)	-0.2±0.3	-1.1±0.4†	+0.2±0.3
HbA1c (mmol/mol)	-0.8±1.0	-7.7±1.5†††	-5.3±3.2
Total cholesterol (mmol/l)	-0.01±0.09	-0.07±014	-0.23±0.2
LDL cholesterol (mmol/l)	-0.05 (-0.41-0.14)	-0.30 (-0.52-0.13)	-0.22 (-0.60-0.17)
HDL cholesterol (mmol/l)	-0.04 (-0.13-0.11)	-0.02 (-0.07-0.07)	0 (-0.23-0.07)
Triglycerides (mmol/l)	+0.07 (-0.23-0.32)	+0.08 (-0-32-0.71)	-0.07 (-0.53-0.49)
eGFR (ml/min/1.73m^2)	-0.9±1.6	2.4±0.02††	-5.2±2.6
Calcification data			
OPG (pg/ml)	+161±46*	-75±66	-286±55‡‡
RANKL (pg/ml)	+45 (-60-106)	+63 (-34-143)	-67 (-144-0)
TRAIL (pg/ml)	+16±5	+14±4	+23±7
Calcium (mmol/l)	+0.01±0.02	-0.01±0.02	-0.01±0.02
CAC score	+4 (-21-66)	0 (-8-4)	+65 (2-309)‡‡

Data are given as mean±SEM or median (25% percentile – 75% percentile), as appropriate. Statistical tests used to assess the differences between the study groups are paired *t*-test or Wilcoxon signed rank test, as appropriate. *for comparison of change within the metformin group, *<0.005. †for comparison of change within the liraglutide group, †<0.05, ††<0.005, †††>0.0005. ‡for comparison of change within the insulin group, ‡<0.005, ‡‡<0.0005. BMI, body mass index; CAC, coronary artery calcification; eGFR, estimated glomerular filtration rate, HDL, high-density lipoprotein; HbA1c, glycated hemoglobin A1c; LDL, low-density lipoprotein; OPG, osteoprotegerin; RANKL, receptor activator of nuclear factor kappa-beta ligand; T2DM, type 2 diabetes mellitus; TRAIL, tumor necrosis factor-related apoptosis-inducing ligand.

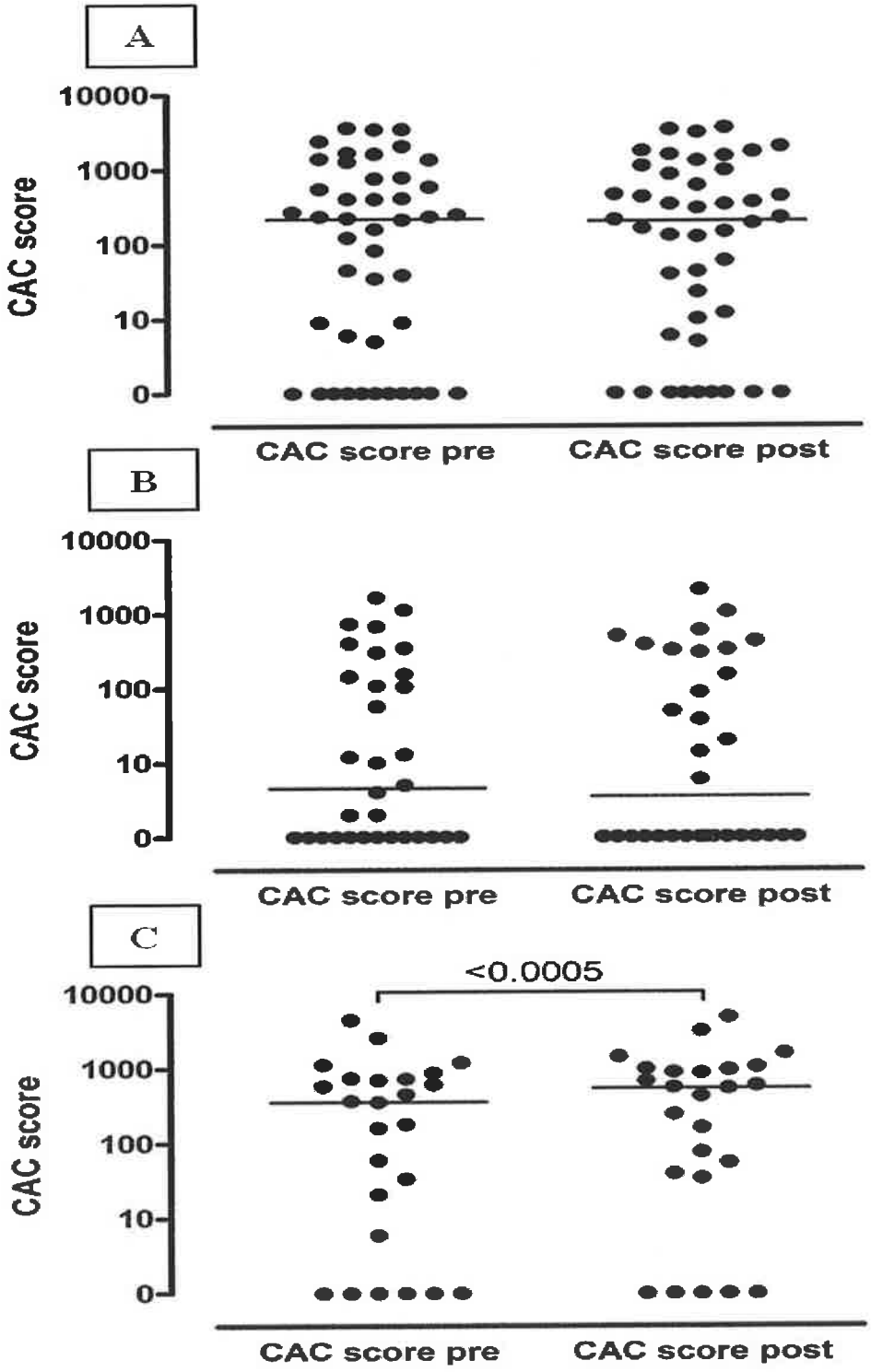

Figure 5.6. CAC scores as measured by MDCT at baseline (pre) and at 16 months (post), stratified into A: metformin, B: liraglutide and C: insulin groups. Datapoints are provided, with lines indicating median value. The Wilcoxon signed rank test was utilized to test for differences in CAC score from pre to post. CAC, coronary artery calcification; IHD, ischemic heart disease; MDCT, multidetector computed tomography.

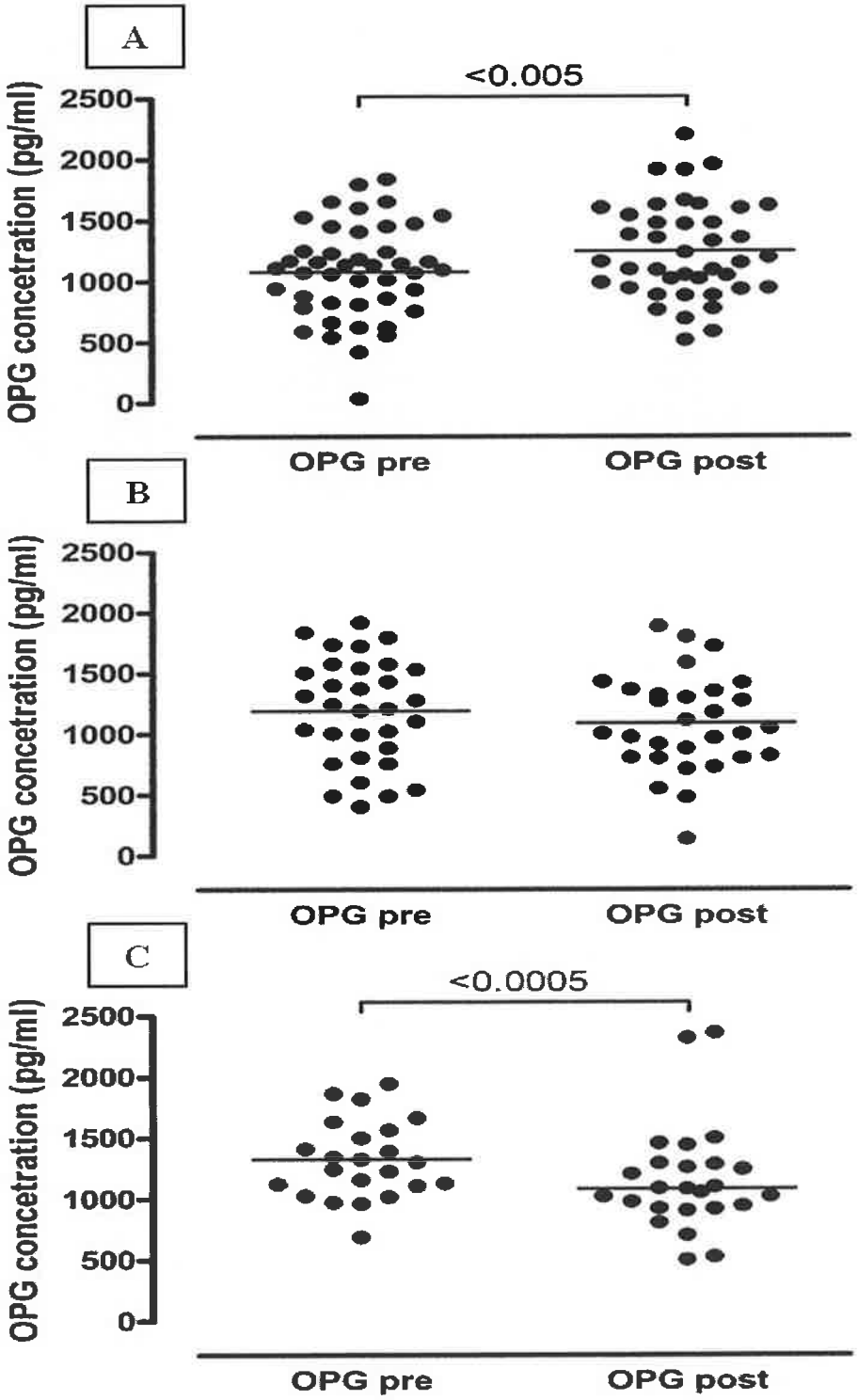

Figure 5.7. Circulating OPG concentrations as measured by ELISA at baseline (pre) and at 16 months (post), stratified into A: metformin, B: liraglutide, and C: insulin groups. Datapoints are provided, with lines indicating mean or median values where appropriate. Paired t-test or wilcoxon signed rank test were utilized, as appropriate, to test for differences in OPG concentrations from pre to post. ELISA, enzyme-linked immunosorbent assay; OPG, osteoprotegerin.

5.2.2.5. Effects of Treatment on CAC, OPG, RANKL and TRAIL

Data from ANCOVA analyses on CAC are presented in table 5.3. In the initial analysis a significant ($p<0.0005$) treatment effect was observed. Exposure to insulin analogue therapy was associated with a significantly greater change (increase) in CAC score over the duration of the study when compared to the metformin or liraglutide groups after post-hoc tests ($p<0.005$ and $p<0.05$, respectively). No difference in CAC change was observed in patients exposed to liraglutide when compared to the metformin control group. These results were maintained when the model was controlled for baseline differences in age, eGFR, weight, duration of diabetes, sulphonylurea use and triglycerides (significance for treatment effect of $p<0.005$, similar findings in the pairwise comparisons). When the model was controlled for all baseline differences, however, including age, eGFR, weight, duration of diabetes, sulphonylurea use, triglycerides and HbA1c, the treatment effect was no longer observed to be significant ($p=0.11$).

With regards to the effects of liraglutide or insulin analogues on the change in OPG, RANKL and TRAIL over the duration of the study, a significant treatment effect was observed with OPG ($p<0.01$). Exposure to insulin analogues was associated with a significant decrease in circulating OPG concentrations over the duration of the study in comparison to the metformin control group ($p<0.01$), but not the liraglutide group ($p=0.1$). These results were maintained when corrected for all baseline differences between the groups. No difference was observed in patients exposed to liraglutide when compared to the metformin control group. No treatment effect was observed on either RANKL or TRAIL.

Table 5.3. Effect of pharmacological interventions on CAC scores.

Model	*p-value*
Model adjusted for: • Baseline CAC score	*<0.0005** • Metformin versus liraglutide: NS† • Liraglutide versus insulin: <0.05† • Insulin versus metformin: <0.005†
Model adjusted for: • Baseline CAC score • + • Age (yrs) • Weight (kg) • eGFR (ml/min/1.73m^2) • Use of sulphonylurea	*<0.05** • Metformin versus liraglutide: NS† • Liraglutide versus insulin: NS† • Insulin versus metformin: <0.05†
Model adjusted for: • Baseline CAC score • Age (yrs) • Weight (kg) • eGFR (ml/min/1.73m^2) • Use of sulphonylurea • + • Time since T2DM dx (yrs)	*<0.05** • Metformin versus liraglutide: NS† • Liraglutide versus insulin: NS† • Insulin versus metformin: <0.05†
Model adjusted for: • Baseline CAC score • Age (yrs) • Weight (kg) • eGFR (ml/min/1.73m^2) • Use of sulphonylurea • Time since T2DM dx (yrs) • + • Triglycerides (mmol/l)	*<0.05** • Metformin versus liraglutide: NS† • Liraglutide versus insulin: NS† • Insulin versus metformin: <0.05†
Model adjusted for: • Baseline CAC score • Age (yrs) • Weight (kg) • eGFR (ml/min/1.73m^2) • Use of sulphonylurea • Time since T2DM dx (yrs) • Triglycerides (mmol/l) • + • HbA1c (mmol/mol)	*0.11**

*p-value for overall ANCOVA. †p-value for the Bonferroni post-hoc test for the difference between the treatment groups. CAC, coronary artery calcification; dx, diagnosis; eGFR, estimated glomerular filtration rate; HbA1c, glycated hemoglobin A1c; LDL, low-density lipoprotein; T2DM, type 2 diabetes mellitus.

In the final analysis, the mean insulin analogue dose per kg per day received by patients in the insulin analogue group was plotted against the change in CAC scores and OPG concentrations across the duration of the study. No significant correlations were observed (figure 5.8).

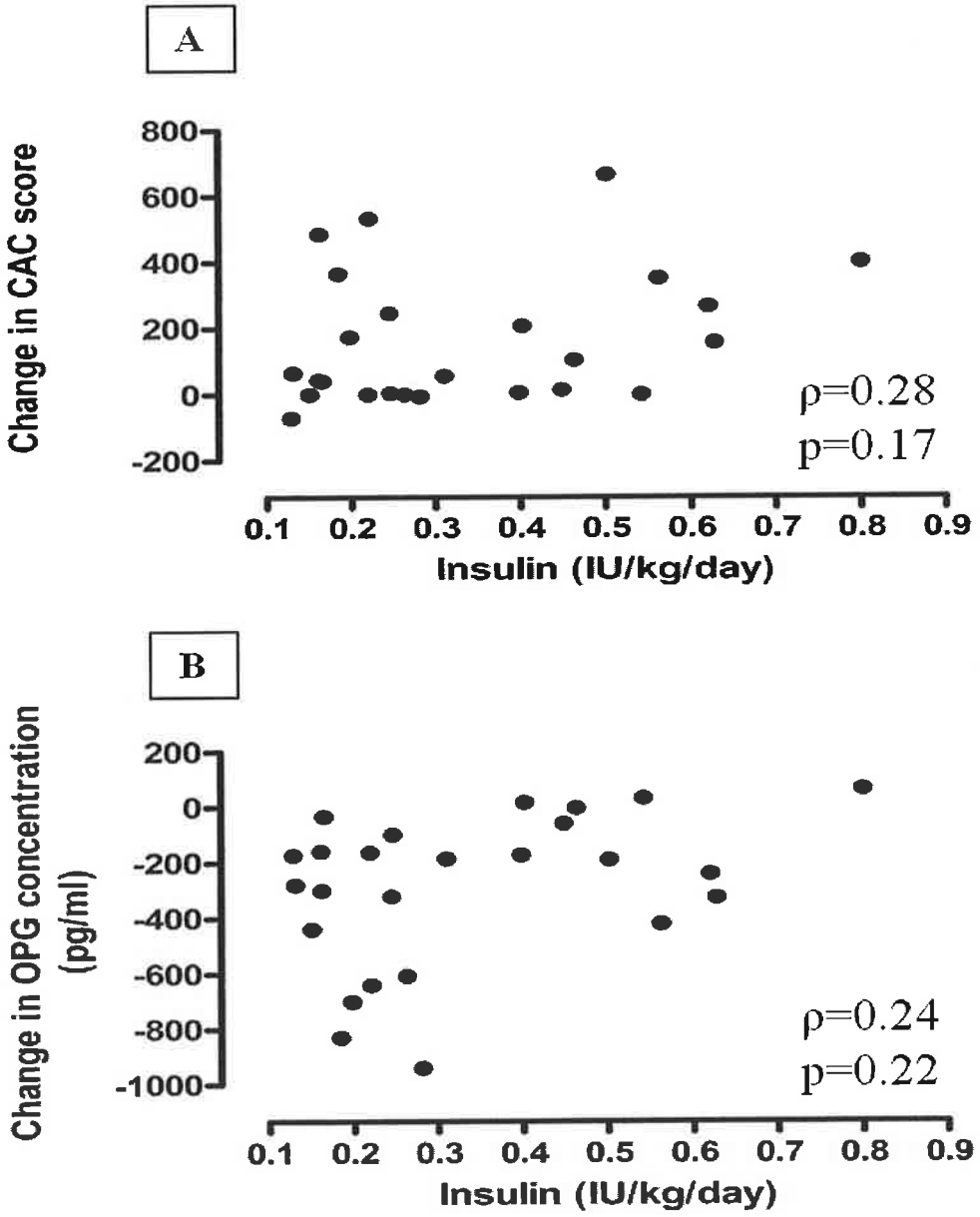

Figure 5.8. Mean insulin analogue dose per kg per day plotted against A: the change in CAC scores as measured by MDCT, and B: the change circulating OPG concentrations over the duration of the study in the insulin group. A non-parametric test (Spearman rank) was used to assess correlation. CAC, coronary artery calcification; MDCT, multidetector computed tomography; OPG, osteoprotegerin.

5.3. Discussion

Study III of the present thesis was comprised of both *in vitro* and *in vivo* research, and extrapolated upon the findings of Study II (that RANKL, whose actions are blocked by OPG, promotes osteoblastic activity in HASMCS) and Study I (that insulin glargine significantly downregulates OPG production and release from HASMCs). The primary goal of Study III, therefore, was to determine whether insulin analogues act to promote VC in both HASMC cultures and a clinical population of patients with T2DM. The effects of liraglutide, an alternative medication to insulin analogue therapy for the treatment of T2DM, was also assessed at the *in vitro* and *in vivo* levels as a clinically meaningful comparator [44].

As a multistep research project, Study III addressed a number of novel areas of interest. Whilst human insulin has previously been reported to decrease the production of OPG and accentuate RANKL-dependent VSMC calcification *in vitro*, the data reported were prelminary in nature, the endpoints of calcification reviewed were suboptimal, and, significantly, no data on the effects of insulin analogues (the mainstay of insulin treatment in clinical practice), existed in the literature. In Study III, therefore, an additional characterization of this effect of insulin was sought, using insulin glargine (a common insulin analogue, and the main insulin analogue used in the clinical study) and assessing both ALP activity in media and the emergence of osteogenic activity in HASMC at the mRNA level [39-41,186]. Furthermore, while insulin analogues has long been used for the treatment of T2DM, a patient population with a high prevalence of VC [42,43], and have been reported to acutely decrease circulating concentrations of OPG in patients with diabetes [21,117], to the best of my knowledge there have been no clinical studies, observational or otherwise, that have examined whether treatment with insulin analogues affects the progression of VC, or whether insulin induces a chronic downregulation of OPG. With regards to liraglutide, this relatively new

medication for the treatment of T2DM, for which receptors on coronary artery ECs exist [194], is being prescribed for this population with increasing frequency [44,274], yet to date there are little to no data regarding its effects on any aspect of the OPG/RANKL/TRAIL system, or on VC itself.

5.3.1. The Effects of Insulin and Liraglutide on Calcifying Activity in HAECs and HASMCs

In the *in vitro* component of Study III, I demonstrated that insulin glargine, when administered at concentrations that are relevant to the *in vivo* setting of T2DM, was associated with a significant increase in both the ALP activity of HASMC cultures, and increased HASMC expression of osteoblastic genes, including Runx2, ALP and BSP (the latter at supraphysiological concentrations of insulin glargine only). Concentrations of BMP-2 and BMP-4 were also measured in the supernatant media of the HASMC population, but were not observed to change in response to insulin glargine, suggesting an alternative mechanism by which insulin glargine led to the increase in osteoblastic activity observed. In contrast to insulin glargine, liraglutide was not observed to exert any effect on either OPG release by HASMCs, or osteoblastic activity. Moreover, in contrast to HASMCs, HAECs, when exposed to both insulin glargine and liraglutide, increased their production of BMP-2 (but not BMP-4).

With regards to previous research in this area, a number of other groups have reported that native insulin may promote osteoblastic activity and VC *in vitro,* but overall there has been a lack of consistency in the data on this issue, and no investigations of insulin analogues. Olesen *et al*, for example, reported in their initial publications that high-dose native insulin, when added to calcifying media, increased osteoblastic activity in HASMCs, but subsequently reported that they could not reproduce these findings. They attributed this discrepancy to heterogeneity between HASMC populations from different donors [39,186]. Yuan *et al.*, however, reported findings in keeping with

Olesen's first study when they described a significant increase in multiple markers of osteoblastic activity in murine CVCs (a sub-population of VSMCs that are particularly prone to undergoing osteoblastic change) [41]. Furthermore, this latter group reported that the effects of native insulin on osteoblastic activity in this study were being mediated by the ERK 1/2, but not the PI3K pathways, a result that may be relevant to the insulin resistant T2DM population, in whom an upregulation of the ERK 1/2 pathway has previously been reported [201]. Finally, and to complicate this scenario further, Wang *et al* reported that exposure to native insulin reduced osteoblastic activity in VSMCs, unless the PI3K pathway was selectively blocked, in which case insulin increased calcifying behaviour (in this context it is noteworthy that downregulation of the PI3K pathway has also been described in T2DM) [40,200].

As noted previously, prior to Study III, there was little to no data on the effects of liraglutide on osteoblastic activity in VSMCs. The only relevant publications in the area came from Nuche-Berenguer *et al.* who examined the effects of GLP-1 on circulating concentrations of OPG and RANKL in atherogenic rats and reported an increase in OPG and a decrease in RANKL, changes which, based on my own results in Study II, may be hypothesized to oppose the process of VC [205]. In a similar manner, another study by this group using exendin-4 (a GLP-1 receptor agonist) in postmenopausal rats also reported an alteration of the OPG/RANKL ratio in favour of OPG [206]. To the best of my knowledge, however, there have been no previous studies examining the effect of GLP-1 or its analogues on endpoints of osteoblastic activity.

Within the context of the evidence base as described above, my own data on insulin glargine and osteoblastic activity is generally in keeping with the initial report by Olesen *et al.,* and the data presented by Yuan *et al.* [39,41] in that I report a clear and consistent increase in osteoblastic activity amongst HASMCs following exposure to

insulin glargine. It is noteworthy, given that the other component of Study III involved examining the effects of insulin analogues *in vivo*, that these changes were produced by insulin glargine at concentrations similar to those of endogenous insulin when reported as part of the insulin resistant state *in vivo [216,217].* One explanation for the discrepancy between my data and the second report by Oleson *et al* could be my use of HASMCs from a single donor, which may have decreased the heterogeneity of my data [186]. While the scope of the present thesis did not extend to manipulating the pathways of insulin signalling, I did measure BMP-2 and BMP-4 concentrations in the supernatant media of HASMCs to determine if the effects of insulin glargine could be mediated by changes in the concentrations of these proteins, but I found no evidence that this was the case. With regards to the data I generated on liraglutide and HASMCs, I note that my findings are not consistent with those of Nuche-Berengue *et al* in that I did not observe liraglutide to exert any effect on OPG release from HASMCs. Whether this discrepancy is due to differences in liraglutide versus native GLP-1 or exendin-4, or whether the longer duration of this group's experiments accounted for the difference is unclear, and will likely require further assessment in the future. In terms of osteoblastic activity, however, my data on liraglutide and HASMCs indicate that this medication does not exert any direct effects, whether beneficial or detrimental, on HASMCs.

Finally, with regards to the experiments involving HAECs, my own earlier data (Study II) have already demonstrated that HAECs are capable of releasing BMP-2, and that this paracrine signal can induce osteoblastic change in HASMCs. In this context, the observation that both insulin glargine and, somewhat surprisingly, liraglutide, increase the release of this protein from HAECs indicates an additional pathway by which insulin glargine may promote VC, and that liraglutide may also stimulate this paracrine effect. It should be noted that while the effects of liraglutide *in vivo* are explored as part of the

second component of Study III, its stimulation of BMP-2 release from HAECs *in vitro* represents a novel and interesting finding, and may merit additional characterization in future research programs.

5.3.1.1. Summary of In Vitro Results

In this, the first component of Study III, I report two additional pathways by which exposure to insulin glargine may lead to increased osteoblastic activity in HASMCs, in addition to the insulin glargine-dependent downregulation of HASMC OPG expression and release already described in Study I. Firstly, osteoblastic activity increased following direct administration of insulin glargine to HASMCs, with previous groups suggesting that osteoblastic activity may be caused, in this setting, by activation of the ERK 1/2 pathway [41]. Secondly, insulin glargine increased the production of BMP-2 by HAECs, an upregulation of a paracrine signal that I have shown earlier in this thesis (Study II) to increase osteoblastic activity in HASMCs. Thus, and with regards to the study of insulin glargine in the clinical setting, I report three pathways in total by which insulin glargine may promote osteoblastic activity and VC in the vessel wall. These are a) the downregulation of OPG release from HASMCs, b) the upregulation of BMP-2 release from HAECs and c) a direct effect of insulin glargine on HASMCs. Finally, I note that while liraglutide was not observed to exert direct effects on HASMCs, it did increase the production of HAEC-derived BMP-2, and as such the hypothesis that liraglutide may exert inhibitory effects on VC *in vivo* is called into question, and is examined closely in the clinical component of Study III.

5.3.2. The Effects of Insulin Analogues Versus Liraglutide on CAC in Patients with T2DM

In the second component of Study III, the *in vitro* observations reported in Study I, Study II and the first component of Study III were amalgamated and tested *in vivo* within the clinical setting of T2DM, a condition that is characterized by

hyperinsulinemia, VC, and excessive rates of CVD [3,42,43,193]. In this prospective, observational study, the first of its kind to measure the effect of commencing insulin analogues or liraglutide on CAC in T2DM, I measured CAC scores pre- and post-commencement of these medications, and, as discussed in the following sections, report a number of relevant findings.

5.3.2.1. Baseline Characteristics of the Study Population

At baseline in this study, CAC score correlated strongly with age. This is a consistent finding with regards to VC and indicated that my study group was similar, in this respect at least, to previous studies on CAC [28,46]. In a similar fashion, I also reported that CAC score was significantly higher in patients with a prior history of IHD. Although this group was relatively small (n=6), this result is also consistent with the recognized ability of CAC to identify/differentiate patients at high risk of CVD [70,75].

With regards to recruitment for this study, it is a salient point that numbers in the insulin analgoue group were lower than the liraglutide or metformin control groups. Although I met my initial, pilot study recruitment targets, optimal recruitment would have involved the attainment of greater numbers of patients in the insulin analogue group. I speculate two reasons why recruitment was relatively low in this, the group of particular interest. The first is that patients with T2DM who require insulin treatment, when compared to those who do not, tend to have more co-morbidities, and as such may have been less eager to enroll in research that at the very least involved 6 additional visits to hospitals over the duration of the study. Furthermore, the use of liraglutide as a step-up treatment by the diabetes teams was observed to increase over the duration of the study at the expense of insulin treatment, and while this increased the numbers eligible for the liraglutide group, it did so at the expense of the insulin analogue group.

As may have been expected for an observational study of this nature, there were significant baseline differences between the groups. Patients assigned to liraglutide by their diabetes team weighed more than those who remained on metformin and those assigned to insulin. This is unsurprising given that part of the reason patients may be assigned to liraglutide is the weight-loss associated with this medication [45]. Equally, it is to be expected that the patients on insulin had a longer duration of diabetes, and a higher HbA1c than the other groups, as insulin is typically employed when blood glucose readings remain high despite the maximal use of oral hypoglycemic medications, and the progressive nature of T2DM observed with increasing age [44,115]. It was somewhat surprising that age was higher in the metformin group, but it should also be noted that this difference likely accounted for the lower eGFR in this group in comparison to the two others. Ultimately, although expected, these differences do represent a limitation of Study III in that baseline differences in certain parameters (duration of diabetes and HbA1c in particular) may also affect CAC progression, and as such may account for some of the changes observed in the study. While the statistical analysis demonstrated in table 5.3 was designed to adjust for baseline differences in these variables, and appears to demonstrate a strong trend indicating that insulin analogue therapy increases CAC progression, statistical significance was lost when all baseline differences were accounted for. Therefore I cannot outrule a confounding effect from these baseline variables. Nonetheless, I also note that this strong trend towards an effect from insulin analogues on CAC progression was observed despite relatively small numbers in a clinical study of this nature, and that the data presented, while insufficient to draw definite conclusions regarding insulin analogues and CAC, does not weaken the hypothesis that insulin may promote VC in T2DM, and instead strengthens the argument for randomized studies into this phenomenon.

5.3.2.2. Change in Baseline Variables Over the Duration of the Study, and the Effects of Treatment on CAC, OPG, RANKL and TRAIL

Over the duration of this study (16 months), significant changes to the baseline variables were observed. Both the insulin analogue and the liraglutide groups experienced a significant reduction in HbA1c, as one might expect, and the liraglutide group also noted a decrease in weight and triglycerides, also in keeping with the expected weight loss effect of this medication [45].

With regards to the variables of interest, it is noteworthy that one of the main findings of Study I, that insulin glargine reduces the release of OPG from HASMCs, was supported *in vivo* by the results of Study III, where a significant reduction in circulating concentrations of OPG were observed in the insulin analogue group. This effect of insulin analogues on OPG was noted to remain significant even when the analysis was corrected for all baseline differences between the groups. Whilst other groups have previously reported that native insulin decreases circulating OPG concentrations in T2DM acutely, and that circulating concentrations of OPG decrease following the commencement of insulin analogues for T1DM, the present study is the first to report the sustained downregulation of OPG by insulin analogues in T2DM [21,117]. Although no significant changes in the circulating concentrations of either RANKL or TRAIL were noted to occur over the duration of the study, it is possible that the reduction in circulating concentrations of OPG in the insulin analgoue group facilitated increased levels of RANKL and TRAIL activity [29].

Upon assessment of the CAC data, a significant increase in CAC score was observed in the insulin analogue group over the duration of the study, a treatment effect that persisted in significance when corrected for baseline variables that are known to affect VC (such as eGFR, age and duration of diabetes), but lost significance when corrected

for *all* baseline differences, including triglyceride and HbA1c levels, between the groups. As previously discussed, the loss of significance of this result indicates that baseline variations between groups may have accounted for the increased CAC progression noted in the insulin group. Equally, is should be noted that triglyceride levels are not recognized as potent risk factors for CAC, and as such their relevance to this endpoint, and their inclusion in the statistical model, may be challenged [28].With regards to HbA1c, however, a limited number of studies have been published indicating that this variable may affect CAC. In an examination of CAC scores over a 2 year period in a type 1 diabetes population, Rewers *et al.*, extracting data from the Coronary Artery Calcification in Type 1 Diabetes (CACTI) study, reported increased CAC in association with higher HbA1c values. Equally, Lahiri *et al.* assessed CAC scores in T2DM patients over 2.5 years and also reported that progression was linked to HbA1c. Finally, I note that a long term follow-up of the Diabetes Control and Complications Trial (DCCT, Nathan et al) reported a lower CAC burden in T1DM patients assigned to intensive glycemic contol compared to conventional control. As such, I note it is possible that HbA1c status may affected the CAC changes observed in the present study.

Ultimately, with regards to the primary endpoint of Study III, I report that insulin analogue therapy was not associated with a significant increase in CAC score when *all* baseline differences were accounted for in this observational study. Nonetheless, I submit that these data demonstrate a strong trend towards an effect, by insulin analgoues, on CAC, and when considered in conjunction with the *in vitro* components of Study I and Study III, the results of this pilot study support additional, potentially randomized research programs, involving larger study cohorts, on insulin analogues and VC in T2DM.

With regards to the liraglutide group, no significant effects of this medication were noted on CAC score or OPG over the duration of the study, even before correcting for baseline differences between the groups. It may be speculated that liraglutide simply has no effect on CAC or, in the context of my *in vitro* data, that the beneficial metabolic effects of liraglutide may be offset by an upregulation of BMP-2 paracrine signaling from HAECs. Regardless of the reason, however, in Study III I report no evidence for an effect by liraglutide on CAC.

5.3.2.3. Summary of In Vivo Results

In the clinical component of Study III, I conducted the first prospective study of the effects of either insulin analogues or liraglutide on CAC in T2DM. Over 100 patients were recruited, and CAC scores were measured in blinded fashion at the beginning and end of a 16 month period. Insulin analogue use was associated with a highly significant decrease in circulating concentrations of OPG, a result that is consistent with Study I, and I report a trend towards significance for an effect of insulin analogues on CAC, an effect that would be consistent with the *in vitro* results of Study II and the *in vitro* component of Study III. If, as is suggested by these results, insulin therapy promotes VC, in the future increasing interest may focus upon avoiding or mitigating this effect. This may involve, as an example, comparing the various insulin analogues available in terms of their effect on VC and favouring those with lesser VC promotion. Equally, it may also involve increased use of alternative agents/strategies for the treatment of T2DM, including the use of GLP-1 analogues such as liraglutide, or more invasive treatment options for T2DM such as gastric bypass surgery. Ultimately, I submit that the results presented here, while not achieving full significance in the final statistical model, nonetheless support the hypothesis that insulin analogue therapy promotes VC, and that the results of this pilot study justify, and provide data with which to design, randomized clinical trials to assess the effects of insulin on VC in the high CVD risk state that is T2DM.

Chapter 6 - General Discussion and Future Directions

The data generated in the present thesis characterize a novel pathway involved in the regulation of VC, starting at the *in vitro* level with HAECs and HASMCs, progressing to the incorporation of paracrine signalling between the two cell populations, testing the model in a perfusing, co-culture artifical capillary system, and then examining the effects of two commonly used medications for T2DM on this pathway *in vitro* and *in vivo* in an T2DM population. I report that OPG functions as an inhibitior of VC by preventing RANKL from inducing BMP-2 release from HAECs, which then act on HASMCs to undergo osteoblastic change. Insulin glargine appears to promote this process in a number of different ways, including the down-regulation of OPG secretion and production by HASMCs, whereas liraglutide does not appear to interact with this system in any significant way. These findings are summarized in figure 6.1. In my clinical study I observed decreased circulating concentrations of OPG, along with increased progression of CAC, in the group commencing insulin analogue therapy, but baseline differences between the groups mean that these results must be interpreted with caution, and are best viewed as support for the performance of future randomized trials on VC.

With T2DM affecting approximately 347 million individuals worldwide [275], and more than 50% of patients with this condition sucumbing to CVD [276], now more than ever we need to identify and develop novel interventions with which to combat these high levels of CV morbidity and mortality. In the last two decades, our perception of VC, in the context of CVD, has changed from an essentially benign to a detrimental process. It is of particular note that this perception change first occurred in the setting of dialysis, where the exceptionally high rates of VC were seen to associate with poor prognosis, and where efforts to reverse or at least slow the progression of VC have been ongoing for the longest time [47,48,132].

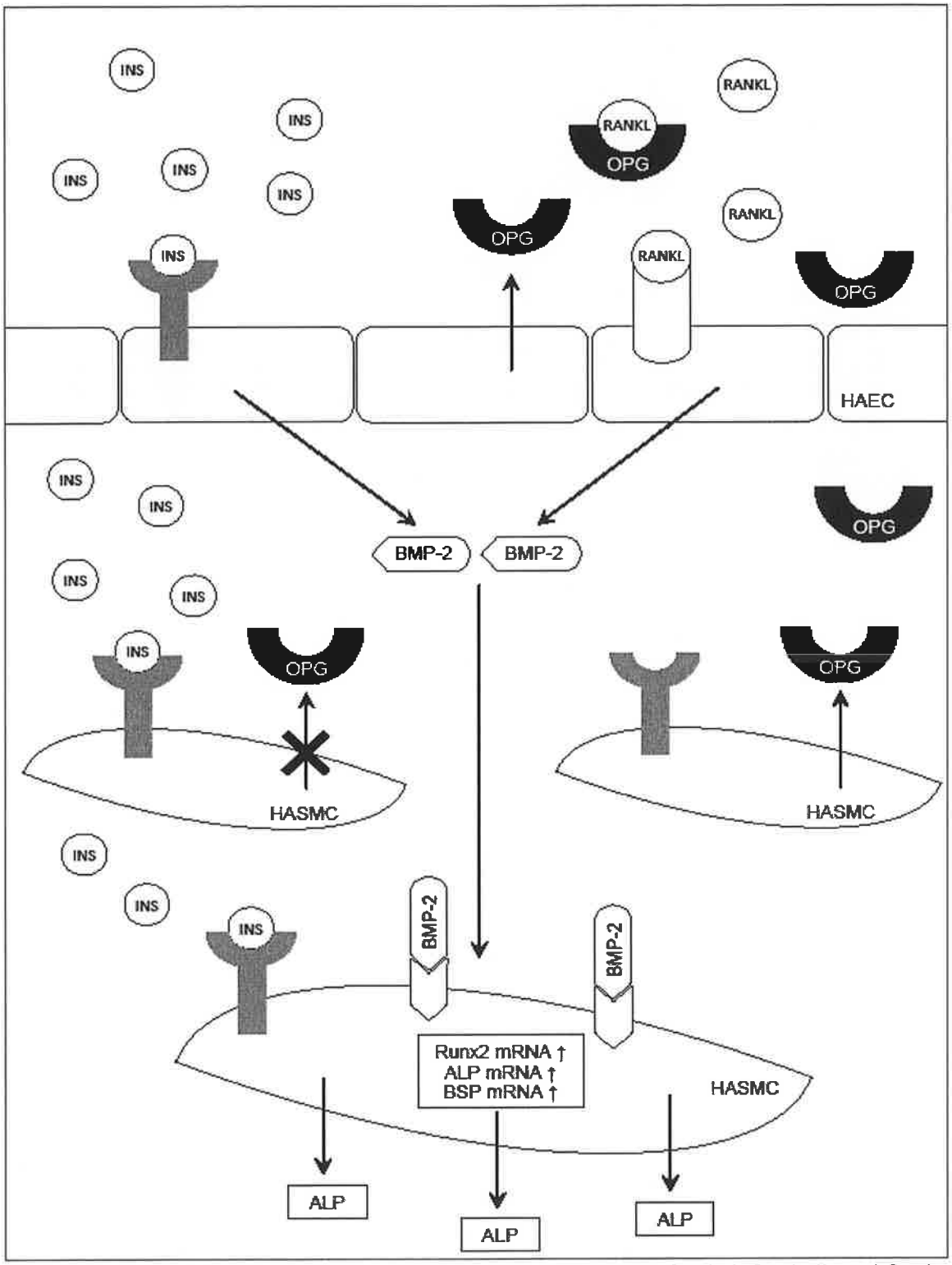

Figure 6.1. Schematic representation, based on data genearted in Study I, Study II, and Study III of the relationships between OPG, RANKL, insulin and BMP-2 in the context of VC. Insulin (left) can be seen binding to HAECs and inducing BMP-2 release, binding to HASMCs and decreasing OPG release, and binding to HASMCs to directly induce osteoblastic activity. RANKL (right) can be seen binding to HAECs and inducing BMP-2 release with OPG (released from HAECs and HASMCs) blocking these actions. BMP-2 (centre) binds to HASMCs and induced osteobalstic activity. ALP, alkaline phosphatase; BMP-2, bone morphogenetic protein-2; BSP, bone sialoprotein; HAEC, human aortic endothelial cell; HASMC, human aortic smooth muscle cell; OPG, osteoprotegerin; RANKL, receptor activator of nuclear factor kappa-beta ligand; Runx2, runt-related transcription factor 2; VC, vascular calcification.

It is only in more recent years that the effects of interventions such as statins and bisphosphonates on VC have been studied in the general population (including those with T2DM). Inhibiting VC, however, has proven exceedingly difficult, as highlighted by an recent aptly titled editorial - Vascular Calcification: Harder Than it Looks [277]. Multiple interrelated promoters and inhibitors of this process have been identified, with a variety of cell lineages potentially involved and differing forms of VC depending on anatamical location and underlying co-morbid conditions. Counterintuitive relationships have complicated our understanding of this condition further, with proteins such as OPG acting in opposing fashion depending on the microenvironment (e.g. skeletal bone versus vascular wall).

In this setting the results of the present thesis can be considered as a timely characterization of a particularly complex set of ligands involved in the VC process. One of the strengths of this thesis is its inclusion of the paracrine signalling that occurs between two major vascular cell populations, ECs and SMCs, in the context of VC. Indeed, it is possible that the assessment of only one cell population at a time when studying a complex process of this nature may be inherently limited, and highlights the need for more complex *in vitro* models of the arterial wall environment before progressing research to the *in vivo* level. With the CELLMAX DUO®, I was able to approximate multiple aspects of *in vivo* vascular physiology, and by doing so I strengthened the evidence base for the role of RANKL and OPG in VC to the degree that clinical studies could now be designed around this system. Ultimately, and with regards to future avenues of research in this area, this is the first major finding of the thesis, a signalling system that appears to promote or inhibit VC depending on the ratio of OPG to RANKL, and, critically, one which we can already manipulate with the use of the medication denosumab. As mentioned previously, denosumab is a recently licensed medication which affects bone turnover, and is an antibody which mimics the

effects of OPG in that it binds to and neutralizes RANKL (but not TRAIL) [130,164]. The administration of denosumab to patients with VC (preferably in a placebo-controlled randomized fashion), to assess its effects on VC in a) T2DM patients and b) patients with ESRF, is a major long-term goal of my research group. The data presented in the present thesis lead to the hypothesis that this treatment may have more success in inhibiting VC than other, less targeted therapies such as statins. Longer-term studies with significantly larger patient populations would be required to determine if an intervention of this nature leads to a reduction in CV events, and may be beyond the scope of our present research program. Demonstrating an inhibitory effect by denosumab on VC, however, would be a significant step towards the performance of such studies.

The other major finding of the present thesis was the significant effects of insulin glargine on OPG secretion and production by HASMCs (which appear to be the dominant source of OPG in the vascular wall environment), and on the development of osteoblastic activity in this cell population following exposure to this medication. Although other groups have reported some preliminary research in this area, my research indicated that the effect extended to that of the insulin analogues currently in clinical use, that insulin glargine promoted VC not only by reducing OPG production, but also by acting directly on HASMCs and by increasing BMP-2 production by HAECs. It is quite notable that despite the assocations between T2DM, VC and the frequent use of exogenous insulin to treat this condition, no group (to the best of my knowledge) has performed prospective research to determine if insulin therapy promotes VC. As noted in the chapter 5 discussion, the approach adopted in my clinical study had some limitations, and as such should be considered a pilot study in many respects. Nonetheless, I report a number of findings in keeping with my *in vitro* research, most notably a highly significant effect by insulin analogue therapy on circulating OPG

concentrations, and in addition a faster progression of CAC in the group exposed to insulin analogues. Certainly, these results do nothing to diminsh the concern that insulin therapy may promote VC, and now provide the evidence base with which formal randomized studies can be performed in an ethical and effective manner. Following on from my results, therefore, additional goals of my research group include a plan to a) perform a statistical analysis on the relationship between insulin analogue therapy and VC progression in, a large T2DM cohort which have had VC assessments performed over time and b) perform a randomized trial of insulin analogue therapy versus GLP-1 analogue therapy incorporating the measurement of both VC and arterial stiffness. The latter study would by necessity require a large cohort of patients and a significant resource allocation, likely involving multiple centres, and as such would optimally be performed after the former analysis was performed.

In addition to the research directions already indicated, the present thesis also raises a number of queries that merit investigation. Certainly the idenitificaiton of a significant effect, by cyclic strain, on OPG production and secretion by vascular cell populations is entirely novel and deserving of additional research. As the laboratory of my research group specializes in experiments involving cyclic strain and shear stress [235], this is within the current capabilities of my group, and a series of experiments identifying the nature and significance of this relationship are of particular interest to the group. Furthermore, the role of TRAIL within the vascular wall remains one of interest. Although no effect by TRAIL on VC was noted in the present thesis, an epidemiological relationship exists between TRAIL and CVD in high CV risk patients, with low TRAIL associated with high CV risk [278]. Therefore it remains possible that an interaction between TRAIL and OPG exists. Such a relationship may be particularly relevant in the setting of an acute injury to the vascular wall, when OPG is released by ECs (along with other acute phase proteins) [144], and it may be hypothesized that TRAIL affects

EC survival. This possibility is currently under investigation by my research group, with preliminary evidence that TRAIL inhibits the inflammatory response of ECs [279]. Finally, I note that the complexity of the interactions between OPG, RANKL and TRAIL, and the various forms (e.g. bound or unbound, in circulation or on cell membanes, the 3 different isomers of RANKL) underpin some of the difficulties in performing research on this group of ligands. Accordingly, my group has commenced planning a collaboration with a research centre in America with access to mass-spectrometry, so that future research involving these ligands can be performed in an isomer specific fashion.

In closing, the issue of VC in T2DM, is one, I submit, that merits a significant degree of research, with the ultimate goal being a reduction in CVD in this high-risk condition. While promoters and inhibits of VC require characterization at the *in vitro* level, this should be done with the greatest degree of appicability to the *in vivo* environment possible, with measures such as the inclusion of co-cultures and hemodynamic forces in the experimental models. I report that insulin analogue therapy may promote VC in T2DM, with *in vitro* evidence that matches preliminary clinical data. This is a significant concern for the evermore prevalent condition of T2DM, and one which deserves additional attention and discussion in the literature. With the concept of VC as a benign phenomenon rapidly fading, the research performed as part of the present thesis joins an ever-growing body of evidence designed to characterize, and ultimately inhibit, this aspect of CVD.

In this following section, the original aims of the present thesis, and the relevant results, are revisited.

6.1. Study I

An investigation of OPG, TRAIL and RANKL secretion from human aortic endothelial cells (HAECs) and human aortic smooth muscle cells (HASMCs) under basal and injurious conditions *in vitro*.

6.1.1. Aims

The purpose of this study was to quantify the release of OPG under basal and injurious states, and to qualify whether RANKL and/or TRAIL was produced in significant amounts by either cell population.

6.1.2. Results

i) OPG was secreted by HAECs and HASMCs. HASMCs secreted OPG in quantities that were 2 orders of magnitude higher than HAECs. TNF-α increased the release of OPG from both cell populations.

ii) Insulin glargine increased OPG release from HAECs (while decreasing its production), but had a quantitatively greater effect on HASMCs, where it significantly reduced both OPG production and release.

iii) Neither RANKL nor TRAIL were produced by either cell population in detectable quantities under any of the experimental conditions tested.

6.2. Study II

The effects of RANKL and/or TRAIL on osteoblastic transformation of HASMCs, the paracrine influence of HAECs on osteoblastic-transformation of HASMCs, and the effects of RANKL on osteoblastic activity in an advanced perfused co-culture model incorporating HAECs and HASMCs.

6.2.1. Aims

i) To determine whether RANKL and/or TRAIL were capable of inducing osteoblastic changes in HASMCs

ii) To determine whether HAECs exerted a paracrine influence on the osteoblastic change of HASMCs, and whether RANKL and/or TRAIL affected this relationship.

iii) To determine whether RANKL and/or TRAIL induced osteoblastic activity in HASMCs when co-cultured with HAECs in a perfused artificial capillary system.

6.2.2. Results

i) Neither RANKL nor TRAIL exerted direct effects on HASMCs.

ii) RANKL acted on HAECS to increase the production of BMP-2, a paracrine signal that increased the osteoblastic transformation of HASMCs.

iii) These findings were subsequently replicated in my perfused co-culture model, providing data with increased comparability to the arterial environment *in vivo*.

6.3. Study III

The effect of insulin analgoues versus liraglutide on the emergence of osteoblastic activity in HASMCs and on CAC score via CT in patients with T2DM.

6.3.1. Aims

i) To determine the effects of insulin glargine and liraglutide on the emergence of osteoblastic activity in HASMCs.

ii) To determine the effects of starting either insulin analgoue therapy or liraglutide on OPG, RANKL,TRAIL, and CAC over a period of 16 months. Patients remaining on metformin±sulphonylurea only constituted the control group.

6.3.2. Results

i) Insulin glargine, but not liraglutide, was associated with a significant increase in osteoblastic activity within HASMC cultures when these medications were applied directly.

ii) Treatment of T2DM with insulin analgoues was associated with a significant decrease in circulating concentrations of OPG, and a trend towards a significant increase in CAC scores, over the study timeframe.

iii) Treatment of T2DM with liraglutide was not associated with any significant change in circulating concentrations of OPG or in CAC scores, over the study timeframe.

References

1. European Heart Network and European Society of Cardiology. European Cardiovascular Disease Statistics 2012 Edition. http://www.escardio.org/about/documents/eu-cardiovascular-disease-statistics-2012.pdf.

2. Irish Heart Foundation. Mortality from cardiovascular disease (CVD) i.e. from coronary heart disease, stroke and other diseases of the circulation in 2006. http://www.irishheart.ie/media/pub/factsheets/cvd_mortality_rates_2007.pdf.

3. Grundy SM, Benjamin IJ, Burke GL *et al.* Diabetes and cardiovascular disease: a statement for healthcare professionals from the American Heart Association. *Circulation* 1999; **100:** 1134-46.

4. Eikelboom JW, Lonn E, Genest J, Jr., Hankey G, Yusuf S. Homocyst(e)ine and cardiovascular disease: a critical review of the epidemiologic evidence. *Ann.Intern.Med.* 1999; **131:** 363-75.

5. Pilz S, Tomaschitz A, Marz W *et al.* Vitamin D, cardiovascular disease and mortality. *Clin.Endocrinol.(Oxf)* 2011; **75:** 575-84.

6. Lippi G, Franchini M, Targher G. Screening and therapeutic management of lipoprotein(a) excess: review of the epidemiological evidence, guidelines and recommendations. *Clin.Chim.Acta* 2011; **412:** 797-801.

7. Greenland P, Alpert JS, Beller GA *et al.* 2010 ACCF/AHA guideline for assessment of cardiovascular risk in asymptomatic adults: a report of the American College of Cardiology Foundation/American Heart Association Task Force on Practice Guidelines. *Circulation* 2010; **122:** e584-e636.

8. Smith SC, Jr., Benjamin EJ, Bonow RO *et al.* AHA/ACCF Secondary Prevention and Risk Reduction Therapy for Patients with Coronary and other Atherosclerotic Vascular Disease: 2011 update: a guideline from the American Heart Association and American College of Cardiology Foundation. *Circulation* 2011; **124:** 2458-73.

9. Banegas JR, Lopez-Garcia E, Dallongeville J *et al.* Achievement of treatment goals for primary prevention of cardiovascular disease in clinical practice across Europe: the EURIKA study. *Eur.Heart J.* 2011; **32:** 2143-52.

10. Smulders YM, Thijs A, Twisk JW. New cardiovascular risk determinants do exist and are clinically useful. *Eur.Heart J.* 2008; **29:** 436-40.

11. Mora S, Musunuru K, Blumenthal RS. The clinical utility of high-sensitivity C-reactive protein in cardiovascular disease and the potential implication of JUPITER on current practice guidelines. *Clin.Chem.* 2009; **55:** 219-28.

12. Nordestgaard BG, Chapman MJ, Ray K *et al.* Lipoprotein(a) as a cardiovascular risk factor: current status. *Eur.Heart J.* 2010; **31:** 2844-53.

13. Couri CE, da Silva GA, Martinez JA, Pereira FA, de Paula FJ. Monckeberg's sclerosis - is the artery the only target of calcification? *BMC.Cardiovasc.Disord.* 2005; **5:** 34.

14. Piers LH, Salachova F, Slart RH *et al.* The role of coronary artery calcification score in clinical practice. *BMC.Cardiovasc.Disord.* 2008; **8:** 38.

15. Shao JS, Cai J, Towler DA. Molecular mechanisms of vascular calcification: lessons learned from the aorta. *Arterioscler.Thromb.Vasc.Biol.* 2006; **26:** 1423-30.

16. Hayden MR, Tyagi SC, Kolb L, Sowers JR, Khanna R. Vascular ossification-calcification in metabolic syndrome, type 2 diabetes mellitus, chronic kidney disease, and calciphylaxis-calcific uremic arteriolopathy: the emerging role of sodium thiosulfate. *Cardiovasc.Diabetol.* 2005; **4:** 4.

17. Demer LL. A skeleton in the atherosclerosis closet. *Circulation* 1995; **92:** 2029-32.

18. Kizu A, Jono S. [Mechanism of vascular calcification]. *Clin.Calcium* 2004; **14:** 92-6.

19. Zhang Y, Khan D, Delling J, Tobiasch E. Mechanisms underlying the osteo- and adipo-differentiation of human mesenchymal stem cells. *ScientificWorldJournal.* 2012; **2012:** 793823.

20. Chen NX, Moe SM. Vascular calcification: pathophysiology and risk factors. *Curr.Hypertens.Rep.* 2012; **14:** 228-37.

21. Xiang GD, Sun HL, Zhao LS, Hou J, Yue L, Xu L. [Changes of osteoprotegerin before and after insulin therapy in type 1 diabetic patients]. *Zhonghua Yi.Xue.Za Zhi.* 2007; **87:** 1234-7.

22. Abedin M, Tintut Y, Demer LL. Vascular calcification: mechanisms and clinical ramifications. *Arterioscler.Thromb.Vasc.Biol.* 2004; **24:** 1161-70.

23. Dao HH, Essalihi R, Bouvet C, Moreau P. Evolution and modulation of age-related medial elastocalcinosis: impact on large artery stiffness and isolated systolic hypertension. *Cardiovasc.Res.* 2005; **66:** 307-17.

24. Demer LL, Tintut Y. Vascular calcification: pathobiology of a multifaceted disease. *Circulation* 2008; **117:** 2938-48.

25. Johnson RC, Leopold JA, Loscalzo J. Vascular calcification: pathobiological mechanisms and clinical implications. *Circ.Res.* 2006; **99:** 1044-59.

26. O'Brien KD. Pathogenesis of calcific aortic valve disease: a disease process comes of age (and a good deal more). *Arterioscler.Thromb.Vasc.Biol.* 2006; **26:** 1721-8.

27. Virmani R, Burke AP, Farb A. Plaque morphology in sudden coronary death. *Cardiologia* 1998; **43:** 267-71.

28. Wexler L, Brundage B, Crouse J *et al.* Coronary artery calcification: pathophysiology, epidemiology, imaging methods, and clinical implications. A

statement for health professionals from the American Heart Association. Writing Group. *Circulation* 1996; **94:** 1175-92.

29. Vitovski S, Phillips JS, Sayers J, Croucher PI. Investigating the interaction between osteoprotegerin and receptor activator of NF-kappaB or tumor necrosis factor-related apoptosis-inducing ligand: evidence for a pivotal role for osteoprotegerin in regulating two distinct pathways. *J.Biol.Chem.* 2007; **282:** 31601-9.

30. Hofbauer LC, Schoppet M. Clinical implications of the osteoprotegerin/RANKL/RANK system for bone and vascular diseases. *JAMA* 2004; **292:** 490-5.

31. Bucay N, Sarosi I, Dunstan CR *et al.* osteoprotegerin-deficient mice develop early onset osteoporosis and arterial calcification. *Genes Dev.* 1998; **12:** 1260-8.

32. Morony S, Tintut Y, Zhang Z *et al.* Osteoprotegerin inhibits vascular calcification without affecting atherosclerosis in ldlr(-/-) mice. *Circulation* 2008; **117:** 411-20.

33. Price PA, June HH, Buckley JR, Williamson MK. Osteoprotegerin inhibits artery calcification induced by warfarin and by vitamin D. *Arterioscler.Thromb.Vasc.Biol.* 2001; **21:** 1610-6.

34. Van CA, Golledge J. Osteoprotegerin, vascular calcification and atherosclerosis. *Atherosclerosis* 2009; **204:** 321-9.

35. Tintut Y, Demer L. Role of osteoprotegerin and its ligands and competing receptors in atherosclerotic calcification. *J.Investig.Med.* 2006; **54:** 395-401.

36. Wu M, Rementer C, Giachelli CM. Vascular calcification: an update on mechanisms and challenges in treatment. *Calcif.Tissue Int.* 2013; **93:** 365-73.

37. Di Iasio, MG, Corrallini, F, Secchiero, P, and Capitani, S. Atlas of Genetics and Cytogenetics in Oncology and Haematology. http://atlasgeneticsoncology.org/Genes/TNFRSF11BID42610ch8q24.html.

38. Osako MK, Nakagami H, Koibuchi N *et al.* Estrogen inhibits vascular calcification via vascular RANKL system: common mechanism of osteoporosis and vascular calcification. *Circ.Res.* 2010; **107:** 466-75.

39. Olesen P, Nguyen K, Wogensen L, Ledet T, Rasmussen LM. Calcification of human vascular smooth muscle cells: associations with osteoprotegerin expression and acceleration by high-dose insulin. *Am.J.Physiol Heart Circ.Physiol* 2007; **292:** H1058-H1064.

40. Wang CC, Sorribas V, Sharma G, Levi M, Draznin B. Insulin attenuates vascular smooth muscle calcification but increases vascular smooth muscle cell phosphate transport. *Atherosclerosis* 2007; **195:** e65-e75.

41. Yuan LQ, Zhu JH, Wang HW *et al.* RANKL is a downstream mediator for insulin-induced osteoblastic differentiation of vascular smooth muscle cells. *PLoS.One.* 2011; **6:** e29037.

42. Lehto S, Niskanen L, Suhonen M, Ronnemaa T, Laakso M. Medial artery calcification. A neglected harbinger of cardiovascular complications in non-insulin-dependent diabetes mellitus. *Arterioscler.Thromb.Vasc.Biol.* 1996; **16:** 978-83.

43. Schurgin S, Rich S, Mazzone T. Increased prevalence of significant coronary artery calcification in patients with diabetes. *Diabetes Care* 2001; **24:** 335-8.

44. Inzucchi SE, Bergenstal RM, Buse JB *et al.* Management of hyperglycemia in type 2 diabetes: a patient-centered approach: position statement of the American Diabetes Association (ADA) and the European Association for the Study of Diabetes (EASD). *Diabetes Care* 2012; **35:** 1364-79.

45. Niswender K, Pi-Sunyer X, Buse J *et al.* Weight change with liraglutide and comparator therapies: an analysis of seven phase 3 trials from the liraglutide diabetes development programme. *Diabetes Obes.Metab* 2013; **15:** 42-54.

46. Allison MA, Criqui MH, Wright CM. Patterns and risk factors for systemic calcified atherosclerosis. *Arterioscler.Thromb.Vasc.Biol.* 2004; **24:** 331-6.

47. Braun J, Oldendorf M, Moshage W, Heidler R, Zeitler E, Luft FC. Electron beam computed tomography in the evaluation of cardiac calcification in chronic dialysis patients. *Am.J.Kidney Dis.* 1996; **27:** 394-401.

48. Oh J, Wunsch R, Turzer M *et al.* Advanced coronary and carotid arteriopathy in young adults with childhood-onset chronic renal failure. *Circulation* 2002; **106:** 100-5.

49. Bunting CH. THE FORMATION OF TRUE BONE WITH CELLULAR (RED) MARROW IN A SCLEROTIC AORTA. *J.Exp.Med.* 1906; **8:** 365-76.

50. Tintut Y, Demer LL. Recent advances in multifactorial regulation of vascular calcification. *Curr.Opin.Lipidol.* 2001; **12:** 555-60.

51. Shanahan CM, Proudfoot D, Tyson KL, Cary NR, Edmonds M, Weissberg PL. Expression of mineralisation-regulating proteins in association with human vascular calcification. *Z.Kardiol.* 2000; **89 Suppl 2:** 63-8.

52. Bostrom K, Watson KE, Horn S, Wortham C, Herman IM, Demer LL. Bone morphogenetic protein expression in human atherosclerotic lesions. *J.Clin.Invest* 1993; **91:** 1800-9.

53. Campbell GR, Campbell JH. Vascular smooth muscle and arterial calcification. *Z.Kardiol.* 2000; **89 Suppl 2:** 54-62.

54. Canfield AE, Sutton AB, Hoyland JA, Schor AM. Association of thrombospondin-1 with osteogenic differentiation of retinal pericytes in vitro. *J.Cell Sci.* 1996; **109 (Pt 2):** 343-53.

55. Proudfoot D, Skepper JN, Shanahan CM, Weissberg PL. Calcification of human vascular cells in vitro is correlated with high levels of matrix Gla protein and low levels of osteopontin expression. *Arterioscler.Thromb.Vasc.Biol.* 1998; **18:** 379-88.

56. Towler DA, Demer LL. Thematic series on the pathobiology of vascular calcification: an introduction. *Circ.Res.* 2011; **108:** 1378-80.

57. Proudfoot D, Shanahan CM. Biology of calcification in vascular cells: intima versus media. *Herz* 2001; **26:** 245-51.

58. Amann K. Media calcification and intima calcification are distinct entities in chronic kidney disease. *Clin.J.Am.Soc.Nephrol.* 2008; **3:** 1599-605.

59. Shanahan CM, Cary NR, Salisbury JR, Proudfoot D, Weissberg PL, Edmonds ME. Medial localization of mineralization-regulating proteins in association with Monckeberg's sclerosis: evidence for smooth muscle cell-mediated vascular calcification. *Circulation* 1999; **100:** 2168-76.

60. Lau WL, Ix JH. Clinical detection, risk factors, and cardiovascular consequences of medial arterial calcification: a pattern of vascular injury associated with aberrant mineral metabolism. *Semin.Nephrol.* 2013; **33:** 93-105.

61. McCullough PA, Agrawal V, Danielewicz E, Abela GS. Accelerated atherosclerotic calcification and Monckeberg's sclerosis: a continuum of advanced vascular pathology in chronic kidney disease. *Clin.J.Am.Soc.Nephrol.* 2008; **3:** 1585-98.

62. Katz R, Wong ND, Kronmal R *et al.* Features of the metabolic syndrome and diabetes mellitus as predictors of aortic valve calcification in the Multi-Ethnic Study of Atherosclerosis. *Circulation* 2006; **113:** 2113-9.

63. Nelson RG, Gohdes DM, Everhart JE *et al.* Lower-extremity amputations in NIDDM. 12-yr follow-up study in Pima Indians. *Diabetes Care* 1988; **11:** 8-16.

64. Mohler ER, III, Gannon F, Reynolds C, Zimmerman R, Keane MG, Kaplan FS. Bone formation and inflammation in cardiac valves. *Circulation* 2001; **103:** 1522-8.

65. Ix JH, Chertow GM, Shlipak MG, Brandenburg VM, Ketteler M, Whooley MA. Association of fetuin-A with mitral annular calcification and aortic stenosis among persons with coronary heart disease: data from the Heart and Soul Study. *Circulation* 2007; **115:** 2533-9.

66. Leopold JA. Cellular mechanisms of aortic valve calcification. *Circ.Cardiovasc.Interv.* 2012; **5:** 605-14.

67. Lee TC, O'Malley PG, Feuerstein I, Taylor AJ. The prevalence and severity of coronary artery calcification on coronary artery computed tomography in black and white subjects. *J.Am.Coll.Cardiol.* 2003; **41:** 39-44.

68. Iribarren C, Sidney S, Sternfeld B, Browner WS. Calcification of the aortic arch: risk factors and association with coronary heart disease, stroke, and peripheral vascular disease. *JAMA* 2000; **283:** 2810-5.

69. Lindroos M, Kupari M, Heikkila J, Tilvis R. Prevalence of aortic valve abnormalities in the elderly: an echocardiographic study of a random population sample. *J.Am.Coll.Cardiol.* 1993; **21:** 1220-5.

70. Rennenberg RJ, Kessels AG, Schurgers LJ, van Engelshoven JM, de Leeuw PW, Kroon AA. Vascular calcifications as a marker of increased cardiovascular risk: a meta-analysis. *Vasc.Health Risk Manag.* 2009; **5:** 185-97.

71. Rumberger JA, Simons DB, Fitzpatrick LA, Sheedy PF, Schwartz RS. Coronary artery calcium area by electron-beam computed tomography and coronary atherosclerotic plaque area. A histopathologic correlative study. *Circulation* 1995; **92:** 2157-62.

72. Taylor AJ, Cerqueira M, Hodgson JM *et al.* ACCF/SCCT/ACR/AHA/ASE/ASNC/NASCI/SCAI/SCMR 2010 Appropriate Use Criteria for Cardiac Computed Tomography. A Report of the American College of Cardiology Foundation Appropriate Use Criteria Task Force, the Society of Cardiovascular Computed Tomography, the American College of Radiology, the American Heart Association, the American Society of Echocardiography, the American Society of Nuclear Cardiology, the North American Society for Cardiovascular Imaging, the Society for Cardiovascular Angiography and Interventions, and the Society for Cardiovascular Magnetic Resonance. *J.Cardiovasc.Comput.Tomogr.* 2010; **4:** 407-33.

73. Agatston AS, Janowitz WR, Hildner FJ, Zusmer NR, Viamonte M, Jr., Detrano R. Quantification of coronary artery calcium using ultrafast computed tomography. *J.Am.Coll.Cardiol.* 1990; **15:** 827-32.

74. Henneman MM, Bax JJ, Schuijf JD *et al.* Global and regional left ventricular function: a comparison between gated SPECT, 2D echocardiography and multi-slice computed tomography. *Eur.J.Nucl.Med.Mol.Imaging* 2006; **33:** 1452-60.

75. Greenland P, Bonow RO, Brundage BH *et al.* ACCF/AHA 2007 clinical expert consensus document on coronary artery calcium scoring by computed tomography in global cardiovascular risk assessment and in evaluation of patients with chest pain: a report of the American College of Cardiology Foundation Clinical Expert Consensus Task Force (ACCF/AHA Writing Committee to Update the 2000 Expert Consensus Document on Electron Beam Computed Tomography) developed in collaboration with the Society of Atherosclerosis Imaging and Prevention and the Society of Cardiovascular Computed Tomography. *J.Am.Coll.Cardiol.* 2007; **49:** 378-402.

76. Vliegenthart R, Oudkerk M, Hofman A *et al.* Coronary calcification improves cardiovascular risk prediction in the elderly. *Circulation* 2005; **112:** 572-7.

77. Raggi P, Shaw LJ, Berman DS, Callister TQ. Prognostic value of coronary artery calcium screening in subjects with and without diabetes. *J.Am.Coll.Cardiol.* 2004; **43:** 1663-9.

78. Wang L, Jerosch-Herold M, Jacobs DR, Jr., Shahar E, Detrano R, Folsom AR. Coronary artery calcification and myocardial perfusion in asymptomatic adults: the MESA (Multi-Ethnic Study of Atherosclerosis). *J.Am.Coll.Cardiol.* 2006; **48:** 1018-26.

79. Goldsmith D, Ritz E, Covic A. Vascular calcification: a stiff challenge for the nephrologist: does preventing bone disease cause arterial disease? *Kidney Int.* 2004; **66:** 1315-33.

80. Roy D, Kauffmann C, Delorme S, Lerouge S, Cloutier G, Soulez G. A literature review of the numerical analysis of abdominal aortic aneurysms treated with endovascular stent grafts. *Comput.Math.Methods Med.* 2012; **2012:** 820389.

81. Cecelja M, Chowienczyk P. Role of arterial stiffness in cardiovascular disease. *JRSM.Cardiovasc.Dis.* 2012; **1**.

82. O'Keefe JH, Jr., Lavie CJ, Nishimura RA, Edwards WD. Degenerative aortic stenosis. One effect of the graying of America. *Postgrad.Med.* 1991; **89:** 143-4.

83. Barasch E, Gottdiener JS, Larsen EK, Chaves PH, Newman AB, Manolio TA. Clinical significance of calcification of the fibrous skeleton of the heart and aortosclerosis in community dwelling elderly. The Cardiovascular Health Study (CHS). *Am.Heart J.* 2006; **151:** 39-47.

84. Cohen MM, Jr. The new bone biology: pathologic, molecular, and clinical correlates. *Am.J.Med.Genet.A* 2006; **140:** 2646-706.

85. Caetano-Lopes J, Canhao H, Fonseca JE. Osteoblasts and bone formation. *Acta Reumatol.Port.* 2007; **32:** 103-10.

86. Komori T. Regulation of osteoblast differentiation by Runx2. *Adv.Exp.Med.Biol.* 2010; **658:** 43-9.

87. Orimo H. The mechanism of mineralization and the role of alkaline phosphatase in health and disease. *J.Nippon Med.Sch* 2010; **77:** 4-12.

88. Schinke T, Karsenty G. Vascular calcification--a passive process in need of inhibitors. *Nephrol.Dial.Transplant.* 2000; **15:** 1272-4.

89. SIFFERT RS. The role of alkaline phosphatase in osteogenesis. *J.Exp.Med.* 1951; **93:** 415-26.

90. Datta HK, Ng WF, Walker JA, Tuck SP, Varanasi SS. The cell biology of bone metabolism. *J.Clin.Pathol.* 2008; **61:** 577-87.

91. Downey PA, Siegel MI. Bone biology and the clinical implications for osteoporosis. *Phys.Ther.* 2006; **86:** 77-91.

92. Towler, D. Vascular calcification: A perspective on an imminent disease epidemic. http://www.nature.com/bonekey/knowledgeenvironment/2008/0802/bonekey20080298/full/bonekey20080298.html#ref32.

93. Mackie EJ, Ahmed YA, Tatarczuch L, Chen KS, Mirams M. Endochondral ossification: how cartilage is converted into bone in the developing skeleton. *Int.J.Biochem.Cell Biol.* 2008; **40:** 46-62.

94. Marie PJ, Kassem M. Osteoblasts in osteoporosis: past, emerging, and future anabolic targets. *Eur.J.Endocrinol.* 2011; **165:** 1-10.

95. Kirton JP, Crofts NJ, George SJ, Brennan K, Canfield AE. Wnt/beta-catenin signaling stimulates chondrogenic and inhibits adipogenic differentiation of pericytes: potential relevance to vascular disease? *Circ.Res.* 2007; **101:** 581-9.

96. Cheng SL, Shao JS, Charlton-Kachigian N, Loewy AP, Towler DA. MSX2 promotes osteogenesis and suppresses adipogenic differentiation of multipotent mesenchymal progenitors. *J.Biol.Chem.* 2003; **278:** 45969-77.

97. Parhami F, Jackson SM, Tintut Y *et al.* Atherogenic diet and minimally oxidized low density lipoprotein inhibit osteogenic and promote adipogenic differentiation of marrow stromal cells. *J.Bone Miner.Res.* 1999; **14:** 2067-78.

98. Massy ZA, Mentaverri R, Mozar A, Brazier M, Kamel S. The pathophysiology of vascular calcification: are osteoclast-like cells the missing link? *Diabetes Metab* 2008; **34 Suppl 1:** S16-S20.

99. Meregalli M, Farini A, Colleoni F, Cassinelli L, Torrente Y. The role of stem cells in muscular dystrophies. *Curr.Gene Ther.* 2012; **12:** 192-205.

100. Speer MY, Yang HY, Brabb T *et al.* Smooth muscle cells give rise to osteochondrogenic precursors and chondrocytes in calcifying arteries. *Circ.Res.* 2009; **104:** 733-41.

101. Doherty TM, Asotra K, Fitzpatrick LA *et al.* Calcification in atherosclerosis: bone biology and chronic inflammation at the arterial crossroads. *Proc.Natl.Acad.Sci.U.S.A* 2003; **100:** 11201-6.

102. Drueke TB. Arterial intima and media calcification: distinct entities with different pathogenesis or all the same? *Clin.J.Am.Soc.Nephrol.* 2008; **3:** 1583-4.

103. Amann K. Media calcification and intima calcification are distinct entities in chronic kidney disease. *Clin.J.Am.Soc.Nephrol.* 2008; **3:** 1599-605.

104. Tintut Y, Patel J, Parhami F, Demer LL. Tumor necrosis factor-alpha promotes in vitro calcification of vascular cells via the cAMP pathway. *Circulation* 2000; **102:** 2636-42.

105. Mody N, Parhami F, Sarafian TA, Demer LL. Oxidative stress modulates osteoblastic differentiation of vascular and bone cells. *Free Radic.Biol.Med.* 2001; **31:** 509-19.

106. Bouletreau PJ, Warren SM, Spector JA *et al.* Hypoxia and VEGF up-regulate BMP-2 mRNA and protein expression in microvascular endothelial cells: implications for fracture healing. *Plast.Reconstr.Surg.* 2002; **109:** 2384-97.

107. Qiao JH, Fishbein MC, Demer LL, Lusis AJ. Genetic determination of cartilaginous metaplasia in mouse aorta. *Arterioscler.Thromb.Vasc.Biol.* 1995; **15:** 2265-72.

108. Schmidt HH, Hill S, Makariou EV, Feuerstein IM, Dugi KA, Hoeg JM. Relation of cholesterol-year score to severity of calcific atherosclerosis and tissue deposition in homozygous familial hypercholesterolemia. *Am.J.Cardiol.* 1996; **77:** 575-80.

109. Sorescu GP, Sykes M, Weiss D *et al.* Bone morphogenic protein 4 produced in endothelial cells by oscillatory shear stress stimulates an inflammatory response. *J.Biol.Chem.* 2003; **278:** 31128-35.

110. Maiellaro K, Taylor WR. The role of the adventitia in vascular inflammation. *Cardiovasc.Res.* 2007; **75:** 640-8.

111. Moreno PR, Fuster V. New aspects in the pathogenesis of diabetic atherothrombosis. *J.Am.Coll.Cardiol.* 2004; **44:** 2293-300.

112. Al-Aly Z, Shao JS, Lai CF *et al.* Aortic Msx2-Wnt calcification cascade is regulated by TNF-alpha-dependent signals in diabetic Ldlr-/- mice. *Arterioscler.Thromb.Vasc.Biol.* 2007; **27:** 2589-96.

113. Lee HL, Woo KM, Ryoo HM, Baek JH. Tumor necrosis factor-alpha increases alkaline phosphatase expression in vascular smooth muscle cells via MSX2 induction. *Biochem.Biophys.Res.Commun.* 2010; **391:** 1087-92.

114. Scatena M, Liaw L, Giachelli CM. Osteopontin: a multifunctional molecule regulating chronic inflammation and vascular disease. *Arterioscler.Thromb.Vasc.Biol.* 2007; **27:** 2302-9.

115. Fonseca VA. Defining and characterizing the progression of type 2 diabetes. *Diabetes Care* 2009; **32 Suppl 2:** S151-S156.

116. Olesen P, Ledet T, Rasmussen LM. Arterial osteoprotegerin: increased amounts in diabetes and modifiable synthesis from vascular smooth muscle cells by insulin and TNF-alpha. *Diabetologia* 2005; **48:** 561-8.

117. Jorgensen GM, Vind B, Nybo M, Rasmussen LM, Hojlund K. Acute hyperinsulinemia decreases plasma osteoprotegerin with diminished effect in type 2 diabetes and obesity. *Eur.J.Endocrinol.* 2009; **161:** 95-101.

118. Stewart BF, Siscovick D, Lind BK *et al.* Clinical factors associated with calcific aortic valve disease. Cardiovascular Health Study. *J.Am.Coll.Cardiol.* 1997; **29:** 630-4.

119. Otto CM, Kuusisto J, Reichenbach DD, Gown AM, O'Brien KD. Characterization of the early lesion of 'degenerative' valvular aortic stenosis. Histological and immunohistochemical studies. *Circulation* 1994; **90:** 844-53.

120. Miller JD, Weiss RM, Heistad DD. Calcific aortic valve stenosis: methods, models, and mechanisms. *Circ.Res.* 2011; **108:** 1392-412.

121. Robicsek F, Thubrikar MJ, Cook JW, Fowler B. The congenitally bicuspid aortic valve: how does it function? Why does it fail? *Ann.Thorac.Surg.* 2004; **77:** 177-85.

122. Nigam V, Srivastava D. Notch1 represses osteogenic pathways in aortic valve cells. *J.Mol.Cell Cardiol.* 2009; **47:** 828-34.

123. Moe SM, Chen NX. Pathophysiology of vascular calcification in chronic kidney disease. *Circ.Res.* 2004; **95:** 560-7.

124. Neven E, D'Haese PC. Vascular calcification in chronic renal failure: what have we learned from animal studies? *Circ.Res.* 2011; **108:** 249-64.

125. Covic A, Kanbay M, Voroneanu L *et al.* Vascular calcification in chronic kidney disease. *Clin.Sci.(Lond)* 2010; **119:** 111-21.

126. Levin A, Bakris GL, Molitch M *et al.* Prevalence of abnormal serum vitamin D, PTH, calcium, and phosphorus in patients with chronic kidney disease: results of the study to evaluate early kidney disease. *Kidney Int.* 2007; **71:** 31-8.

127. Shanahan CM, Crouthamel MH, Kapustin A, Giachelli CM. Arterial calcification in chronic kidney disease: key roles for calcium and phosphate. *Circ.Res.* 2011; **109:** 697-711.

128. Zhu D, Mackenzie NC, Farquharson C, Macrae VE. Mechanisms and clinical consequences of vascular calcification. *Front Endocrinol.(Lausanne)* 2012; **3:** 95.

129. Mazzaferro S, Pasquali M, Rotondi S, Tartaglione L. Does any therapy exist for vascular calcifications in uremia? *J.Nephrol.* 2011; **24 Suppl 18:** S16-S24.

130. Helas S, Goettsch C, Schoppet M *et al.* Inhibition of receptor activator of NF-kappaB ligand by denosumab attenuates vascular calcium deposition in mice. *Am.J.Pathol.* 2009; **175:** 473-8.

131. Shao JS, Cheng SL, Charlton-Kachigian N, Loewy AP, Towler DA. Teriparatide (human parathyroid hormone (1-34)) inhibits osteogenic vascular calcification in diabetic low density lipoprotein receptor-deficient mice. *J.Biol.Chem.* 2003; **278:** 50195-202.

132. Jamal SA, Vandermeer B, Raggi P *et al.* Effect of calcium-based versus non-calcium-based phosphate binders on mortality in patients with chronic kidney disease: an updated systematic review and meta-analysis. *Lancet* 2013; **382:** 1268-77.

133. Rodriguez M, guilera-Tejero E, Mendoza FJ, Guerrero F, Lopez I. Effects of calcimimetics on extraskeletal calcifications in chronic kidney disease. *Kidney Int.Suppl* 2008; S50-S54.

134. Shea MK, O'Donnell CJ, Hoffmann U *et al.* Vitamin K supplementation and progression of coronary artery calcium in older men and women. *Am.J.Clin.Nutr.* 2009; **89:** 1799-807.

135. Auriemma M, Carbone A, Di LL *et al.* Treatment of cutaneous calciphylaxis with sodium thiosulfate: two case reports and a review of the literature. *Am.J.Clin.Dermatol.* 2011; **12:** 339-46.

136. Essalihi R, Dao HH, Gilbert LA *et al.* Regression of medial elastocalcinosis in rat aorta: a new vascular function for carbonic anhydrase. *Circulation* 2005; **112:** 1628-35.

137. Novo G, Fazio G, Visconti C *et al.* Atherosclerosis, degenerative aortic stenosis and statins. *Curr.Drug Targets.* 2011; **12:** 115-21.

138. Collin-Osdoby P, Rothe L, Anderson F, Nelson M, Maloney W, Osdoby P. Receptor activator of NF-kappa B and osteoprotegerin expression by human microvascular endothelial cells, regulation by inflammatory cytokines, and role in human osteoclastogenesis. *J.Biol.Chem.* 2001; **276:** 20659-72.

139. Simonet WS, Lacey DL, Dunstan CR *et al.* Osteoprotegerin: a novel secreted protein involved in the regulation of bone density. *Cell* 1997; **89:** 309-19.

140. Tsuda E, Goto M, Mochizuki S *et al.* Isolation of a novel cytokine from human fibroblasts that specifically inhibits osteoclastogenesis. *Biochem.Biophys.Res.Commun.* 1997; **234:** 137-42.

141. Yun TJ, Chaudhary PM, Shu GL *et al.* OPG/FDCR-1, a TNF receptor family member, is expressed in lymphoid cells and is up-regulated by ligating CD40. *J.Immunol.* 1998; **161:** 6113-21.

142. Yamaguchi K, Kinosaki M, Goto M *et al.* Characterization of structural domains of human osteoclastogenesis inhibitory factor. *J.Biol.Chem.* 1998; **273:** 5117-23.

143. Vinholt PJ, Overgaard M, Diederichsen AC *et al.* An ELISA for the quantitation of von Willebrand factor: osteoprotegerin complexes in plasma. *Thromb.Res.* 2013; **131:** 396-400.

144. Zannettino AC, Holding CA, Diamond P *et al.* Osteoprotegerin (OPG) is localized to the Weibel-Palade bodies of human vascular endothelial cells and is physically associated with von Willebrand factor. *J.Cell Physiol* 2005; **204:** 714-23.

145. Khosla S. Minireview: the OPG/RANKL/RANK system. *Endocrinology* 2001; **142:** 5050-5.

146. Corallini F, Rimondi E, Secchiero P. TRAIL and osteoprotegerin: a role in endothelial physiopathology? *Front Biosci.* 2008; **13:** 135-47.

147. Anderson DM, Maraskovsky E, Billingsley WL *et al.* A homologue of the TNF receptor and its ligand enhance T-cell growth and dendritic-cell function. *Nature* 1997; **390:** 175-9.

148. Yasuda H, Shima N, Nakagawa N *et al.* Osteoclast differentiation factor is a ligand for osteoprotegerin/osteoclastogenesis-inhibitory factor and is identical to TRANCE/RANKL. *Proc.Natl.Acad.Sci.U.S.A* 1998; **95:** 3597-602.

149. Wong BR, Josien R, Lee SY *et al.* TRANCE (tumor necrosis factor [TNF]-related activation-induced cytokine), a new TNF family member predominantly expressed in T cells, is a dendritic cell-specific survival factor. *J.Exp.Med.* 1997; **186:** 2075-80.

150. Josien R, Wong BR, Li HL, Steinman RM, Choi Y. TRANCE, a TNF family member, is differentially expressed on T cell subsets and induces cytokine production in dendritic cells. *J.Immunol.* 1999; **162:** 2562-8.

151. Lum L, Wong BR, Josien R *et al.* Evidence for a role of a tumor necrosis factor-alpha (TNF-alpha)-converting enzyme-like protease in shedding of TRANCE, a TNF family member involved in osteoclastogenesis and dendritic cell survival. *J.Biol.Chem.* 1999; **274:** 13613-8.

152. Hofbauer LC, Heufelder AE. Role of receptor activator of nuclear factor-kappaB ligand and osteoprotegerin in bone cell biology. *J.Mol.Med.(Berl)* 2001; **79:** 243-53.

153. Ikeda T, Kasai M, Utsuyama M, Hirokawa K. Determination of three isoforms of the receptor activator of nuclear factor-kappaB ligand and their differential expression in bone and thymus. *Endocrinology* 2001; **142:** 1419-26.

154. Wiley SR, Schooley K, Smolak PJ *et al.* Identification and characterization of a new member of the TNF family that induces apoptosis. *Immunity.* 1995; **3:** 673-82.

155. Pitti RM, Marsters SA, Ruppert S, Donahue CJ, Moore A, Ashkenazi A. Induction of apoptosis by Apo-2 ligand, a new member of the tumor necrosis factor cytokine family. *J.Biol.Chem.* 1996; **271:** 12687-90.

156. MacFarlane M, Ahmad M, Srinivasula SM, Fernandes-Alnemri T, Cohen GM, Alnemri ES. Identification and molecular cloning of two novel receptors for the cytotoxic ligand TRAIL. *J.Biol.Chem.* 1997; **272:** 25417-20.

157. Pan G, O'Rourke K, Chinnaiyan AM *et al.* The receptor for the cytotoxic ligand TRAIL. *Science* 1997; **276:** 111-3.

158. Sheridan JP, Marsters SA, Pitti RM *et al.* Control of TRAIL-induced apoptosis by a family of signaling and decoy receptors. *Science* 1997; **277:** 818-21.

159. Ashkenazi A, Dixit VM. Death receptors: signaling and modulation. *Science* 1998; **281:** 1305-8.

160. Sato K, Niessner A, Kopecky SL, Frye RL, Goronzy JJ, Weyand CM. TRAIL-expressing T cells induce apoptosis of vascular smooth muscle cells in the atherosclerotic plaque. *J.Exp.Med.* 2006; **203:** 239-50.

161. Cross SS, Yang Z, Brown NJ *et al.* Osteoprotegerin (OPG)--a potential new role in the regulation of endothelial cell phenotype and tumour angiogenesis? *Int.J.Cancer* 2006; **118:** 1901-8.

162. Di Iasio, MG, Melloni, E, Secchiero, P, and Capitani, S. Atlas of Genetics and Cytogenetics in Oncology and Haematology. http://atlasgeneticsoncology.org/Genes/TNFSF10ID42632ch3q26.html.

163. Sadler JE. Biochemistry and genetics of von Willebrand factor. *Annu.Rev.Biochem.* 1998; **67:** 395-424.

164. Cummings SR, San MJ, McClung MR *et al.* Denosumab for prevention of fractures in postmenopausal women with osteoporosis. *N.Engl.J.Med.* 2009; **361:** 756-65.

165. Kong YY, Yoshida H, Sarosi I *et al.* OPGL is a key regulator of osteoclastogenesis, lymphocyte development and lymph-node organogenesis. *Nature* 1999; **397:** 315-23.

166. Baud'huin M, Duplomb L, Ruiz VC, Fortun Y, Heymann D, Padrines M. Key roles of the OPG-RANK-RANKL system in bone oncology. *Expert.Rev.Anticancer Ther.* 2007; **7:** 221-32.

167. Wong BR, Josien R, Lee SY, Vologodskaia M, Steinman RM, Choi Y. The TRAF family of signal transducers mediates NF-kappaB activation by the TRANCE receptor. *J.Biol.Chem.* 1998; **273:** 28355-9.

168. Galibert L, Tometsko ME, Anderson DM, Cosman D, Dougall WC. The involvement of multiple tumor necrosis factor receptor (TNFR)-associated factors in the signaling mechanisms of receptor activator of NF-kappaB, a member of the TNFR superfamily. *J.Biol.Chem.* 1998; **273:** 34120-7.

169. Armstrong AP, Tometsko ME, Glaccum M, Sutherland CL, Cosman D, Dougall WC. A RANK/TRAF6-dependent signal transduction pathway is essential for osteoclast cytoskeletal organization and resorptive function. *J.Biol.Chem.* 2002; **277:** 44347-56.

170. Kostenuik PJ, Nguyen HQ, McCabe J *et al.* Denosumab, a fully human monoclonal antibody to RANKL, inhibits bone resorption and increases BMD in knock-in mice that express chimeric (murine/human) RANKL. *J.Bone Miner.Res.* 2009; **24:** 182-95.

171. Schoppet M, Al-Fakhri N, Franke FE *et al.* Localization of osteoprotegerin, tumor necrosis factor-related apoptosis-inducing ligand, and receptor activator of nuclear factor-kappaB ligand in Monckeberg's sclerosis and atherosclerosis. *J.Clin.Endocrinol.Metab* 2004; **89:** 4104-12.

172. Davenport C, Ashley DT, O'Sullivan EP *et al.* Identifying coronary artery disease in men with type 2 diabetes: osteoprotegerin, pulse wave velocity, and other biomarkers of cardiovascular risk. *J.Hypertens.* 2011; **29:** 2469-75.

173. Nybo M, Rasmussen LM. The capability of plasma osteoprotegerin as a predictor of cardiovascular disease: a systematic literature review. *Eur.J.Endocrinol.* 2008; **159:** 603-8.

174. Min H, Morony S, Sarosi I *et al.* Osteoprotegerin reverses osteoporosis by inhibiting endosteal osteoclasts and prevents vascular calcification by blocking a process resembling osteoclastogenesis. *J.Exp.Med.* 2000; **192:** 463-74.

175. Orita Y, Yamamoto H, Kohno N *et al.* Role of osteoprotegerin in arterial calcification: development of new animal model. *Arterioscler.Thromb.Vasc.Biol.* 2007; **27:** 2058-64.

176. Bennett BJ, Scatena M, Kirk EA *et al.* Osteoprotegerin inactivation accelerates advanced atherosclerotic lesion progression and calcification in older ApoE-/- mice. *Arterioscler.Thromb.Vasc.Biol.* 2006; **26:** 2117-24.

177. Samelson EJ, Miller PD, Christiansen C *et al.* RANKL inhibition with denosumab does not influence 3-year progression of aortic calcification or incidence of adverse cardiovascular events in postmenopausal women with osteoporosis and high cardiovascular risk. *J.Bone Miner.Res.* 2013.

178. Collin-Osdoby P. Regulation of vascular calcification by osteoclast regulatory factors RANKL and osteoprotegerin. *Circ.Res.* 2004; **95:** 1046-57.

179. Dhore CR, Cleutjens JP, Lutgens E *et al.* Differential expression of bone matrix regulatory proteins in human atherosclerotic plaques. *Arterioscler.Thromb.Vasc.Biol.* 2001; **21:** 1998-2003.

180. Sandberg WJ, Yndestad A, Oie E *et al.* Enhanced T-cell expression of RANK ligand in acute coronary syndrome: possible role in plaque destabilization. *Arterioscler.Thromb.Vasc.Biol.* 2006; **26:** 857-63.

181. Kiechl S, Werner P, Knoflach M, Furtner M, Willeit J, Schett G. The osteoprotegerin/RANK/RANKL system: a bone key to vascular disease. *Expert.Rev.Cardiovasc.Ther.* 2006; **4:** 801-11.

182. Ndip A, Williams A, Jude EB *et al.* The RANKL/RANK/OPG signaling pathway mediates medial arterial calcification in diabetic Charcot neuroarthropathy. *Diabetes* 2011; **60:** 2187-96.

183. Panizo S, Cardus A, Encinas M *et al.* RANKL increases vascular smooth muscle cell calcification through a RANK-BMP4-dependent pathway. *Circ.Res.* 2009; **104:** 1041-8.

184. Kaden JJ, Bickelhaupt S, Grobholz R *et al.* Receptor activator of nuclear factor kappaB ligand and osteoprotegerin regulate aortic valve calcification. *J.Mol.Cell Cardiol.* 2004; **36:** 57-66.

185. Xie H, Xie PL, Wu XP *et al.* Omentin-1 attenuates arterial calcification and bone loss in osteoprotegerin-deficient mice by inhibition of RANKL expression. *Cardiovasc.Res.* 2011; **92:** 296-306.

186. Olesen M, Skov V, Mechta M, Mumm BH, Rasmussen LM. No influence of OPG and its ligands, RANKL and TRAIL, on proliferation and regulation of the calcification process in primary human vascular smooth muscle cells. *Mol.Cell Endocrinol.* 2012; **362:** 149-56.

187. Byon CH, Sun Y, Chen J *et al.* Runx2-upregulated receptor activator of nuclear factor kappaB ligand in calcifying smooth muscle cells promotes migration and osteoclastic differentiation of macrophages. *Arterioscler.Thromb.Vasc.Biol.* 2011; **31:** 1387-96.

188. Kim HH, Shin HS, Kwak HJ *et al.* RANKL regulates endothelial cell survival through the phosphatidylinositol 3'-kinase/Akt signal transduction pathway. *FASEB J.* 2003; **17:** 2163-5.

189. Chasseraud M, Liabeuf S, Mozar A *et al.* Tumor necrosis factor-related apoptosis-inducing ligand and vascular calcification. *Ther.Apher.Dial.* 2011; **15:** 140-6.

190. Di Bartolo BA, Cartland SP, Harith HH, Bobryshev YV, Schoppet M, Kavurma MM. TRAIL-Deficiency Accelerates Vascular Calcification in Atherosclerosis via Modulation of RANKL. *PLoS.One.* 2013; **8:** e74211.

191. Stolar MW, Chilton RJ. Type 2 diabetes, cardiovascular risk, and the link to insulin resistance. *Clin.Ther.* 2003; **25 Suppl B:** B4-31.

192. Forst T, Pfutzner A, Kann P, Lobmann R, Schafer H, Beyer J. Association between diabetic-autonomic-C-fibre-neuropathy and medial wall calcification and the significance in the outcome of trophic foot lesions. *Exp.Clin.Endocrinol.Diabetes* 1995; **103:** 94-8.

193. Shanik MH, Xu Y, Skrha J, Dankner R, Zick Y, Roth J. Insulin resistance and hyperinsulinemia: is hyperinsulinemia the cart or the horse? *Diabetes Care* 2008; **31 Suppl 2:** S262-S268.

194. Nystrom T, Gutniak MK, Zhang Q *et al.* Effects of glucagon-like peptide-1 on endothelial function in type 2 diabetes patients with stable coronary artery disease. *Am.J.Physiol Endocrinol.Metab* 2004; **287:** E1209-E1215.

195. The diabetes pandemic. *Lancet* 2011; **378:** 99.

196. Wilcox G. Insulin and insulin resistance. *Clin.Biochem.Rev.* 2005; **26:** 19-39.

197. Sung KC, Choi JH, Gwon HC *et al.* Relationship between insulin resistance and coronary artery calcium in young men and women. *PLoS.One.* 2013; **8:** e53316.

198. Zhou YB, Zhang J, Cai Y *et al.* Insulin resistance induces medial artery calcification in fructose-fed rats. *Exp.Biol.Med.(Maywood.)* 2012; **237:** 50-7.

199. Ahmadi N, Tirunagaram S, Hajsadeghi F *et al.* Concomitant insulin resistance and impaired vascular function is associated with increased coronary artery calcification. *Int.J.Cardiol.* 2010; **144:** 163-5.

200. Bouzakri K, Roques M, Gual P *et al.* Reduced activation of phosphatidylinositol-3 kinase and increased serine 636 phosphorylation of insulin receptor substrate-1 in primary culture of skeletal muscle cells from patients with type 2 diabetes. *Diabetes* 2003; **52:** 1319-25.

201. Carlson CJ, Koterski S, Sciotti RJ, Poccard GB, Rondinone CM. Enhanced basal activation of mitogen-activated protein kinases in adipocytes from type 2 diabetes: potential role of p38 in the downregulation of GLUT4 expression. *Diabetes* 2003; **52:** 634-41.

202. Drucker DJ. The biology of incretin hormones. *Cell Metab* 2006; **3:** 153-65.

203. Hirata Y, Kurobe H, Nishio C *et al.* Exendin-4, a glucagon-like peptide-1 receptor agonist, attenuates neointimal hyperplasia after vascular injury. *Eur.J.Pharmacol.* 2013; **699:** 106-11.

204. Deacon CF. Potential of liraglutide in the treatment of patients with type 2 diabetes. *Vasc.Health Risk Manag.* 2009; **5:** 199-211.

205. Nuche-Berenguer B, Moreno P, Esbrit P *et al.* Effect of GLP-1 treatment on bone turnover in normal, type 2 diabetic, and insulin-resistant states. *Calcif.Tissue Int.* 2009; **84:** 453-61.

206. Nuche-Berenguer B, Moreno P, Portal-Nunez S, Dapia S, Esbrit P, Villanueva-Penacarrillo ML. Exendin-4 exerts osteogenic actions in insulin-resistant and type 2 diabetic states. *Regul.Pept.* 2010; **159:** 61-6.

207. Chaykovska L, von WK, Rahnenfuhrer J *et al.* Effects of DPP-4 inhibitors on the heart in a rat model of uremic cardiomyopathy. *PLoS.One.* 2011; **6:** e27861.

208. von Offenberg SN, Cummins PM, Birney YA, Cullen JP, Redmond EM, Cahill PA. Cyclic strain-mediated regulation of endothelial matrix metalloproteinase-2 expression and activity. *Cardiovasc.Res.* 2004; **63:** 625-34.

209. Redmond EM, Cahill PA, Sitzmann JV. Perfused transcapillary smooth muscle and endothelial cell co-culture--a novel in vitro model. *In Vitro Cell Dev.Biol.Anim* 1995; **31:** 601-9.

210. Ardanaz N, Pagano PJ. Hydrogen peroxide as a paracrine vascular mediator: regulation and signaling leading to dysfunction. *Exp.Biol.Med.(Maywood.)* 2006; **231:** 237-51.

211. Rongen GA, Smits P, Thien T. Endothelium and the regulation of vascular tone with emphasis on the role of nitric oxide. Physiology, pathophysiology and clinical implications. *Neth.J.Med.* 1994; **44:** 26-35.

212. Neuhaus W, Lauer R, Oelzant S, Fringeli UP, Ecker GF, Noe CR. A novel flow based hollow-fiber blood-brain barrier in vitro model with immortalised cell line PBMEC/C1-2. *J.Biotechnol.* 2006; **125:** 127-41.

213. Sakao S, Taraseviciene-Stewart L, Wood K, Cool CD, Voelkel NF. Apoptosis of pulmonary microvascular endothelial cells stimulates vascular smooth muscle cell growth. *Am.J.Physiol Lung Cell Mol.Physiol* 2006; **291:** L362-L368.

214. Chiu JJ, Usami S, Chien S. Vascular endothelial responses to altered shear stress: pathologic implications for atherosclerosis. *Ann.Med.* 2009; **41:** 19-28.

215. Astles JR, Sedor FA, Toffaletti JG. Evaluation of the YSI 2300 glucose analyzer: algorithm-corrected results are accurate and specific. *Clin.Biochem.* 1996; **29:** 27-31.

216. Tsukuda K, Kikuchi M, Irie S *et al.* Evaluation of the 24-hour profiles of physiological insulin, glucose, and C-peptide in healthy Japanese volunteers. *Diabetes Technol.Ther.* 2009; **11:** 499-508.

217. Costa CH, Batista MC, Moises VA, Kohlmann NB, Ribeiro AB, Zanella MT. Serum insulin levels, 24-hour blood pressure profile, and left ventricular mass in nonobese hypertensive patients. *Hypertension* 1995; **26:** 1085-8.

218. R&D, Systems. Human Osteoprotegerin/TNFRSF11B Antibody. http://www.rndsystems.com/pdf/af805.pdf.

219. R&D, Systems. Recombinant Human Noggin. http://www.rndsystems.com/pdf/6057-NG.pdf.

220. Buse JB, Rosenstock J, Sesti G *et al.* Liraglutide once a day versus exenatide twice a day for type 2 diabetes: a 26-week randomised, parallel-group, multinational, open-label trial (LEAD-6). *Lancet* 2009; **374:** 39-47.

221. Kim HJ, Zhao H, Kitaura H *et al.* Glucocorticoids suppress bone formation via the osteoclast. *J.Clin.Invest* 2006; **116:** 2152-60.

222. Alcaraz C, De DM, Pastor MJ, Escribano JM. Comparison of a radioimmunoprecipitation assay to immunoblotting and ELISA for detection of antibody to African swine fever virus. *J.Vet.Diagn.Invest* 1990; **2:** 191-6.

223. Smith PK, Krohn RI, Hermanson GT *et al.* Measurement of protein using bicinchoninic acid. *Anal.Biochem.* 1985; **150:** 76-85.

224. Olivares-Navarrete R, Hyzy S, Wieland M, Boyan BD, Schwartz Z. The roles of Wnt signaling modulators Dickkopf-1 (Dkk1) and Dickkopf-2 (Dkk2) and cell maturation state in osteogenesis on microstructured titanium surfaces. *Biomaterials* 2010; **31:** 2015-24.

225. Vik A, Mathiesen EB, Brox J *et al.* Serum osteoprotegerin is a predictor for incident cardiovascular disease and mortality in a general population: the Tromso Study. *J.Thromb.Haemost.* 2011; **9:** 638-44.

226. Sambrook J, Fritsch E, Maniatis T. *Molecular cloning: a laboratory manual. New York: Cold Spring Harbor Laboratory Press*, 1989.

227. Chomczynski P, Sacchi N. Single-step method of RNA isolation by acid guanidinium thiocyanate-phenol-chloroform extraction. *Anal.Biochem.* 1987; **162:** 156-9.

228. Livak KJ, Schmittgen TD. Analysis of relative gene expression data using real-time quantitative PCR and the 2(-Delta Delta C(T)) Method. *Methods* 2001; **25:** 402-8.

229. Levey AS, Bosch JP, Lewis JB, Greene T, Rogers N, Roth D. A more accurate method to estimate glomerular filtration rate from serum creatinine: a new prediction equation. Modification of Diet in Renal Disease Study Group. *Ann.Intern.Med.* 1999; **130:** 461-70.

230. Malyankar UM, Scatena M, Suchland KL, Yun TJ, Clark EA, Giachelli CM. Osteoprotegerin is an alpha vbeta 3-induced, NF-kappa B-dependent survival factor for endothelial cells. *J.Biol.Chem.* 2000; **275:** 20959-62.

231. Secchiero P, Corallini F, Pandolfi A *et al.* An increased osteoprotegerin serum release characterizes the early onset of diabetes mellitus and may contribute to endothelial cell dysfunction. *Am.J.Pathol.* 2006; **169:** 2236-44.

232. Watt V, Chamberlain J, Steiner T, Francis S, Crossman D. TRAIL attenuates the development of atherosclerosis in apolipoprotein E deficient mice. *Atherosclerosis* 2011; **215:** 348-54.

233. Falschlehner C, Schaefer U, Walczak H. Following TRAIL's path in the immune system. *Immunology* 2009; **127:** 145-54.

234. Bornfeldt KE, Tabas I. Insulin resistance, hyperglycemia, and atherosclerosis. *Cell Metab* 2011; **14:** 575-85.

235. Cummins PM, von Offenberg SN, Killeen MT, Birney YA, Redmond EM, Cahill PA. Cyclic strain-mediated matrix metalloproteinase regulation within the vascular endothelium: a force to be reckoned with. *Am.J.Physiol Heart Circ.Physiol* 2007; **292:** H28-H42.

236. Mackey RH, Venkitachalam L, Sutton-Tyrrell K. Calcifications, arterial stiffness and atherosclerosis. *Adv.Cardiol.* 2007; **44:** 234-44.

237. Popa C, Netea MG, van Riel PL, van der Meer JW, Stalenhoef AF. The role of TNF-alpha in chronic inflammatory conditions, intermediary metabolism, and cardiovascular risk. *J.Lipid Res.* 2007; **48:** 751-62.

238. Raghavan VA. Insulin resistance and atherosclerosis. *Heart Fail.Clin.* 2012; **8:** 575-87.

239. Moschen AR, Kaser A, Enrich B *et al.* The RANKL/OPG system is activated in inflammatory bowel disease and relates to the state of bone loss. *Gut* 2005; **54:** 479-87.

240. Bouis D, Hospers GA, Meijer C, Molema G, Mulder NH. Endothelium in vitro: a review of human vascular endothelial cell lines for blood vessel-related research. *Angiogenesis.* 2001; **4:** 91-102.

241. Popov D, Simionescu M. Cellular mechanisms and signalling pathways activated by high glucose and AGE-albumin in the aortic endothelium. *Arch.Physiol Biochem.* 2006; **112:** 265-73.

242. Giri H, Muthuramu I, Dhar M, Rathnakumar K, Ram U, Dixit M. Protein tyrosine phosphatase SHP2 mediates chronic insulin-induced endothelial inflammation. *Arterioscler.Thromb.Vasc.Biol.* 2012; **32:** 1943-50.

243. Carmody SR, Wente SR. mRNA nuclear export at a glance. *J.Cell Sci.* 2009; **122:** 1933-7.

244. Greenbaum D, Colangelo C, Williams K, Gerstein M. Comparing protein abundance and mRNA expression levels on a genomic scale. *Genome Biol.* 2003; **4:** 117.

245. Ishida A, Fujita N, Kitazawa R, Tsuruo T. Transforming growth factor-beta induces expression of receptor activator of NF-kappa B ligand in vascular endothelial cells derived from bone. *J.Biol.Chem.* 2002; **277:** 26217-24.

246. Pascal LE, True LD, Campbell DS *et al.* Correlation of mRNA and protein levels: cell type-specific gene expression of cluster designation antigens in the prostate. *BMC.Genomics* 2008; **9:** 246.

247. Laurent JM, Vogel C, Kwon T *et al.* Protein abundances are more conserved than mRNA abundances across diverse taxa. *Proteomics.* 2010; **10:** 4209-12.

248. Vogel C, Marcotte EM. Insights into the regulation of protein abundance from proteomic and transcriptomic analyses. *Nat.Rev.Genet.* 2012; **13:** 227-32.

249. Kostenuik PJ. Osteoprotegerin and RANKL regulate bone resorption, density, geometry and strength. *Curr.Opin.Pharmacol.* 2005; **5:** 618-25.

250. Bowsher RR, Sailstad JM. Insights in the application of research-grade diagnostic kits for biomarker assessments in support of clinical drug development: bioanalysis of circulating concentrations of soluble receptor activator of nuclear factor kappaB ligand. *J.Pharm.Biomed.Anal.* 2008; **48:** 1282-9.

251. Chamoux E, Houde N, L'Eriger K, Roux S. Osteoprotegerin decreases human osteoclast apoptosis by inhibiting the TRAIL pathway. *J.Cell Physiol* 2008; **216:** 536-42.

252. Davenport C, Kenny H, Ashley DT, O'Sullivan EP, Smith D, O'Gorman DJ. The effect of exercise on osteoprotegerin and TNF-related apoptosis-inducing ligand in obese patients. *Eur.J.Clin.Invest* 2012; **42:** 1173-9.

253. Ishimura N, Isomoto H, Bronk SF, Gores GJ. Trail induces cell migration and invasion in apoptosis-resistant cholangiocarcinoma cells. *Am.J.Physiol Gastrointest.Liver Physiol* 2006; **290:** G129-G136.

254. Gochuico BR, Zhang J, Ma BY, Marshak-Rothstein A, Fine A. TRAIL expression in vascular smooth muscle. *Am.J.Physiol Lung Cell Mol.Physiol* 2000; **278:** L1045-L1050.

255. Spierings DC, de Vries EG, Vellenga E *et al.* Tissue distribution of the death ligand TRAIL and its receptors. *J.Histochem.Cytochem.* 2004; **52:** 821-31.

256. Pritzker LB, Scatena M, Giachelli CM. The role of osteoprotegerin and tumor necrosis factor-related apoptosis-inducing ligand in human microvascular endothelial cell survival. *Mol.Biol.Cell* 2004; **15:** 2834-41.

257. Chapman GB, Durante W, Hellums JD, Schafer AI. Physiological cyclic stretch causes cell cycle arrest in cultured vascular smooth muscle cells. *Am.J.Physiol Heart Circ.Physiol* 2000; **278:** H748-H754.

258. Kusumi A, Sakaki H, Kusumi T *et al.* Regulation of synthesis of osteoprotegerin and soluble receptor activator of nuclear factor-kappaB ligand in normal human osteoblasts via the p38 mitogen-activated protein kinase pathway by the application of cyclic tensile strain. *J.Bone Miner.Metab* 2005; **23:** 373-81.

259. Kusumi A, Kusumi T, Miura J, Tateishi T. Passage-affected competitive regulation of osteoprotegerin synthesis and the receptor activator of nuclear factor-kappaB ligand mRNA expression in normal human osteoblasts stimulated by the application of cyclic tensile strain. *J.Bone Miner.Metab* 2009; **27:** 653-62.

260. Nguyen KQ, Olesen P, Ledet T, Rasmussen LM. Bone morphogenetic proteins regulate osteoprotegerin and its ligands in human vascular smooth muscle cells. *Endocrine.* 2007; **32:** 52-8.

261. Schoppet M, Kavurma MM, Hofbauer LC, Shanahan CM. Crystallizing nanoparticles derived from vascular smooth muscle cells contain the calcification inhibitor osteoprotegerin. *Biochem.Biophys.Res.Commun.* 2011; **407:** 103-7.

262. Ferrari-Lacraz, S and Ferrari, S. Effects of RANKL Inhibition on Inflammation and Immunity. http://www.nature.com/bonekey/knowledgeenvironment/2009/0903/bonekey20090369/pdf/bonekey20090369.pdf.

263. Takemura A, Iijima K, Ota H *et al.* Sirtuin 1 retards hyperphosphatemia-induced calcification of vascular smooth muscle cells. *Arterioscler.Thromb.Vasc.Biol.* 2011; **31:** 2054-62.

264. Jono S, McKee MD, Murry CE *et al.* Phosphate regulation of vascular smooth muscle cell calcification. *Circ.Res.* 2000; **87:** E10-E17.

265. Shioi A, Nishizawa Y, Jono S, Koyama H, Hosoi M, Morii H. Beta-glycerophosphate accelerates calcification in cultured bovine vascular smooth muscle cells. *Arterioscler.Thromb.Vasc.Biol.* 1995; **15:** 2003-9.

266. Candido R, Toffoli B, Corallini F *et al.* Human full-length osteoprotegerin induces the proliferation of rodent vascular smooth muscle cells both in vitro and in vivo. *J.Vasc.Res.* 2010; **47:** 252-61.

267. Moran CS, McCann M, Karan M, Norman P, Ketheesan N, Golledge J. Association of osteoprotegerin with human abdominal aortic aneurysm progression. *Circulation* 2005; **111:** 3119-25.

268. Corallini F, Gonelli A, D'Aurizio F, di Iasio MG, Vaccarezza M. Mesenchymal stem cells-derived vascular smooth muscle cells release abundant levels of osteoprotegerin. *Eur.J.Histochem.* 2009; **53:** 19-24.

269. Tseng W, Graham LS, Geng Y *et al.* PKA-induced receptor activator of NF-kappaB ligand (RANKL) expression in vascular cells mediates osteoclastogenesis but not matrix calcification. *J.Biol.Chem.* 2010; **285:** 29925-31.

270. Tenenbaum HC, Heersche JN. Differentiation of osteoblasts and formation of mineralized bone in vitro. *Calcif.Tissue Int.* 1982; **34:** 76-9.

271. Mori K, Shioi A, Jono S, Nishizawa Y, Morii H. Dexamethasone enhances In vitro vascular calcification by promoting osteoblastic differentiation of vascular smooth muscle cells. *Arterioscler.Thromb.Vasc.Biol.* 1999; **19:** 2112-8.

272. Krause C, Guzman A, Knaus P. Noggin. *Int.J.Biochem.Cell Biol.* 2011; **43:** 478-81.

273. Gouverneur M, Berg B, Nieuwdorp M, Stroes E, Vink H. Vasculoprotective properties of the endothelial glycocalyx: effects of fluid shear stress. *J.Intern.Med.* 2006; **259:** 393-400.

274. Pottegard A, Bjerregaard BK, Larsen MD *et al.* Use of exenatide and liraglutide in Denmark: a drug utilization study. *Eur.J.Clin.Pharmacol.* 2013.

275. Danaei G, Finucane MM, Lu Y *et al.* National, regional, and global trends in fasting plasma glucose and diabetes prevalence since 1980: systematic analysis of health examination surveys and epidemiological studies with 370 country-years and 2.7 million participants. *Lancet* 2011; **378:** 31-40.

276. Morrish NJ, Wang SL, Stevens LK, Fuller JH, Keen H. Mortality and causes of death in the WHO Multinational Study of Vascular Disease in Diabetes. *Diabetologia* 2001; **44 Suppl 2:** S14-S21.

277. Kovacic JC, Randolph GJ. Vascular calcification: harder than it looks. *Arterioscler.Thromb.Vasc.Biol.* 2011; **31:** 1249-50.

278. Volpato S, Ferrucci L, Secchiero P *et al.* Association of tumor necrosis factor-related apoptosis-inducing ligand with total and cardiovascular mortality in older adults. *Atherosclerosis* 2011; **215:** 452-8.

279. Forde H, Davenport C, McLoughlin A, Hynes L, Smith D, and Cummins PM. TRAIL reduces constitutive and stimulated IL-6 release from human aortic endothelial cells . Irish Endocrine Society Annual General Meeting 2014 .